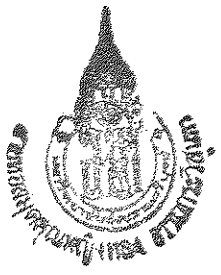

Chemical Constituents from the Twigs of *Garcinia parvifolia*

Wanpen Naklue

A Thesis Submitted in Partial Fulfillment of the Requirements
for the Degree of Master of Science in Organic Chemistry
Prince of Songkla University
2006

ISBN 974-11-4308-7

Thesis Title Chemical Constituents from the Twigs of *Garcinia parvifolia*

Author Miss Wanpen Naklue

Major Program Organic Chemistry

Advisory Committee

V. Rukachaisirikul .....Chairman

(Assoc. Prof. Dr. Vatcharin Rukachaisirikul)

Suda Chakthong .....Committee

(Dr. Suda Chakthong)

Examining Committee

V. Rukachaisirikul .....Chairman

(Assoc. Prof. Dr. Vatcharin Rukachaisirikul)

Suda Chakthong .....Committee

(Dr. Suda Chakthong)

C. Karalai .....Committee

(Assoc. Prof. Dr. Chatchanok Karalai)

.....Committee

(Asst. Prof. Dr. Anuchit Plubrukarn)

The Graduate School, Prince of Songkla University, has approved this thesis as partial fulfillment of the requirements for the Master of Science Degree in Organic Chemistry

.....

(Assoc. Prof. Dr. Surapon Arrykul)

Dean of Graduate School

ชื่อวิทยานิพนธ์	องค์ประกอบทางเคมีจากกิ่งชะมวงเล็ก (*Garcinia parvifolia*)
ผู้เขียน	นางสาววันเพ็ญ นาเกลือ
สาขาวิชา	เคมีอินทรีย์
ปีการศึกษา	2548

บทคัดย่อ

ส่วนสกัดหยาบเมธานอลของกิ่งชะมวงเล็ก เมื่อนำมาแยกและทำให้บริสุทธิ์ด้วยวิธีทางโครมาโทกราฟี สามารถแยกสารใหม่ 13 สาร ได้แก่สารประเภท methyl benzoate จำนวน 2 สาร (**GP2** และ **GP7**) สารประเภท benzopyran จำนวน 5 สาร (**GP1, GP3, GP4, GP5** และ **GP6**) สารประเภท depsidone จำนวน 2 สาร (**GP12** และ **GP14**) สารประเภท xanthone จำนวน 3 สาร (**GP8, GP9** และ **GP11**) และสารประเภท benzocyclooctene จำนวน 1 สาร (**GP10**) รวมทั้งสารที่ทราบโครงสร้างแล้วจำนวน 7 สาร ได้แก่สารประเภท depsidone จำนวน 1 สาร (**GP18**) สารประเภท xanthone จำนวน 5 สาร (**GP15, GP16, GP17, GP19** และ **GP20**) และสารอนุพันธ์ของ cyclohexenone จำนวน 1 สาร (**GP13**) โครงสร้างของสารทั้งหมดวิเคราะห์โดยใช้ข้อมูลทางสเปกโทรสโกปี โดยเฉพาะ 1D และ 2D NMR สเปกโทรสโกปี และการเปรียบเทียบข้อมูลกับสารที่มีการรายงานโครงสร้างมาแล้ว

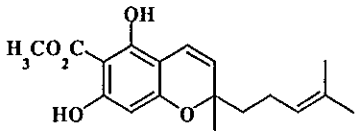

GP1

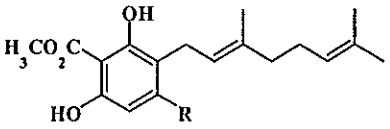

GP2: R = OCH_3

GP7: R = OH

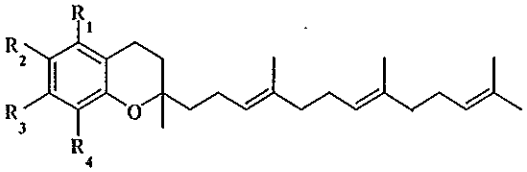

GP3: $R_1 = H, R_2 = R_3 = CH_3, R_4 = OH$

GP4: $R_1 = R_4 = CH_3, R_2 = H, R_4 = OH$

GP5: $R_1 = R_3 = H, R_2 = CH_3, R_4 = OH$

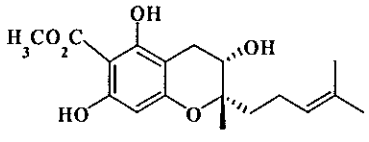

GP6

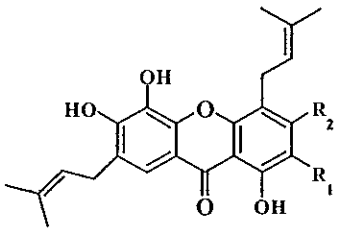

GP8: $R_1 = H, R_2 = OCH_3$

GP9: $R_1 =$ 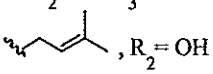 $, R_2 = OH$

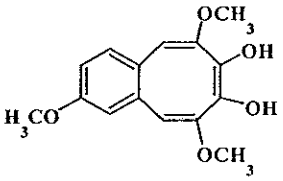

GP10

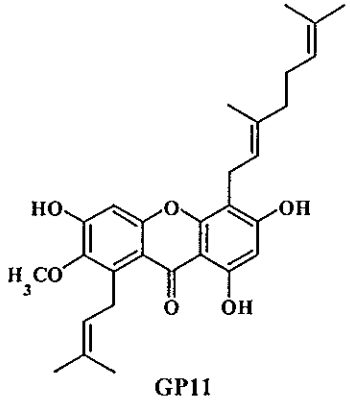

GP11

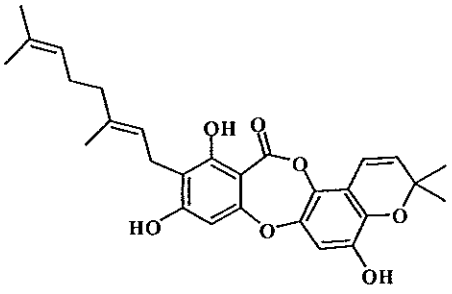

GP12

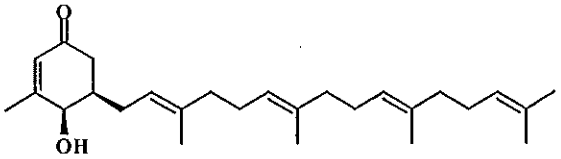

GP13

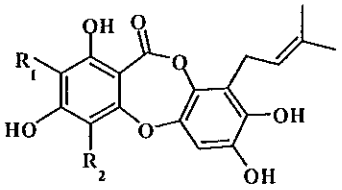

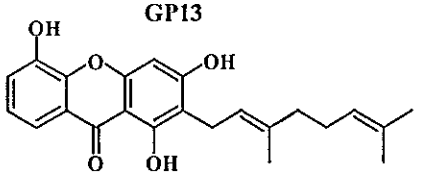

GP15

GP14: $R_1 = H, R_2 =$ 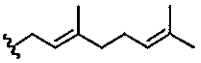

GP18: $R_1 =$ 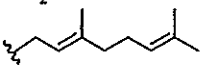 $, R_2 = H$

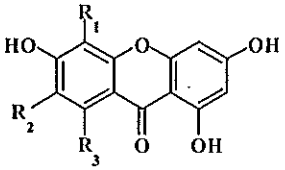

GP16: $R_1 = H, R_2 = OCH_3, R_3 =$ 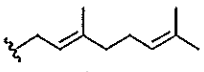

GP17: $R_1 = H, R_2 = OCH_3, R_3 =$ 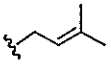

GP19: $R_1 = OH, R_2 = R_3 = H$

GP20: $R_1 = R_3 = OH, R_2 =$ OH

Thesis Title	Chemical Constituents from the Twigs of *Garcinia parvifolia*
Author	Miss Wanpen Naklue
Major Program	Organic Chemistry
Academic Year	2005

ABSTRACT

The crude methanol extract from the twigs of *Garcinia parvifolia* was separated by chromatographic methods to yield thirteen new compounds: two methyl benzoates (**GP2** and **GP7**), five benzopyrans (**GP1, GP3, GP4, GP5** and **GP6**), two depsidones (**GP12** and **GP14**), three xanthones (**GP8, GP9** and **GP11**) and one benzocyclooctene (**GP10**) together with seven known compounds: one depsidone (**GP18**), five xanthones (**GP15, GP16, GP17, GP19** and **GP20**) and one cyclohexenone derivative (**GP13**). The structures were determined by analysis of 1D and 2D NMR spectroscopic data and comparison of the NMR data with those reported in literature.

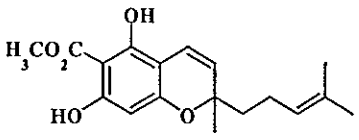

GP1

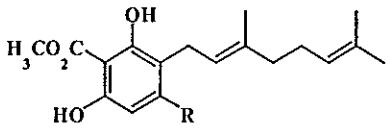

GP2: R = OCH_3

GP7: R = OH

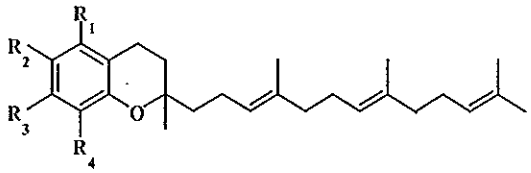

GP3: R_1 = H, R_2 = R_3 = CH_3, R_4 = OH

GP4: R_1 = R_4 = CH_3, R_2 = H, R_4 = OH

GP5: R_1 = R_3 = H, R_2 = CH_3, R_4 = OH

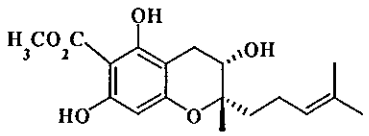

GP6

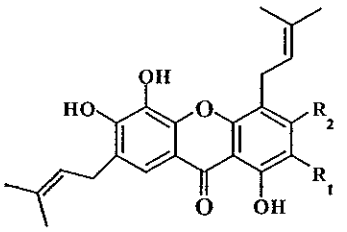

GP8: R_1 = H, R_2 = OCH_3

GP9: R_1 = 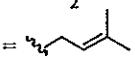 , R_2 = OH

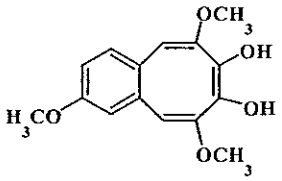

GP10

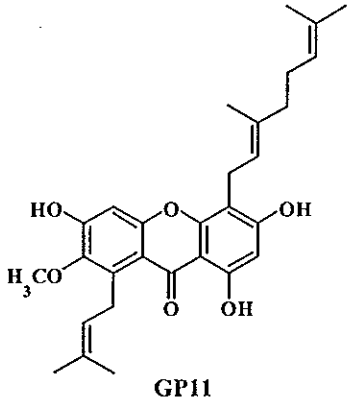

GP11

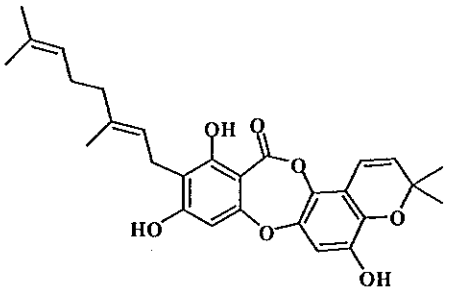

GP12

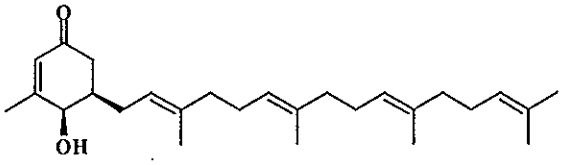

GP13

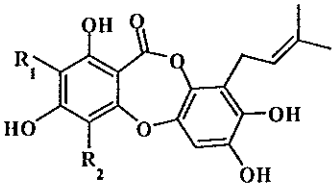

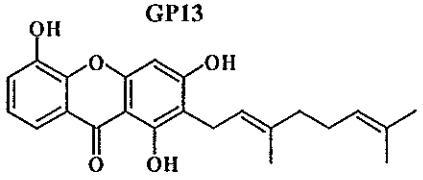

GP15

GP14: R_1 = H, R_2 = 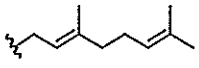

GP18: R_1 = 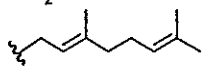 , R_2 = H

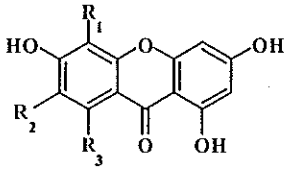

GP16: R_1 = H, R_2 = OCH_3, R_3 = 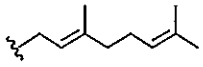

GP17: R_1 = H, R_2 = OCH_3, R_3 = 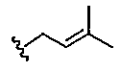

GP19: R_1 = OH, R_2 = R_3 = H

GP20: R_1 = R_3 = OH, R_2 = OH

ACKNOWLEDGEMENT

I wish to express my deepest and sincere gratitude to my supervisor, Associate Professor Dr. Vatcharin Rukachaisirikul, for her valuable instruction, expert guidance and excellent suggestion. I would also like to express my appreciation to her for correction of my thesis. Everything will always be kept in my mind.

My sincere thanks are expressed to Dr. Suda Chakthong, my co-advisor, for her collaboration. I would like to extend my appreciation to the staff of the Department of Chemistry, Faculty of Science, Prince of Songkla University and to those in the Herbarium of Biology Department, Faculty of Science, Prince of Songkla University, for making this thesis possible.

This work was made possible by a scholarship from the Development and Promotion of Science and Technology Talents Project and the Higher Education Development Project: Postgraduate Education and Research Program in Chemistry, funded by the Royal Thai Government.

Finally, none of this would have been possible without love and encouragement of my family and friends. I thank them all for their understanding during all of the times when I could not be with them. Their steady love, indeed, supported me.

Wanpen Naklue

CONTENTS

CONTENTS (Continued)

LIST OF TABLES

LIST OF TABLES (Continued)

LIST OF TABLES (Continued)

LIST OF TABLES (Continued)

LIST OF TABLES (Continued)

LIST OF ILLUSTRATIONS

LIST OF ILLUSTRATIONS (Continued)

LIST OF ILLUSTRATIONS (Continued)

LIST OF ILLUSTRATIONS (Continued)

LIST OF ILLUSTRATIONS (Continued)

LIST OF ILLUSTRATIONS (Continued)

LIST OF ILLUSTRATIONS (Continued)

LIST OF ILLUSTRATIONS (Continued)

LIST OF ABBREVIATIONS AND SYMBOLS

s	=	*singlet*
d	=	*doublet*
t	=	*triplet*
q	=	*quartet*
m	=	*multiplet*
brs	=	*broad singlet*
brd	=	*broad doublet*
brq	=	*broad quartet*
dd	=	*doublet of doublet*
dt	=	*doublet of triplet*
mt	=	*multiplet of triplet*
ddd	=	*doublet of doublet of doublet*
δ	=	chemical shift relative to TMS
J	=	coupling constant
m/z	=	a value of mass divided by charge
°C	=	degree celcius
R_f	=	retention factor
g	=	gram
ml	=	milliliter
cm^{-1}	=	reciprocal centimeter (wavenumber)
nm	=	nanometer
λ_{max}	=	maximum wavelength
ν	=	absorption frequency
ε	=	Molar extinction coefficient
Hz	=	Hertz

LIST OF ABBREVIATIONS AND SYMBOLS (Continued)

MHz	=	megaHertz
ppm	=	part per million
$[\alpha]_D$	=	specific rotation
c	=	concentration
UV	=	Ultraviolet
IR	=	Infrared
NMR	=	Nuclear Magnetic Resonance
2D NMR	=	Two Dimentional Nuclear Magnetic Resonance
MS	=	Mass spectroscopy
HMQC	=	Heteronuclear Multiple Quantum Coherence
HMBC	=	Heteronuclear Multiple Bond Correlation
COSY	=	Correlation spectroscopy
DEPT	=	Distortionless Enhancement by Polarization Transfer
NOE	=	Nuclear Overhauser Effect
TLC	=	Thin-Layer Chromatography
DMSO	=	dimethylsulphoxide
MeOH	=	methanol
CD_3OD	=	deuteromethanol
$CDCl_3$	=	deuterochlorofrom
ASA	=	anisaldehyde-sulphuric acid in acetic acid solution

1. INTRODUCTION

1.1 Introduction

Garcinia parvifolia, a plant belonging to the Guttiferae family, is widely distributed in the southern part of Thailand, Malaya, Sumatra, Borneo. *G. parvifolia* is a small to medium tree and once reaching 33 m tall, 240 cm girth; rarely a shrub. Inner bark with opaque, yellow exudate. Very similar to *G. cowa*, but leaves abruptly tapering into the tip. Male flowers with slender stalk 4-10 mm long, 7-10 mm wide, petals pale, clear yellow, 4 x 2.5 – 6 x 4 mm, not reflexed; female with calyx 4-6 mm wide. Fruits roundish or elongate, not grooved, occasionally umbonate, stigma and calyx generally deeply sunken, stigma only 1.5 mm wide; seated on persistent petals and sepals. Seeds small, embedded in much pulp. *G. parvifolia* is closely related to *G. nigrolineata* (Whitmore, 1973). In Thailand, *G. parvifolia* has a local name, "Cha maung lek". (Smitinand, 2001)

1.2 Review of Literatures

Plants in the *Garcinia* genus (Guttiferae) are well known to be rich in a variety of compounds: xanthones (Soemiati, 2004; Sherley, 2004; Wahyuni, 2004; Abe, 2004; 2003; Chanmahasathien, 2003a,b; Suksamrarn, 2002; 2003; Chiang, 2003; Ito, 2003b; Rukachaisirikul, 2000a, 2003a,b; 2005c,d; Jantan, 2002; Nilar, 2002; Xu, 2001; Huang, 2001; Thoison, 2000), benzophenones (Merza, 2004; Williams, 2003; Chiang, 2003; Rukachaisirikul, 2003a; Abe, 2004; Ito, 2003a; Lakshmi, 2002; Huang, 2001; Ali, 2000), biflavonoids (Parveen, 2004; Abe, 2004; Thoison, 2000), benzophenone-xanthone dimmers (Kosela, 1999; 2000), chalcones (Ilyas, 2002), flavones (Farombi, 2002), depsidones (Xu, 2000) and triterpenes (Vieira, 2004a,b; Rukachaisirikul, 2003a; 2000b; 2005b; Weng, 2003a,b; Thoison, 2000; Nguyen,

2000). Some of these exhibit a wide range of biological and pharmacological activities, e.g., cytotoxic (Sherley, 2004; Soemiati, 2004; Williams, 2003; Xu, 2000; Thoison, 2000; Kosela, 2000), anti-inflammatory (Weng, 2003a,b), antimicrobial (Kosela, 2000), antifungal (Farombi, 2002; Kosela, 2000), antibacterial (Sherley, 2004; Lakshmi, 2002; Rukachaisirikul, 2000a; 2003b), antimalarial (Hay, 2004a; Kosela, 2000), anti-HIV (Rukachaisirikul, 2003a) and antioxidant (Hay, 2004b; Farombi, 2002) activities.

Chemical constituents isolated from plants of the genus *Garcinia* in 2004 have been reported (Sukpondma, 2005). The continuing search using SciFinder database revealed additional chemical constituents in 2005 which were summarized in **Table 1.**

Table 1 Compounds from the genus *Garcinia* in 2005

Scientific name	Investigated part	Compounds	Structures	References
G. bancana	twigs	[1,1'-biphenyl]-2-(3-methyl-2-butenyl)-3-methoxy-4,4',5,6-tetraol	3a	Rukachaisirikul, *et al.*, 2005a
		garcinol	1b	
		isogarcinol	1a	
		(-)-mellein	7g	
		8-(OH)-6-(OCH_3)-3-pentylisocoumarin	7h	
		blumenol C *O*-β-D-glucoside	7c	
		lupeol	5n	
		stigmasterol	7d	
	leaves	quercetin 3-*O*-α-L-rhamnoside	4b	
		kaemferol 3-*O*-α-L-rhamnoside	4a	

Table 1 (Continued)

Scientific name	Investigated part	Compounds	Structures	References
G. bracteata	bark	garcibracteatone	6.6d	Thoison, *et al.*, 2005
		xerophenone C	1i	
		5-*O*-methylxanthone V_1	6.3ii	
		nemorosonol	1j	
		10-*O*-methylmaclura-xanthone	6.3bb	
	leaves	neoisobractatin A	6.6b	
		neoisobractatin B	6.6c	
		bracteaxanthone I	6.3y	
		bracteaxanthone II	6.3jj	
		macluraxanthone	6.3aa	
		cudraxanthone R	6.3kk	
		gerontoxanthone I	6.3z	
G. cowa	latex	cowagarcinone A	6.3r	Mahabusara-kum, *et al.*, 2005
		cowagarcinone B	6.3dd	
		cowagarcinone C	6.3cc	
		cowagarcinone D	6.3ee	
		cowagarcinone E	6.3f	
		cowaxanthone	6.3g	
		cowanin	6.3d	
		cowanol	6.3e	
		1,3,6-tri(OH)-7-(OCH_3)-2,5-*bis*(3-methyl-2-butenyl)xanthone	6.3q	
		mangostinone	6.2k	
		fuscaxanthone A	6.3rr	

Table 1 (Continued)

Scientific name	Investigated part	Compounds	Structures	References
G. dulcis	green fruits	dulcinoside	4e	Deachathai, *et al.*, 2005
		dulcisisoflavone	4o	
		dulcisxanthone A	6.2o	
		sphaerobioside acetate	4m	
		camboginol	1b	
		octadecanoic acid-2,3-di(OH)propyl ester	7j	
		derriscannoside A	4p	
		1,6-di(OH)-3,7-di(OCH_3)-2-(3-methyl-2-butenyl)xanthone	6.3yy	
		cowanin	6.3d	
		cowaxanthone	6.3g	
		1,7-di(OH)-3-(OCH_3)-2-(3-methyl-2-butenyl)-xanthone	6.2q	
		1,5,8-tri(OH)-3-(OCH_3)-2-(3-methyl-2-butenyl)-xanthone	6.3ss	
		chandalone	4n	
		lupalbigenin	4k	
		BR-xanthone A	6.3mm	
		α-mangostin	6.3h	
		isolupalbigenin	4l	

Table 1 (Continued)

Scientific name	Investigated part	Compounds	Structures	References
		6,8,12-tri(OH)-7-(3-methyl-2-butenyl)-2-methyl-2-(4-methyl-3-pentenyl)pyrano(2′,-3′:7, 8)xanthone	6.3ee	
		2-(OH)-l,2,3-propanetricarboxylic acid-1,3-dimethylester	7i	
		vitexin	4f	
		morelloflavone	2b	
		clusiaphenone B	1o	
		mangostenol	6.3i	
		cratoxylone	6.3k	
		garcinone D	6.3j	
	ripe fruits	dulcisflavan	4j	
		dulcisxanthone B	6.3c	
		camboginol	1b	
		octadecanoic acid-2,3-di(OH)propyl ester	7j	
		1,5,8-tri(OH)-3-(OCH_3)-2-(3-methyl-2-butenyl)xanthone	6.3ss	
		BR-xanthone A	6.3mm	
		mangostin	6.3h	
		morelloflavone	2b	
		mangostenol	6.3i	
		isonormangostin	6.3nn	

Table 1 (Continued)

Scientific name	Investigated part	Compounds	Structures	References
		1,6-di(OH)-7-(OCH_3)-8-(3,7-dimethyl-2,6-octadienyl)-2′,2′-dimethylpyrano[3,2-b]xanthen-9-one	6.3rr	
		tovophyllin A	6.3v	
		betulinic acid	5q	
		kaemferol 3-*O*-β-glucopyranosyl-7-*O*-α-rhamnopyranoside	4c	
		garcinone B	6.3w	
		1,3,6-tri(OH)-7-(OCH_3)-2,5-*bis*(3-methyl-2-butenyl)xanthone	6.3q	
		1,6-di(OH)-7-(OCH_3)-8-(3-methyl-2-butenyl)-2′,2′-dimethylchromeno[5′,6′: 2,3]xanthone	6.3aaa	
		8-desoxygartanin	6.2j	
		gartanin	6.3gg	
		morusignin J	6.3pp	
		apigenin	4h	
		cambogin	1a	
		kaemferol 3,7-di-*O*-α-L-rhamnopyranoside	4d	
		(-)-epicatechin	4i	

Table 1 (Continued)

Scientific name	Investigated part	Compounds	Structures	References
G. griffithii	stem bark	guttiferone I	1n	Nilar, *et al.*, 2005
		cambogin	1a	
		1,7-di(OH)xanthone	6.1c	
		1,3,6,7-tetra(OH)-xanthone	6.3l	
		1,3,5,6-tetra(OH)-xanthone	6.3m	
G. hanburyi	fruits	hanburinone	6.5q	Sukpondma, *et al.*, 2005a
		isomoreollin B	6.5t	
		morellin	6.5r	
		moreollic acid	6.5u	
		morellic acid	6.5s	
G. hombroniana	leaves	garcihombronane B	5d	Rukachaisirikul, *et al.*, 2005b
		garcihombronane C	5e	
		garcihombronane D	5k	
		garcihombronane E	5l	
		garcihombronane F	5f	
		garcihombronane G	5g	
		garcihombronane H	5h	
		garcihombronane I	5i	
		garcihombronane J	5j	
		methyl (25*R*)-3β-(OH)-23-oxo-9,15-lanostadien-26-oate	5m	
		vitexin	4f	
		isovitexin	4g	

Table 1 (Continued)

Scientific name	Investigated part	Compounds	Structures	References
		blumenol C 9-*O*-*β*-D-apiofuranosyl-(1⟶6)-*β*-D-glucopyranoside	7b	
		vomifoliol 9-*O*-*β*-D-apiofuranosyl-(1⟶6)-*β*-D-glucopyranoside	7a	
G. humilis	stem and bark	guttiferone G	1l	Herath, *et al.*, 2005
		guttiferone I	1n	
G. kola	roots	3″,4′,4‴,5,5″,7,7″-hepta(OH)-3,8″-biflavanone	2e	Han, *et al.*, 2005
G. linii	roots	linixanthone A	6.4b	Chen, *et al.*, 2005
		linixanthone B	6.2m	
		linixanthone C	6.2c	
		garcibiphenyl A	3d	
		garcibiphenyl B	3e	
		garcibenzopyran	7f	
		10-O-methylmacluraxanthone	6.3bb	
		rheediachromenoxan-thone	6.2l	
		globulixanthone D	6.2d	
		1,6-di(OH)-5,7-di(OCH_3)xanthone	6.3uu	
		1,5-di(OH)xanthone	6.1b	

Table 1 (Continued)

Scientific name	Investigated part	Compounds	Structures	References
		1,5-di(OH)-3-(OCH_3)-xanthone	6.2e	
		1,6-di(OH)-3,5-di(OCH_3)-xanthone	6.3tt	
		1,6-di(OH)-3,5,7-tri(OCH_3)xanthone	6.4a	
		1,6-di(OH)-5-(OCH_3)-xanthone	6.2f	
		1,6-di(OH)-7-(OCH_3)-xanthone	6.2g	
		1,7-di(OH)xanthone	6.1c	
		5-(OH)-1-(OCH_3)-xanthone	6.1a	
		acuparin	3f	
G. mangostana	heartwood	mangoxanthone	6.3ll	Nilar, *et al.*, 2005
		3′,6-di(OH)-2,4,4′-tri(OCH_3)benzophenone	1p	
		dulxanthone D	6.3b	
		1,3,7-tri(OH)-2-(OCH_3)xanthone	6.3vv	
		1,3,5-tri(OH)-13,13-dimethyl-2H-pyran[7,6-*b*]xanthen-9-one	6.3s	
G. macrophylla	twigs	guttiferone A	1k	Williams, *et al.*, 2005
		guttiferone G	1l	
		friedelin	5p	

Table 1 (Continued)

Scientific name	Investigated part	Compounds	Structures	References
G. nigrolineata	twigs	nigrolineabenzopyran A	7e	Rukachaisirikul, *et al.*, 2005d
		nigrolineabiphenyl A	3b	
		nigrolineabiphenyl B	3c	
		nigrolineaxanthone T	6.3o	
		nigrolineaxanthone U	6.3p	
		nigrolineaxanthone V	6.3u	
		nigrolineaxanthone W	6.3xx	
		dulxanthone A	6.3n	
		nigrolineaxanthone A	6.2p	
		1,3,5-tri(OH)-4-(3-(OH)-3-methylbutyl)xanthone	6.2i	
		forbexanthone	6.3t	
		tovophyllin A	6.3v	
		6-deoxyjacareubin	6.2a	
		morusignin C	6.3oo	
		ananixanthone	6.2b	
		1,5-di(OH)-6′,6′-dimethylpyrano[2′,3′-:3,2]xanthone	6.2r	
		morusignin I	6.3hh	
		rheediaxanthone A	6.3qq	
G. polyantha	stem bark	bangangxanthone A	6.3ff	Lannang, *et al.*, 2005
		bangangxanthone B	6.2s	
		1,5-di(OH)xanthone	6.1b	
		2-(OH)-1,7-di(OCH_3)-xanthone	6.2n	

Table 1 (Continued)

Scientific name	Investigated part	Compounds	Structures	References
		friedelin	5p	
		oleanolic acid	5o	
		lupeol	5n	
G. scortechinii	fruits	scortechinone A	6.5a	Sukpondma,
		scortechinone B	6.5b	*et al.*, 2005b
		scortechinone C	6.5c	
		scortechinone D	6.5d	
		scortechinone E	6.5e	
		scortechinone F	6.5f	
		scortechinone H	6.5g	
		scortechinone I	6.5l	
		scortechinone M	6.5i	
		scortechinone L	6.5h	
		scortechinone P	6.5n	
		scortechinone Q	6.5v	
		scortechinone R	6.5k	
		scortechinone S	6.5o	
		scortechinone T	6.5p	
		scortechinone U	6.2t	
		scortechinone V	6.2u	
		scortechinone W	6.2v	
		scortechinone X	6.6a	
		scortechterpene A	5a	
		scortechterpene B	5b	
		(+)-volkensiflavone	2a	
		(+)-morelloflavone	2b	

Table 1 (Continued)

Scientific name	Investigated part	Compounds	Structures	References
		germacra-4(15),5*E*,-10(14)-trien-1β-ol	5c	
	stem bark	scortechinone A	6.5a	Rukachaisirikul,
		scortechinone B	6.5b	*et al.*, 2005c
		scortechinone D	6.5d	
		scortechinone F	6.5f	
		scortechinone I	6.5l	
		scortechinone J	6.5w	
		scortechinone L	6.5h	
		scortechinone M	6.5i	
		scortechinone N	6.5j	
		scortechinone O	6.5m	
		scortechinone P	6.5n	
		4",5"-dihydro-1,5-di(OH)-6',6'-dimethylpyrano-(2',3':6,7)-4",4",5"-trimethylfurano(2",3"-:3,4)xanthone	6.3ww	
G. smeathmannii	stem bark	smeathxanthone A	6.3zz	Komguem, et
		smeathxanthone B	6.3x	al., 2005
		1,3,5-tri(OH)xanthone	6.2h	
		1,5-di(OH)xanthone	6.1b	
G. xanthochymus	fruits	guttiferone H	1g	Baggett, et al.,
		gambogenone	1h	2005
		aristophenone A	1m	
		xanthochymol	1e	
		guttiferone E	1f	

Table 1 (Continued)

Scientific name	Investigated part	Compounds	Structures	References
		cycloxanthochymol	1d	
		isoxanthochymol	1c	
		alloathyriol	6.3a	
		amentoflavone	2f	
		3,8″-biapigenin	2d	
		(±)-fukugetin	2b	
		(±)-fukugiside	2c	
		(±)-volkensiflavone	2a	

Structures of Compounds Isolated from Plants of the genus *Garcinia*

1. Benzophenones

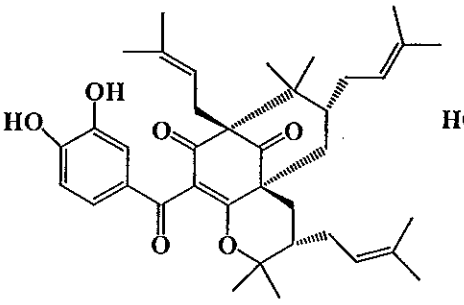

1a: cambogin (isogarcinol)

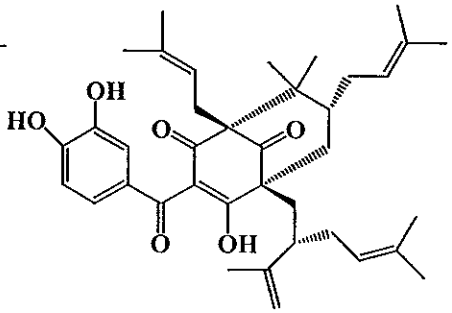

1b: camboginol (garcinol)

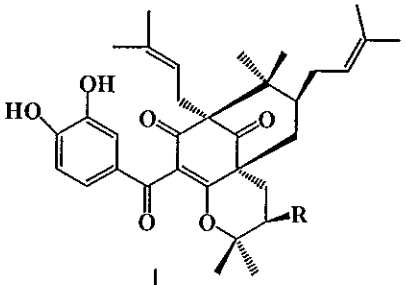

1c: R = : isoxanthochymol

1d: R = : cycloxanthochymol

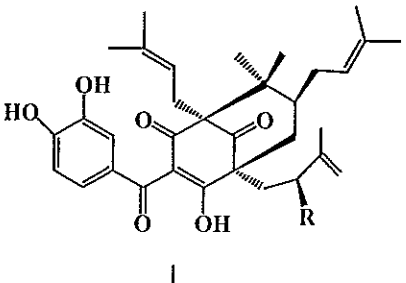

1e: R = : xanthochymol

1f: R = : guttiferone E

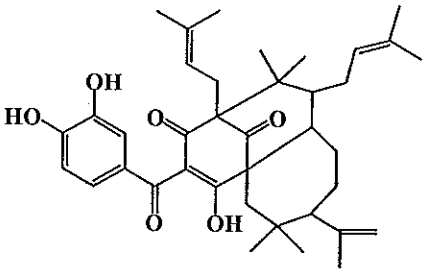

1g: guttiferone H

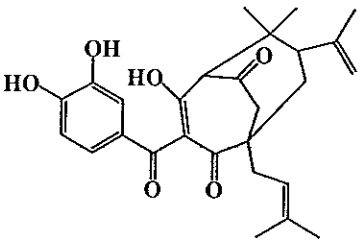

1h: gambogenone

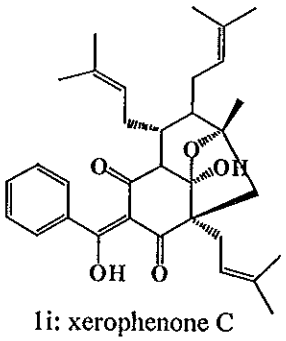

1i: xerophenone C

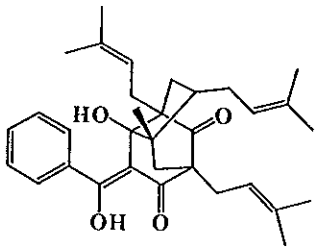

1j: nemorosonol

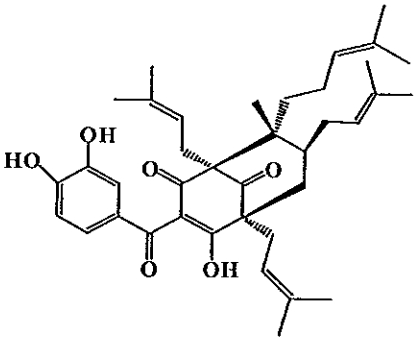

1k: guttiferone A

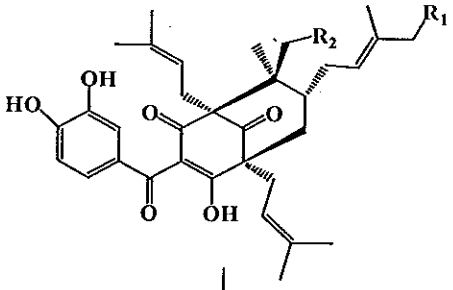

1l: $R_1 = R_2 =$ 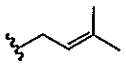 : guttiferone G

1m: $R_1 = R_2 = H$: aristophenone

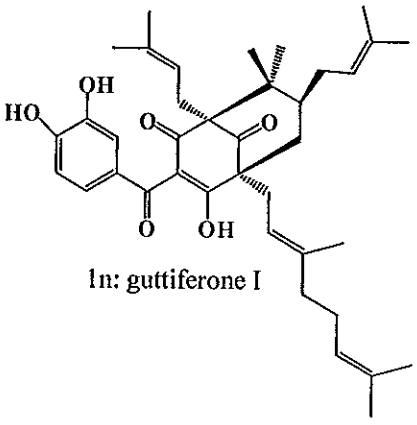

1n: guttiferone I

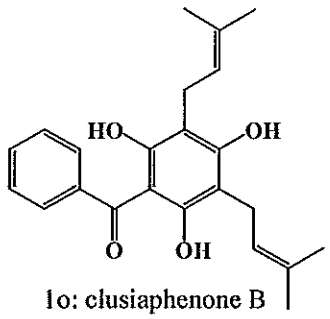

1o: clusiaphenone B

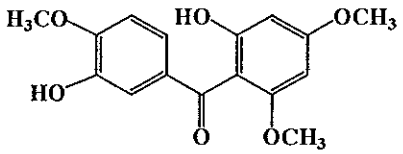

1p: 3',6-di(OH)-2,4,4'-tri(OCH_3)benzophenone

2. Biflavanoids

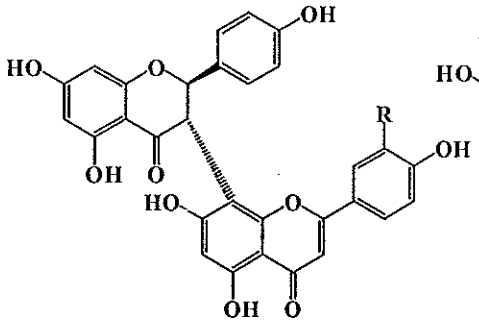

2a: R = H : volkensiflavone

2b: R = OH : morelloflavone (fukugetin)

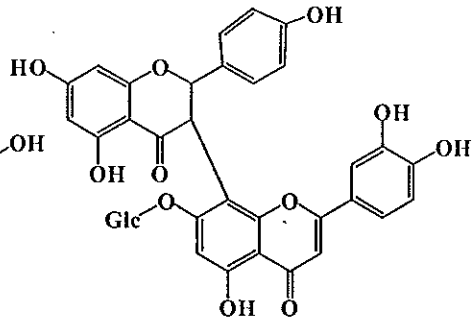

2c: fukugiside

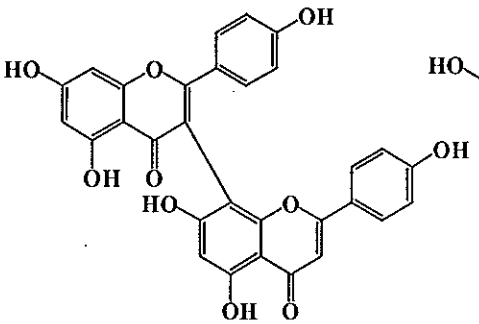

2d: 3,8"-biapigenin

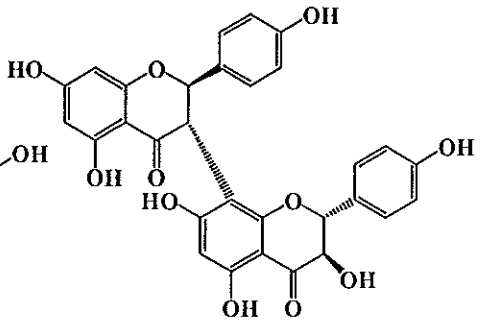

2e: 3",4',4'",5,5",7,7"-hepta(OH)-3,8"-biflavone

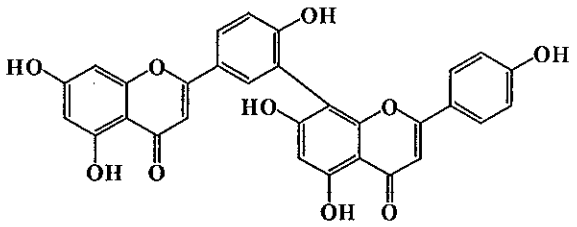

2f: amentoflavone

3. Biphenyls

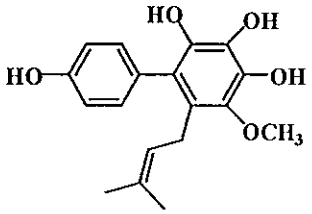

3a: [1,1'-biphenyl]-2-(3-methyl-2-butenyl)-3-(OCH_3)-4,4',5,6-tetraol

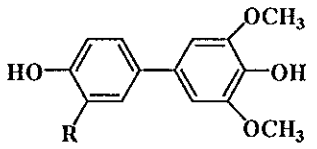

3b: R = OH : nigrolineabiphenyl A

3c: R = OCH_3 : nigrolineabiphenyl B

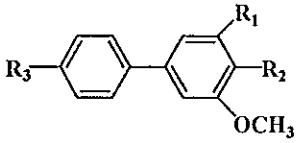

3d: $R_1 = R_3 = OH$, $R_2 = H$: garcibiphenyl A

3e: $R_1 = R_3 = OH$, $R_2 = CH_2CH=C(CH_3)_2$: garcibiphenyl B

3f: $R_1 = OCH_3$, $R_2 = OH$, $R_3 = H$: acuparin

4. Flavanoids

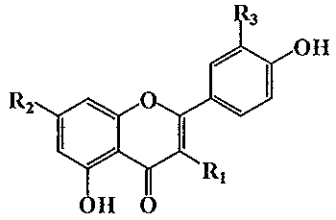

4a: R_1 = O-α-L-rhamnose, R_2 = OH, R_3 = H : kaemferol 3-*O*-α-L-rhamnoside

4b: R_1 = O-α-L-rhamnose, R_2 = R_3 = OH : quercetin 3-*O*-α-L-rhamnoside

4c: R_1 = O-β-D-glucose, R_2 = O-α-L-rhamnose, R_3 = H : kaemferol 3-O-β-D-glucopyranosyl-7-*O*-α-L-rhamnopyranoside

4d: R_1 = R_2 = O-α-L-rhamnose, R_3 = H : kaemferol 3,7-di-*O*-α-L-rhamnopyranoside

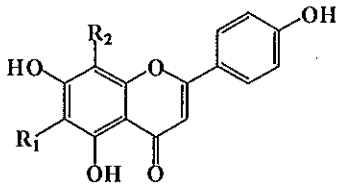

4e: R_1 = β-D-glucose (6 → 1)-α-L-rhamnose, R_2 = H : dulcinoside

4f: R_1 = H, R_2 = β-D-glucose : vitexin

4g: R_1 = β-D-glucose, R_2 = H : isovitexin

4h: R_1 = R_2 = H : apigenin

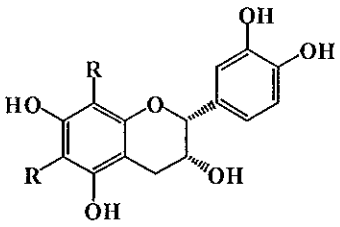

4i: R =H : (-)-epicatechin

4j: R =OH : dulcisflavan

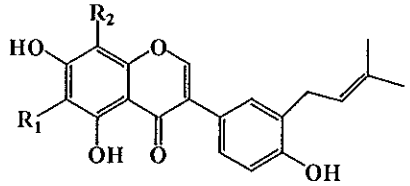

4k: R_1 = 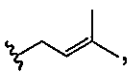 , R_2 = H : lupalbigenin

4l: R_1 = H, R_2 = 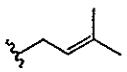 : isolupalbigenin

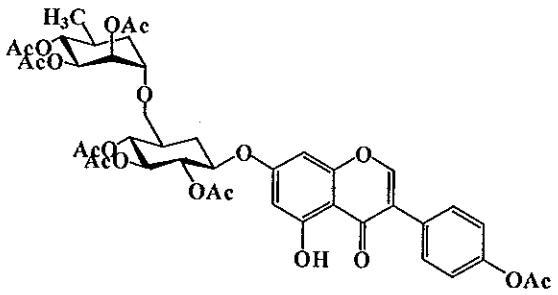

4m: sphaerobioside acetate

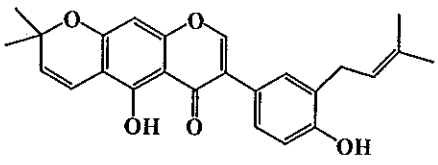

4n: chandalone

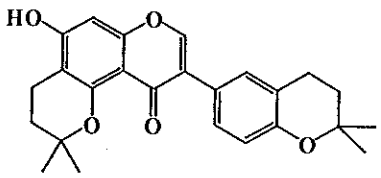

4o: dulcisisoflavone

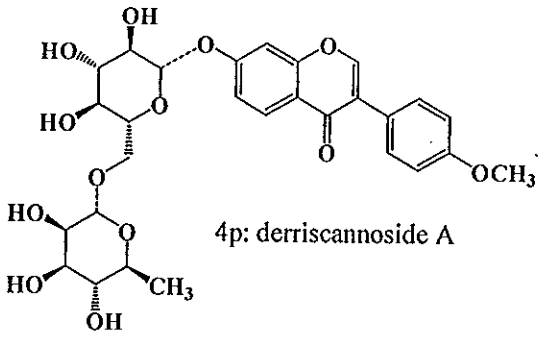

4p: derriscannoside A

5. Terpenoids

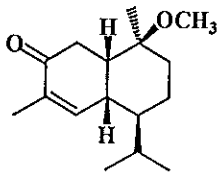

5a: scortechterpene A

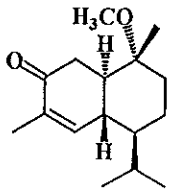

5b: scortechterpene B

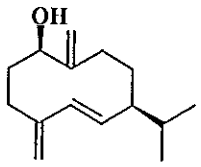

5c: germacra-4(15),5E,-10(14)-trien-1-ol

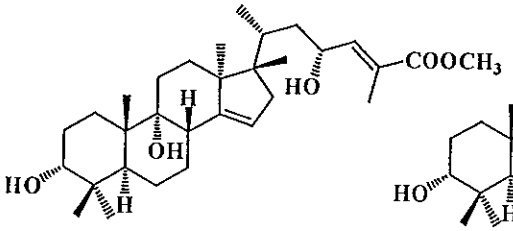

5d: garcihombronane B

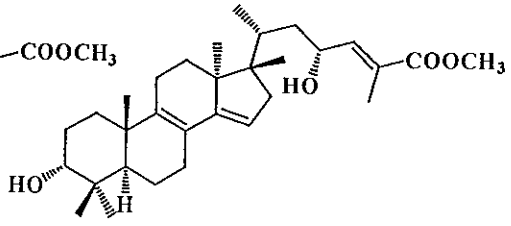

5e: garcihombronane C

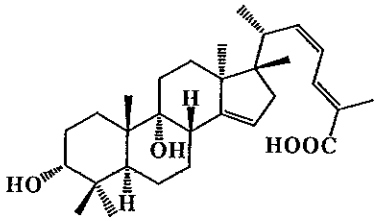

5f: garcihombronane F

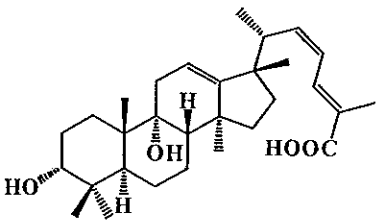

5g: garcihombronane G

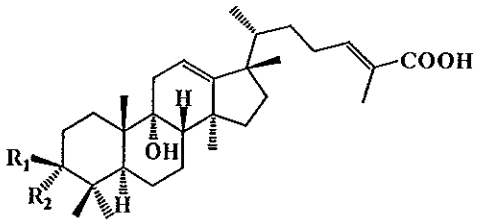

5h: R_1 = H, R_2 = OH : garcihombronane H

5i: R_1 = OH, R_2 = H : garcihombronane I

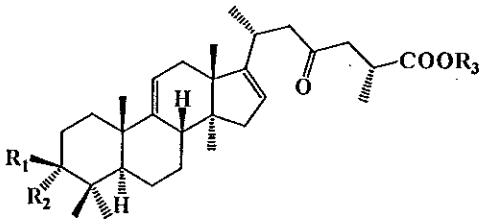

5j: R_1 = H, R_2 = OH, R_3 = CH_3 : garcihombronane J

5k: R_1 = OH, R_2 = R_3 = H : garcihombronane D

5l: R_1 = R_3 = H, R_2 = OH : garcihombronane E

5m: R_1 = OH, R_2 = H, R_3 = CH_3 : methyl (25R)-3β-(OH)-23-oxo-9,15-lanostadien-26-oate

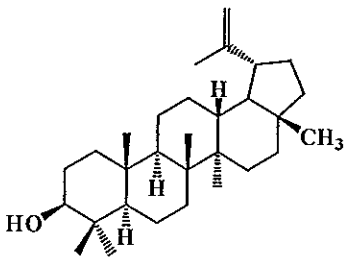

5n: lupeol

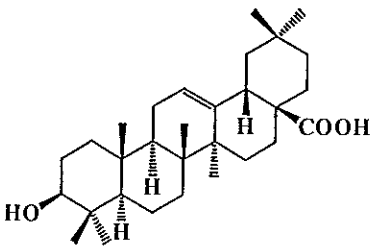

5o: oleanolic acid

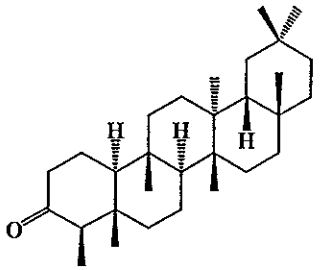

5p: friedelin

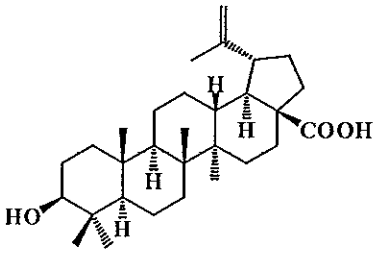

5q: betulinic acid

6. Xanthones

6.1 Dioxygenated xanthones

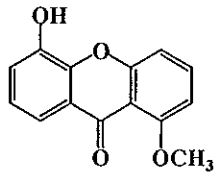

6.1a: 5-(OH)-1-(OCH_3)xanthone

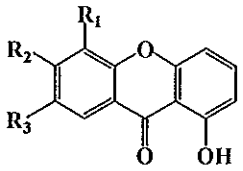

6.1b: R_1 = OH, R_2 = R_3 = H : 1,5-di(OH)xanthone

6.1c: R_1 = R_2 = H, R_3 = OH : 1,7-di(OH)xanthone

6.2 Trioxygenated xanthones

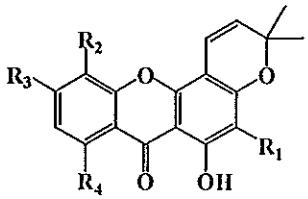

6.2a: R_1 = R_3 = R_4 = H, R_2 = OH : 6-deoxyjacareubin

6.2b: R_1 = 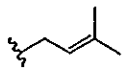 , R_2 = = OH, R_3 = R_4 = H : ananixanthone

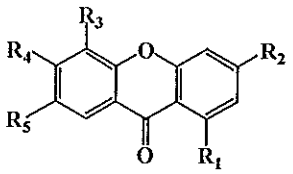

6.2c: R_1 = OH, R_2 = H, R_3 = R_4 = OCH_3, R_5 = 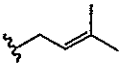 : linixanthone C

6.2d: R_1 = R_4 = OH, R_2 = H, R_3 = OCH_3, R_5 = 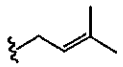 : globulixanthone D

6.2e: R_1 = R_3 = OH, R_2 = OCH_3, R_4 = R_5 = H : 1,5-di(OH)-3-(OCH_3)xanthone

6.2f: R_1 = R_4 = OH, R_2 = R_5 = H, R_3 = OCH_3: 1,6-di(OH)-5-(OCH_3)xanthone

6.2g: R_1 = R_4 = OH, R_2 = R_3 = H, R_5 = OCH_3: 1,6-di(OH)-7-(OCH_3)xanthone

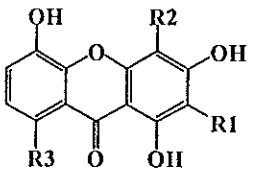

6.2h: R_1 = R_2 = R_3 = H : 1,3,5-tri(OH)xanthone

6.2i: R_1 = R_3 = H, R_2 = 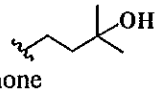 : 1,3,5-tri(OH)-4-(3-(OH)-3-methylbutyl)xanthone

6.2j: R_1 = R_2 = 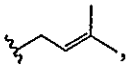 , R_3 = H : 8-desoxygartanin

6.2k: R_1 = 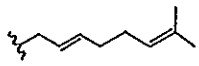 , R_2 = R_3 = H : mangostinone

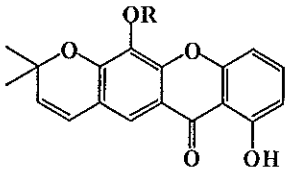

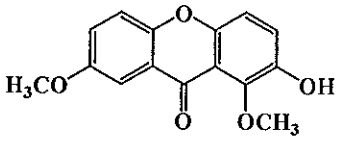

6.2l: R = H : rheediachromenoxanthone

6.2n: 2-(OH)-1,7-di(OCH_3)xanthone

6.2m: R = CH_3 : linixanthone B

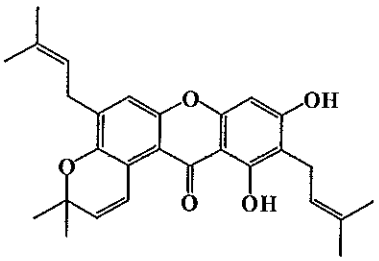

6.2o: dulcisxanthone A

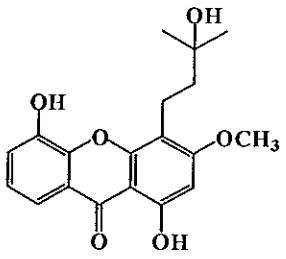

6.2p: nigrolineaxanthone A

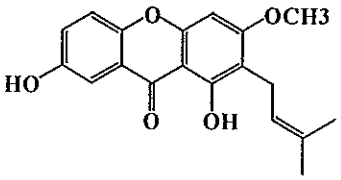

6.2q: 1,7-di(OH)-3-(OCH_3)-2-(3-methyl-2-butenyl)xanthone

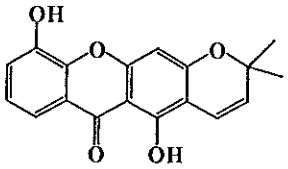

6.2r: 1,5-di(OH)-6',6'-dimethylpyrano[2',3':3,2]xanthone

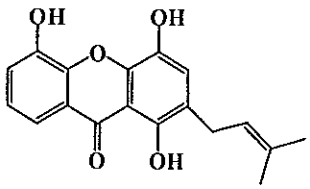

6.2s: bangangxanthone B

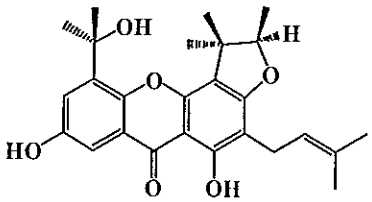

6.2t: scortechinone U

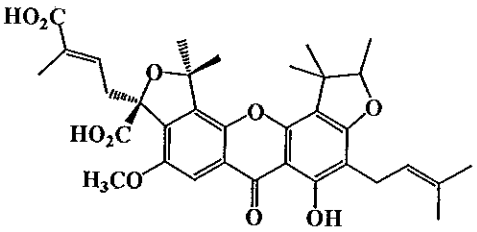

6.2u: scortechinone V

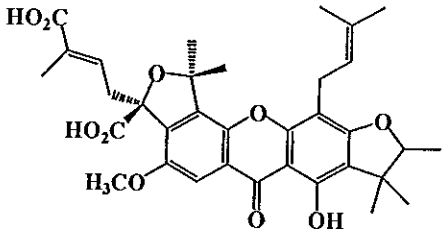

6.2v: scortechinone W

6.3 Tetraoxygenated xanthones

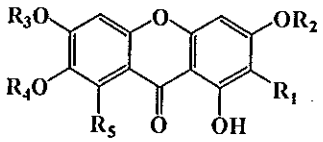

6.3a: $R_1 = R_2 = R_3 = R_5 = H$, $R_4 = CH_3$: alloathyriol

6.3b: $R_1 = R_2 = R_3 = H$; $R_4 = CH_3$, $R_5 =$ 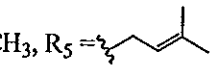 : dulxanthone D

6.3c: $R_1 =$ 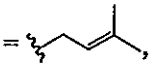 , $R_2 = CH_3$, $R_3 = R_4 = H$, $R_5 =$ 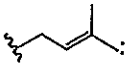 : dulcisxanthone B

6.3d: $R_1 =$ 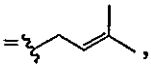 , $R_2 = R_3 = H$, $R_4 = CH_3$, $R_5 =$ 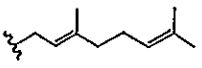
: cowanin

6.3e: $R_1 =$ 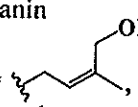 , $R_2 = R_3 = H$, $R_4 = CH_3$, $R_5 =$ 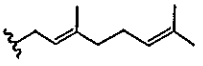
: cowanol

6.3f: $R_1 =$ 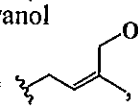 , $R_2 = R_3 = H$, $R_4 = CH_3$, $R_5 =$ 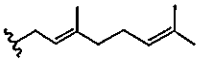
: cowagarcinone E

6.3g: $R_1 =$ 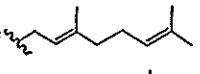 , $R_2 = R_3 = R_5 = H$, $R_4 = CH_3$: cowaxanthone

6.3h: $R_1 = R_5 =$ 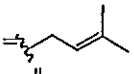 , $R_2 = R_3 = H$, $R_4 = CH_3$: α-mangostin

6.3i: $R_1 =$ 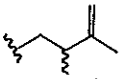 , $R_2 = R_3 = H$, $R_4 = CH_3$, $R_5 =$ 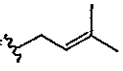 : mangostenol

6.3j: $R_1 =$ 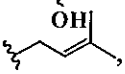 , $R_2 = R_3 = H$, $R_4 = CH_3$, $R_5 =$ 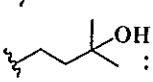 : garcinone D

6.3k: $R_1 =$ 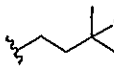 , $R_2 = R_3 = H$, $R_4 = CH_3$, $R_5 =$ 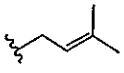 : cratoxylone

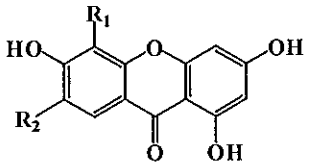

6.3l: R_1 = H, R_2 = OH : 1,3,6,7-tetra(OH)xanthone

6.3m: R_1 = OH, R_2 = H : 1,3,5,6-tetra(OH)xanthone

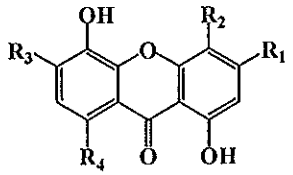

6.3n: R_1 = OCH_3, R_2 = 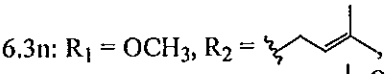 , R_3 = OH, R_4 = H : dulxanthone A

6.3o: R_1 = OCH_3, R_2 = 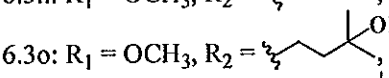 , R_3 = OH, R_4 = H : nigrolineaxanthone T

6.3p: R_1 = R_4 = OH, R_2 = 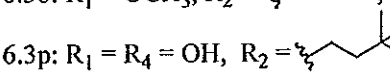 , R_3 = H : nigrolineaxanthone U

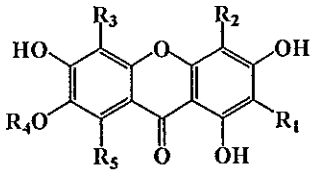

6.3q: R_1 = 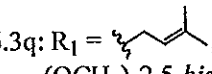 , R_2 = R_5 = H, R_3 = , R_4 = CH_3 : 1,3,6-tri(OH)-7-(OCH_3)-2,5-*bis*(3-methyl-2-butenyl)xanthone

6.3r: R_1 = 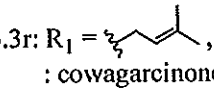 , R_2 = H, R_3 = , R_4 = CH_3, R_5 = : cowagarcinone A

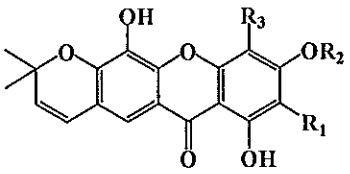

6.3s: R_1 = R_2 = R_3 = H : 1,3,5-tri(OH)-13,13-dimethyl-2H-pyran[7,6-b]xanthen-9-one

6.3t: R_1 = R_3 = H, R_2 = CH_3 : forbexanthone

6.3u: R_1 = H, R_2 = CH_3, R_3 = 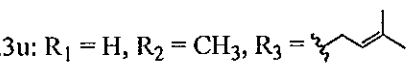 : nigrolineaxanthone V

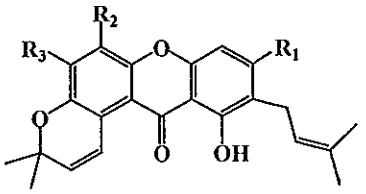

6.3v: $R_1 = R_3 = OH$, R_2 = 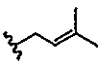 : tovophyllin A

6.3w: $R_1 = R_3 = OH$, $R_2 = H$: garcinone B

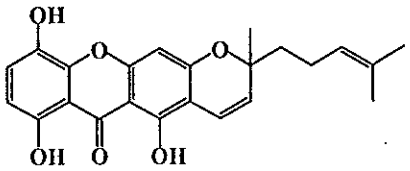

6.3x: smeathxanthone B

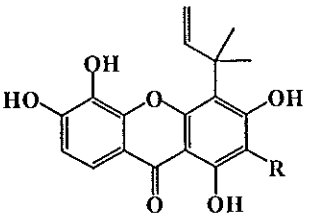

6.3y: R = 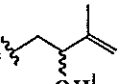 : bracteaxanthone I

6.3z: R = 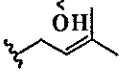 : gerontoxanthone I

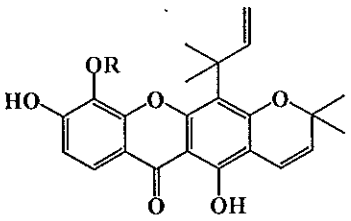

6.3aa: R = H : macluraxanthone

6.3bb: R = CH_3 : 10-*O*-methyl-macluraxanthone

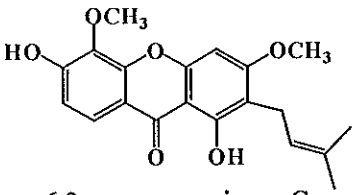

6.3cc: cowagarcinone C

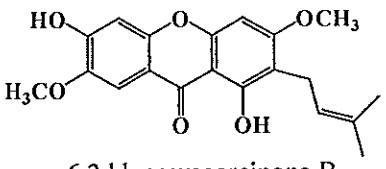

6.3dd: cowagarcinone B

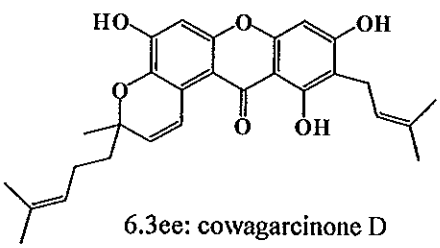

6.3ee: cowagarcinone D

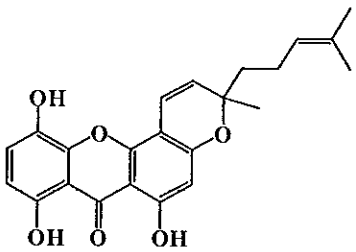

6.3ff: bangangxanthone A

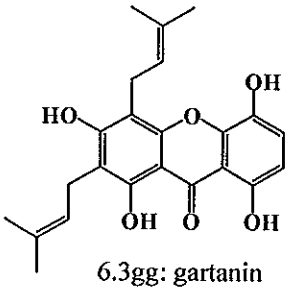

6.3gg: gartanin

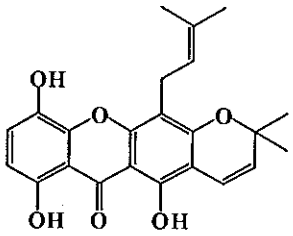

6.3hh: morusignin I

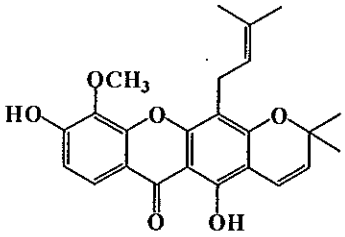

6.3ii: 5-*O*-methylxanthone V_1

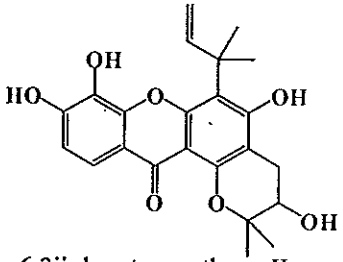

6.3jj: bracteaxanthone II

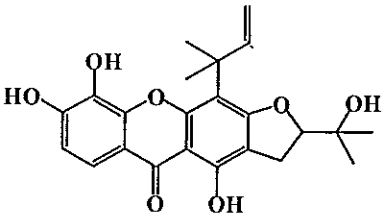

6.3kk: cudraxanthone R

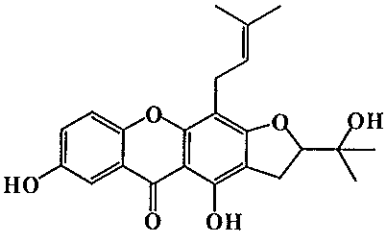

6.3ll: mangoxanthone

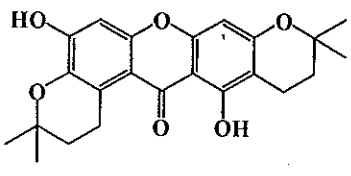

6.3mm: BR-xanthone A

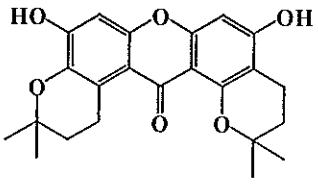

6.3nn: isonormangostin

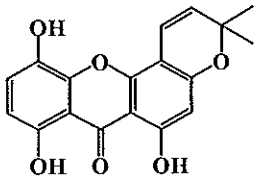

6.3oo: morusignin C

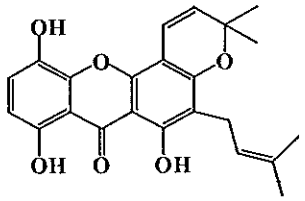

6.3pp: morusignin J

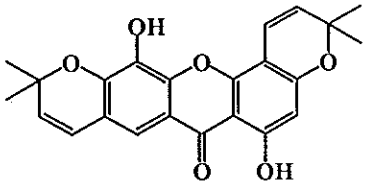

6.3qq: rheediaxanthone A

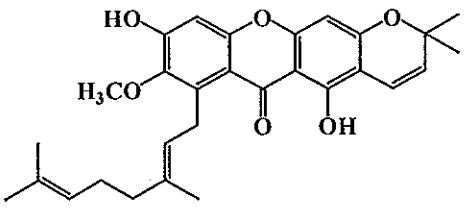

6.3rr: fuscaxanthone A

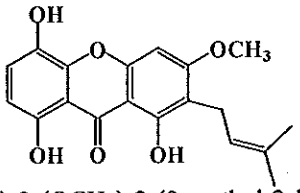

6.3ss: 1,5,8-tri(OH)-3-(OCH_3)-2-(3-methyl-2-butenyl)xanthone

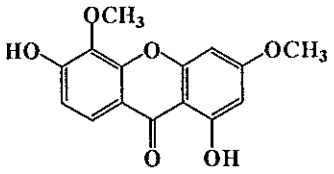

6.3tt: 1,6-di(OH)-3,5-di(OCH_3)xanthone

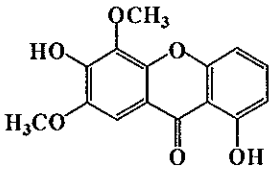

6.3uu: 1,6-di(OH)-5,7-di(OCH_3)xanthone

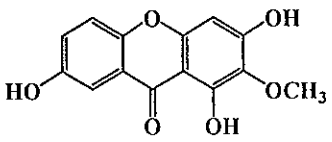

6.3vv: 1,3,7-tri(OH)-2-(OCH_3)xanthone

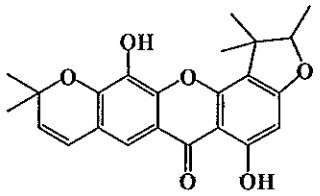

6.3ww: 4",5"-dihydro-1,5-di(OH)-6',6'-dimethylpyrano(2',3':6,7)-4",4",5"-trimethylfurano(2",3":3,4)xanthone

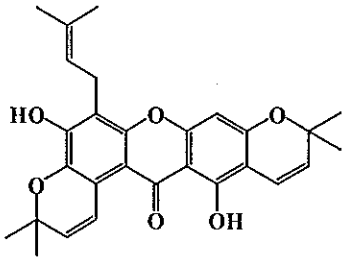

6.3xx: nigrolineaxanthone W

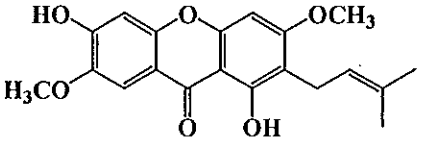

6.3yy: l,6-di(OH)-3,7-di(OCH_3)-2-(3-methyl-2-butenyl)xanthone

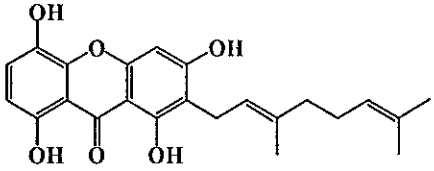

6.3zz: smeathxanthone A

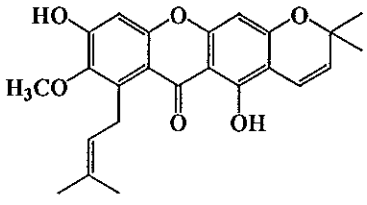

6.3aaa: l,6-di(OH)-7-(OCH_3)-8-(3-methyl-2-butenyl)-2',2'-dimethylchromeno [5',6': 2,3]xanthone

6.4 Pentaoxygenated xanthones

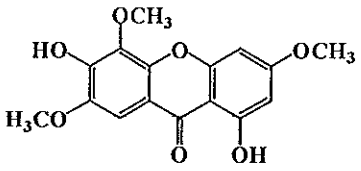

6.4a: 1,6-di(OH)-3,5,7-tri(OCH_3)xanthone

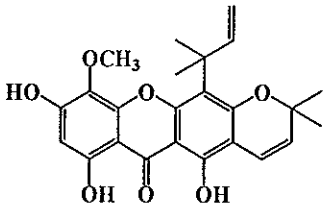

6.4b: linixanthone A

6.5 Caged-polyprenylated xanthones

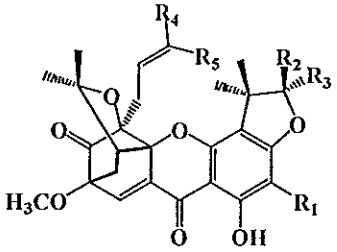

6.5a: R_1 = 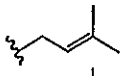 , $R_2 = R_4 = R_5 = CH_3$, R_3 = H : scortechinone A

6.5b: R_1 = 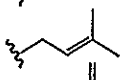 , R_2 = H, $R_3 = R_4 = CH_3$, $R_5 = CO_2H$: scortechinone B

6.5c: R_1 = 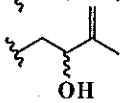 , R_2 = H, $R_3 = R_4 = CH_3$, $R_5 = CO_2H$: scortechinone C

6.5d: $R_1 = R_3$ = H, $R_2 = R_4 = R_5 = CH_3$: scortechinone D

6.5e: $R_1 = R_2$ = H, $R_3 = R_4 = R_5 = CH_3$: scortechinone E

6.5f: R_1 = 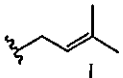 , R_2 = H, $R_3 = R_5 = CH_3$, $R_4 = CO_2H$: scortechinone F

6.5g: R_1 = 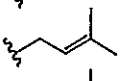 , R_2 = H, $R_3 = R_5 = CH_3$, R_4 = CHO : scortechinone H

6.5h: R_1 = 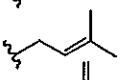 , R_2 = H, $R_3 = R_4 = R_5 = CH_3$: scortechinone L

6.5i: R_1 = 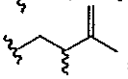 , R_2 = H, $R_3 = R_4 = CH_3$, $R_5 = CO_2H$: scortechinone M

6.5j: R_1 = 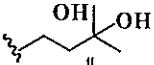 , R_2 = H, $R_3 = R_4 = CH_3$, $R_5 = CO_2H$: scortechinone N

6.5k: R_1 = 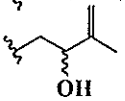 , $R_2 = R_4 = CH_3$, R_3 = H, $R_5 = CO_2H$: scortechinone R

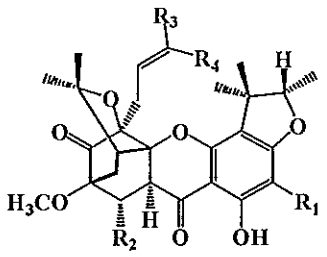

6.5l: R_1 = 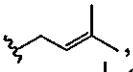 , $R_2 = OCH_3$, $R_3 = CH_3$, $R_4 = CO_2H$: scortechinone I

6.5m: R_1 = 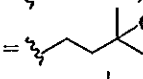 , $R_2 = OCH_3$, $R_3 = CH_3$, $R_4 = CO_2H$: scortechinone O

6.5n: R_1 = 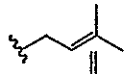 , $R_2 = OH$, $R_3 = CH_3$, $R_4 = CO_2H$: scortechinone P

6.5o: R_1 = 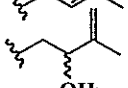 , $R_2 = OCH_3$, $R_3 = CH_3$, $R_4 = CO_2H$: scortechinone S

6.5p: R_1 = 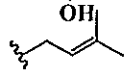 , $R_2 = OCH_3$, $R_3 = CHO$, $R_4 = CH_3$: scortechinone T

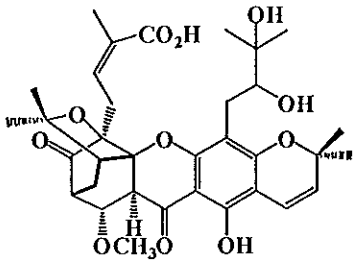

6.5q: hanburinone

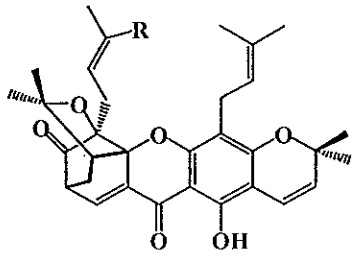

6.5r: R = CHO: morellin

6.5s: R = CO_2H : morellic acid

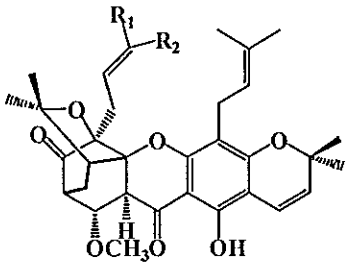

6.5t: R_1 = CHO, $R_2 = CH_3$: isomoreollin B

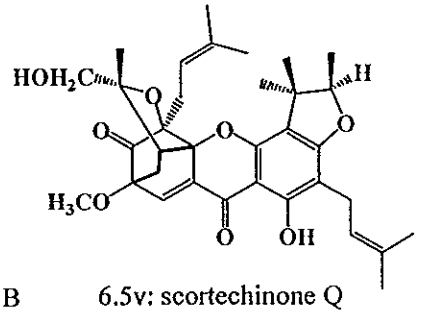

6.5v: scortechinone Q

6.5u: $R_1 = CH_3$, $R_2 = CO_2H$: moreollic acid

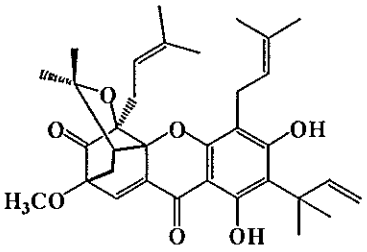

6.5w: scortechinone J

6.6 Rearranged xanthones

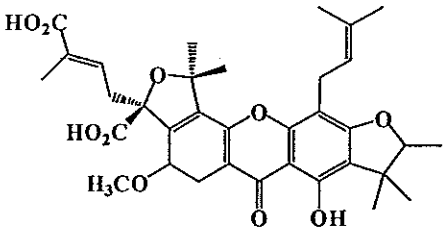

6.6a: scortechinone X

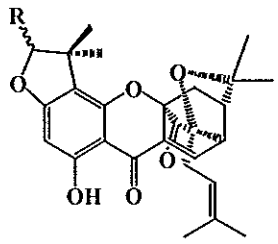

6.6b: R = —CH_3 : neoisobractatin A

6.6c: R = ''''CH_3 : neoisobractatin B

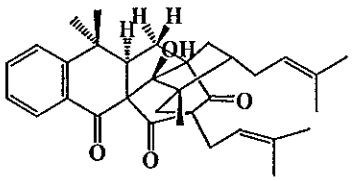

6.6d: garcibracteatone

7. Miscellaneous

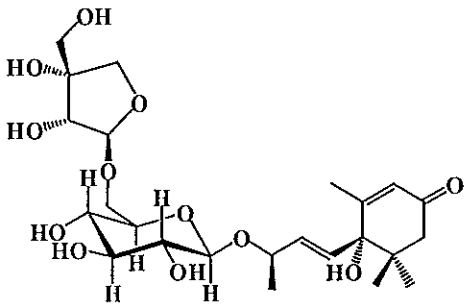

7a: vomifoliol 9-*O*-β-D-apiofuranosyl-(1→6)-β-D-glucopyranoside

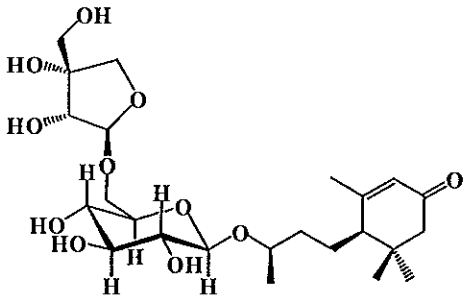

7b: blumenol C 9-*O*-*β*-D-apiofuranosyl-(1→6)-*β*-D-glucopyranoside

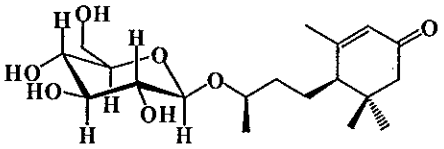

7c: blumenol C *O*-*β*-D-glucoside

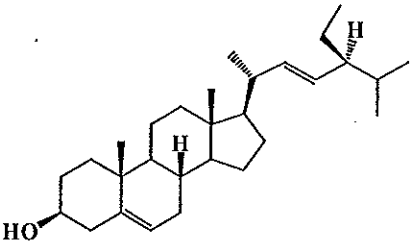

7d: stigmasterol

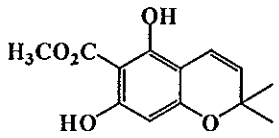

7e: nigrolineabenzopyran A

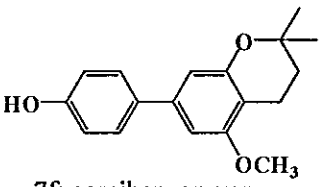

7f: garcibenzopyran

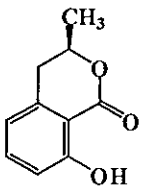

7g: (-)-mellein

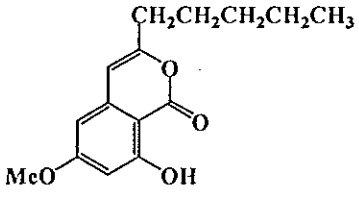

7h: 8-(OH)-6-(OCH$_3$)-3-pentylisocoumarin

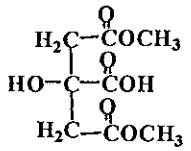

7i: 2-(OH)-1,2,3-propanetricarboxylic acid-1,3-dimethylester

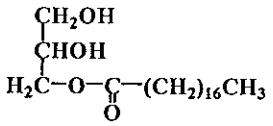

7j: octadecanoic acid-2,3-di(OH) propyl ester

1.3 The Objective

Based on the literature search, phytochemical investigation on the latex (Patthalung, 1988), leaves (Xu, 2000) and bark (Xu, 2001) of *G. parvifolia* resulted in the isolation of ten xanthones and four depsidones which exhibited strong cytotoxic activity (Xu, 2000). We are interested in investigation of its twigs in order to separate additional chemical constituents. This research involved isolation, purification and structure elucidation of chemical constituents from the twigs of *G. parvifolia* which were collected at Trang province.

Structures of Compounds Isolated from *Garcinia parvifolia*

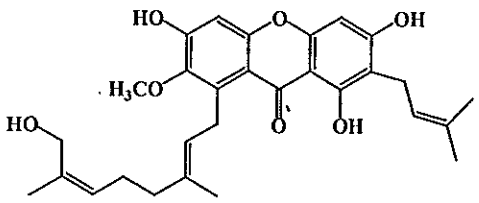

1: parvixanthone A

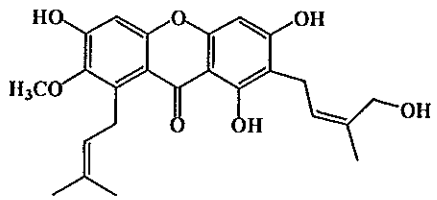

2: parvixanthone B

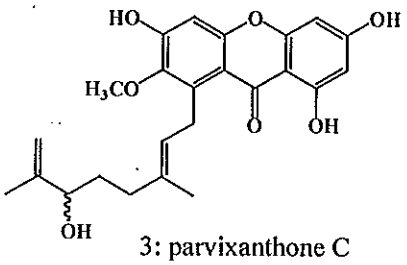

3: parvixanthone C

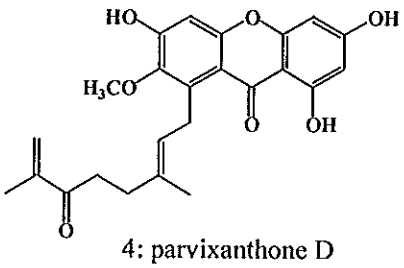

4: parvixanthone D

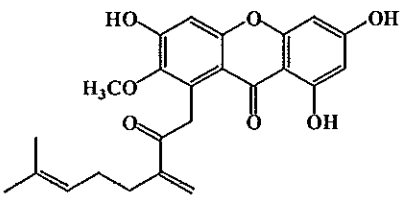

5: parvixanthone E

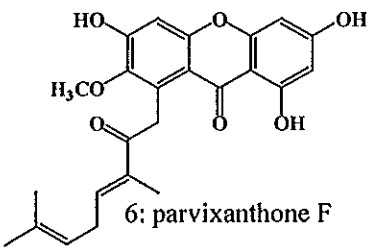

6: parvixanthone F

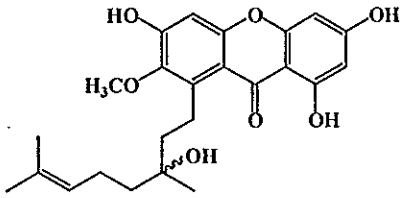

7: parvixanthone G

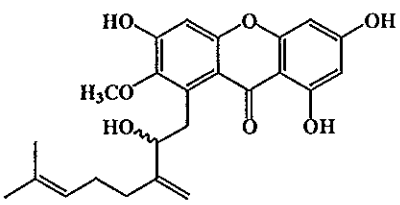

8: parvixanthone H

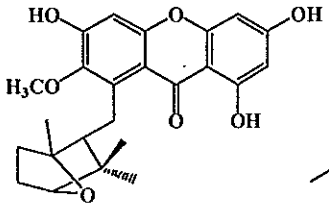

9: parvixanthone I

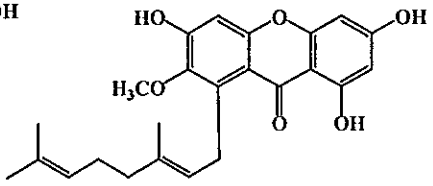

10: rubraxanthone

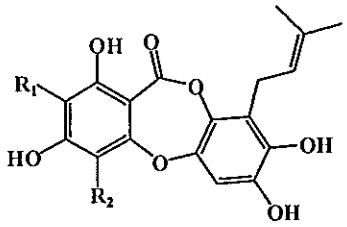

11: $R_1 = R_2 =$ 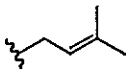 : garcidepsidone A

12: $R_1 =$ 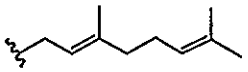 , $R_2 = H$: garcidepsidone B

13: $R_1 =$ 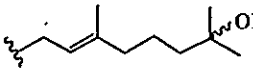 , $R_2 = H$: garcidepsidone C

14: $R_1 =$ 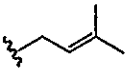 , $R_2 = H$: garcidepsidone D

2. EXPERIMENTAL

2.1 Chemicals and instruments

Melting points were determined on an electrothermal melting point apparatus (Electrothermal 9100) and reported without correction. Infrared spectra (IR) were obtianed on a FTS165 FT-IR spectrometer or a Perkin Elmer Spectrum GX FT-IR system and recorded on wavenumber (cm^{-1}). ^{1}H and ^{13}C-Nuclear magnetic resonance spectra (^{1}H and ^{13}C NMR) were recorded on a FTNMR, Bruker Avance 300 MHz or a Varian UNITY INOVA 500 MHz spectrometer using tetramethylsilane (TMS) as an internal standard. Spectra were recorded as chemical shift parameter (δ) value in ppm down field from TMS (δ 0.00). Ultraviolet spectra (UV) were measured with an UV-160A spectrophotometer (SHIMADSU). Principle bands (λ_{max}) were recorded as wavelengths (nm) and log ε in MeOH solution. Optical rotation was measured in MeOH solution with sodium D line (590 nm) on an AUTOPOL® II automatic polarimeter. Quick column chromatography, thin-layer chromatography (TLC) and precoated thin-layer chromatography were performed on silica gel 60 GF_{254} (Merck) or reverse phase C-18 silica gel. Column chromatography was performed on silica gel (Merck) type 100 (70-230 Mesh ASTM) or reverse phase C-18 silica gel. The solvents for extraction and chromatography were distilled at their boiling point ranges prior to use except for petroleum ether (bp. 40-60°C) and ethyl acetate which were analytical grade reagent.

2.2 Plant material

The twigs of *G. parvifolia* were collected at Trang Province, Thailand. A voucher specimen is deposited in the Herbarium of the Department of Biology, Faculty of Science, Prince of Songkla University, Hat Yai, Songkhla, Thailand.

2.3 Isolation and extraction

The twigs of *G. parvifolia* (2.4 kg), cut into small segments, were extracted with MeOH (12 L) for three times. After filtration, the filtrate was evaporated to dryness under reduced pressure to give a crude MeOH extract as a dark brown gum in 102.5 g.

2.4 Chemical investigation of the crude MeOH extract

The crude extract was primarily tested for its solubility in various solvents at room temperature. The results were demonstrated in **Table 2.**

Table 2 Solubility of the crude extract in various solvents at room temperature

Solvent	Solubility at room temperature
Petroleum ether	-
Chloroform	+ (pale yellow solution)
Ethyl acetate	++ (dark brown solution)
Acetone	++ (red solid in dark brown solution)
MeOH	+++ (dark brown solution)
Water	+ (pale yellow solution)
10% HCl	-
10% NaOH	+++ (dark brown solution)
10% $NaHCO_3$	++ (dark brown solution)

Symbol meaning: + slightly soluble, ++ moderately soluble, +++ well soluble,
- insoluble

The solubility results indicated that the crude extract contained acidic and polar constituents. Chromatogram characteristics on normal phase TLC of the crude extract, using 100%$CHCl_3$ as a mobile phase, showed seven UV-active spots with the R_f values of 0.70, 0.61, 0.54, 0.45, 0.36, 0.21 and 0.16.

Chromatogram characteristics on normal phase TLC of the crude extract, using 100%$CHCl_3$ as a mobile phase, showed clear resolution. Further purification by quick column chromatography over silica gel was performed. Elution was conducted initially with 100%hexane and gradually enriched with chloroform and MeOH until 100%MeOH. Fractions with the similar chromatogram characteristics were combined and evaporated to dryness under reduced pressure to afford eleven subfractions, as shown in **Table 3.**

Table 3 Subfractions obtained from the crude extract by quick column chromatography over silica gel

Fraction	Mobile phase	Weight (mg)	Physical appearance
A	100%Hexane-20%$CHCl_3$/Hexane	264.4	Yellow liguid
B	20%$CHCl_3$/Hexane	299.6	Yellow-brown gum
C	50%$CHCl_3$/Hexane	283.9	Yellow-brown gum
D	70%$CHCl_3$/Hexane-100%$CHCl_3$	1794.8	Red-brown gum
E	0.2-0.7%MeOH/$CHCl_3$	1059.0	Red-brown gum
F	1%MeOH/$CHCl_3$	272.4	Brown-black gum
G	3%MeOH/$CHCl_3$	3203.6	Brown-black gum
H	5%MeOH/$CHCl_3$	604.2	Brown-black gum
I	10%MeOH/$CHCl_3$	3052.3	Brown-black gum
J	20-40%MeOH/$CHCl_3$	1643.4	Brown-black gum
K	40-100%MeOH/$CHCl_3$	3301.9	Brown-black gum

Fraction A Chromatogram characteristics on normal phase TLC with 100%$CHCl_3$ showed no definite spot under UV and ASA reagent. Further investigation was then not carried out.

Fraction B Chromatogram characteristics on normal phase TLC with 100%$CHCl_3$ showed three UV-active spots with the R_f values of 0.75, 0.70 and 0.61. This fraction was separated by column chromatography over silica gel. Elution was conducted initially with 20%$CHCl_3$/Petrol, gradually enriched with $CHCl_3$ and finally with 100%$CHCl_3$. Fractions with the similar chromatogram characteristics were combined

and evaporated to dryness under reduced pressure to afford seven subfractions, as shown in **Table 4.**

Table 4 Subfractions obtained from the fraction B by column chromatography over silica gel

Fraction	Mobile phase	Weight (mg)	Physical appearance
BA	20%$CHCl_3$/Petrol	18.6	Yellow gum
BB	20%$CHCl_3$/Petrol	25.4	Yellow gum
BC	20%$CHCl_3$/Petrol	17.4	Yellow gum
BD	20%$CHCl_3$/Petrol	13.0	Yellow-brown gum
BE	20-30%$CHCl_3$/Petrol	14.6	Yellow-brown gum
BF	40%$CHCl_3$/Petrol	14.9	Yellow-brown gum
BG	40-100%$CHCl_3$/Petrol	82.3	Yellow-brown gum

Fraction BA Chromatogram characteristics on normal phase TLC with 40%$CHCl_3$/Petrol showed no definite spot under UV and ASA reagent. Further investigation was then not carried out.

Fraction BB Chromatogram characteristics on normal phase TLC with 40%$CHCl_3$/Petrol showed three UV-active spots with the R_f values of 0.52, 0.44 and 0.38. This fraction was separated by column chromatography over silica gel. Elution was conducted initially with 2%EtOAc/Petrol, gradually enriched with EtOAc and finally with 45%EtOAc/Petrol. Fractions with the similar chromatogram characteristics were combined and evaporated to dryness under reduced pressure to afford three subfractions, as shown in **Table 5.**

Table 5 Subfractions obtained from the fraction BB by column chromatography over silica gel

Fraction	Mobile phase	Weight (mg)	Physical appearance
BB1	2%EtOAc/Petrol	17.3	Yellow gum
BB2	2%EtOAc/Petrol	6.0	Yellow gum
BB3	2-45%EtOAc/Petrol	0.7	Yellow-brown gum

Fraction BB1 Chromatogram characteristics on normal phase TLC with 2%EtOAc/Petrol showed three UV-active spots with the R_f values of 0.77, 0.63 and 0.44. Because the ^1H NMR data indicated the presence of many compounds, it was not further investigated.

Fraction BB2 Chromatogram characteristics on normal phase TLC with 2%EtOAc/Petrol showed one UV-active spot with the R_f value of 0.38. It was named as **GP1**.

$[\alpha]^{29}_D$	-36.43 (c = 0.06, MeOH)
UV λ_{max}(nm)(MeOH)(log ε)	227 (3.17), 254 (4.39), 262 (4.49), 278 (3.25), 333 (2.82)
FTIR(neat): υ (cm^{-1})	3431, 1668
^1H NMR($CDCl_3$)(δ_{ppm})(300 MHz) :	6.65 (*dd, J* = 10.0 and 0.6 Hz, 1H), 5.96 (*brs*, 1H), 5.41 (*d, J* = 10.0 Hz, 1H), 5.08 (*mt, J* = 7.0 Hz, 1H), 4.03 (*s*, 3H), 2.06 (*m*, 2H), 1.69 (*m*, 2H), 1.66 (*s*, 3H), 1.57 (*s*, 3H), 1.39 (*s*, 3H)
^{13}C NMR($CDCl_3$)(δ_{ppm}) (75 MHz):	169.79, 161.00, 131.83, 124.71, 123.87, 116.43, 102.13, 96.54, 93.37, 80.22, 52.46, 41.65, 27.12, 25.65, 22.61, 17.61
DEPT 90°	CH : 124.71, 123.87, 116.43, 96.54
DEPT 135°	CH_2 : 41.65, 22.61
	CH_3 : 52.46, 27.12, 25.65, 17.61
EIMS (*m/z*) (% rel. int.)	318 (15), 271 (9), 235 (97), 203 (100)

Fraction BB3 Chromatogram characteristics on normal phase TLC with 2%EtOAc/Petrol showed none of well-separated spots under UV and ASA reagent. Because of low quantity, it was not further investigated.

Fraction BC Chromatogram characteristics on normal phase TLC with 40%$CHCl_3$/Petrol showed four UV-active spots with the R_f values of 0.52, 0.44, 0.38 and 0.29. This fraction was separated by column chromatography over silica gel. Elution was conducted initially with 2%EtOAc/Petrol, gradually enriched with EtOAc and finally with 30%EtOAc/Petrol. Fractions with the similar chromatogram

characteristics were combined and evaporated to dryness under reduced pressure to afford four subfractions, as shown in **Table 6.**

Table 6 Subfractions obtained from the fraction BC by column chromatography over silica gel

Fraction	Mobile phase	Weight (mg)	Physical appearance
BC1	2%EtOAc/Petrol	1.4	Yellow gum
BC2	2%EtOAc/Petrol	8.3	Yellow gum
BC3	2%EtOAc/Petrol	3.3	Yellow-brown gum
BC4	2-30%EtOAc/Petrol	3.6	Yellow-brown gum

Fraction BC1 Chromatogram characteristics on normal phase TLC with 2%EtOAc/Petrol showed no definite spot under UV and ASA reagent. Further investigation was then not carried out.

Fraction BC2 Chromatogram characteristics on normal phase TLC with 2%EtOAc/Petrol showed two UV-active spots with the R_f values of 0.54 and 0.42. Because the ^1H NMR data indicated the presence of many compounds, it was not further investigated.

Fraction BC3 Chromatogram characteristics on normal phase TLC with 2%EtOAc/Petrol showed one UV-active spot with the R_f value of 0.38. The ^1H NMR data indicated the presence of **GP1** as a major component. Further investigation was then not carried out.

Fraction BC4 Chromatogram characteristics on normal phase TLC with 2%EtOAc/Petrol showed one UV-active spot with the R_f value of 0.23. It was named as **GP2.**

UV λ_{max}(nm)(MeOH)(log ε) 223 (4.36), 268 (4.15), 317 (3.40)

FTIR(neat): υ (cm^{-1}) 3433, 1662

^1H NMR($CDCl_3$)(δ_{ppm})(300 MHz) : 6.07 (*s*, 1H), 5.16 (*mt*, J = 6.9 Hz, 1H), 5.07 (*mt*, J = 6.9 Hz, 1H), 4.03 (*s*, 3H), 3.83 (*s*, 3H), 3.26 (*d*, J = 6.9 Hz, 2H), 2.00 (*m*, 4H), 1.76 (*s*, 3H), 1.64 (*s*, 3H), 1.58 (*s*, 3H)

^{13}C NMR($CDCl_3$)(δ_{ppm})(75 MHz):	169.97, 164.15, 160.80, 158.60, 134.82, 131.37, 124.48, 122.53, 109.00, 93.50, 91.57, 55.62, 52.41, 39.79, 26.75, 25.67, 21.46, 17.66, 16.04
DEPT 90°	CH : 124.48, 122.53, 91.57
DEPT 135°	CH_2 : 39.79, 26.75, 21.46
	CH_3 : 55.62, 52.41, 25.67, 17.66, 16.04
EIMS (*m/z*) (% rel. int.)	334 (4), 264 (8), 233 (46), 219 (21), 211 (69), 179 (100)

Fraction BD Chromatogram characteristics on normal phase TLC with 40%$CHCl_3$/Petrol showed four UV-active spots with the R_f values of 0.52, 0.44, 0.38 and 0.28. The ^{1}H NMR data indicated the presence of many compounds. Therefore, it was not further investigated.

Fraction BE Chromatogram characteristics on normal phase TLC with 40%$CHCl_3$/Petrol showed one UV-active spot with the R_f value of 0.36. The ^{1}H NMR data indicated the presence of many compounds. Thus, it was not further investigated.

Fraction BF Chromatogram characteristics on normal phase TLC with 40%$CHCl_3$/Petrol showed three UV-active spots with the R_f values of 0.38, 0.25 and 0.11. The ^{1}H NMR data indicated the presence of many compounds. Therefore, it was not further investigated.

Fraction BG Chromatogram characteristics on normal phase TLC with 40%$CHCl_3$/Petrol showed none of well-separated spots under UV and ASA reagent. It was not further investigated.

Fraction C Chromatogram characteristics on normal phase TLC with 40%$CHCl_3$/Petrol showed four UV-active spots with the R_f values of 0.61, 0.54, 0.50 and 0.45. This fraction was separated by column chromatography over silica gel. Elution was conducted initially with 3%EtOAc/Petrol, gradually enriched with EtOAc and finally with 50%EtOAc/Petrol. Fractions with the similar chromatogram characteristics were combined and evaporated to dryness under reduced pressure to afford six subfractions, as shown in **Table 7**.

Table 7 Subfractions obtained from the fraction C by column chromatography over silica gel

Fraction	Mobile phase	Weight (mg)	Physical appearance
CA	3%EtOAc/Petrol	18.3	Yellow gum
CB	3%EtOAc/Petrol	20.2	Yellow gum
CC	3%EtOAc/Petrol	12.4	Yellow-brown gum
CD	3-10%EtOAc/Petrol	16.3	Yellow-brown gum
CE	10-50%EtOAc/Petrol	46.2	Yellow-brown gum
CF	20-50%EtOAc/Petrol	92.1	Yellow-brown gum

Fraction CA Chromatogram characteristics on normal phase TLC with 3%EtOAc/Petrol showed two UV-active spots with the R_f values of 0.48 and 0.41. The ^1H NMR data indicated the presence of **GP3** as a major component. Further investigation was then not carried out.

Fraction CB Chromatogram characteristics on normal phase TLC with 3%EtOAc/Petrol showed one UV-active spot with the R_f value of 0.41. The ^1H NMR data indicated the presence of **GP4** as a major component. Further investigation was then not carried out.

Fraction CC Chromatogram characteristics on normal phase TLC with 3%EtOAc/Petrol showed two UV-active spots with the R_f values of 0.41 and 0.30. This fraction was separated by column chromatography over silica gel. Elution was conducted initially with 2%EtOAc/Petrol, gradually enriched with EtOAc and finally with 30%EtOAc/Petrol. Fractions with the similar chromatogram characteristics were combined and evaporated to dryness under reduced pressure to afford four subfractions, as shown in **Table 8.**

Table 8 Subfractions obtained from the fraction CC by column chromatography over silica gel

Fraction	Mobile phase	Weight (mg)	Physical appearance
CC1	2%EtOAc/Petrol	0.3	Yellow gum
CC2	2%EtOAc/Petrol	2.4	Yellow gum
CC3	2%EtOAc/Petrol	9.5	Yellow-brown gum
CC4	2-30%EtOAc/Petrol	9.5	Yellow-brown gum

Fraction CC1 Chromatogram characteristics on normal phase TLC with 3%EtOAc/Petrol showed no definite spot under UV and ASA reagent. Further investigation was then not carried out.

Fraction CC2 Chromatogram characteristics on normal phase TLC with 3%EtOAc/Petrol showed one UV-active spot with the R_f value of 0.41. Because the ^1H NMR data indicated the presence of many compounds, it was not further investigated.

Fraction CC3 Chromatogram characteristics on normal phase TLC with 3%EtOAc/Petrol showed one UV-active spot with the R_f value of 0.41. The ^1H NMR data indicated the presence of **GP4** as a major component. Further investigation was then not carried out.

Fraction CC4 Chromatogram characteristics on normal phase TLC with 3%EtOAc/Petrol showed none of well-separated spots under UV and ASA reagent. It was not further investigated.

Fraction CD Chromatogram characteristics on normal phase TLC with 3%EtOAc/Petrol showed three UV-active spots with the R_f values of 0.41, 0.30 and 0.25. Because the ^1H NMR data indicated the presence of many compounds, it was not further investigated.

Fraction CE Chromatogram characteristics on normal phase TLC with 3%EtOAc/Petrol showed two UV-active spots with the R_f values of 0.25 and 0.19. This fraction was separated by column chromatography over silica gel. Elution was conducted initially with 15%$CHCl_3$/Petrol, gradually enriched with $CHCl_3$ and finally with 25%$CHCl_3$/Petrol. Fractions with the similar chromatogram characteristics were

combined and evaporated to dryness under reduced pressure to afford three subfractions, as shown in **Table 9**.

Table 9 Subfractions obtained from the fraction CE by column chromatography over silica gel

Fraction	Mobile phase	Weight (mg)	Physical appearance
CE1	15%$CHCl_3$/Petrol	20.3	Yellow gum
CE2	15-25%$CHCl_3$/Petrol	14.5	Yellow gum
CE3	25%$CHCl_3$/Petrol	14.3	Yellow-brown gum

Fraction CE1 Chromatogram characteristics on normal phase TLC with 3%EtOAc/Petrol showed no definite spot under UV and ASA reagent. Further investigation was then not carried out.

Fraction CE2 Chromatogram characteristics on normal phase TLC with 3%EtOAc/Petrol showed two UV-active spots with the R_f values of 0.25 and 0.19. Because the ^1H NMR data indicated the presence of many compounds, it was not further investigated.

Fraction CE3 Chromatogram characteristics on normal phase TLC with 3%EtOAc/Petrol showed none of well-separated spots under UV and ASA reagent. It was not further investigated.

Fraction CF Chromatogram characteristics on normal phase TLC with 3%EtOAc/Petrol showed none of well-separated spots under UV and ASA reagent. It was not further investigated.

Fraction D Chromatogram characteristics on normal phase TLC with 100%$CHCl_3$ showed six UV-active spots with the R_f values of 0.71, 0.70, 0.61, 0.50, 0.45 and 0.32. This fraction was separated by column chromatography over Sephadex LH 20. Elution was conducted with 100%MeOH. Fractions with the similar chromatogram characteristics were combined and evaporated to dryness under reduced pressure to afford five subfractions, as shown in **Table 10**.

Table 10 Subfractions obtained from the fraction D by column chromatography over Sephadex LH 20

Fraction	Weight (mg)	Physical appearance
DA	4.0	Yellow gum
DB	1492.4	Yellow gum
DC	66.2	Yellow-brown gum
DD	15.3	Yellow-brown gum
DE	4.7	Yellow-brown gum

Fraction DA Chromatogram characteristics on normal phase TLC with 50%$CHCl_3$/Petrol showed no definite spot under UV and ASA reagent. Further investigation was then not carried out.

Fraction DB Chromatogram characteristics on normal phase TLC with 50%$CHCl_3$/Petrol showed four UV-active spots with the R_f values of 0.65, 0.44, 0.23 and 0.15. This fraction was separated by column chromatography over silica gel. Elution was conducted initially with 40%$CHCl_3$/Petrol, gradually enriched with $CHCl_3$ and finally with 100%$CHCl_3$. Fractions with the similar chromatogram characteristics were combined and evaporated to dryness under reduced pressure to afford six subfractions, as shown in **Table 11.**

Table 11 Subfractions obtained from the fraction DB by column chromatography over silica gel

Fraction	Mobile phase	Weight (mg)	Physical appearance
DB1	40%$CHCl_3$/Petrol	43.7	Yellow gum
DB2	40%$CHCl_3$/Petrol	72.4	Yellow gum
DB3	40%$CHCl_3$/Petrol	12.3	Yellow gum
DB4	50%$CHCl_3$/Petrol	70.3	Yellow-brown gum
DB5	60-80%$CHCl_3$/Petrol	294.3	Yellow-brown gum
DB6	100%$CHCl_3$	277.3	Yellow-brown gum

Fraction DB1 Chromatogram characteristics on normal phase TLC with 40%$CHCl_3$/Petrol showed none of well-separated spots under UV and ASA

reagent. Because the ^{1}H NMR data indicated the presence of many compounds, it was not further investigated.

Fraction DB2 Chromatogram characteristics on normal phase TLC with 40%$CHCl_3$/Petrol showed two UV-active spots with the R_f values of 0.58 and 0.35. The ^{1}H NMR data indicated the presence of **GP4** as a major component. Further investigation was then not carried out.

Fraction DB3 Chromatogram characteristics on normal phase TLC with 40%$CHCl_3$/Petrol showed two UV-active spots with the R_f values of 0.49 and 0.29. Because the ^{1}H NMR data indicated the presence of many compounds, it was not further investigated.

Fraction DB4 Chromatogram characteristics on normal phase TLC with 40%$CHCl_3$/Petrol showed three UV-active spots with the R_f values of 0.40, 0.35 and 0.20. This fraction was separated by flash column chromatography over silica gel. Elution was conducted with 4%Acetone/Petrol. Fractions with the similar chromatogram characteristics were combined and evaporated to dryness under reduced pressure to afford five subfractions, as shown in **Table 12.**

Table 12 Subfractions obtained from the fraction DB4 by flash column chromatography over silica gel

Fraction	Weight (mg)	Physical appearance
DB41	2.2	Yellow gum
DB42	8.5	Colorless gum
DB43	4.8	Yellow gum
DB44	20.1	Yellow gum
DB45	12.0	Yellow-brown gum

Fraction DB41 Chromatogram characteristics on normal phase TLC with 2%Acetone/Petrol showed no definite spot under UV and ASA reagent. Further investigation was then not carried out.

Fraction DB42 Chromatogram characteristics on normal phase TLC with 2%Acetone/Petrol showed one UV-active spot with the R_f value of 0.27. It was named as **GP4.**

$[\alpha]^{29}_D$	+53.02 (c = 0.16, MeOH)
UV λ_{max}(nm)(MeOH)(log ε)	207 (4.24), 226 (3.11), 301 (3.10)
FTIR(neat):υ (cm^{-1})	3431
^{1}H NMR($CDCl_3$)(δ_{ppm})(300 MHz) :	5.14 (*m*, 1H), 5.10 (*m*, 2H), 4.44 (*brs*, 1H), 2.32 (*m*, 1H), 2.20 (*s*, 3H), 2.19 (*s*, 3H), 2.11 (*m*, 3H), 2.07 (*m*, 4H), 2.00 (*m*, 4H), 1.68 (*m*, 2H), 1.68 (*s*, 3H), 1.60 (*brs*, 3H), 1.59 (*m*, 2H), 1.59 (*s*, 6H), 1.26 (*s*, 3H)
^{13}C NMR($CDCl_3$)(δ_{ppm}) (75 MHz):	145.86, 144.72, 135.20, 134.97, 131.24, 126.89, 124.39, 124.24, 124.18, 122.22, 117.28, 115.17, 74.96, 39.82, 39.72, 31.27, 26.76, 26.65, 25.69, 23.83, 22.20, 20.62, 17.68, 16.00, 15.85, 12.25, 11.98
DEPT 90°	CH : 124.39, 124.24, 124.18
DEPT 135°	CH_2 : 39.82, 39.72, 31.27, 26.76, 26.65, 22.20, 20.62
	CH_3 : 25.69, 23.83, 17.68, 16.00, 15.85, 12.25, 11.98
EIMS (*m/z*) (% rel. int.)	426 (3), 410 (15), 322 (7), 191 (10), 151 (30), 135 (13), 123 (16), 109 (21), 97 (25), 95 (27), 83 (28), 81 (42), 69 (100), 57 (53)

Fraction DB43 Chromatogram characteristics on normal phase TLC with 2%Acetone/Petrol showed three UV-active spots with the R_f values of 0.27, 0.17 and 0.12. Because the ^{1}H NMR data indicated the presence of many compounds, it was not further investigated.

Fraction DB44 Chromatogram characteristics on normal phase TLC with 2%Acetone/Petrol showed one UV-active spot with the R_f value of 0.12. It was named as **GP3**.

$[\alpha]^{29}_D$	-3.21 (c = 0.27, MeOH)
UV λ_{max}(nm)(MeOH)(log ε)	208 (4.23), 227 (3.14), 298 (3.09)
FTIR(neat):υ (cm^{-1})	3420

^{1}H NMR($CDCl_3$)(δ_{ppm})(300 MHz) :		6.36 (*brs*, 1H), 5.12 (*m*, 3H), 4.35 (*brs*, 1H), 2.67 (*t*, *J* = 6.6 Hz, 2H), 2.13 (*s*, 6H), 2.12 (*m*, 2H), 2.07 (*m*, 6H), 1.96 (*m*, 2H), 1.75 (*m*, 2H), 1.68 (*s*, 3H), 1.66 (*m*, 1H), 1.61 (*s*, 3H), 1.60 (*s*, 3H), 1.58 (*s*, 3H), 1.54 (*m*, 1H), 1.26 (*s*, 3H)
^{13}C NMR($CDCl_3$)(δ_{ppm}) (75 MHz):		146.28, 145.70, 135.09, 134.96, 131.25, 125.82, 124.42, 124.36, 124.21, 121.65, 118.24, 112.16, 75.23, 39.80, 39.72, 31.44, 26.77, 26.61, 25.69, 24.01, 22.29, 17.68, 16.00, 15.89, 11.90, 11.85
DEPT 90°	CH :	124.42, 124.36, 124.21, 112.16
DEPT 135°	CH_2 :	39.80, 39.72, 31.44, 26.77, 26.61, 22.29
	CH_3 :	25.69, 24.01, 17.68, 16.00, 15.89, 11.90, 11.85
EIMS (*m/z*) (% rel. int.)		410 (56), 206 (9), 191 (17), 151 (100), 69 (53)

Fraction DB45 Chromatogram characteristics on normal phase TLC with 2%Acetone/Petrol showed none of well-separated spots under UV and ASA reagent. It was not further investigated.

Fraction DB5 Chromatogram characteristics on normal phase TLC with 40%$CHCl_3$/Petrol showed none of well-separated spots under UV and ASA reagent. It was not further investigated.

Fraction DB6 Chromatogram characteristics on normal phase TLC with 40%$CHCl_3$/Petrol showed no definite spot under UV and ASA reagent. Further investigation was then not carried out.

Fraction DC Chromatogram characteristics on normal phase TLC with 50%$CHCl_3$/Petrol showed one UV-active spot with the R_f value of 0.15. Because the ^{1}H NMR data indicated the presence of many compounds, it was not further investigated.

Fraction DD Chromatogram characteristics on normal phase TLC with 50%$CHCl_3$/Petrol showed two UV-active spots with the R_f values of 0.15 and 0.12. Because the ^{1}H NMR data indicated the presence of many compounds, it was not further investigated.

Fraction DE Chromatogram characteristics on normal phase TLC with 50%$CHCl_3$/Petrol showed none of well-separated spots under UV and ASA reagent. Because of low quantity, it was not further investigated.

Fraction E Chromatogram characteristics on normal phase TLC with 100%$CHCl_3$ showed six UV-active spots with the R_f values of 0.71, 0.70, 0.54, 0.45, 0.36 and 0.26. This fraction was separated by column chromatography over Sephadex LH 20. Elution was conducted with 100%MeOH. Fractions with the similar chromatogram characteristics were combined and evaporated to dryness under reduced pressure to afford six subfractions, as shown in **Table 13.**

Table 13 Subfractions obtained from the fraction E by column chromatography over Sephadex LH 20

Fraction	Weight (mg)	Physical appearance
EA	4.7	Yellow gum
EB	170.2	Yellow gum
EC	390.6	Yellow gum
ED	210.7	Yellow-brown gum
EE	3.0	Yellow-brown gum
EF	3.1	Yellow-brown gum

Fraction EA Chromatogram characteristics on normal phase TLC with 50%$CHCl_3$/Petrol showed no definite spot under UV and ASA reagent. Further investigation was then not carried out.

Fraction EB Chromatogram characteristics on normal phase TLC with 50%$CHCl_3$/Petrol showed three UV-active spots with the R_f values of 0.25, 0.15 and 0.09. Because the ^1H NMR data indicated the presence of many compounds, it was not further investigated.

Fraction EC Chromatogram characteristics on normal phase TLC with 50%$CHCl_3$/Petrol showed two UV-active spots with the R_f values of 0.21 and 0.15. This fraction was separated by column chromatography over silica gel. Elution was conducted initially with 2%EtOAc/Petrol, gradually enriched with EtOAc and finally

with 100%EtOAc. Fractions with the similar chromatogram characteristics were combined and evaporated to dryness under reduced pressure to afford five subfractions, as shown in **Table 14.**

Table 14 Subfractions obtained from the fraction EC by column chromatography over silica gel

Fraction	Mobile phase	Weight (mg)	Physical appearance
EC1	2%EtOAc/Petrol	9.3	Yellow gum
EC2	2-4%EtOAc/Petrol	96.9	Yellow gum
EC3	4-10%EtOAc/Petrol	107.1	Yellow gum
EC4	10-15%EtOAc/Petrol	73.3	Yellow-brown gum
EC5	15-100%EtOAc/Petrol	27.4	Yellow-brown gum

Fraction EC1 Chromatogram characteristics on normal phase TLC with 5%EtOAc/Petrol showed no definite spot under UV and ASA reagent. Further investigation was then not carried out.

Fraction EC2 Chromatogram characteristics on normal phase TLC with 5%EtOAc/Petrol showed three UV-active spots with the R_f values of 0.77, 0.59 and 0.31. This fraction was separated by column chromatography over silica gel. Elution was conducted with 30%$CHCl_3$/Petrol. Fractions with the similar chromatogram characteristics were combined and evaporated to dryness under reduced pressure to afford three subfractions, as shown in **Table 15.**

Table 15 Subfractions obtained from the fraction EC2 by column chromatography over silica gel

Fraction	Weight (mg)	Physical appearance
EC21	3.5	Yellow gum
EC22	12.9	Yellow gum
EC23	43.2	Yellow gum

Fraction EC21 Chromatogram characteristics on normal phase TLC with 40%$CHCl_3$/Petrol showed no definite spot under UV and ASA reagent. Further investigation was then not carried out.

Fraction EC22 Chromatogram characteristics on normal phase TLC with 40%$CHCl_3$/Petrol showed one major UV-active spot with the same R_f value as **GP4**. Further investigation was then not carried out.

Fraction EC23 Chromatogram characteristics on normal phase TLC with 40%$CHCl_3$/Petrol showed one major UV-active spot with the same R_f value as **GP3**. Further investigation was then not carried out.

Fraction EC3 Chromatogram characteristics on normal phase TLC with 5%EtOAc/Petrol showed two UV-active spots with the R_f values of 0.31 and 0.24. This fraction was separated by column chromatography over silica gel. Elution was conducted with 30%$CHCl_3$/Petrol. Fractions with the similar chromatogram characteristics were combined and evaporated to dryness under reduced pressure to afford two subfractions, as shown in **Table 16**.

Table 16 Subfractions obtained from the fraction EC3 by column chromatography over silica gel

Fraction	Weight (mg)	Physical appearance
EC31	41.3	Yellow gum
EC32	22.4	Colorless gum

Fraction EC31 Chromatogram characteristics on normal phase TLC with 40%$CHCl_3$/Petrol showed no definite spot under UV and ASA reagent. Further investigation was then not carried out.

Fraction EC32 Chromatogram characteristics on normal phase TLC with 40%$CHCl_3$/Petrol showed one UV-active spot with the R_f value of 0.30. It was named as **GP5**.

$[\alpha]^{28}_D$ +26.24 (c = 0.31, MeOH)

UV λ_{max}(nm)(MeOH)(log ε) 206 (4.17), 223 (3.21), 297 (2.41)

FTIR(neat):υ (cm^{-1})	3387
^{1}H NMR($CDCl_3$)(δ_{ppm})(300 MHz) :	6.47 (*d*, *J* = 2.7 Hz, 1H), 6.37 (*d*, *J* = 2.7 Hz, 1H), 5.11 (*m*, 3H), 2.69 (*t*, *J* = 6.6 Hz, 2H), 2.12 (*m*, 2H), 2.12 (*s*, 3H), 2.07 (*m*, 2H), 2.01 (*m*, 2H), 1.97 (*m*, 4H), 1.76 (*m*, 2H), 1.69 (*m*, 1H), 1.68 (*s*, 3H), 1.60 (*s*, 3H), 1.59 (*s*, 3H), 1.58 (*s*, 3H), 1.53 (*m*, 1H), 1.26 (*s*, 3H)
^{13}C NMR($CDCl_3$)(δ_{ppm}) (75 MHz):	147.75, 145.99, 135.13, 134.97, 131.25, 127.36, 124.42, 124.31, 121.25, 115.66, 112.61, 75.34, 39.71, 39.69, 31.38, 26.77, 26.60, 25.69, 24.03, 22.49, 22.18, 17.68, 16.04, 16.00, 15.87
DEPT 90°	CH : 124.42, 124.31, 115.66, 112.61
DEPT 135°	CH_2 : 39.71, 39.69, 31.38, 26.77, 26.60, 22.49, 22.18
	CH_3 : 25.69, 24.03, 17.68, 16.04, 16.00, 15.87
EIMS (*m/z*) (% rel. int.)	396 (100), 177 (16), 137 (19), 83 (20), 81 (23), 69 (32)

Fraction EC4 Chromatogram characteristics on normal phase TLC with 5%EtOAc/Petrol showed two UV-active spots with the R_f values of 0.15 and 0.13. Because the ^{1}H NMR data indicated the presence of many compounds, it was not further investigated.

Fraction EC5 Chromatogram characteristics on normal phase TLC with 5%EtOAc/Petrol showed none of well-separated spots under UV and ASA reagent. It was not further investigated.

Fraction ED Chromatogram characteristics on normal phase TLC with 50%$CHCl_3$/Petrol showed three UV-active spots with the R_f values of 0.38, 0.29 and 0.19. This fraction was separated by column chromatography over Sephadex LH 20. Elution was conducted with 100%MeOH. Fractions with the similar chromatogram characteristics were combined and evaporated to dryness under reduced pressure to afford four subfractions, as shown in **Table 17.**

Table 17 Subfractions obtained from the fraction ED by column chromatography over Sephadex LH 20

Fraction	Weight (mg)	Physical appearance
ED1	38.6	Yellow gum
ED2	18.3	Yellow gum
ED3	12.9	Yellow gum
ED4	34.3	Yellow-brown gum

Fraction ED1 Chromatogram characteristics on normal phase TLC with 40%$CHCl_3$/Petrol showed one major UV-active spot with the same R_f value as **GP5**. Further investigation was then not carried out.

Fraction ED2 Chromatogram characteristics on normal phase TLC with 40%$CHCl_3$/Petrol showed two UV-active spots with the R_f values of 0.30 and 0.17. Further purification was performed by precoated TLC, using 3%EtOAc/Petrol as a mobile phase (9 runs), to afford two bands.

Band 1 was obtained as a yellow gum in 3.0 mg. Chromatogram characteristics on normal phase TLC with 3%EtOAc/Petrol showed one UV-active spot with the R_f value of 0.30. The ^1H NMR data indicated the presence of many compounds. Because of low quantity, it was not further investigated.

Band 2 was obtained as a yellow gum in 4.3 mg. Chromatogram characteristics on normal phase TLC with 3%EtOAc/Petrol showed one UV-active spot with the R_f value of 0.17. It was named as **GP6**.

$[\alpha]^{28}_D$	-21.15 (c = 0.07, MeOH)
UV λ_{max}(nm)(MeOH)(log ε)	232 (4.16), 272 (4.37), 311 (2.32)
FTIR(neat): υ (cm^{-1})	3430, 1662
^1H NMR($CDCl_3$)(δ_{ppm})(300 MHz) :	6.00 (*s*, 1H), 5.12 (*mt*, *J* = 7.2 Hz, 1H), 4.73 (*t*, *J* = 8.7 Hz, 1H), 4.03 (*s*, 3H), 3.03 (*d*, *J* = 8.7 Hz, 2H), 2.11 (*m*, 2H), 1.68 (*s*, 3H), 1.63 (*s*, 3H), 1.60 (*m*, 2H), 1.29 (*s*, 3H)

^{13}C NMR($CDCl_3$)(δ_{ppm}) (75 MHz): 169.82, 167.06, 132.20, 124.03, 105.08, 93.00, 91.01, 90.83, 73.70, 52.36, 36.68, 26.65, 25.66, 22.72, 21.93, 17.65

DEPT 90° CH : 124.03, 91.01, 90.83

DEPT 135° CH_2 : 36.68, 26.65, 21.93

CH_3 : 52.36, 25.66, 22.72, 17.65

EIMS (*m/z*) (% rel. int.) 336 (43), 279 (15), 251 (19), 210 (61), 209 (43), 178 (36), 177 (38), 167 (24), 149 (100), 109 (22), 97 (20), 83 (21), 69 (32), 57 (34)

Fraction ED3 Chromatogram characteristics on normal phase TLC with 40%$CHCl_3$/Petrol showed one major UV-active spot with the same R_f value as **GP7**. Further investigation was then not carried out.

Fraction ED4 Chromatogram characteristics on normal phase TLC with 40%$CHCl_3$/Petrol showed none of well-separated spots under UV and ASA reagent. It was not further investigated.

Fraction EE Chromatogram characteristics on normal phase TLC with 50%$CHCl_3$/Petrol showed one UV-active spot with the R_f value of 0.11. It was named as **GP7**.

UV λ_{max}(nm)(MeOH)(log ε) 224 (4.38), 271 (4.20), 315 (3.42)

FTIR(neat):υ (cm^{-1}) 3433, 1660

^{1}H NMR($CDCl_3$)(δ_{ppm})(300 MHz) : 6.00 (*brs*, 1H), 5.99 (*s*, 1H), 5.23 (*mt*, J = 7.2 Hz, 1H), 5.05 (*mt*, J = 6.9 Hz, 1H), 4.04 (*s*, 3H), 3.35 (*d*, J = 7.2 Hz, 2H), 2.07 (*m*, 4H), 1.80 (*s*, 3H), 1.67 (*s*, 3H), 1.59 (*s*, 3H)

^{13}C NMR($CDCl_3$)(δ_{ppm}) (75 MHz): 169.98, 162.31, 138.72, 131.96, 123.79, 121.69, 105.98, 96.03, 93.71, 52.43, 39.70, 26.39, 25.64, 21.64, 17.67, 16.16

DEPT 90° CH : 123.79, 121.69, 96.03

DEPT 135° CH_2 : 39.70, 26.39, 21.64

CH_3 : 52.43, 25.64, 17.67, 16.16

EIMS (*m/z*) (% rel. int.) 320 (9), 219 (100), 197 (39), 165 (25), 69 (20)

Fraction EF Chromatogram characteristics on normal phase TLC with 50%$CHCl_3$/Petrol showed none of well-separated spots under UV and ASA reagent. It was not further investigated.

Fraction F Chromatogram characteristics on normal phase TLC with 100%$CHCl_3$ showed three UV-active spots with the R_f values of 0.45, 0.39 and 0.32. This fraction was separated by column chromatography over Sephadex LH 20. Elution was conducted with 100%MeOH. Fractions with the similar chromatogram characteristics were combined and evaporated to dryness under reduced pressure to afford five subfractions, as shown in **Table 18.**

Table 18 Subfractions obtained from the fraction F by column chromatography over Sephadex LH 20

Fraction	Weight (mg)	Physical appearance
FA	4.3	Yellow gum
FB	57.6	Yellow gum
FC	10.4	Yellow gum
FD	18.3	Yellow-brown gum
FE	24.2	Yellow-brown gum

Fraction FA Chromatogram characteristics on normal phase TLC with 50%$CHCl_3$/Petrol showed no definite spot under UV and ASA reagent. Further investigation was then not carried out.

Fraction FB Chromatogram characteristics on normal phase TLC with 50%$CHCl_3$/Petrol showed six UV-active spots with the R_f values of 0.41, 0.37, 0.19, 0.16, 0.15 and 0.09. Therefore, it was not further investigated.

Fraction FC Chromatogram characteristics on normal phase TLC with 50%$CHCl_3$/Petrol showed three UV-active spots with the R_f values of 0.21, 0.11 and 0.10. Thus, it was not further investigated.

Fraction FD Chromatogram characteristics on normal phase TLC with 50%$CHCl_3$/Petrol showed three UV-active spots with the R_f values of 0.16, 0.13 and 0.08. The ^1H NMR data indicated the presence of **GP7** as a major component. Further investigation was then not carried out.

Fraction FE Chromatogram characteristics on normal phase TLC with 50%$CHCl_3$/Petrol showed none of well-separated spots under UV and ASA reagent. It was not further investigated.

Fraction G Chromatogram characteristics on normal phase TLC with 100%$CHCl_3$ showed eight UV-active spots with the R_f values of 0.70, 0.45, 0.39, 0.32, 0.27, 0.21, 0.16 and 0.07. This fraction was separated by column chromatography over silica gel. Elution was conducted initially with 100%CH_2Cl_2, gradually enriched with MeOH and finally with 100%MeOH. Fractions with the similar chromatogram characteristics were combined and evaporated to dryness under reduced pressure to afford eight subfractions, as shown in **Table 19**.

Table 19 Subfractions obtained from the fraction G by column chromatography over silica gel

Fraction	Mobile phase	Weight (mg)	Physical appearance
GA	100%CH_2Cl_2	297.3	Yellow gum
GB	100%CH_2Cl_2	203.0	Yellow gum
GC	100%CH_2Cl_2	182.8	Yellow gum
GD	100%CH_2Cl_2	52.1	Yellow-brown gum
GE	100%CH_2Cl_2	238.3	Yellow-brown gum
GF	5-10%CH_2Cl_2/MeOH	148.2	Yellow-brown gum
GG	10-25%CH_2Cl_2/MeOH	834.1	Yellow-brown gum
GH	25-100%CH_2Cl_2/MeOH	108.7	Yellow-brown gum

Fraction GA Chromatogram characteristics on normal phase TLC with 100%CH_2Cl_2 showed many UV-active spots. Therefore, it was not further investigated.

Fraction GB Chromatogram characteristics on normal phase TLC with 100%CH_2Cl_2 showed three UV-active spots with the R_f values of 0.47, 0.39 and 0.22.

This fraction was separated by column chromatography over Sephadex LH 20. Elution was conducted with 100%MeOH. Fractions with the similar chromatogram characteristics were combined and evaporated to dryness under reduced pressure to afford six subfractions, as shown in **Table 20.**

Table 20 Subfractions obtained from the fraction GB by column chromatography over Sephadex LH 20

Fraction	Weight (mg)	Physical appearance
GB1	72.1	Yellow gum
GB2	44.3	Yellow gum
GB3	9.4	Yellow gum
GB4	33.4	Yellow-brown gum
GB5	51.3	Yellow-brown gum
GB6	7.0	Yellow-brown gum

Fraction GB1 Chromatogram characteristics on normal phase TLC with 80%$CHCl_3$/Petrol showed no definite spot under UV and ASA reagent. Further investigation was then not carried out.

Fraction GB2 Chromatogram characteristics on normal phase TLC with 80%$CHCl_3$/Petrol showed two UV-active spots with the R_f values of 0.33 and 0.22. The ^1H NMR data indicated the presence of **GP5** as a major component. Further investigation was then not carried out.

Fraction GB3 Chromatogram characteristics on normal phase TLC with 80%$CHCl_3$/Petrol showed no definite spot under UV and ASA reagent. Further investigation was then not carried out.

Fraction GB4 Chromatogram characteristics on normal phase TLC with 80%$CHCl_3$/Petrol showed one major UV-active spot with the same R_f as **GP7.** Further investigation was then not carried out.

Fraction GB5 Chromatogram characteristics on normal phase TLC with 80%$CHCl_3$/Petrol showed two UV-active spots with the R_f values of 0.33 and 0.21. This fraction was separated by column chromatography over silica gel. Elution was conducted initially with 10%EtOAc/Petrol, gradually enriched with EtOAc and

finally with 100%EtOAc. Fractions with the similar chromatogram characteristics were combined and evaporated to dryness under reduced pressure to afford five subfractions, as shown in **Table 21.**

Table 21 Subfractions obtained from the fraction GB5 by column chromatography over silica gel

Fraction	Mobile phase	Weight (mg)	Physical appearance
GB51	10%EtOAc/Petrol	4.6	Yellow gum
GB52	10%EtOAc/Petrol	9.2	Yellow gum
GB53	10%EtOAc/Petrol	4.5	Yellow gum
GB54	10-30%EtOAc/Petrol	17.9	Yellow-brown gum
GB55	30-100%EtOAc/Petrol	8.5	Yellow-brown gum

Fraction GB51 Chromatogram characteristics on normal phase TLC with 10%Acetone/Petrol showed no definite spot under UV and ASA reagent. Further investigation was then not carried out.

Fraction GB52 Chromatogram characteristics on normal phase TLC with 10%Acetone/Petrol showed one UV-active spot with the R_f value of 0.28. It was named as **GP8.**

UV λ_{max}(nm)(MeOH)(log ε) 236 (4.19), 254 (4.48), 285 (3.65), 328 (3.60)

FTIR(neat): υ (cm^{-1}) 3410, 1644

^{1}H NMR($CDCl_3$)(δ_{ppm})(300 MHz) : 13.12 (*s*, 1H), 7.60 (*s*, 1H), 6.37 (*s*, 1H), 6.12 (*s*, 1H), 5.61 (*s*, 1H), 5.35 (*mt*, J = 7.5 Hz, 1H), 5.22 (*brs*, 1H), 3.91 (*s*, 3H), 3.49 (*d*, J = 5.7 Hz, 2H), 3.42 (*d*, J = 7.5 Hz, 2H), 1.85 (*s*, 3H), 1.77 (*s*, 3H), 1.76 (*s*, 3H), 1.71 (*s*, 3H)

^{13}C NMR($CDCl_3$)(δ_{ppm}) (75 MHz): 180.69, 163.62, 162.17, 153.77, 147.75, 143.76, 134.34, 131.67, 130.14, 125.36, 122.89, 121.08, 117.10, 113.34, 107.31, 102.99, 94.36, 56.07, 28.39, 25.83, 25.63, 21.72, 17.86

DEPT 90° CH : 122.89, 121.08, 117.10, 94.39

DEPT 135° CH_2 : 28.39, 21.72

CH_3 : 56.07, 25.83, 25.63, 17.86

EIMS (*m/z*) (% rel. int.) 410 (29), 394 (32), 376 (57), 354 (23), 294 (100), 251 (29), 234 (33), 219 (57), 203 (81), 197 (37), 177 (36), 165 (79), 149 (63), 85 (53), 71 (73), 69 (78)

Fraction GB53 Chromatogram characteristics on normal phase TLC with 10%Acetone/Petrol showed no definite spot under UV and ASA reagent. Further investigation was then not carried out.

Fraction GB54 Chromatogram characteristics on normal phase TLC with 10%Acetone/Petrol showed showed one UV-active spot with the R_f value of 0.22. It was named as **GP9**.

UV λ_{max}(nm)(MeOH)(log ε) 256 (4.46), 286 (3.68), 329 (3.60)

FTIR(neat): υ (cm^{-1}) 3346, 1641

^{1}H NMR($CDCl_3$)(δ_{ppm})(300 MHz) : 13.32 (*s*, 1H), 7.58 (*s*, 1H), 6.43 (*s*, 1H), 6.15 (*brs*, 1H), 5.67 (*brs*, 1H), 5.34 (*mt*, J = 7.5 Hz, 1H), 5.28 (*mt*, J = 7.2 Hz, 1H), 5.25 (*mt*, J = 6.6 Hz, 1H), 3.52 (*d*, J = 6.6 Hz, 2H), 3.46 (*d*, J = 7.2 Hz, 2H), 3.41 (*d*, J = 7.5 Hz, 2H), 1.85 (*s*, 6H), 1.78 (*d*, J = 1.2 Hz, 3H), 1.77 (*s*, 3H), 1.75 (*s*, 3H), 1.73 (*s*, 3H)

^{13}C NMR($CDCl_3$)(δ_{ppm}) (75 MHz): 180.68, 160.34, 158.62, 152.56, 147.69, 143.67, 135.83, 134.39, 133.50, 130.08, 125.27, 122.33, 121.40, 121.09, 117.11, 113.38, 108.94, 105.22, 102.91, 28.47, 25.87, 25.84, 25.70, 22.02, 21.63, 17.95, 17.86

DEPT 90° CH : 122.33, 121.40, 121.09, 117.11

DEPT 135° CH_2 : 28.47, 22.02, 21.63

CH_3 : 25.87, 25.84, 25.70, 17.95, 17.86

EIMS (*m/z*) (% rel. int.) 464 (58), 463 (50), 446 (25), 420 (36), 409 (50), 408 (46), 394 (37), 352 (68), 336 (25), 308 (26), 297 (31), 149 (44), 85 (55), 71 (79)

Fraction GB55 Chromatogram characteristics on normal phase TLC with 10%Acetone/Petrol showed none of well-separated spots under UV and ASA reagent. It was not further investigated.

Fraction GB6 Chromatogram characteristics on normal phase TLC with 80%$CHCl_3$/Petrol showed none of well-separated spots under UV and ASA reagent. It was not further investigated.

Fraction GC Chromatogram characteristics on normal phase TLC with 100%CH_2Cl_2 showed four UV-active spots with the R_f values of 0.47, 0.39, 0.34 and 0.26. This fraction was separated by column chromatography over Sephadex LH 20. Elution was conducted with 100%MeOH. Fractions with the similar chromatogram characteristics were combined and evaporated to dryness under reduced pressure to afford four subfractions, as shown in **Table 22.**

Table 22 Subfractions obtained from the fraction GC by column chromatography over Sephadex LH 20

Fraction	Weight (mg)	Physical appearance
GC1	37.6	Yellow gum
GC2	92.2	Yellow gum
GC3	45.3	Yellow gum
GC4	4.3	Yellow-brown gum

Fraction GC1 Chromatogram characteristics on normal phase TLC with 100%$CHCl_3$ showed no definite spot under UV and ASA reagent. Further investigation was then not carried out.

Fraction GC2 Chromatogram characteristics on normal phase TLC with 100%$CHCl_3$ showed one UV-active spot with the R_f value of 0.19. Because the ^1H NMR data indicated the presence of many compounds, it was not further investigated.

Fraction GC3 Chromatogram characteristics on normal phase TLC with 100%$CHCl_3$ showed three UV-active spots with the R_f values of 0.34, 0.26 and 0.17. This fraction was separated by column chromatography over silica gel. Elution was conducted with 20%EtOAc/Petrol. Fractions with the similar chromatogram characteristics were combined and evaporated to dryness under reduced pressure to afford three subfractions, as shown in **Table 23.**

Table 23 Subfractions obtained from the fraction GC3 by column chromatography over silica gel

Fraction	Weight (mg)	Physical appearance
GC31	24.3	Yellow gum
GC32	6.9	Colorless gum
GC33	10.3	Yellow gum

Fraction GC31 Chromatogram characteristics on normal phase TLC with 10%EtOAc/Petrol showed two UV-active spots with the R_f values of 0.48 and 0.39. Because the ^1H NMR data indicated the presence of many compounds, it was not further investigated.

Fraction GC32 Chromatogram characteristics on normal phase TLC with 10%EtOAc/Petrol showed one UV-active spot with the R_f values of 0.22. It was named as **GP10.**

UV λ_{max}(nm)(MeOH)(log ε) 211 (4.10), 270 (3.73), 294 (3.09)

FTIR(neat):υ (cm^{-1}) 3417

^1H NMR($CDCl_3$)(δ_{ppm})(300 MHz) : 7.04 (*dd*, J = 8.0 and 2.1 Hz, 1H), 7.00 (*d*, J = 2.1 Hz, 1H), 6.97 (*d*, J = 8.0 Hz, 1H), 6.72 (*s*, 2H), 5.16 (*brs*, 1H), 5.04 (*brs*, 1H), 3.96 (*s*, 3H), 3.95 (*s*, 6H)

^{13}C NMR($CDCl_3$)(δ_{ppm}) (75 MHz): 147.72, 146.67, 145.01, 134.16, 134.09, 133.11, 120.03, 114.64, 109.69, 104.02, 56.44, 56.08

EIMS (*m/z*) (% rel. int.) 276 (100), 261 (18), 233 (35), 138 (10)

Fraction GC33 Chromatogram characteristics on normal phase TLC with 10%EtOAc/Petrol showed none of well-separated spots under UV and ASA reagent. It was not further investigated.

Fraction GC4 Chromatogram characteristics on normal phase TLC with 100%$CHCl_3$ showed none of well-separated spots under UV and ASA reagent. It was not further investigated.

Fraction GD Chromatogram characteristics on normal phase TLC with 100%CH_2Cl_2 showed three UV-active spots with the R_f values of 0.56, 0.47 and 0.37. Because the ^1H NMR data indicated the presence of many compounds, it was not further investigated.

Fraction GE Chromatogram characteristics on normal phase TLC with 100%CH_2Cl_2 showed four UV-active spots with the R_f values of 0.34, 0.30, 0.24 and 0.18. This fraction was separated by column chromatography over Sephadex LH 20. Elution was conducted with 100%MeOH. Fractions with the similar chromatogram characteristics were combined and evaporated to dryness under reduced pressure to afford four subfractions, as shown in **Table 24.**

Table 24 Subfractions obtained from the fraction GE by column chromatography over Sephadex LH 20

Fraction	Weight (mg)	Physical appearance
GE1	101.6	Yellow gum
GE2	66.7	Yellow gum
GE3	66.7	Yellow gum
GE4	6.3	Yellow-brown gum

Fraction GE1 Chromatogram characteristics on normal phase TLC with 20%EtOAc/Petrol showed no definite spot under UV and ASA reagent. Further investigation was then not carried out.

Fraction GE2 Chromatogram characteristics on normal phase TLC with 20%EtOAc/Petrol showed none of well-separated spots under UV and ASA reagent. It was not further investigated.

Fraction GE3 Chromatogram characteristics on normal phase TLC with 20%EtOAc/Petrol showed four UV-active spots with the R_f values of 0.34, 0.21, 0.12 and 0.05. This fraction was separated by column chromatography over silica gel. Elution was conducted with 20%EtOAc/Petrol. Fractions with the similar chromatogram characteristics were combined and evaporated to dryness under reduced pressure to afford four subfractions, as shown in **Table 25.**

Table 25 Subfractions obtained from the fraction GE3 by column chromatography over silica gel

Fraction	Weight (mg)	Physical appearance
GE31	29.7	Yellow gum
GE32	2.0	Yellow gum
GE33	2.2	Yellow gum
GE34	16.8	Yellow-brown gum

Fraction GE31 Chromatogram characteristics on normal phase TLC with 20%EtOAc/Petrol showed many UV-active spots. Thus, it was not further investigated.

Fraction GE32 Chromatogram characteristics on normal phase TLC with 20%EtOAc/Petrol showed one UV-active spot with the R_f value of 0.20. It was named as **GP11.**

UV λ_{max}(nm)(MeOH)(log ε) 241 (4.01), 257 (3.82), 317 (3.15), 359 (2.59)

FTIR(neat):υ (cm^{-1}) 3394, 1646

^{1}H NMR($CDCl_3$)(δ_{ppm})(300 MHz) : 13.35 (*s*, 1H), 6.88 (*s*, 1H), 6.33 (*brs*, 1H), 6.25 (*s*, 1H), 6.00 (*brs*, 1H), 5.97 (*brs*, 1H), 5.28 (*mt*, J = 6.6 Hz, 1H), 5.27 (*mt*, J = 6.0 Hz, 1H), 5.03 (*mt*, J = 6.6 Hz, 1H), 4.10 (*d*, J = 6.0 Hz, 2H), 3.82 (*s*, 3H), 3.53 (*d*, J = 6.6 Hz, 2H), 2.09 (*m*, 4H), 1.89 (*d*, J = 0.9 Hz, 3H), 1.83 (*d*, J = 1.2 Hz, 3H), 1.70 (*d*, J = 1.2 Hz, 3H), 1.66 (*d*, J = 0.9 Hz, 3H), 1.60 (*d*, J = 0.9 Hz, 3H)

^{13}C NMR($CDCl_3$)(δ_{ppm}) (75 MHz): 182.39, 161.68, 155.81, 154.58, 154.00, 142.67, 138.76, 137.06, 135.69, 124.27, 123.72, 123.08, 121.26, 112.20, 104.08, 101.56, 98.53, 62.12, 39.70, 26.55, 26.38, 25.83, 25.65, 21.62, 18.24, 17.97

DEPT 90° CH : 123.72, 123.08, 121.26, 101.56, 98.53

DEPT 135° CH_2 : 39.70, 26.55, 26.38, 21.62

CH_3 : 62.12 , 25.83, 25.65, 18.24, 17.97

EIMS (*m/z*) (% rel. int.) 478 (59), 463 (21), 435 (43), 409 (100), 367 (26), 355 (37), 339 (26), 323 (25), 167 (29), 149 (96), 111 (23), 109 (27), 97 (35), 83 (52), 71 (63)

Fraction GE33 Chromatogram characteristics on normal phase TLC with 20%EtOAc/Petrol showed one UV-active spot with the R_f value of 0.06. It was named as **GP12.**

UV λ_{max}(nm)(MeOH)(log ε) 221 (4.09), 272 (3.16), 281 (3.15), 327 (2.59)

FTIR(neat):υ (cm^{-1}) 3363, 1657

^{1}H NMR($CDCl_3$)(δ_{ppm})(300 MHz) : 11.36 (*s*, 1H), 6.76 (*d*, *J* = 10.2 Hz, 1H), 6.69 (*s*, 1H), 6.29 (*s*, 1H), 6.26 (*s*, 1H), 5.75 (*d*, *J* = 10.2 Hz, 1H), 5.39 (*brs*, 1H), 5.23 (*mt*, *J* = 7.2 Hz, 1H), 5.04 (*mt*, *J* = 6.6 Hz, 1H), 3.41 (*d*, *J* = 7.2 Hz, 2H), 2.08 (*m*, 4H), 1.80 (*s*, 6H), 1.68 (*s*, 3H), 1.59 (*s*, 3H), 1.46 (*s*, 6H)

^{13}C NMR($CDCl_3$)(δ_{ppm}) (75 MHz): 168.50, 162.60, 162.41, 160.08, 143.10, 142.24, 140.25, 136.45, 132.58, 132.25, 132.06, 123.58, 120.67, 116.22, 113.80, 110.76, 106.43, 100.52, 98.53, 77.21, 39.67, 27.70, 26.25, 25.65, 21.95, 17.70, 16.23

DEPT 90° CH : 132.06, 123.58, 120.67, 116.22, 106.43, 100.52

DEPT 135° CH_2 : 39.67, 26.25, 21.95

CH_3 : 27.70, 25.65, 17.70, 16.23

EIMS (*m/z*) (% rel. int.) 478 (100), 463 (26), 409 (35), 393 (56), 355 (92), 219 (35), 203 (36), 165 (36), 149 (65), 135 (33), 83 (29), 81 (33)

Fraction GE34 Chromatogram characteristics on normal phase TLC with 20%EtOAc/Petrol showed none of well-separated spots under UV and ASA reagent. It was not further investigated.

Fraction GE4 Chromatogram characteristics on normal phase TLC with 20%EtOAc/Petrol showed none of well-separated spots under UV and ASA reagent. Because of low quantity, it was not further investigated.

Fraction GF Chromatogram characteristics on normal phase TLC with 100%CH_2Cl_2 showed one UV-active spot with the R_f value of 0.18. This fraction was separated by column chromatography over Sephadex LH 20. Elution was conducted with MeOH. Fractions with the similar chromatogram characteristics were combined and evaporated to dryness under reduced pressure to afford four subfractions, as shown in **Table 26.**

Table 26 Subfractions obtained from the fraction GF by column chromatography over Sephadex LH 20

Fraction	Weight (mg)	Physical appearance
GF1	18.3	Yellow gum
GF2	44.3	Yellow gum
GF3	69.3	Yellow gum
GF4	17.7	Yellow-brown gum

Fraction GF1 Chromatogram characteristics on normal phase TLC with 20%EtOAc/Petrol showed no definite spot under UV and ASA reagent. Further investigation was then not carried out.

Fraction GF2 Chromatogram characteristics on normal phase TLC with 20%EtOAc/Petrol showed two UV-active spots with the R_f values of 0.27

and 0.22. Further purification was performed by precoated TLC, using 10%EtOAc/Petrol as a mobile phase (8 runs), to afford two bands.

Band 1 was obtained as a yellow gum in 10.3 mg. Chromatogram characteristics on normal phase TLC with 20%EtOAc/Petrol showed one UV-active spot with the R_f value of 0.27. Because the ^1H NMR data indicated the presence of many compounds, it was not further investigated.

Band 2 was obtained as a yellow gum in 9.6 mg. Chromatogram characteristics on normal phase TLC with 20%EtOAc/Petrol showed one UV-active spot with the R_f value of 0.20. It was named as **GP13**.

$[\alpha]^{29}_D$	+60.01 (c = 0.01, $CHCl_3$)
UV λ_{max}(nm)(MeOH)(log ε)	205 (3.82), 234 (2.23), 277 (2.01)
FTIR(neat): υ (cm^{-1})	3404, 1655
^1H NMR($CDCl_3$)(δ_{ppm})(300 MHz) :	5.84 (*brq*, *J* = 1.2 Hz, 1H), 5.20 (*mt*, *J* = 6.0 Hz, 1H), 5.09 (*m*, 3H), 4.15 (*brd*, *J* = 6.0 Hz, 1H), 2.54 (*brd*, *J* = 13.5 Hz, 1H), 2.36 (*m*, 1H), 2.17 (*m*, 1H), 2.16 (*m*, 1H), 2.14 (*m*, 1H), 2.13 (*m*, 6H), 2.06 (*m*, 2H), 2.04 (*brt*, *J* = 1.2 Hz, 3H), 2.00 (*m*, 2H), 1.95 (*m*, 2H), 1.68 (*brd*, *J* = 0.9 Hz, 3H), 1.64 (*brd*, *J* = 0.9 Hz, 3H), 1.62 (*s*, 3H), 1.59 (*s*, 6H)
^{13}C NMR($CDCl_3$)(δ_{ppm}) (75 MHz):	196.45, 162.96, 138.54, 135.47, 134.98, 131.29, 126.85, 124.39, 124.17, 123.81, 120.73, 73.71, 43.62, 41.37, 39.85, 39.73, 39.69, 31.01, 26.77, 26.61, 26.47, 25.70, 20.32, 17.69, 16.29, 16.07, 16.01
DEPT 90°	CH : 126.85, 124.39, 124.17, 123.81, 120.73, 73.71, 43.62
DEPT 135°	CH_2 : 41.37, 39.85, 39.73, 39.69, 31.01, 26.77, 26.61, 26.47
	CH_3 : 25.70, 20.32, 17.69, 16.29, 16.07, 16.01

Fraction GF3 Chromatogram characteristics on normal phase TLC with 20%EtOAc/Petrol showed no definite spot under UV and ASA reagent. Further investigation was then not carried out.

Fraction GF4 Chromatogram characteristics on normal phase TLC with 20%EtOAc/Petrol showed none of well-separated spots under UV and ASA reagent. Therefore, it was not further investigated.

Fraction GG Chromatogram characteristics on normal phase TLC with 100%CH_2Cl_2 showed four UV-active spots with the R_f values of 0.26, 0.18, 0.15 and 0.09. Because the ^1H NMR data indicated the presence of many compounds, it was not further investigated.

Fraction GH Chromatogram characteristics on normal phase TLC with 100%CH_2Cl_2 showed none of well-separated spots under UV and ASA reagent. It was not further investigated.

Fraction H Chromatogram characteristics on normal phase TLC with 100%$CHCl_3$ showed five UV-active spots with the R_f values of 0.28, 0.27, 0.21, 0.16 and 0.12. This fraction was separated by column chromatography over silica gel. Elution was conducted initially with 0.5%MeOH/CH_2Cl_2, gradually enriched with MeOH and finally with 100%MeOH. Fractions with the similar chromatogram characteristics were combined and evaporated to dryness under reduced pressure to afford six subfractions, as shown in **Table 27.**

Table 27 Subfractions obtained from the fraction H by column chromatography over silica gel.

Fraction	Mobile phase	Weight (mg)	Physical appearance
HA	0.5%MeOH/CH_2Cl_2	10.1	Yellow gum
HB	1.5%MeOH/CH_2Cl_2	6.5	Yellow gum
HC	1.5%MeOH/CH_2Cl_2	7.0	Yellow gum
HD	3%MeOH/CH_2Cl_2	46.4	Yellow-brown gum
HE	3-15%MeOH/CH_2Cl_2	93.8	Yellow brown gum
HF	30-100%MeOH/CH_2Cl_2	203.6	Yellow-brown gum

Fraction HA Chromatogram characteristics on normal phase TLC with 0.25%MeOH/CH_2Cl_2 showed two UV-active spots with the R_f values of 0.83 and 0.65. Because the ^1H NMR data indicated the presence of many compounds, it was not further investigated.

Fraction HB Chromatogram characteristics on normal phase TLC with 0.25%MeOH/CH_2Cl_2 showed two UV-active spots with the R_f values of 0.59 and 0.52. The ^1H NMR data indicated the presence of **GP3** and **GP4** as major components. Further investigation was then not carried out.

Fraction HC Chromatogram characteristics on normal phase TLC with 0.25%MeOH/CH_2Cl_2 showed three UV-active spots with the R_f values of 0.55, 0.52 and 0.46. The ^1H NMR data indicated the presence of **GP3** and **GP5** as major components. Further investigation was then not carried out.

Fraction HD Chromatogram characteristics on normal phase TLC with 0.25%MeOH/CH_2Cl_2 showed three UV-active spots with the R_f values of 0.48, 0.42 and 0.37. Because the ^1H NMR data indicated the presence of many compounds, it was not further investigated.

Fraction HE Chromatogram characteristics on normal phase TLC with 0.25%MeOH/CH_2Cl_2 showed three UV-active spots with the R_f values of 0.46, 0.38 and 0.33. Because the ^1H NMR data indicated the presence of many compounds, it was not further investigated.

Fraction HF Chromatogram characteristics on normal phase TLC with 0.25%MeOH/CH_2Cl_2 showed four UV-active spots with the R_f values of 0.38, 0.37, 0.33 and 0.24. Because the ^1H NMR data indicated the presence of many compounds, it was not further investigated.

Fraction I Chromatogram characteristics on normal phase TLC with 100%$CHCl_3$ showed two UV-active spots with the R_f values of 0.07 and 0.05. This fraction was separated by column chromatography over silica gel. Elution was conducted initially with 100%CH_2Cl_2, gradually enriched with MeOH and finally with 100%MeOH. Fractions with the similar chromatogram characteristics were combined and

evaporated to dryness under reduced pressure to afford nine subfractions, as shown in **Table 28.**

Table 28 Subfractions obtained from the fraction I by column chromatography over silica gel

Fraction	Mobile phase	Weight (mg)	Physical appearance
IA	100%/CH_2Cl_2	19.3	Yellow gum
IB	100%/CH_2Cl_2	48.2	Yellow gum
IC	0.5%MeOH/CH_2Cl_2	23.2	Yellow gum
ID	2%MeOH/CH_2Cl_2	16.5	Yellow gum
IE	2%MeOH/CH_2Cl_2	13.5	Yellow gum
IF	3%MeOH/CH_2Cl_2	24.2	Yellow gum and white solid
IG	3-10%MeOH/CH_2Cl_2	57.2	Yellow-brown gum
IH	10-30%MeOH/CH_2Cl_2	206.3	Yellow -brown gum
II	30-100%MeOH/CH_2Cl_2	2340.9	Yellow-brown gum

Fraction IA Chromatogram characteristics on normal phase TLC with 0.25%MeOH/CH_2Cl_2 showed two UV-active spots with the R_f values of 0.71 and 0.68. Because the ^1H NMR data indicated the presence of many compounds, it was not further investigated.

Fraction IB Chromatogram characteristics on normal phase TLC with 0.25%MeOH/CH_2Cl_2 showed three UV-active spots with the R_f values of 0.68, 0.59 and 0.51. The ^1H NMR data indicated the presence of **GP3** and **GP4** as major components. Further investigation was then not carried out.

Fraction IC Chromatogram characteristics on normal phase TLC with 0.25%MeOH/CH_2Cl_2 showed three UV-active spots with the R_f values of 0.54, 0.51 and 0.17. The ^1H NMR data indicated the presence of **GP4** and **GP5** as major components. Further investigation was then not carried out.

Fraction ID Chromatogram characteristics on normal phase TLC with 0.25%MeOH/CH_2Cl_2 showed one major UV-active spot with the same R_f value as **GP5**. Further investigation was then not carried out.

Fraction IE Chromatogram characteristics on normal phase TLC with 0.25%MeOH/CH_2Cl_2 showed one major UV-active spot with the same R_f value as **GP12**. Further investigation was then not carried out.

Fraction IF Chromatogram characteristics on normal phase TLC with 0.25%MeOH/CH_2Cl_2 showed two UV-active spots with the R_f values of 0.29 and 0.20. The ^1H NMR data indicated the presence of **GP10** and **stigmasterol** as major components. Further investigation was then not carried out.

Fraction IG Chromatogram characteristics on normal phase TLC with 0.25%MeOH/CH_2Cl_2 showed three UV-active spots with the R_f values of 0.29, 0.25 and 0.20. The ^1H NMR data indicated the presence of **GP10** as a major component. Further investigation was then not carried out.

Fraction IH Chromatogram characteristics on normal phase TLC with 0.25%MeOH/CH_2Cl_2 showed two UV-active spots with the R_f values of 0.19 and 0.13. This fraction was separated by column chromatography over silica gel. Elution was conducted initially with 100%CH_2Cl_2, gradually enriched with MeOH and finally with 10%MeOH/CH_2Cl_2. Fractions with the similar chromatogram characteristics were combined and evaporated to dryness under reduced pressure to afford four subfractions, as shown in **Table 29.**

Table 29 Subfractions obtained from the fraction IH by column chromatography over silica gel

Fraction	Mobile phase	Weight (mg)	Physical appearance
IH1	100%CH_2Cl_2	0.9	Yellow gum
IH2	100%CH_2Cl_2	30.9	Yellow gum
IH3	0.25%MeOH/CH_2Cl_2	103.9	Yellow gum
IH4	5-10%MeOH/CH_2Cl_2	8.4	Yellow-brown gum

Fraction IH1 Chromatogram characteristics on normal phase TLC with 0.25%MeOH/CH_2Cl_2 showed no definite spot under UV and ASA reagent. Further investigation was then not carried out.

Fraction IH2 Chromatogram characteristics on normal phase TLC with 0.25%MeOH/CH_2Cl_2 showed three UV-active spots with the R_f values of 0.47, 0.39 and 0.34. Because the ^1H NMR data indicated the presence of many compounds, it was not further investigated.

Fraction IH3 Chromatogram characteristics on normal phase TLC with 0.25%MeOH/CH_2Cl_2 showed four UV-active spots with the R_f values of 0.42, 0.34, 0.25 and 0.22. This fraction was separated by flash column chromatography over silica gel. Elution was conducted with 100%$CHCl_3$. Fractions with the similar chromatogram characteristics were combined and evaporated to dryness under reduced pressure to afford three subfractions, as shown in **Table 30.**

Table 30 Subfractions obtained from the fraction IH3 by flash column chromatography over silica gel

Fraction	Weight (mg)	Physical appearance
IH31	15.9	Yellow gum
IH32	34.5	Yellow gum
IH33	39.7	Yellow gum

Fraction IH31 Chromatogram characteristics on normal phase TLC with 0.25%MeOH/CH_2Cl_2 showed one UV-active spot with the R_f value of 0.22. Because the ^1H NMR data indicated the presence of many compounds, it was not further investigated.

Fraction IH32 Chromatogram characteristics on normal phase TLC with 0.25%MeOH/CH_2Cl_2 showed one UV-active spot with the R_f value of 0.30. It was named as **GP14.**

UV λ_{max}(nm)(MeOH)(log ε) 223 (3.59), 276 (3.43), 319 (2.82)

FTIR(neat):υ (cm^{-1}) 3373, 1656

^1H NMR($CDCl_3$)(δ_{ppm})(300 MHz) : 10.72 (*s*, 1H), 6.69 (*s*, 1H), 6.29 (*s*, 1H), 6.23 (*brs*, 1H), 5.59 (*brs*, 1H), 5.53 (*brs*, 1H), 5.25 (*mt*, J = 6.9 Hz, 1H), 5.20 (*mt*, J = 6.9 Hz, 1H), 5.05 (*mt*, J = 6.9 Hz, 1H), 3.57 (*d*, J = 6.9 Hz,

	4H), 2.13 (*m*, 4H), 1.86 (*s*, 3H), 1.83 (*s*, 3H), 1.76 (*s*, 3H), 1.67 (*s*, 3H), 1.60 (*s*, 3H)
^{13}C NMR($CDCl_3$)(δ_{ppm}) (75 MHz):	168.32, 163.20, 162.64, 158.74, 143.41, 141.95, 139.83, 139.36, 136.70, 135.86, 132.24, 123.63, 121.30, 120.15, 119.95, 111.18, 105.39, 100.90, 99.29, 39.65, 26.31, 25.76, 25.69, 23.92, 22.44, 17.99, 17.70, 16.35
DEPT 90°	CH : 123.63, 121.30, 120.15, 105.39, 100.90
DEPT 135°	CH_2 : 39.65, 26.31, 23.92, 22.44
	CH_3 : 25.76, 25.69, 17.99, 17.70, 16.35
EIMS (*m/z*) (% rel. int.)	480 (71), 424 (44), 357 (73), 301 (57), 298 (100), 283 (51), 165 (43), 149 (68), 71 (33), 69 (60)

Fraction IH33 Chromatogram characteristics on normal phase TLC with 0.25%MeOH/CH_2Cl_2 showed two UV-active spots with the R_f values of 0.42 and 0.34. Because the ^{1}H NMR data indicated the presence of many compounds, it was not further investigated.

Fraction IH4 Chromatogram characteristics on normal phase TLC with 0.25%MeOH/CH_2Cl_2 showed none of well-separated spots under UV and ASA reagent. It was not further investigated.

Fraction II Chromatogram characteristics on normal phase TLC with 0.25%MeOH/CH_2Cl_2 showed two UV-active spots with the R_f values of 0.10 and 0.07. This fraction was separated by column chromatography over Sephadex LH 20. Elution was conducted with 100%MeOH. Fractions with the similar chromatogram characteristics were combined and evaporated to dryness under reduced pressure to afford four subfractions, as shown in **Table 31.**

Table 31 Subfractions obtained from the fraction II by column chromatography over Sephadex LH 20

Fraction	Weight (mg)	Physical appearance
II1	737.3	Yellow gum
II 2	584.4	Yellow gum
II3	828.2	Yellow gum
II4	51.7	Yellow-brown gum

Fraction II1 Chromatogram characteristics on normal phase TLC with 20%Acetone/Petrol showed no definite spot under UV and ASA reagent. Further investigation was then not carried out.

Fraction II2 Chromatogram characteristics on normal phase TLC with 20%Acetone/Petrol showed two UV-active spots with the R_f values of 0.28 and 0.25. Because the ^1H NMR data indicated the presence of many compounds, it was not further investigated.

Fraction II3 Chromatogram characteristics on normal phase TLC with 20%Acetone/Petrol showed three UV-active spots with the R_f values of 0.30, 0.20 and 0.13. This fraction was separated by flash column chromatography over silica gel. Elution was conducted with 100%$CHCl_3$. Fractions with the similar chromatogram characteristics were combined and evaporated to dryness under reduced pressure to afford four subfractions, as shown in **Table 32.**

Table 32 Subfractions obtained from the fraction II3 by column chromatography over silica gel

Fraction	Weight (mg)	Physical appearance
II31	14.3	Yellow gum
II32	42.9	Yellow gum
II33	529.3	Yellow gum
II34	169.3	Yellow-brown gum

Fraction II31 Chromatogram characteristics on normal phase TLC with 20%Acetone/Petrol showed one UV-active spot with the R_f value of 0.30. Because the ^1H NMR data indicated the presence of many compounds, it was not further investigated.

Fraction II32 Chromatogram characteristics on normal phase TLC with 20%Acetone/Petrol showed three UV-active spots with the R_f values of 0.34, 0.30 and 0.25. This fraction was separated by flash column chromatography over silica gel. Elution was conducted with 10%Acetone/Petrol. Fractions with the similar chromatogram characteristics were combined and evaporated to dryness under reduced pressure to afford three subfractions, as shown in **Table 33.**

Table 33 Subfractions obtained from the fraction II32 by column chromatography over silica gel

Fraction	Weight (mg)	Physical appearance
II321	5.0	Yellow gum
II322	6.6	Yellow gum
II323	13.3	Yellow gum

Fraction II321 Chromatogram characteristics on normal phase TLC with 20%Acetone/Petrol showed no definite spot under UV and ASA reagent. Further investigation was then not carried out.

Fraction II322 Chromatogram characteristics on normal phase TLC with 20%Acetone/Petrol showed one UV-active spot with the R_f value of 0.34. It was named as **GP15.**

UV λ_{max}(nm)(MeOH)(log ε) 243 (4.19), 273 (3.65), 317 (3.61)

FTIR(neat):υ (cm^{-1}) 3400, 1651

^1H NMR($CDCl_3$)(δ_{ppm})(300 MHz) : 13.05 (*s*, 1H), 7.72 (*dd*, J = 7.5 and 1.8 Hz, 1H), 7.23 (*dd*, J = 7.5 and 1.8 Hz, 1H), 7.16 (*t*, J = 7.5 Hz, 1H), 6.46 (*s*, 1H), 5.29 (*mt*, J = 6.6 Hz, 1H), 5.08 (*mt*, J = 6.6 Hz, 1H), 3.40 (*d*, J = 6.6

Hz, 2H), 2.07 (*m*, 2H), 1.99 (*m*, 2H), 1.82 (*s*, 3H), 1.65 (*s*, 3H), 1.58 (*s*, 3H)

^{13}C NMR($CDCl_3$)(δ_{ppm}) (75 MHz): 180.80, 162.80, 160.40, 155.00, 145.30, 145.00, 135.95, 131.28, 124.30, 123.49, 121.80, 121.40, 119.89, 116.09, 110.80, 102.80, 93.38, 39.73, 26.62, 25.51, 21.24, 17.52, 16.05

Fraction II323 Chromatogram characteristics on normal phase TLC with 20%Acetone/Petrol showed none of well-separated spots under UV and ASA reagent. Thus, it was not further investigated

Fraction II33 Chromatogram characteristics on normal phase TLC with 20%Acetone/Petrol showed three UV-active spots with the R_f values of 0.30, 0.20 and 0.15. This fraction was separated by flash column chromatography over silica gel. Elution was conducted with 10%Acetone/Petrol. Fractions with the similar chromatogram characteristics were combined and evaporated to dryness under reduced pressure to afford five subfractions, as shown in **Table 34.**

Table 34 Subfractions obtained from the fraction II33 by column chromatography over silica gel

Fraction	Weight (mg)	Physical appearance
II331	24.3	Yellow gum
II332	82.1	Yellow gum
II333	79.0	Yellow gum
II334	42.4	Yellow-brown gum
II335	52.3	Yellow-brown gum

Fraction II331 Chromatogram characteristics on normal phase TLC with 30%Acetone/Petrol showed no definite spot under UV and ASA reagent. Further investigation was then not carried out.

Fraction II332 Chromatogram characteristics on normal phase TLC with 30%Acetone/Petrol showed one UV-active spot with the R_f

value of 0.30. This fraction was separated by column chromatography over Sephadex LH 20. Elution was conducted with 100%MeOH. Fractions with the similar chromatogram characteristics were combined and evaporated to dryness under reduced pressure to afford three subfractions, as shown in **Table 35.**

Table 35 Subfractions obtained from the fraction II332 by column chromatography over Sephadex LH 20

Fraction	Weight (mg)	Physical appearance
II3321	29.3	Yellow gum
II3322	11.3	Yellow gum
II3323	10.3	Yellow gum

Fraction II3321 Chromatogram characteristics on normal phase TLC with 30%Acetone/Petrol showed no definite spot under UV and ASA reagent. Further investigation was then not carried out.

Fraction II3322 Chromatogram characteristics on normal phase TLC with 30%Acetone/Petrol showed one UV-active spot with the R_f value of 0.30. It was named as **GP16.**

UV λ_{max}(nm)(MeOH)(log ε) 239 (4.19), 253 (4.38), 312 (3.61), 351 (2.58)

FTIR(neat):υ (cm^{-1}) 3366, 1646

^{1}H NMR($CDCl_3$+CD_3OD)(δ_{ppm})(300 MHz) :13.67 (*brs*, 1H), 6.76 (*s*, 3H), 6.25 (*d*, *J* = 1.8 Hz, 1H), 6.18 (*d*, *J* = 1.8 Hz, 1H), 5.25 (*brt*, *J* = 6.6 Hz, 1H), 5.03 (*brt*, *J* = 6.6 Hz, 1H), 4.09 (*d*, *J* = 6.6 Hz, 2H), 3.78 (*s*, 3H), 2.07 (*m*, 2H), 2.00 (*m*, 2H), 1.82 (*s*, 3H), 1.60 (*s*, 3H), 1.54 (*s*, 3H)

^{13}C NMR($CDCl_3$+CD_3OD)(δ_{ppm}) (75 MHz): 181.85, 162.20, 157.03, 155.61, 143.17, 142.70, 137.41, 135.24, 131.10, 124.31, 123.37, 111.67, 103.21, 101.85, 97.93,

93.43, 61.28, 39.69, 26.54, 26.22, 25.49, 17.53, 16.34

Fraction II3323 Chromatogram characteristics on normal phase TLC with 30%Acetone/Petrol showed none of well-separated spots under UV and ASA reagent. Therefore, it was not further investigated

Fraction II333 Chromatogram characteristics on normal phase TLC with 30%Acetone/Petrol showed three UV-active spots with the R_f values of 0.34, 0.30 and 0.25. This fraction was separated by column chromatography over Sephadex LH 20. Elution was conducted with 100%MeOH. Fractions with the similar chromatogram characteristics were combined and evaporated to dryness under reduced pressure to afford four subfractions, as shown in **Table 36.**

Table 36 Subfractions obtained from the fraction II333 by column chromatography over Sephadex LH 20

Fraction	Weight (mg)	Physical appearance
II3331	13.3	Yellow gum
II3332	23.2	Yellow gum
II3333	4.3	Yellow gum
II3334	9.2	Yellow gum

Fraction II3331 Chromatogram characteristics on normal phase TLC with 30%Acetone/Petrol showed no definite spot under UV and ASA reagent. Further investigation was then not carried out.

Fraction II3332 Chromatogram characteristics on normal phase TLC with 30%Acetone/Petrol showed none of well-separated spots under UV and ASA reagent. Therefore, it was not further investigated.

Fraction II3333 Chromatogram characteristics on normal phase TLC with 30%Acetone/Petrol showed one UV-active spot with the R_f values of 0.25. It was named as **GP17.**

UV λ_{max}(nm)(MeOH)(log ε)	238 (4.09), 251 (4.08), 312 (3.42), 353 (2.85)
FTIR(neat):υ (cm^{-1})	3371, 1643
^{1}H NMR($CDCl_3$+CD_3OD)(δ_{ppm})(300 MHz) :	13.63 (*brs*, 1H), 6.77 (*s*, 1H), 6.26 (*d*, *J* = 2.1 Hz, 1H), 6.19 (*d*, *J* = 2.1 Hz, 1H), 5.27 (*mt*, *J* = 6.0 Hz, 1H), 4.09 (*d*, *J* = 6.0 Hz, 2H), 3.79 (*s*, 3H), 1.84 (*s*, 3H), 1.69 (*s*, 3H)
^{13}C NMR($CDCl_3$+CD_3OD)(δ_{ppm}) (75 MHz):	181.93, 164.70, 164.00, 156.10, 155.63, 143.10, 137.30, 131.83, 123.30, 112.00, 101.87, 97.93, 92.60, 61.34, 26.34, 25.75, 18.10

Fraction II3334 Chromatogram characteristics on normal phase TLC with 30%Acetone/Petrol showed none of well-separated spots under UV and ASA reagent. Thus, it was not further investigated

Fraction II334 Chromatogram characteristics on normal phase TLC with 30%Acetone/Petrol showed one UV-active spot with the R_f values of 0.34. This fraction was separated by flash column chromatography over silica gel. Elution was conducted with 2%MeOH/$CHCl_3$. Fractions with the similar chromatogram characteristics were combined and evaporated to dryness under reduced pressure to afford three subfractions, as shown in **Table 37.**

Table 37 Subfractions obtained from the fraction II334 by flash column chromatography over silica gel

Fraction	Weight (mg)	Physical appearance
II3341	13.4	Yellow gum
II3342	16.3	Yellow gum
II3343	6.4	Yellow gum

Fraction II3341 Chromatogram characteristics on normal phase TLC with 30%Acetone/Petrol showed no definite spot under UV and ASA reagent. Further investigation was then not carried out.

Fraction II3342 Chromatogram characteristics on normal phase TLC with 30%Acetone/Petrol showed one UV-active spot with the R_f value of 0.34. It was named as **GP18.**

UV λ_{max}(nm)(MeOH)(log ε)	231 (3.69), 281 (3.57), 324 (2.82)
FTIR(neat):υ (cm^{-1})	3381, 1660
^{1}H NMR($CDCl_3$)(δ_{ppm})(300 MHz) :	11.30 (*s*, 1H), 6.67 (*s*, 1H), 6.47 (*brs*, 1H), 6.27 (*s*, 1H), 5.73 (*brs*, 1H), 5.59 (*brs*, 1H), 5.25 (*mt*, *J* = 7.2 Hz, 1H), 5.22 (*mt*, *J* = 7.2 Hz, 1H), 5.04 (*mt*, *J* = 6.9 Hz, 1H), 3.55 (*d*, *J* = 7.2 Hz, 2H), 3.39 (*d*, *J* = 7.2 Hz, 2H), 2.09 (*m*, 2H), 2.06 (*m*, 2H), 1.84 (*s*, 3H), 1.80 (*s*, 3H), 1.75 (*s*, 3H), 1.67 (*s*, 3H), 1.58 (*s*, 3H)
^{13}C NMR($CDCl_3$)(δ_{ppm}) (75 MHz):	168.70, 162.60, 162.34, 160.08, 143.43, 141.84, 139.82, 139.72, 136.18, 135.68, 132.12, 123.65, 120.76, 120.31, 110.91, 105.09, 100.33, 98.53, 39.68, 26.30, 25.77, 25.65, 23.88, 21.95, 17.98, 17.68, 16.22
DEPT 90°	CH : 123.65, 120.76, 120.31, 105.09, 100.33
DEPT 135°	CH_2 : 39.68, 26.30, 23.88, 21.95
	CH_3 : 25.77, 25.65, 17.98, 17.68, 16.22

Fraction II3343 Chromatogram characteristics on normal phase TLC with 30%Acetone/Petrol showed none of well-separated spots under UV and ASA reagent. Therefore, it was not further investigated

Fraction II335 Chromatogram characteristics on normal phase TLC with 30%Acetone/Petrol showed none of well-separated spots under UV and ASA reagent. Thus, it was not further investigated

Fraction II34 Chromatogram characteristics on normal phase TLC with 20%Acetone/Petrol showed none of well-separated spots under UV and ASA reagent. It was not further investigated.

Fraction II4 Chromatogram characteristics on normal phase TLC with 20%Acetone/Petrol showed none of well-separated spots under UV and ASA reagent. It was not further investigated.

Fraction J Chromatogram characteristics on reverse phase TLC with 50%H_2O/MeOH showed two UV-active spots with the R_f values of 0.32 and 0.39. This fraction was separated by column chromatography over reverse phase silica gel. Elution was conducted initially with 50%H_2O/MeOH, gradually enriched with MeOH and finally with 100%MeOH. Fractions with the similar chromatogram characteristics were combined and evaporated to dryness under reduced pressure to afford three subfractions, as shown in **Table 38.**

Table 38 Subfractions obtained from the fraction J by column chromatography over reverse phase silica gel

Fraction	Mobile phase	Weight (mg)	Physical appearance
JA	50%H_2O/MeOH	413.4	Brown gum
JB	60-80%H_2O/MeOH	132.5	Brown gum
JC	60-100%H_2O/MeOH	216.3	Brown gum

Fraction JA Chromatogram characteristics on reverse phase TLC with 50%H_2O/MeOH showed no definite spot under UV and ASA reagent. Further investigation was then not carried out.

Fraction JB Chromatogram characteristics on reverse phase TLC with 50%H_2O/MeOH showed two UV-active spots with the R_f values of 0.32 and 0.39. This fraction was separated by column chromatography over Sephadex LH 20. Elution was conducted with 100%MeOH. Fractions with the similar chromatogram characteristics were combined and evaporated to dryness under reduced pressure to afford four subfractions, as shown in **Table 39.**

Table 39 Subfractions obtained from the fraction JB by column chromatography over Sephadex LH 20

Fraction	Weight (mg)	Physical appearance
JB1	43.2	Yellow-brown gum
JB2	18.4	Yellow-brown gum
JB3	23.2	Yellow-brown gum
JB4	21.6	Yellow-brown gum

Fraction JB1 Chromatogram characteristics on reverse phase TLC with 50%H_2O/MeOH showed no definite spot under UV and ASA reagent. Further investigation was then not carried out.

Fraction JB2 Chromatogram characteristics on reverse phase TLC with 50%H_2O/MeOH showed two UV-active spots with the R_f values of 0.32 and 0.39. This fraction was separated by column chromatography over Sephadex LH 20. Elution was conducted with 100%MeOH. Fractions with the similar chromatogram characteristics were combined and evaporated to dryness under reduced pressure to afford three subfractions, as shown in **Table 40.**

Table 40 Subfractions obtained from the fraction JB2 by column chromatography over Sephadex LH 20

Fraction	Weight (mg)	Physical appearance
JB2-1	4.2	Yellow gum
JB2-2	2.1	Yellow gum
JB2-3	10.3	Yellow gum

Fraction JB2-1 Chromatogram characteristics on reverse phase TLC with 50%H_2O/MeOH showed no definite spot under UV and ASA reagent. Further investigation was then not carried out.

Fraction JB2-2 Chromatogram characteristics on reverse phase TLC with 50%H_2O/MeOH showed one UV-active spot with the R_f value of 0.32. It was named as **GP19.**

UV λ_{max}(nm)(MeOH)(log ε)	236 (3.61), 253 (3.90), 273 (3.40), 312 (2.94), 365 (2.37)
FTIR(neat):υ (cm^{-1})	3231, 1657
^{1}H NMR(CD_3OD)(δ_{ppm})(300 MHz) :	7.56 (*d, J* = 8.7 Hz, 1H), 6.87 (*d, J* = 8.7 Hz, 1H), 6.42 (*d, J* = 2.1 Hz, 1H), 6.16 (*d, J* = 2.1 Hz, 1H)
^{13}C NMR(CD_3OD)(δ_{ppm})(75 MHz) :	180.20, 166.00, 163.30, 158.00, 152.30, 146.30, 132.80, 115.40, 112.80, 112.10, 101.40, 97.80, 93.20

Fraction JB2-3 Chromatogram characteristics on reverse phase TLC with 50%H_2O/MeOH showed one UV-active spot with the R_f value of 0.39. The ^{1}H NMR data indicated the presence of **GP20** as a major component. Further investigation was then not carried out.

Fraction JB3 Chromatogram characteristics on reverse phase TLC with 50%H_2O/MeOH showed one UV-active spot with the R_f values 0.39. This fraction was separated by column chromatography over Sephadex LH 20. Elution was conducted with 100%MeOH. Fractions with the similar chromatogram characteristics were combined and evaporated to dryness under reduced pressure to afford three subfractions, as shown in **Table 41.**

Table 41 Subfractions obtained from the fraction JB3 by column chromatography over Sephadex LH 20

Fraction	Weight (mg)	Physical appearance
JB3-1	1.4	Yellow gum
JB3-2	9.8	Yellow gum
JB3-3	7.2	Yellow gum

Fraction JB3-1 Chromatogram characteristics on reverse phase TLC with 50%H_2O/MeOH showed no definite spots under UV and ASA reagent. Further investigation was then not carried out.

Fraction JB3-2 Chromatogram characteristics on reverse phase TLC with 50%H_2O/MeOH showed one UV-active spot with the R_f value of 0.39. It was named as **GP20.**

UV λ_{max}(nm)(MeOH)(log ε)	236 (3.60), 253 (3.72), 272 (3.43), 313 (2.94), 365 (2.41)
FTIR(neat): υ (cm^{-1})	3231, 1655
^{1}H NMR(CD_3OD)(δ_{ppm})(300 MHz) :	7.44 (*s*, 1H), 6.82 (*s*, 1H), 6.28 (*d*, J = 2.4 Hz, 1H), 6.15 (*d*, J = 2.4 Hz, 1H)
^{13}C NMR(CD_3OD)(δ_{ppm})(75 MHz) :	179.73, 164.84, 162.93, 157.99, 153.77, 151.81, 143.38, 112.47, 107.80, 102.10, 101.94, 97.36, 93.30

Fraction JB3-3 Chromatogram characteristics on reverse phase TLC with 50%H_2O/MeOH showed none of well-separated spots under UV and ASA reagent. Therefore, it was not further investigated.

Fraction JB4 Chromatogram characteristics on reverse phase TLC with 50%H_2O/MeOH showed none of well-separated spots under UV and ASA reagent. Therefore, it was not further investigated.

Fraction JC Chromatogram characteristics on reverse phase TLC with 50%H_2O/MeOH showed none of well-separated spots under UV and ASA reagent. Therefore, it was not further investigated.

Fraction K Chromatogram characteristics on reverse phase TLC with 50%H_2O/MeOH showed none of well-separated spots under UV and ASA reagent. Therefore, it was not further investigated.

3. RESULTS AND DISCUSSION

The crude methanol extract from the twigs of *G. parvifolia* was separated by chromatographic methods to yield thirteen new compounds: two methyl benzoates (**GP2** and **GP7**), five benzopyrans (**GP1, GP3, GP4, GP5** and **GP6**), two depsidones (**GP12** and **GP14**), three xanthones (**GP8, GP9** and **GP11**) and one benzocyclooctene (**GP10**) together with seven known compounds: one depsidone (**GP18**), five xanthones (**GP15, GP16, GP17, GP19** and **GP20**) and one cyclohexenone derivative (**GP13**). The structures were determined by analysis of 1D and 2D NMR spectroscopic data and comparison of the NMR data with those reported in literature.

3.1 Methyl benzoate derivatives

3.1.1 Compound GP7

Compound **GP7** with the molecular formula $C_{18}H_{24}O_5$ from EIMS (*m/z* 320) (**Figure 1**) was isolated as a colorless gum. It exhibited UV (**Figure 2**) absorption bands at 224, 271 and 315 nm while hydroxyl and conjugated ester carbonyl absorption bands were found at 3433 and 1660 cm^{-1}, respectively, in the IR spectrum (**Figure 3**). The ^1H NMR spectrum (**Figure 4**) (**Table 42**) contained signals of one hydroxyl group (δ_H 5.99, *s*), one aromatic proton (δ_H 6.00, *s*), one geranyl unit [δ_H 5.23 (*mt*, J = 7.2 Hz, 1H), 5.05 (*mt*, J = 6.9 Hz, 1H), 3.35 (*d*, J = 7.2 Hz, 2H), 2.07 (*m*, 4H), 1.80 (*s*, 3H) 1.67 (*s*, 3H) and 1.59 (*s*, 3H)] and one methoxyl group (δ_H 4.04, *s*). The carbon signal at δ_C 169.98 together with its HMBC correlation (**Figure 8**) with the methoxy protons confirmed the presence of the methyl ester group. The hydroxyl group (δ_H 5.99, 2-OH) and the geranyl unit were adjacent and located at C-2 (δ_C 162.31) and C-3 (δ_C 105.98), respectively, on the basis of HMBC correlations of 2-OH/C-1 (δ_C 93.71), C-2 and C-3 and those of H-7 (δ_H 3.35)/C-2, C-3 and C-4 (δ_C 162.31). Signal enhancement of 2-OH in the NOEDIFF experiment (**Figure 9**), upon irradiation of H_2-7, supported the conclusion. The aromatic proton was attributed to H-5 according to ^3J correlations with C-1 and C-3. Furthermore, a HMBC correlation between H-5 and the carbonyl carbon (C-17) together with the chemical-shift value of

C-1 established the attachment of the ester functionality at C-1. The assigned location of H-5, the ester moiety and the geranyl unit was further confirmed since irradiation of H-5 did not affect any proton signals in the NOEDIFF experiment. Because of no other signals were observed in the ^{1}H NMR spectrum, the substituents at C-4 and C-6 were hydroxyl groups. Thus, **GP7** was determined as methyl 2,4,6-trihydroxy-3-(3,7-dimethylocta-2,6-dienyl)benzoate, a new methyl benzoate derivative.

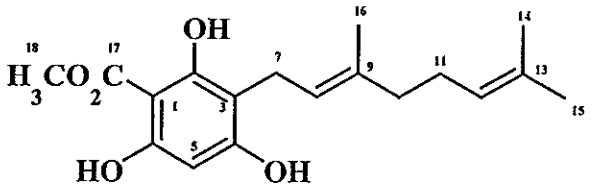

Table 42 The 300 MHz NMR data of compound GP7 in $CDCl_3$

Position	δ_H (*mult.*, J_{Hz})	δ_C (C-type)	HMBC correlations	NOE
1		93.71 (C)		
2-OH	5.99 (*s*)	162.31 (C)	C-1, C-2, C-3	
3		105.98 (C)		
4-OH		162.31 (C)		
5	6.00 (*s*)	96.03 (CH)	C-1, C-3, C-4, C-6, C-17	
6-OH		162.31 (C)		
7	3.35 (*d*, 7.2)	21.64 (CH_2)	C-2, C-3, C-4, C-8	2-OH, H-8, H-16
8	5.23 (*mt*, 7.2)	121.69 (CH)	C-4	H-7, H-10
9		138.72 (C)		
10	2.07 (*m*)	39.70 (CH_2)	C-8, C-11, C-12	
11	2.07 (*m*)	26.39 (CH_2)	C-9, C-10, C-13	
12	5.05 (*mt*, 6.9)	123.79 (CH)		H-10, H-15
13		131.96 (C)		
14	1.59 (*s*)	17.67 (CH_3)	C-12, C-13, C-15	H-11

Table 42 (Continued)

Position	δ_H (*mult.*, J_{Hz})	δ_C (C-type)	HMBC correlations	NOE
15	1.67 (*s*)	25.64 (CH_3)	C-12, C-13, C-14	H-12
16	1.80 (*s*)	16.16 (CH_3)	C-8, C-9, C-10	H-7, H-11
17		169.98 (C=O)		
18-OCH_3	4.04 (*s*)	52.43 (CH_3)	C-17	

3.1.2 Compound GP2

Compound **GP2** with the molecular formula $C_{19}H_{26}O_5$ from EIMS (*m/z* 334) (**Figure 10**) was isolated as a colorless gum. Its UV (**Figure 11**) and IR (**Figure 12**) absorption bands were almost identical to those of **GP7**. The ^{1}H NMR spectrum (**Figure 13**) (**Table 43**) contained signals of one aromatic proton (δ_H 6.07, *s*), one geranyl unit [δ_H 5.16 (*mt*, J = 6.9 Hz, 1H), 5.07 (*mt*, J = 6.9 Hz, 1H), 3.26 (*d*, J = 6.9 Hz, 2H), 2.00 (*m*, 4H), 1.76 (*s*, 3H) 1.64 (*s*, 3H) and 1.58 (*s*, 3H)] and two methoxyl groups [δ_H 4.03 (*s*) and 3.83 (*s*)]. The ^{1}H NMR data were similar to those of **GP7** except for the additional signal of the methoxyl group (δ_H 3.83) in **GP2**. The methoxyl group was located at C-4 (δ_C 164.15) on the basis of a HMBC correlation between the methoxy protons with C-4 (**Figure 17**). Signal enhancement of H-5 and H_3-14 after irradiation at 4-OCH_3 in the NOEDIFF experiment (**Figure 18**) supported the assigned location of the methoxyl group. The remaining HMBC correlations were similar to those found in **GP7**. Thus, **GP2** was determined as methyl 2,6-dihydroxy-4-methoxy-3-(3,7-dimethylocta-2,6-dienyl)benzoate, a new methyl ether derivative of **GP7**.

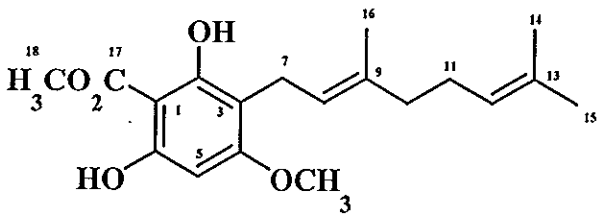

Table 43 The 300 MHz NMR data of compound GP2 in $CDCl_3$

Position	δ_H(*mult.*, J_{Hz})	δc (C-type)	HMBC correlations	NOE
1		109.00 (C)		
2-OH		158.60 (C)		
3		93.50 (C)		
3		164.15 (C)		
4-OCH_3	3.83 (*s*)	55.62 (CH_3)	C-4	H-5, H-14
5	6.07 (*s*)	91.57 (CH)	C-1, C-3, C-4, C-6	3-OCH_3
6-OH		160.80 (C)		
7	3.26 (*d*, 6.9)	21.46 (CH_2)	C-2, C-3, C-4, C-8, C-9	
8	5.16 (*mt*, 6.9)	122.53 (CH)		
9		134.82 (C)		
10	2.00 (*m*)	39.79 (CH_2)	C-11	
11	2.00 (*m*)	26.75 (CH_2)		
12	5.07 (*mt*, 6.9)	124.48 (CH)		
13		131.37 (C)		
14	1.58 (*s*)	17.66 (CH_3)	C-12, C-13, C-15	
15	1.64 (*s*)	25.67 (CH_3)	C-12, C-13, C-14	
16	1.76 (*s*)	16.04 (CH_3)	C-8, C-9	
17		169.97 (C=O)		
18-OCH_3	4.03 (*s*)	52.41 (CH_3)	C-17	

3.2 Benzopyran derivatives

3.2.1 Compound GP1

Compound **GP1** with the molecular formula $C_{18}H_{22}O_5$ from EIMS (*m/z* 318) (**Figure 19**) was isolated as a colorless gum. It exhibited UV absorption bands at 227, 254, 262, 278 and 333 nm (**Figure 20**), indicating the presence of a longer conjugation than that in **GP2** and **GP7**. The IR absorption bands (**Figure 21**) were similar to those of **GP7**. The ^1H NMR spectrum (**Figure 22**) (**Table 44**) contained signals of one aromatic proton (δ_H 5.96, *s*), two olefinic protons of a chromene ring

[δ_H 6.65 (*dd*, J = 10.0 and 0.6 Hz, 1H) and 5.41 (*d*, J = 10.0 Hz, 1H)], one 4-methyl-3-pentenyl unit [δ_H 5.08 (*mt*, J = 7.0 Hz, 1H), 2.06 (*m*, 2H), 1.69 (*m*, 2H), 1.66 (*s*, 3H) and 1.57 (*s*, 3H)], one methyl group (δ_H 1.39, *s*) and one methoxyl group (δ_H 4.03, *s*). The ^{1}H NMR data were similar to those of **GP7** except for the fact that signals of the geranyl substituent in **GP7** were replaced by signals of two olefinic protons of the chromene ring, the 4-methyl-3-pentenyl unit and the methyl group in **GP1**. ^3J HMBC correlations (**Figure 27**) between H-3 (δ_H 5.41) of the chromene ring with C-4a (δ_C 102.13), C-9 (δ_C 41.65) of the 4-methyl-3-pentenyl unit and C-15 (δ_C 27.12) of the quaternary methyl group established the attachment of the chromene ring at C-4a and C-8a (δ_C 161.00) with an ether linkage at C-8a. These also revealed the linkage of the 4-methyl-3-prenyl unit and H_3-15 at C-2 of the chromene ring. Signal enhancement of H-4 (δ_H 6.65), H_2-10 (δ_H 2.06) and H_3-15 (δ_H 1.39), upon irradiation of H-3 in the NOEDIFF experiment (**Figure 28**), supported these assignments. In addition, H-8 showed a zig-zag coupling with H-4 in the COSY spectrum (**Figure 25**). Thus, **GP1** was determined as 2-methyl-2-(4-methyl-3-pentenyl)-6-methylcarboxybenzopyran-5,7-diol, a new benzopyran derivative.

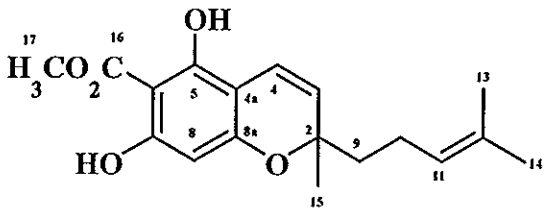

Table 44 The 300 MHz NMR data of compound GP1 in $CDCl_3$

Position	δ_H (*mult.*, J_{Hz})	δc (C-type)	HMBC correlations	NOE
2		80.22 (C)		
3	5.41 (*d*, 10.0)	124.71 (CH)	C-2, C-4a, C-9, C-15	H-4, H-10, H-15
4	6.65 (*dd*, 10.0, 0.6)	116.43 (CH)	C-2, C-4a, C-8a	H-3
4a		102.13 (C)		
5-OH		161.00 (C)		
6		93.37 (C)		

Table 44 (Continued)

Position	δ_H (*mult.*, J_{Hz})	δc (C-type)	HMBC correlations	NOE
7-OH		161.00 (C)		
8	5.96 (*brs*)	96.54 (CH)	C-4a, C-6, C-8a,C-16	
8a		161.00 (C)		
9	1.69 (*m*)	41.65 (CH_2)	C-2, C-3, C-10, C-11, C-15	
10	2.06 (*m*)	22.61 (CH_2)	C-9, C-11, C-12	H-9, H-11, H-13, H-15
11	5.08 (*mt*, 7.0)	123.87 (CH)	C-13, C-14	H-10, H-14
12		131.83 (C)		
13	1.57 (*s*)	17.61 (CH_3)	C-11, C-12, C-14	H-10
14	1.66 (*s*)	25.65 (CH_3)	C-11, C-12, C-13	H-11
15	1.39 (*s*)	27.12 (CH_3)	C-2, C-3, C-9	H-3, H-10
16		169.79 (C=O)		
17-OCH_3	4.03 (*s*)	52.46 (CH_3)	C-16	

3.2.2 Compound GP6

Compound **GP6** with the molecular formula $C_{18}H_{24}O_6$ from EIMS (*m/z* 336) (**Figure 29**) was isolated as a colorless gum. Its UV (**Figure 30**) and IR (**Figure 31**) absorption bands were almost identical to those of **GP7**. The ^{1}H NMR spectrum (**Figure 32**) (**Table 45**) contained signals of one aromatic proton (δ_H 6.00, *s*), one 4-methyl-3-pentenyl unit [δ_H 5.12 (*mt*, J = 7.2 Hz, 1H), 2.11 (*m*, 2H), 1.60 (*m*, 2H), 1.68 (*s*, 3H) and 1.63 (*s*, 3H)], one oxymethine proton (δ_H 4.73, *t*, J = 8.7 Hz, 1H), two methylene protons (δ_H 3.03, *d*, J = 8.7 Hz, 2H), one methyl group (δ_H 1.29, *s*) and one methoxyl group (δ_H 4.03, *s*). The ^{1}H NMR data revealed the replacement of the olefinic proton signal of the chromene unit in **GP1** with signal of the oxymethine (δ_H

4.73) and methylene (δ_H 3.03) protons in **GP6**. ^3J HMBC correlations (**Figure 36**) of the oxymethine proton/C-9 (δ_C 36.68) and C-15 (δ_C 22.72) as well as those of the methylene protons/C-2 (δ_C 73.70) and C-8a (δ_C 167.06) established the location of these protons at C-3 and C-4, respectively. The relative configuration of the methyl group at C-2 and the hydroxyl group at C-3 was assigned as *trans* since irradiation of H-3 enhanced the signal intensity of H_3-15 in the NOEDIFF experiment (**Figure 37**). Thus, **GP6** was determined as 2-methyl-2-(4-methyl-3-pentenyl)-6-methylcarboxy-3,4-dihydrobenzopyran-3,5,7-triol, a new dihydrobenzopyran derivative.

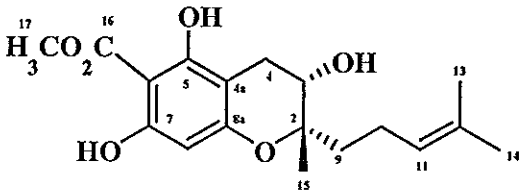

Table 45 The 300 MHz NMR data of compound GP6 in $CDCl_3$

Position	δ_H (*mult.*, J_{Hz})	δc (C-type)	HMBC correlations	NOE
2		73.70 (C)		
3	4.73 (*t*, 8.7)	91.01 (CH)	C-9, C-15	H-4, H-15
4	3.03 (*d*, 8.7)	26.65 (CH_2)	C-2, C-3, C-4a, C-8a	H-3
4a		105.08 (C)		
5-OH		167.06 (C)		
6		93.00 (C)		
7-OH		167.06 (C)		
8	6.00 (*s*)	90.83 (CH)	C-16	
8a		167.06 (C)		
9	1.60 (*m*)	36.68 (CH_2)	C-4a, C-6, C-8a	H-11
10	2.11 (*m*)	21.93 (CH_2)	C-11, C-12, C-15	H-11
11	5.12 (*mt*, 7.2)	124.03 (CH)	C-9, C-11, C-12	H-14
12		132.20 (C)		
13	1.63 (*s*)	17.65 (CH_3)	C-14	H-10

Table 45 (Continued)

Position	δ_H (*mult.*, J_{Hz})	δ_C (C-type)	HMBC correlations	NOE
14	1.68 (*s*)	25.66 (CH_3)	C-13	H-11
15	1.29 (*s*)	22.72 (CH_3)	C-2, C-3, C-9	H-3, H-4
16		169.82 (C=O)		
17-OCH_3	4.03 (*s*)	52.36 (CH_3)	C-16	

3.2.3 Compound GP3

Compound **GP3** with the molecular formula $C_{28}H_{42}O_2$ from EIMS (*m/z* 410) (**Figure 38**) was isolated as a yellow gum. It exhibited UV (**Figure 39**) absorption bands at 208, 227 and 298 nm while a hydroxyl absorption band was found at 3420 cm^{-1} in the IR spectrum (**Figure 40**). The ^1H NMR spectrum (**Figure 41**) (**Table 46**) contained signals of one aromatic proton (δ_H 6.36, *brs*), one hydroxyl group (δ_H 4.35, *brs*), four methylene protons of a chroman ring [δ_H 2.67 (*t*, J = 6.6 Hz, 2H) and 1.75 (*m*, 2H)], one 4,8,12-trimethyltrideca-3,7,11-trienyl unit [δ_H 5.12 (*m*, 3H), 2.12 (*m*, 2H), 2.07 (*m*, 6H), 1.96 (*m*, 2H), 1.66 (*m*, 1H), 1.54 (*m*, 1H), 1.68 (*s*, 3H), 1.61 (*s*, 3H), 1.60 (*s*, 3H) and 1.58 (*s*, 3H)], two aromatic methyl groups [δ_H 2.13 (*s*, 6H)] and one quaternary methyl group [δ_H 1.26 (*s*, 3H)]. The presence of 4,8,12-trimethyltrideca-3,7,11-trienyl moiety was established by COSY (**Figure 44**), HMQC (**Figure 45**) and HMBC (**Figure 46**) correlations. The singlet aromatic proton at δ_H 6.36 was assigned as H-5, according to ^3J HMBC correlations of H-5 with C-4 (δ_C 22.29), C-7 (δ_C 125.82), C-8a (δ_C 145.70) and C-26 (δ_C 11.85). These also indicated the attachment of the methyl group (δ_H 2.13, H_3-26) and the methylene protons (δ_H 2.67, H_2-4) at C-6 (δ_C 121.65) and C-4a (δ_C 118.24), respectively. The HMBC cross peaks between the other methylene protons (δ_H 1.75, H_2-3) of the chroman ring and C-4a, C-9 (δ_C 39.80) and C-25 (δ_C 24.10) constructed the chroman ring carrying the methyl group and 4,8,12-trimethyltrideca-3,7,11-trienyl moiety at C-2. These further indicated the formation of the chroman ring at C-4a and C-8a with an ether linkage at

C-8a. Irradiation of H_2-4 in NOEDIFF (**Figure 47**) experiment affected signal intensity of H_2-3, H-5 and H_3-25. The location of the remaining aromatic methyl group was assigned at C-7 (δ_C 125.82) on the basis of the chemical-shift values of C-8 (δ_C 146.28) and C-8a which suggested the presence of two adjacent oxysubstituents. Thus, **GP3** was determined as 2,6,7-trimethyl-2-(4,8,12-trimethyltrideca-3,7,11-trienyl)-3,4-dihydrobenzopyran-8-ol, a new dihydrobenzopyran derivative.

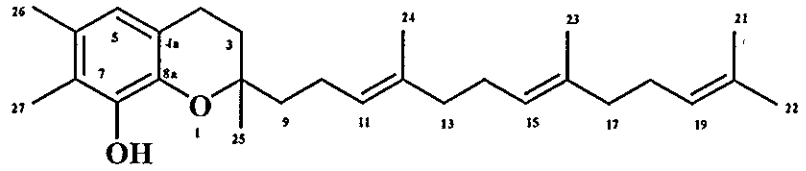

Table 46 The 300 MHz NMR data of compound GP3 in $CDCl_3$

Position	δ_H (*mult.*, J_{Hz})	δ_C (C-type)	HMBC correlations	NOE
2		75.23 (C)		
3	1.75 (*m*)	31.44 (CH_2)	C-2, C-4, C-4a, C-9, C-25	
4	2.67 (*t, 6.6*)	22.29 (CH_2)	C-2, C-3, C-4a, C-5, C-8a	H-3, H-5, H-25
4a		118.24 (C)		
5	6.36 (*brs*)	112.16 (CH)	C-4, C-6, C-7, C-8a, C-26	H-4, H-26
6		121.65 (C)		
7		125.82 (C)		
8-OH	4.35 (*brs*)	146.28 (C)		
8a		145.70 (C)		
9	1.66 (*m*)	39.80 (CH_2)	C-2, C-3, C-25	
	1.54 (*m*)			
10	2.07 (*m*)	26.77 (CH_2)[a]	C-2, C-11, C-12	
11	5.12 (*m*)	124.36 (CH)[b]	C-9	
12		135.09 (C)[c]		

Table 46 (Continued)

Position	δ_H (*mult.*, J_{Hz})	δ_C (C-type)	HMBC correlations	NOE
13	2.12 (*m*)	39.80 (CH_2)		
14	2.07 (*m*)	26.61 (CH_2)[a]	C-15, C-16	H-23
15	5.12 (*m*)	124.42 (CH)[b]	C-13, C-23	
16		134.96 (C)[c]		
17	1.96 (*m*)	39.72 (CH_2)	C-15, C-16, C-23	
18	2.07 (*m*)	26.77 (CH_2)[a]	C-19, C-20	H-21
19	5.12 (*m*)	124.21 (CH)[b]	C-18	
20		131.25 (C)		
21	1.60 (*s*)	17.68 (CH_3)	C-19, C-20, C-22	H-18
22	1.68 (*s*)	25.69 (CH_3)	C-19, C-20, C-21	
23	1.58 (*s*)	16.00 (CH_3)	C-15, C-16, C-17	
24	1.61 (*s*)	15.89 (CH_3)	C-11, C-12, C-13	
25	1.26 (*s*)	24.01 (CH_3)	C-2, C-3, C-9	H-3, H-4
26	2.13 (*s*)	11.85 (CH_3)	C-5, C-6, C-7	H-5
27	2.13 (*s*)	11.90 (CH_3)	C-6, C-7, C-8	

[a,b,c] Chemical shifts with the same index may be interchanged.

3.2.4 Compound GP5

Compound **GP5** with the molecular formula $C_{27}H_{40}O_2$ from EIMS (*m/z* 396) (**Figure 48**) was isolated as a colorless gum. It exhibited UV (**Figure 49**) and IR (**Figure 50**) absorption bands almost identical to those of **GP3**. The ^{1}H NMR spectrum (**Figure 51**) (**Table 47**) contained signals of two *meta*-aromatic protons [δ_H 6.47 (*d*, J = 2.7 Hz, 1H) and 6.37 (*d*, J = 2.7 Hz, 1H)], four methylene protons of a chroman ring [δ_H 2.69 (*t*, J = 6.6 Hz, 2H) and 1.76 (*m*, 2H)], one 4,8,12-trimethyltrideca-3,7,11-trienyl unit [δ_H 5.11 (*m*, 3H), 2.12 (*m*, 2H), 2.07 (*m*, 2H), 2.01 (*m*, 2H), 1.97 (*m*, 4H), 1.69 (*m*, 1H), 1.53 (*m*, 1H), 1.68 (*s*, 3H), 1.60 (*s*, 3H), 1.59 (*s*, 3H) and 1.58 (*s*, 3H)], one aromatic methyl group [δ_H 2.12 (*s*, 3H)] and one

oxyquaternary methyl group [δ_H 1.26 (*s*, 3H)]. The ^{1}H NMR data were similar to those of **GP3** except that signals for the aromatic proton and one of the aromatic methyl signals in **GP3** were replaced by signals of two *meta*-aromatic protons (δ_H 6.47 and 6.37) in **GP5**. The higher field aromatic proton was attributed to H-5 according to its ^3J HMBC correlations (**Figure 55**) with C-4 (*δc* 22.49), C-7 (*δc* 115.66), C-8a (*δc* 145.99) and C-26 (*δc* 16.00). The other *meta*-aromatic proton and the aromatic methyl group were then located at C-7 and C-6 (*δc* 127.36), respectively. Signal enhancement of both H-4 and H_3-26 after irradiation of H-5 in the NOEDIFF experiment (**Figure 56**) supported above assignment. The remaining HMBC correlations and NOEDIFF results were similar to those of **GP3**. Thus, **GP5** was determined as 2,6-dimethyl-2-(4,8,12-trimethyltrideca-3,7,11-trienyl)-3,4-dihydrobenzopyran-8-ol, a new dihydro-benzopyran derivative.

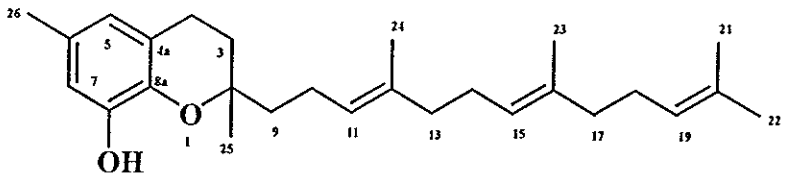

Table 47 The 300 MHz NMR data of compound GP5 in $CDCl_3$

Position	δ_H (*mult.*, J_{Hz})	*δc* (C-type)	HMBC correlations	NOE
2		75.34 (C)		
3	1.76 (*m*)	31.38 (CH_2)	C-2, C-4, C-4a, C-9, C-25	
4	2.69 (*t*, 6.6)	22.49 (CH_2)	C-2, C-3, C-4a, C-5, C-8, C-8a	H-5, H-25
4a		121.25 (C)		
5	6.37 (*d*, 2.7)	112.61 (CH)	C-4, C-7, C-8a, C-26	H-4, H-26
6		127.36 (C)		

Table 47 (Continued)

Position	δ_H (*mult.*, J_{Hz})	δc (C-type)	HMBC correlations	NOE
7	6.47 (*d*, 2.7)	115.66 (CH)	C-5, C-8, C-8a, C-26	H-26
8-OH		147.75 (C)		
8a		145.99 (C)		
9	1.69 (*m*)	39.69 (CH_2)[a]	C-2, C-3, C-10, C-25	
	1.53 (*m*)			
10	2.12 (*m*)	22.18 (CH_2)	C-2, C-11, C-12	H-24
11	5.11 (*m*)	124.31 (CH)[b]	C-9	
12		135.13 (C)[c]		
13	1.97 (*m*)	39.71 (CH_2)[a]	C-11, C-12, C-14	
14	2.07 (*m*)	26.60 (CH_2)		
15	5.11 (*m*)	124.42 (CH)[b]	C-13, C-14	
16		134.97 (C)[c]		
17	1.97 (*m*)	39.71 (CH_2)[a]	C-15, C-16, C-18	
18	2.01 (*m*)	26.77 (CH_2)	C-17	
19	5.11 (*m*)	124.31 (CH)[b]	C-21, C-22	
20		131.25 (C)		
21	1.60 (*s*)	15.87 (CH_3)	C-19, C-20, C-22	
22	1.68 (*s*)	25.69 (CH_3)	C-19, C-20	H-19
23	1.59 (*s*)	17.68 (CH_3)	C-15, C-16	
24	1.58 (*s*)	16.04 (CH_3)[d]	C-11, C-12	
25	1.26 (*s*)	24.03 (CH_3)	C-2, C-3, C-9	H-4, H-9, H-10
26	2.12 (*s*)	16.00 (CH_3)[d]	C-5, C-6, C-7	H-5, H-7

[a,b,c,d] Chemical shifts with the same index may be interchanged.

3.2.5 Compound GP4

Compound **GP4** was isolated as a colorless gum. It showed the molecular ion at *m/z* 426 ($C_{28}H_{42}O_3$) from EIMS (**Figure 57**), which was higher than that of **GP3** by one oxygen atom. Its UV (**Figure 58**) and IR (**Figure 59**) absorption bands were almost identical to those of **GP3**. The ^{1}H NMR spectrum (**Figure 60**) (**Table 48**) contained signals of one hydroxyl group (δ_H 4.44, *brs*), four methylene protons of a chroman ring [δ_H 2.32 (*m*, 1H), 2.11 (*m*, 1H), 1.68 (*m*, 2H)], one 4,8,12-trimethyltrideca-3,7,11-trienyl unit [δ_H 5.14 (*m*, 1H), 5.10 (*m*, 2H), 2.11 (*m*, 2H), 2.07 (*m*, 4H), 2.00 (*m*, 4H), 1.59 (*m*, 2H), 1.68 (*s*, 3H), 1.60 (*brs*, 3H) and 1.59 (*s*, 6H)], two aromatic methyl groups [δ_H 2.20 (*s*, 3H) and 2.19 (*s*, 3H)] and one oxyquarternary methyl group [δ_H 1.26 (*s*, 3H)]. The ^{1}H NMR data were similar to those of **GP3** except for the disappearance of the aromatic proton in **GP4**. The EIMS data revealed the presence of an additional hydroxyl group in **GP4**. HMBC correlations (**Figure 64**) of H_2-4 (δ_H 2.32 and 2.11)/C-4a (δ_C 117.28) and C-5 (δ_C 115.17) and those of H_3-26 (δ_H 2.20)/C-4a, C-5 and C-6 (δ_C 126.89) established the linkage of the methyl group at C-5. The other aromatic methyl group (δ_C 2.19) was attached to C-8 (δ_C 122.22) on the basis of HMBC correlations of H_3-27/C-7 (δ_C 144.72), C-8 and C-8a (δ_C 145.86) and the chemical-shift values of C-6, C-7 and C-8a. Signal enhancement of H_3-27 after irradiation of H_3-25 in the NOEDIFF experiment (**Figure 65**) supported above assignment. Thus, **GP4** was determined as 2,5,8-trimethyl-2-(4,8,12-trimethyltrideca-3,7,11-trienyl)-3,4-dihydrobenzopyran-6,7-diol, a new dihydrobenzopyran derivative.

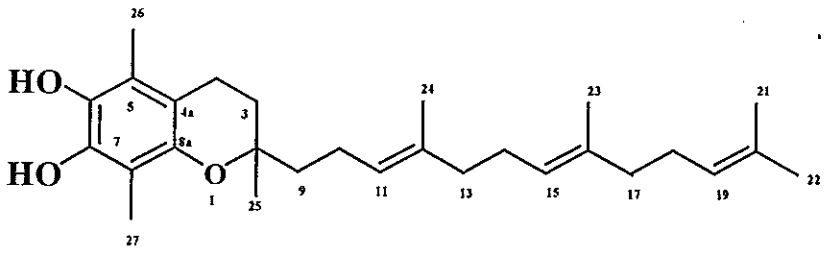

Table 48 The 300 MHz NMR data of compound GP4 in $CDCl_3$

Position	δ_H (*mult.*, J_{Hz})	δc (C-type)	HMBC correlations	NOE
2		74.96 (C)		
3	1.68 (*m*)	31.27 (CH_2)	C-4, C-4a, C-25	
4	2.32(*m*)	20.62 (CH_2)	C-2, C-3, C-4a, C-5	H-9, H-25
	2.11(*m*)			
4a		117.28 (C)		
5		115.17 (C)		
6-OH		126.89 (C)		
7-OH	4.44 (*brs*)	144.72 (C)	C-7, C-8	
8		122.22 (C)		
8a		145.86 (C)		
9	1.59 (*m*)	39.82 (CH_2)	C-3, C-10, C-25	
10	2.11(*m*)	22.20 (CH_2)	C-11, C-12	
11	5.10 (*m*)	124.24 (CH)	C-9, C-13, C-24	
12		135.20 (C)		
13	2.00 (*m*)	39.72 (CH_2)	C-11, C-12, C-14, C-15, C-24	
14	2.07 (*m*)	26.76 (CH_2)	C-13, C-15, C-16	
15	5.14 (*m*)	124.18 (CH)	C-13, C-17, C-23	
16		134.97 (C)		
17	2.00 (*m*)	39.72 (CH_2)	C-15, C-18, C-19, C-23	
18	2.07 (*m*)	26.65 (CH_2)	C-16, C-19, C-20	
19	5.10 (*m*)	124.39 (CH)	C-17, C-18, C-20, C-21	

Table 48 (Continued)

Position	δ_H (*mult.*, J_{Hz})	δ_C (C-type)	HMBC correlations	NOE
20		131.24 (C)		
21	1.60 (*brs*)	17.68 (CH_3)	C-19, C-20, C-22	
22	1.68 (*s*)	25.69 (CH_3)	C-19, C-20, C-21	
23	1.59 (*s*)	15.85 (CH_3) [a]	C-15, C-16, C-17	
24	1.59 (*s*)	16.00 (CH_3) [a]	C-11, C-12, C-13	
25	1.26 (*s*)	23.83 (CH_3)	C-2, C-3, C-9	H-3, H-4, H-9, H-27
26	2.20 (*s*)	11.98 (CH_3) [b]	C-4a, C-5, C-6	
27	2.19 (*s*)	12.25 (CH_3) [b]	C-7, C-8, C-8a	

[a,b] Chemical shifts with the same index may be interchanged.

3.3 Depsidone derivatives

3.3.1 Compound GP18

Compound **GP18** was isolated as a yellow gum. It exhibited UV (**Figure 66**) absorption bands at 231, 281 and 324 nm while the hydroxyl and conjugated carbonyl absorption bands were found at 3381 and 1660 cm^{-1}, respectively, in the IR spectrum (**Figure 67**). The ^1H NMR spectrum (**Figure 68**) (**Table 49**) contained signals of one chelated hydroxyl group (δ_H 11.30, *s*), two aromatic protons [δ_H 6.67 (*s*, 1H) and 6.27 (*s*, 1H)], one geranyl unit [δ_H 5.22 (*mt*, J = 7.2 Hz, 1H), 5.04 (*mt*, J = 6.9 Hz, 1H), 3.39 (*d*, J = 7.2 Hz, 2H), 2.09 (*m*, 2H), 2.06 (*m*, 2H), 1.80 (*s*, 3H), 1.67 (*s*, 3H) and 1.58 (*s*, 3H)] and one prenyl unit [δ_H 5.25 (*mt*, J = 7.2 Hz, 1H), 3.55 (*d*, J = 7.2 Hz, 2H), 1.84 (*s*, 3H) and 1.75 (*s*, 3H)]. The chemical-shift values of the chelated hydroxy proton (δ_H 11.30) and the ester carbonyl carbon (δ_C 168.70) indicated that **GP18** had a depsidone chromophore. In the HMBC spectrum (**Figure 72**), the chelated hydroxy proton, which was located at the peri-position to the lactone carbonyl group, showed correlations with C-1 (δ_C 162.60), C-2 (δ_C 110.91) and C-11a (δ_C 98.53). The geranyl unit was then linked at C-2 on the basis of HMBC correlations between H_2-12 (δ_H

3.39)/C-1, C-2 and C-3 (δ_C 162.34). The aromatic proton (δ_H 6.27) was located at C-4 (δ_C 100.33) according to the HMBC correlations of H-4/C-2, C-3, C-4a (δ_C 160.08) and C-11a. The remaining aromatic proton at δ_H 6.67 was attributed to H-6 due to its HMBC correlations with C-5a (δ_C 141.84), C-7 (δ_C 143.43), C-8 (δ_C 136.18) and C-9a (δ_C 139.82). ^3J HMBC correlations between the methylene protons [H_2-22 (δ_H 3.35)] and C-8 and C-9a established the attachment of the prenyl unit at C-9 (δ_C 135.68). According to the chemical-shift values of C-3, C-7 and C-8, these carbons carried hydroxyl substituents. Signal enhancement of H-6 in the NOEDIFF experiment **(Figure 73)**, upon irradiation of H-4, supported above assignment. Thus, **GP18** was 1,3,7,8-tetrahydoxy-9-(3-methylbut-2-enyl)-2-(3,7-dimethylocta-2,6-dienyl)dibenzo-[*b,e*][1,4]dioxepin-11-one (garcidepsidone B), previously isolated from leaves of *Garcinia parvifolia* (Xu, 2000).

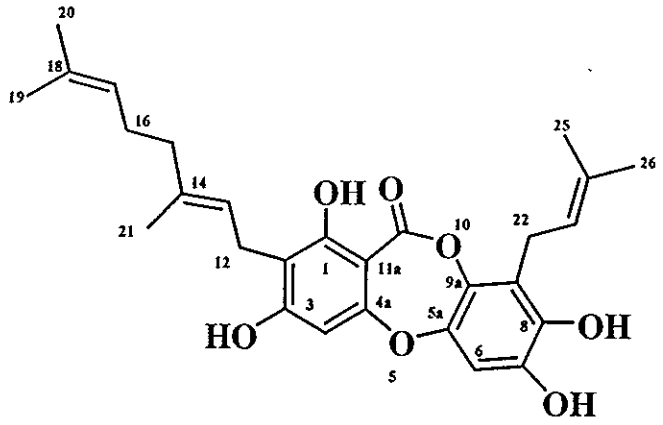

Table 49 The 300 MHz NMR data of compound GP18 in $CDCl_3$

Position	δ_H (*mult.*, J_{Hz})	δ_C (C-type)	HMBC correlations	NOE
1-OH	11.30 (*s*)	162.60 (C)	C-1, C-2, C-11a	
2		110.91 (C)		
3-OH		162.34 (C)		
4	6.27 (*s*)	100.33 (CH)	C-2, C-3, C-4a, C-11a	H-6

Table 49 (Continued)

Position	δ_H (*mult.*, J_{Hz})	δ_C (C-type)	HMBC correlations	NOE
4a		160.08 (C)		
5a		141.84 (C)[a]		
6	6.67 (*s*)	105.09 (CH)	C-5a, C-7, C-8, C-9a	H-4
7-OH		143.43 (C)[a]		
8-OH		136.18 (C)[b]		
9		135.68 (C)		
9a		139.82 (C)[b]		
11		168.70 (C=O)		
11a		98.53 (C)		
12	3.39 (*d*, 7.2)	21.95 (CH_2)	C-1, C-2, C-3, C-13, C-14	H-13, H-21
13	5.22 (*mt*, 7.2)	120.76 (CH)	C-12, C-15, C-21	
14		139.72 (C)		
15	2.09 (*m*)	39.68 (CH_2)	C-13, C-14, C-16, C-17, C-21	
16	2.06 (*m*)	26.30 (CH_2)	C-14, C-16, C-17	
17	5.04 (*mt*, 6.9)	123.65 (CH)	C-15, C-16, C-19, C-20	
18		132.12 (C)		
19	1.58 (*s*)	17.68 (CH_3)	C-17, C-18, C-20	
20	1.67 (*s*)	25.65 (CH_3)	C-17, C-18, C-19	
21	1.80 (*s*)	16.22 (CH_3)	C-13, C-14, C-15	
22	3.55 (*d*, 7.2)	23.88 (CH_2)	C-8, C-9a, C-23, C-26	H-23, H-25
23	5.25 (*mt*, 7.2)	120.31 (CH)	C-26, C-25	H-22, H-26
24		136.18 (C)		
25	1.84 (*s*)	17.98 (CH_3)	C-23, C-24, C-26	
26	1.75 (*s*)	25.77 (CH_3)	C-23, C-24, C-25	

[a,b] Chemical shifts with the same index may be interchanged.

3.3.2 Compound GP14

Compound **GP14** with the molecular formula $C_{28}H_{32}O_7$ from EIMS (*m/z* 480) (**Figure 74**) was isolated as a yellow gum. It exhibited UV (**Figure 75**) and IR (**Figure 76**) absorption bands similar to those of **GP18**. The ^{1}H NMR spectrum (**Figure 77**) (**Table 50**) contained signals of one chelated hydroxyl group (δ_H 10.72, *s*), two aromatic protons [δ_H 6.69 (*s*, 1H) and 6.29 (*s*, 1H)], three hydroxyl groups [δ_H 6.23 (*brs*, 1H), 5.59 (*brs*, 1H) and 5.53 (*brs*, 1H)], one prenyl unit [δ_H 5.25 (*mt*, J = 6.9 Hz, 1H), 3.57 (*d*, J = 6.9 Hz, 2H), 1.83 (*s*, 3H) and 1.76 (*s*, 3H)] and one geranyl unit [δ_H 5.20 (*mt*, J = 6.9 Hz, 1H), 5.05 (*mt*, J = 6.9 Hz, 1H), 3.57 (*d*, J = 6.9 Hz, 2H), 2.13 (*m*, 4H), 1.86 (*s*, 3H), 1.67 (*s*, 3H) and 1.60 (*s*, 3H)]. The ^{1}H NMR data were similar to those of **GP18** except for the differences in the HMBC correlations (**Figure 81**) observed in left hand ring. ^3J HMBC correlations of the aromatic proton δ_H 6.29/C-4 (δ_C 111.18) and C-11a (δ_C 99.29) established the attachment of the aromatic proton at C-2 (δ_C 100.90). The location of the geranyl group at C-4 was confirmed by ^3J HMBC correlations of the methylene protons (δ_H 3.57)/C-3 (δ_C 162.64) and C-4a (δ_C 158.74). Signal enhancement of H_2-12 (δ_H 3.57), H-13 (δ_H 5.20) and H_3-21 (δ_H 1.86) in the NOEDIFF experiment (**Figure 82**) after irradiation of H-6 (δ_H 6.69) confirmed the close proximity of H-6 and the geranyl group. The remaining HMBC correlations and NOEDIFF results were similar to those found in **GP18**. Therefore, **GP14** was determined as 1,3,7,8-tetrahydroxy-9-(3-methylbut-2-enyl)-4-(3,7-dimethylocta-2,6-dienyl)dibenzo[*b,e*][1,4]dioxepin-11-one, a new depsidone derivative.

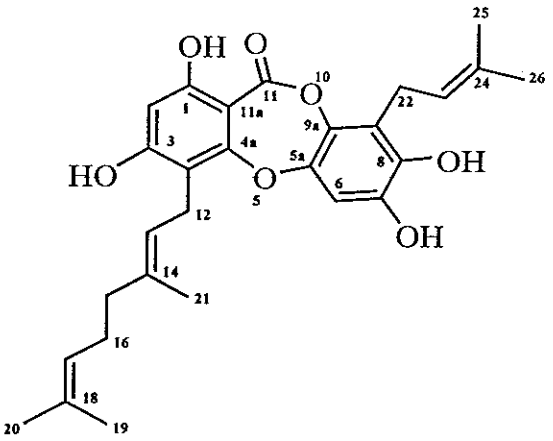

Table 50 The 300 MHz NMR data of compound GP14 in $CDCl_3$

Position	δ_H (*mult.*, J_{Hz})	δc (C-type)	HMBC correlations	NOE
1-OH	10.72 (*s*)	163.20 (C)	C-1, C-2, C-11, C-11a	
2	6.29 (*s*)	100.90 (CH)	C-4, C-11a, C-12	
3-OH	6.23 (*brs*)	162.64 (C)	C-2, C-3, C-4	
4		111.18 (C)		
4a		158.74 (C)		
5a		143.41 (C)		
6	6.69 (*s*)	105.39 (CH)	C-5a, C-7, C-8, C-9a	H-12, H-13, H-21
7-OH	5.53 (*brs*)	141.95 (C)	C-6, C-7, C-8	
8-OH	5.59 (*brs*)	139.83 (C)	C-7, C-8, C-9	
9		119.95 (C)		
9a		135.86 (C)		
11		168.32 (C)		
11a		99.29 (C)		
12	3.57 (*d*, 6.9)	22.44 (CH_2)	C-3, C-4, C-4a, C-13, C-14, C-21	H-6, H-13, H-21
13	5.20 (*mt*, 6.9)	121.30 (CH)	C-4, C-12, C-15, C-21	H-6, H-12, H-15

Table 50 (Continued)

Position	δ_H (*mult.*, J_{Hz})	δ_C (C-type)	HMBC correlations	NOE
14		139.36 (C)		
15	2.13 (*m*)	39.65 (CH_2)	C-13, C-14, C-16, C-17	
16	2.13 (*m*)	26.31 (CH_2)	C-14, C-15, C-17, C-18	
17	5.05 (*mt*, 6.9)	123.63 (CH)	C-19	H-15, H-16, H-20
18		132.24 (C)		
19	1.60 (*s*)	17.70 (CH_3)	C-17, C-18, C-20	H-16
20	1.67 (*s*)	25.69 (CH_3)	C-17, C-18	H-17
21	1.86 (*s*)	16.35 (CH_3)	C-13, C-14, C-15	H-6, H-12, H-16
22	3.57 (*d*, 6.9)	23.92 (CH_2)	C-8, C-9a, C-22, C-23	H-23, H-25
23	5.25 (*mt*, 6.9)	120.15 (CH)	C-22, C-25, C-26	H-22, H-26
24		136.70 (C)		
25	1.83 (s)	17.99 (CH_3)	C-23, C-24, C-26	H-22
26	1.76 (s)	25.76 (CH_3)	C-23, C-24, C-25	H-23

3.3.3 Compound GP12

Compound **GP12** with the molecular formula $C_{28}H_{30}O_7$ from EIMS (*m/z* 478) **(Figure 83)** was isolated as a yellow gum. The UV **(Figure 84)** and IR **(Figure 85)** absorption bands indicated the presence of the depsidone chromophore. The ^1H NMR spectrum **(Figure 86)** **(Table 51)** contained signals of one chelated hydroxyl proton (δ_H 11.36, *s*), two aromatic protons [δ_H 6.69 (*s*, 1H) and 6.29 (*s*, 1H)], two hydroxyl groups [δ_H 6.26 (*brs*, 1H) and 5.39 (*brs*, 1H)], two olefinic protons of a dimethyl chromene ring [δ_H 6.76 (*d*, J = 10.2 Hz, 1H), 5.75 (*d*, J = 10.2 Hz, 1H) and 1.46 (*s*, 6H)] and one geranyl unit [δ_H 5.23 (*mt*, J = 7.2 Hz, 1H), 5.04 (*mt*, J = 6.6 Hz, 1H),

3.41 (*d*, J = 7.2 Hz, 2H), 2.08 (*m*, 4H), 1.80 (*s*, 3H), 1.68 (*s*, 3H) and 1.59 (*s*, 3H)]. The ^{1}H NMR data were similar to those of **GP18** except for the fact that signals of the prenyl substituent in **GP18** were replaced by signals of the dimethylchromene ring in **GP12.** The HMBC correlations (**Figure 90**) between olefinic proton, H-22 (δ_H 6.76), with C-8 (δ_C 136.45), C-9a (δ_C 132.58) and C-24 (δ_C 77.21) and those of H-23 with C-9 (δ_C 113.80) and C-24, established the attachment of the chromene ring at C-9 with an ether linkage at C-8. The remaining HMBC correlations and NOEDIFF results were similar to those found in **GP18.** Thus, **GP12** was determined as 1,3,7-trihydroxy-2-(3,7-dimethylocta-2,6-dienyl)-24,24-dimethyl-2H-pyran[9,8-*b*]dibenzo-[*b,e*][1,4]dioxepin-11-one, a new depsidone derivative.

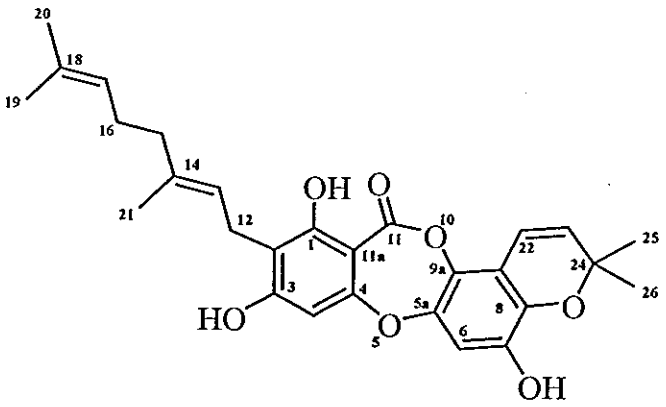

Table 51 The 300 MHz NMR data of compound GP12 in $CDCl_3$

Position	δ_H (*mult.*, J_{Hz})	δc (C-type)	HMBC correlations	NOE
1-OH	11.36 (*s*)	162.41 (C)	C-1, C-2, C-11a	
2		110.76 (C)		
3-OH	6.26 (*brs*)	162.60 (C)		
4	6.29 (*s*)	100.52 (CH)	C-1, C-2, C-3, C-4a, C-11a	H-6
4a		160.08 (C)		
5a		142.24 (C)		

Table 51 (Continued)

Position	δ_H (*mult.*, J_{Hz})	δ_C (C-type)	HMBC correlations	NOE
6	6.69 (*s*)	106.43 (CH)	C-5a, C-7, C-8, C-9a, C-24	H-4
7-OH	5.39 (*brs*)	143.10 (C)		
8		136.45 (C)		
9		113.80 (C)		
9a		132.58 (C)		
11		168.50 (C)		
11a		98.53 (C)		
12	3.41 (*d*, 7.2)	21.95 (CH_2)	C-1, C-2, C-3, C-13, C-14	H-13, H-21
13	5.23 (*mt*, 7.2)	120.67 (CH)		
14		140.25 (C)		
15	2.08 (*m*)	39.67 (CH_2)	C-14, C-16	
16	2.08 (*m*)	26.25 (CH_2)	C-14, C-15	
17	5.04 (*mt*, 6.6)	123.58 (CH)		H-15, H-20
18		132.25 (C)		
19	1.59 (*s*)	17.70 (CH_3)	C-17, C-18, C-20	
20	1.68 (*s*)	25.65 (CH_3)	C-17, C-18, C-19	
21	1.80 (*s*)	16.23 (CH_3)	C-13, C-14, C-15	
22	6.76 (*d*, 10.2)	116.22 (CH)	C-8, C-9a, C-24	H-23
23	5.75 (*d*, 10.2)	132.06 (CH)	C-9, C-24	H-22, H-25, H-26
24		77.21 (C)		
25	1.46 (*s*)	27.70 (CH_3)	C-23, C-24, C-26	
26	1.46 (*s*)	27.70 (CH_3)	C-23, C-24, C-25	

3.4 Xanthone derivatives

3.4.1 Compound GP9

Compound **GP9** with the molecular formula $C_{28}H_{32}O_6$ by EIMS (*m/z* 464) **(Figure 91)** was isolated as a yellow gum. It exhibited UV **(Figure 92)** absorption bands of a xanthone chromophore at 256, 286 and 329 nm while the hydroxyl and conjugated carbonyl absorption bands were found at 3346 and 1641 cm^{-1}, respectively, in the IR spectrum **(Figure 93)**. The ^1H NMR spectrum **(Figure 94)** **(Table 52)** contained signals of one chelated hydroxyl group (δ_H 13.32, *s*), one aromatic proton (δ_H 7.58, *s*), three prenyl units: unit 1 [δ_H 5.28 (*mt*, J = 7.2 Hz, 1H), 3.46 (*d*, J = 7.2 Hz, 2H), 1.85 (*s*, 3H) and 1.78 (*d*, J = 1.2 Hz, 3H)], unit 2 [δ_H 5.25 (*mt*, J = 6.6 Hz, 1H), 3.52 (*d*, J = 6.6 Hz, 2H), 1.85 (*s*, 3H) and 1.73 (*s*, 3H)] and unit 3 [δ_H 5.34 (*mt*, J = 7.5 Hz, 1H), 3.41 (*d*, J = 7.5 Hz, 2H), 1.77 (*s*, 3H) and 1.75 (*s*, 3H)] and three hydroxyl groups [δ_H 6.43 (*s*), 6.15 (*brs*) and 5.67 (*brs*)]. The ^{13}C NMR **(Figure 95)** **(Table 52)**, DEPT **(Figure 96)** and HMQC **(Figure 97)** data indicated that **GP9** consisted of 15 quaternary, 4 methine, 3 methylene and 6 methyl carbons. The location of all substituents was established by HMBC data **(Figure 98)** as follows. The chelated hydroxyl group was placed at C-1 (δ_C 158.62), a peri-position of the xanthone carbonyl group, and gave a ^2J cross peak with C-1 and ^3J ones with C-2 (δ_C 108.94) and C-9a (δ_C 102.91). ^3J HMBC correlations between the methyene protons [H_2-11, (δ_H 3.46)] of the prenyl unit 1 and C-1 and C-3 (δ_C 160.34) and those between the methylene protons [H_2-16, (δ_H 3.52)] of the prenyl unit 2 and C-3 and C-4a (δ_C 152.56) established the attachment of the prenyl units I and II at C-2 and C-4 (δ_C 105.22), respectively. The singlet aromatic proton at δ_H 7.58 was attributed to H-8 on the basis of the chemical-shift value and ^3J HMBC correlations of H-8/C-6 (δ_C 147.69), C-9 (δ_C 180.68) and C-10a (δ_C 143.67). The prenyl unit 3 was linked at C-7 due to HMBC correlations between the methylene protons [H_2-21 (δ_H 3.41)] with C-6, C-7 (δ_C 125.27) and C-8 (δ_C 117.11). According to the chemical-shift values of C-3 and C-6, these carbons carried hydroxyl substituents. Furthermore, HMBC correlations of the hydroxy proton (δ_H 6.43)/C-2, C-3 and C-4 and those of the

hydroxy proton (δ_H 6.15)/C-5, C-6 and C-7 established the linkage of these hydroxyl groups at C-3 and C-6, respectively. Thus, the remaining hydroxy proton at δ 5.67 belonged to the C-5 hydroxyl group. Signal enhancement in the NOEDIFF experiment of H_2-11 and H-17 upon irradiation of 3-OH (**Figure 100**) and that of H_2-21 after irradiation of H-8 (**Figure 99**) supported the assigned location of all prenyl substituents. Therefore, **GP9** was determined as 1,3,5,6-tetrahydroxy-2,4,7-tri(3-methylbutyl-2-enyl)xanthone, a new tetraoxygenated xanthone.

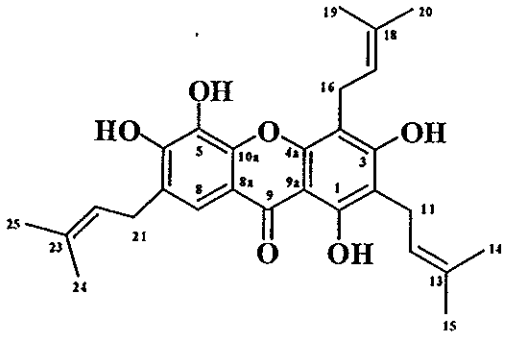

Table 52 The 300 MHz NMR data of compound GP9 in $CDCl_3$

Position	δ_H (*mult.*, J_{Hz})	δc (C-type)	HMBC correlations	NOE
1-OH	13.32 (*s*)	158.62(C)	C-1, C-2, C-9a	
2		108.94 (C)		
3-OH	6.43 (*s*)	160.34 (C)	C-2, C-3, C-4	H-11, H-12, H-17
4		105.22 (C)		
4a		152.56 (C)		
5-OH	5.67 (*brs*)	130.08 (C)		
6-OH	6.15 (*brs*)	147.69 (C)	C-5, C-6, C-7	
7		125.27 (C)		
8	7.58 (*s*)	117.11 (CH)	C-6, C-9, C-10a, C-21	H-21, H-22
8a		113.38 (C)		
9		180.68 (C=O)		
9a		102.91 (C)		

Table 52 (Continued)

Position	δ_H (*mult.*, J_{Hz})	δ_C (C-type)	HMBC correlations	NOE
10a		143.67 (C)		
11	3.46 (*d*, 7.2)	21.63 (CH_2)	C-1, C-2, C-3, C-12, C-13	1-OH, 3-OH, H-14
12	5.28 (*mt*, 7.2)	121.40 (CH)		3-OH, H-11, H-15
13		135.83 (C)		
14	1.85 (*s*)	17.95 (CH_3)	C-12, C-13, C-15	
15	1.78 (*d*, 1.2)	25.84 (CH_3)	C-12, C-13, C-14	
16	3.52 (*d*, 6.6)	22.02 (CH_2)	C-3, C-4, C-4a, C-17, C-18	3-OH, H-17, H-19
17	5.25 (*mt*, 6.6)	122.33 (CH)		
18		133.50 (C)		
19	1.85 (*s*)	17.95 (CH_3)	C-17, C-18, C-20	
20	1.73 (*s*)	25.70 (CH_3)	C-17, C-18	
21	3.41 (*d*, 7.5)	28.47 (CH_2)	C-6, C-7, C-8, C-22, C-23	H-8, H-22, H-24
22	5.34 (*mt*, 7.5)	121.09 (CH)	C-21	H-8, H-21, H-25
23		134.39 (C)		
24	1.75 (*s*)	17.86 (CH_3)	C-22, C-23, C-25	
25	1.77 (*s*)	25.87 (CH_3)	C-22, C-23, C-24	

3.4.2 Compound GP8

Compound **GP8** with the molecular formula $C_{24}H_{26}O_6$ by EIMS (*m/z* 410) (**Figure 101**) was isolated as a yellow gum. The UV (**Figure 102**) and IR (**Figure 103**) absorption bands were similar to those of **GP9**, indicating that **GP8** had a xanthone chromophore. The ^{1}H NMR spectrum (**Figure 104**) (**Table 53**) contained signals of one chelated hydroxyl group (δ_H 13.12, *s*), two hydroxyl groups [δ_H 6.12 (*s*)

and 5.61 (*s*)], two aromatic protons [δ_H 7.60 (*s*) and 6.37 (*s*)], two prenyl units: unit 1 [δ_H 5.22 (*brs*, 1H), 3.49 (*d*, J = 5.7 Hz, 2H), 1.85 (*s*, 3H) and 1.71 (*s*, 3H)] and unit 2 [δ_H 5.35 (*mt*, J = 7.5 Hz, 1H), 3.42 (*d*, J = 7.5 Hz, 2H), 1.76 (*s*, 3H) and 1.77 (*s*, 3H)] and one methoxyl group (δ_H 3.91, *s*). Its ^{1}H NMR data were similar to those of **GP9** except that one of the prenyl signals in **GP9** was replaced by signal of a singlet aromatic proton at δ_H 6.37 in **GP8**. This proton was attributed to H-2 due to HMBC correlations of H-2/C-3 (δ_C 163.62), C-4 (δ_C 107.31), and C-9a (δ_C 102.99) (**Figure 108**). The additional methoxyl group was located at C-3 on the basis of a HMBC correlation of 3-OCH_3/C-3. The enhancement observed between H-2 and the methoxy protons in the NOEDIFF experiment (**Figure 109**) confirmed the assignment. The remaining HMBC correlations and NOEDIFF results were similar to those found in **GP9**. Thus, **GP8** as determined as 1,5,6-trihydroxy-3-methoxy-4,7-di(3-methylbutyl-2-enyl)xanthone, a new tetraoxygenated xanthone.

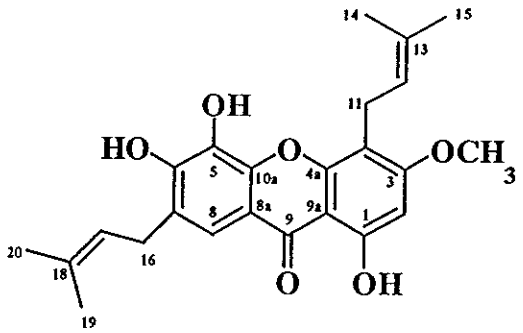

Table 53 The 300 MHz NMR data of compound GP8 in $CDCl_3$

Position	δ_H (*mult.*, J_{Hz})	δc (C-type)	HMBC correlations	NOE
1-OH	13.12 (*s*)	162.17(C)	C-1, C-2, C-9a	
2	6.37 (*s*)	94.36 (CH)	C-1, C-3, C-4, C-9a	3-OCH_3
3		163.62 (C)		
3-OCH_3	3.91 (*s*)	56.07 (CH_3)	C-3	
4		107.31 (C)		
4a		153.77 (C)		
5-OH	5.61 (*s*)	130.14 (C)		

Table 53 (Continued)

Position	δ_H (*mult.*, J_{Hz})	δc (C-type)	HMBC correlations	NOE
6-OH	6.12 (*s*)	147.75 (C)		
7		125.36 (C)		
8	7.60 (*s*)	117.10 (CH)	C-6, C-9, C-10a, C-16	H-16, H-17
8a		113.34 (C)		
9		180.69 (C=O)		
9a		102.99 (C)		
10a		143.76 (C)		
11	3.49 (*d*, 5.7)	21.72 (CH_2)	C-3, C-4, C-4a, C-12, C-13	H-12, H-14
12	5.22 (*brs*)	122.89 (CH)		
13		131.67 (C)		
14	1.85 (*s*)	17.86 (CH_3)	C-12, C-13, C-15	H-11
15	1.71 (*s*)	25.63 (CH_3)	C-12, C-13, C-14	
16	3.42 (*d*, 7.5)	28.39 (CH_2)	C-6, C-7, C-8, C-17, C-18	H-8, H-17, H-19
17	5.35 (*mt*, 7.5)	121.08 (CH)	C-19, C-20	H-8, H-16, H-20
18		134.34 (C)		
19	1.76 (*s*)	17.86 (CH_3)	C-17, C-18, C-20	
20	1.77 (*s*)	25.83 (CH_3)	C-17, C-18, C-19	

3.4.3 Compound GP20

Compound **GP20** was isolated as a yellow gum. It exhibited UV (**Figure 110**) absorption bands of a xanthone chromophore at 236, 253, 272, 313 and 365 nm while the hydroxyl and conjugated carbonyl absorption bands were found at 3231 and 1655 cm^{-1}, respectively, in the IR spectrum (**Figure 111**). The ^1H NMR spectrum (**Figure 112**) (**Table 54**) contained signals of two singlet aromatic protons (δ_H 7.44 and 6.82 and two *meta*-coupled aromatic protons [δ_H 6.28, J = 2.4 Hz and 6.15, J = 2.4 Hz].

The ^{13}C NMR (**Figure 113**) (**Table 54**) and HMQC (**Figure 114**) data indicated that compound **GP20** consisted of 13 carbons: 9 quarternary and 4 methine carbons. The aromatic proton at δ_H 7.44 was attributed to H-8 on the basis of the chemical-shift value and HMBC correlations (**Figure 115**) of H-8/C-6 (δ_C 153.77), C-7 (δ_C 143.38), C-9 (δ_C 179.73) and C-10a (δ_C 151.81). The aromatic proton at δ_H 6.82 gave ^2J cross peaks with C-6 and C-10a and ^3J ones with C-7 and C-8a (δ_C 112.47), indicating its attachment at C-5 (δ_C 102.10). Two *meta*-coupled aromatic protons (δ_H 6.15 and 6.28) were assigned as H-2 and H-4, respectively, according to HMBC cross peaks of H-2/C-1 (δ_C 162.93), C-3 (δ_C 164.84), C-4 (δ_C 93.30) and C-9a (δ_C 101.94) and those of H-4/C-2 (δ_C 97.36), C-3, C-4a (δ_C 157.99), C-9 (δ_C 179.73) and C-9a. The chemical-shift values of C-3, C-6 and C-7 suggested the substituents to be hydroxyl groups. Thus, **GP20** was determined as 1,3,6,7-tetrahydroxyxanthone (norathyriol), isolated from *Hypericum sampsonii* (Don, 2004).

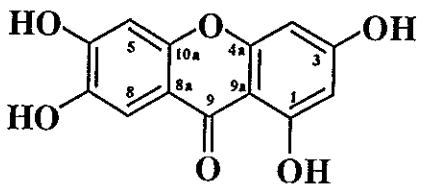

Table 54 The 300 MHz NMR data of compound GP20 in CD_3OD

Position	δ_H (*mult.*, J_{Hz})	δ_C (C-type)	HMBC correlations
1-OH		162.93 (C)	
2	6.15 (*d*, 2.4)	97.36 (CH)	C-1, C-3, C-4, C-9a
3-OH		164.84 (C)	
4	6.28 (*d*, 2.4)	93.30 (CH)	C-2, C-3, C-4a, C-9, C-9a
4a		157.99 (C)	
5	6.82 (*s*)	102.10 (CH)	C-6, C-7, C-8a, C-9, C-10a
6-OH		153.77 (C)*	
7-OH		143.38 (C)	
8	7.44 (*s*)	107.80 (CH)	C-6, C-7, C-9, C-10a

Table 54 (Continued)

Position	δ_H (*mult.*, J_{Hz})	δc (C-type)	HMBC correlations
8a		112.47 (C)	
9		179.73 (C=O)	
9a		101.94 (C)	
10a		151.81 (C)*	

* interchangeable

3.4.4 Compound GP19

Compound **GP19** was isolated as a yellow gum. The UV (**Figure 116**) and IR (**Figure 117**) absorption bands were similar to those of **GP20**. The ^{1}H NMR spectrum (**Figure 118**) (**Table 55**) contained signals of two *ortho*-coupled aromatic protons [δ_H 7.56, J = 8.7 Hz and 6.87, J = 8.7 Hz] and two *meta*-coupled aromatic protons [δ_H 6.42, J = 2.1 Hz and 6.16, J = 2.1 Hz]. The ^{1}H NMR data and HMBC correlations (**Figure 120**) of ring B were similar to those of **GP20**. The *ortho*-coupled aromatic protons at δ_H 7.56 and δ_H 6.87 were attributed to H-8 and H-7, respectively, on the basis of the chemical-shift value of H-8 and HMBC correlations of H-8/C-6 (δ_C 152.30), C-9 (δ_C 180.20) and C-10a (δ_C 146.30) and those of H-7/C-6 and C-8a (δ_C 112.10). Thus, **GP19** was determined as 1,3,5,6-tetrahydroxyxanthone, isolated from *Hypericum scabrum* (Tanaka, 2004).

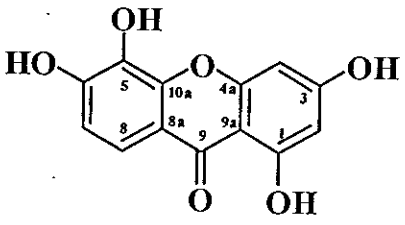

Table 55 The 300 MHz NMR data of compound GP19 in CD_3OD

Position	δ_H (*mult.*, J_{Hz})	δc (C-type)	HMBC correlations
1-OH		163.30 (C)	
2	6.16 (*d*, 2.1)	97.80 (CH)	C-1, C-3, C-4, C-9a
3-OH		166.00 (C)	
4	6.42 (*d*, 2.1)	93.20 (CH)	C-2, C-3, C-4a, C-9a
4a		158.00 (C)	
5-OH		132.80 (C)	
6-OH		152.30 (C)	
7	6.87 (*d*, 8.7)	112.80 (CH)	C-5, C-6, C-8a, C-10a
8	7.56 (*d*, 8.7)	115.40 (CH)	C-6, C-9, C-10a
8a		112.10 (C)	
9		180.20 (C=O)	
9a		101.40 (C)	
10a		146.30 (C)	

3.4.5 Compound GP17

Compound **GP17** was isolated as a yellow gum. The UV (**Figure 121**) and IR (**Figure 122**) absorption bands were similar to those of **GP20**. The ^{1}H NMR spectrum (**Figure 123**) (**Table 56**) contained signals of one chelated hydroxyl group (δ_H 13.63, *s*), three aromatic protons [δ_H 6.77, (*s*), 6.26 (*d*, J = 2.1 Hz) and 6.19 (*d*, J = 2.1 Hz)], one prenyl unit [δ_H 5.27 (*mt*, J = 6.0 Hz, 1H), 4.09 (*d*, J = 6.0 Hz, 2H), 1.84 (*s*, 3H) and 1.69 (*s*, 3H)] and one methoxyl group (δ_H 3.79, *s*). The ^{1}H NMR data were similar to those of **GP20** except for the replacement of the H-8 signal in **GP20** with the prenyl signal in **GP17**. The appearance of the methylene protons of the prenyl group at lower field together with the HMBC correlations (**Figure 126**) of H_2-11/C-7 (δ_C 143.10), C-8 (δ_C 137.30) and C-8a (δ_C 112.00) supported above conclusion. The additional methoxyl group was located at C-7 on the basis of a HMBC correlation of 7-OCH_3/C-7. The remaining HMBC correlations were almost identical to those found

in **GP20**. Thus, **GP17** was determined as 1,3,6-trihydroxy-7-methoxy-8-(3-methylbutyl-2-enyl)xanthone (dulxanthone D) isolate from *Garcinia mangostana* (Nilar, 2005).

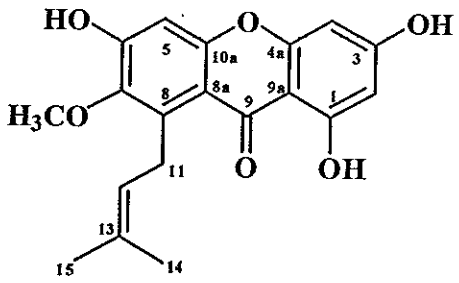

Table 56 The 300 MHz NMR data of compound GP17 in $CDCl_3$ + CD_3OD

Position	δ_H (*mult.*, J_{Hz})	δc (C-type)	HMBC correlations
1-OH	13.63 (*brs*)	164.00 (C)	
2	6.19 (*d*, 2.1)	97.93 (CH)	C-1, C-3, C-4, C-9a
3-OH		164.70 (C)	
4	6.26 (*d*, 2.1)	92.60 (CH)	C-2, C-3, C-4a, C-9a
4a		156.10 (C)	
5	6.77 (*s*)	101.87 (CH)	C-6, C-7, C-8a, C-9, C-10a
6-OH		155.63 (C)	
7		143.10 (C)	
7-OCH_3	3.79 (*s*)	61.34 (CH_3)	C-7
8		137.30 (C)	
8a		112.00 (C)	
9		181.93 (C=O)	
9a		101.87 (C)	
10a		155.63 (C)	
11	4.09 (*d*, 6.0)	26.34 (CH_2)	C-7, C-8, C-8a, C-12, C-13
12	5.27 (*mt*, 6.0)	123.30 (CH)	
13		131.83 (C)	
14	1.84 (*s*)	18.10 (CH_3)	C-12, C-13, C-15
15	1.69 (*s*)	25.75 (CH_3)	C-12, C-13, C-14

3.4.6 Compound GP16

Compound **GP16** was isolated as a yellow gum. The UV (**Figure 127**) absorption bands at 239, 253, 312 and 351 nm and IR absorption bands at 3366 and 1646 cm^{-1} (**Figure 128**) indicated that **GP16** had a xanthone chromophore. The ^1H NMR spectrum (**Figure 129**) (**Table 57**) contained signals of one chelated hydroxyl group (δ_H 13.67, *s*), three aromatic protons [δ_H 6.76 (*s*), 6.25 (*d*, J = 1.8 Hz) and 6.18 (*d*, J = 1.8 Hz)], one geranyl unit [δ_H 5.25 (*brt*, J = 6.6 Hz, 1H), 5.03 (*brt*, J = 6.6 Hz, 1H), 4.09 (*d*, J = 6.6 Hz, 2H), 2.07 (*m*, 2H), 2.00 (*m*, 2H), 1.82 (*s*, 3H), 1.60 (*s*, 3H) and 1.54 (*s*, 3H)] and one methoxyl group (δ_H 3.78, *s*). The ^1H NMR data were similar to those of **GP17** except for the replacement of the prenyl signal in **GP17** with one geranyl signal in **GP16**. The chemical-shift values of methylene protons (H_2-11) and their HMBC correlations (**Figure 132**) with C-7 (δ_C 143.17), C-8 (δ_C 137.41) and C-8a (δ_C 111.67) established the attachment of the geranyl group at C-8. Signal enhancement of H_2-11 and H-12 in the NOEDIFF experiment (**Figure 133**) upon irradiation of the methoxy protons confirmed above assignment. Thus, **GP16** was determined as rubraxanthone, previously isolated from latex of *Garcinia parvifolia* (Patthalung, 1988).

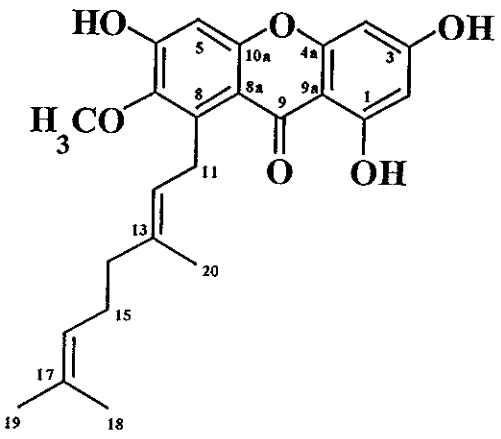

Table 57 The 300 MHz NMR data of compound GP16 in $CDCl_3$ + CD_3OD

Position	δ_H (*mult.*, J_{Hz})	δc (C-type)	HMBC correlations	NOE
1-OH	13.67 (*brs*)	162.20 (C)	C-1, C-2, C-9a	
2	6.18 (*d*, 1.8)	97.93 (CH)	C-1, C-3, C-4, C-9a	
3-OH		157.03 (C)		
4	6.25 (*d*, 1.8)	93.43 (CH)	C-2, C-3, C-4a, C-9a	
4a		157.03 (C)		
5	6.76 (*s*)	101.85 (CH)	C-6, C-7, C-8a, C-9, C-10a	
6-OH		142.70 (C)		
7		143.17 (C)		
7-OCH_3	3.78 (*s*)	61.28 (CH_3)	C-7	H-11, H-12, H-20
8		137.41 (C)		
8a		111.67 (C)		
9		181.85 (C=O)		
9a		103.21 (C)		
10a		155.61 (C)		
11	4.09 (*d*, 6.6)	26.22 (CH_2)	C-7, C-8, C-8a, C-12, C-13	H-12, H-20
12	5.25(*brt*, 6.6)	123.37 (CH)	C-8, C-11, C-14, C-20	H-11, 7-OCH_3
13		135.24 (C)		
14	2.00 (*m*)	39.69 (CH_2)	C-12, C-13, C-15, C-16, C-20	
15	2.07 (*m*)	26.54 (CH_2)	C-13, C-14, C-16, C-17	
16	5.03(*brt*, 6.6)	124.31 (CH)	C-15, C-18, C-19	
17		131.10 (C)		
18	1.54 (*s*)	17.53 (CH_3)	C-16, C-17, C-19	H-14, H-19
19	1.60 (*s*)	25.49 (CH_3)	C-16, C-17, C-18	
20	1.82 (*s*)	16.34 (CH_3)	C-12, C-13, C-14	H-11, 7-OCH_3

3.4.7 Compound GP11

Compound **GP11** with the molecular formula $C_{29}H_{34}O_6$ by EIMS (*m/z* 478) (**Figure 134**) was isolated as a yellow gum. The UV (**Figure 135**) and IR (**Figure 136**) absorption bands were similar to those of **GP16**, indicating that **GP11** had a xanthone chromophore. The ^{1}H NMR spectrum (**Figure 137**) (**Table 58**) contained signals of one chelated hydroxyl group (δ_H 13.35, *s*), two singlet aromatic protons (δ_H 6.88 and 6.25), two hydroxyl groups [δ_H 6.33 (*brs*) and 5.97 (*brs*)], one prenyl unit [δ_H 5.27 (*mt*, J = 6.0 Hz, 1H), 4.10 (*d*, J = 6.0 Hz, 2H), 1.83 (*d*, J = 1.2 Hz, 3H) and 1.70 (*d*, J = 1.2 Hz, 3H)], one geranyl unit [δ_H 5.28 (*mt*, J = 6.6 Hz, 1H), 5.03 (*mt*, J = 6.6 Hz, 1H), 3.53 (*d*, J = 6.6 Hz, 2H), 2.09 (*m*, 4H), 1.89 and (*d*, J = 0.9 Hz, 3H), 1.66 (*d*, J = 0.9 Hz, 3H) and 1.60 (*d*, J = 0.9 Hz, 3H)] and one methoxyl group (δ_H 3.82, *s*). The ^{1}H NMR data were similar to those of **GP17** except for the replacement of one aromatic proton signal (δ_H 6.26) in **GP17** with the geranyl signal in **GP11**. The geranyl group was located at C-4 (δ_C 104.08) on the basis of HMBC correlations (**Figure 141**) between methylene protons, H_2-11, with C-3 (δ_C 138.76), C-4 and C-4a (δ_C 154.00). The remaining HMBC correlations were almost identical to those found in **GP17**. Thus, **GP11** was determined as 1,3,6-trihydroxy-7-methoxy-8-(3-methylbutyl-2-enyl)-4-(3,7-dimethylocta-2,6-dienyl)xanthone, a new tetraoxygenated xanthone.

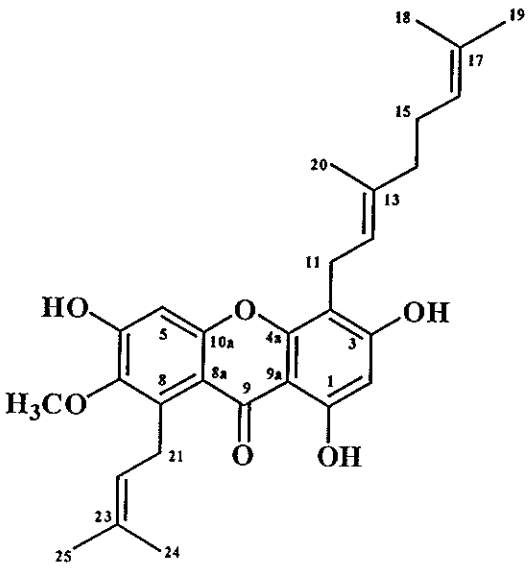

Table 58 The 300 MHz NMR data of compound GP11 in $CDCl_3$

Position	δ_H (*mult.*, J_{Hz})	δ_C (C-type)	HMBC correlations	NOE
1-OH	13.35 (*s*)	161.68 (C)	C-1, C-2, C-9a	
2	6.25 (*s*)	98.53 (CH)	C-1, C-9a	
3-OH	5.97 (*brs*)	138.76 (C)	C-3	
4		104.08 (C)		
4a		154.00 (C)		
5	6.88 (*s*)	101.56 (CH)	C-6, C-7, C-10a	
6-OH	6.33 (*brs*)	155.81 (C)		
7		142.67 (C)		
7-OCH_3	3.82 (*s*)	62.12 (CH_3)	C-7	H-21, H-24
8		137.06 (C)		
8a		112.20 (C)		
9		182.39 (C=O)		
9a		104.08 (C)		
10a		154.58 (C)		
11	3.53 (*d*, 6.6)	21.62 (CH_2)	C-3, C-4, C-4a, C-12 C-13	H-12, H-20
12	5.28 (*mt*, 6.6)	121.26 (CH)	C-14	H-11, H-14
13		138.76 (C)		
14	2.09 (*m*)	39.70 (CH_2)	C-15, C-20	H-12
15	2.09 (*m*)	26.38 (CH_2)	C-14, C-20	H-16
16	5.03 (*mt*, 6.6)	123.72 (CH)		H-19
17		124.27 (C)		
18	1.60 (*d*, 0.9)	17.97 (CH_3)	C-16, C-17	
19	1.66 (*d*, 0.9)	25.65 (CH_3)	C-16, C-17, C-18	
20	1.89 (*d*, 0.9)	18.24 (CH_3)	C-12, C-13, C-14	H-11, H-14
21	4.10 (*d*, 6.0)	26.55 (CH_2)	C-7, C-8, C-8a, C-22, C-23	7-OCH_3, H-22, H-24

Table 58 (Continued)

Position	δ_H (*mult.*, J_{Hz})	δ_C (C-type)	HMBC correlations	NOE
22	5.27 (*mt*, 6.0)	123.08 (CH)	C-8, C-25	
23		135.69 (C)		
24	1.83 (*d*, 1.2)	18.24 (CH_3)	C-22, C-23, C-25	H-21, H-25
25	1.70 (*d*, 1.2)	25.83 (CH_3)	C-22, C-23, C-24	H-22, H-24

3.4.8 Compound GP15

Compound **GP15** was isolated as a yellow gum. It exhibited UV (**Figure 142**) absorption bands of a xanthone chromophore at 243, 273 and 317 nm while the hydroxyl and conjugated carbonyl absorption bands were found at 3400 and 1651 cm^{-1}, respectively, in the IR spectrum (**Figure 143**). The ^1H NMR spectrum (**Figure 144**) (**Table 59**) contained signals of one chelated hydroxyl group (δ_H 13.05, *s*), one singlet aromatic proton (δ_H 6.46), three aromatic protons of 1,2,3-trisubstituted benzene [δ_H 7.72 (*dd*, J = 7.5 and 1.8 Hz), 7.23 (*dd*, J = 7.5 and 1.8 Hz), 7.16, (*t*, J = 7.5 Hz)] and one geranyl unit [δ_H 5.29 (*mt*, J = 6.6 Hz, 1H), 5.08 (*mt*, J = 6.6 Hz, 1H), 3.40 (*d*, J = 6.6 Hz, 2H), 2.07 (*m*, 2H), 1.99 (*m*, 2H), 1.82 (*s*, 3H), 1.65 (*s*, 3H) and 1.58 (*s*, 3H)]. The HMBC correlations (**Figure 147**) between the chelated hydroxy proton and C-2 (δ_C 110.80) together with those between the methylene protons (H_2-11, δ_H 3.40) and C-1 (δ_C 160.40), C-2 and C-3 (δ_C 162.80) established the attachment of the geranyl group at C-2. The singlet aromatic proton (δ_H 6.46) was then attribute to H-4 according to its HMBC cross peaks with C-2, C-3, C-4a (δ_C 155.00), C-9 (δ_C 180.80) and C-9a (δ_C 102.80). The remaining aromatic protons of the 1,2,3-trisubstituted benzene at δ_H 7.23, 7.16 and 7.72 were assigned as H-6, H-7 and H-8, respectively, on the basis of the chemical-shift value of H-8, their multiplicities and HMBC correlations. The substituents at C-3 and C-5 were hydroxyl groups according to chemical-shift values of C-3 and C-5 (**Figure 145**) (**Table 59**). Thus, **GP15** was

determined as mangostinone, previously isolated from green fruit of *Garcinia mangostana* (Suksamrarn, 2002).

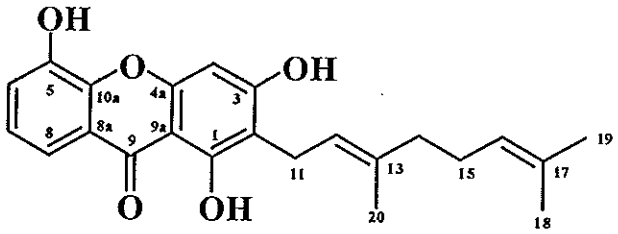

Table 59 The 300 MHz NMR data of compound GP15 in $CDCl_3$

Position	δ_H (*mult.*, J_{Hz})	δc (C-type)	HMBC correlations	NOE
1-OH	13.05 (*s*)	160.40 (C)	C-1, C-2, C-9a	
2		110.80 (C)		
3-OH		162.80 (C)		
4	6.46 (*s*)	93.38 (CH)	C-2, C-3, C-4a, C-9, C-9a	
4a		155.00 (C)		
5		145.30 (C)		
6	7.23 (*dd*, 7.5, 1.8)	119.89 (CH)	C-8, C-10a	
7	7.16 (*t*, 7.5)	123.49 (CH)	C-5, C-8, C-8a	
8	7.72 (*dd*, 7.5, 1.8)	116.09 (CH)	C-6, C-9, C-10a	
8a		121.40 (C)		
9		180.80 (C)		
9a		102.80 (C)		
10a		145.00 (C)		
11	3.40 (*d*, 6.6)	21.24 (CH_2)	C-1, C-2, C-3, C-12, C-13	H-12, H-20
12	5.29 (*mt*, 6.6)	121.80 (CH)	C-2, C-11, C-14, C-20	H-11, H-14
13		135.95 (C)		
14	1.99 (*m*)	39.73 (CH_2)	C-12, C-13, C-15, C-20	

Table 59 (Continued)

Position	δ_H (*mult.*, J_{Hz})	δc (C-type)	HMBC correlations	NOE
15	2.07 (*m*)	26.62 (CH_2)	C-13, C-14, C-16, C-17	H-14, H-18
16	5.08 (*mt*, 6.6)	124.30 (CH)	C-14, C-15, C-18, C-19	
17		131.28 (C)		
18	1.65 (*s*)	25.51 (CH_3)	C-16, C-17, C-19	H-15
19	1.58 (*s*)	17.52 (CH_3)	C-16, C-17, C-18	H-16
20	1.82 (*s*)	16.05 (CH_3)	C-12, C-13, C-14	H-11, H-14

3.5 Benzocyclooctene derivative

3.5.1 Compound GP10

Compound **GP10** with the molecular formula $C_{15}H_{16}O_5$ from EIMS (*m/z* 276) **(Figure 148)** was isolated as a colorless gum. It exhibited UV **(Figure 149)** absorption bands at 211, 270 and 294 nm while a hydroxyl absorption band was found at 3471 cm^{-1} in the IR spectrum **(Figure 150)**. The ^{13}C NMR **(Figure 152)** **(Table 60)** and DEPT **(Figure 153)** data revealed the presence of 7 quaternary, 5 methine and 3 methyl carbons. These results together with the molecular formula established a benzocyclooctene skeleton. The ^1H NMR spectrum **(Figure 151)** **(Table 60)** contained signals of three protons of 1,2,4-trisubstituted benzene [δ_H 7.04 (*dd*, J = 8.0 and 2.1 Hz, 1H), 7.00 (*d*, J = 2.1 Hz, 1H) and 6.97 (*d*, J = 8.0 Hz, 1H)], two identical protons [δ_H 6.72 (*s*, 2H)] and three methoxyl groups [δ_H 3.96 (*s*, 3H) and 3.95 (*s*, 6H)]. The protons of the 1,2,4-trisubstituted benzene at δ_H 7.00, 7.04 and 6.97 were assigned as H-7, H-9 and H-10, respectively, on the basis of HMBC correlations **(Figure 155)** and their multiplicities. The methoxyl group (δ_H 3.96) was linked at C-8 (δ_C 146.67) due to a HMBC correlation with C-8. Two identical protons of the eight-membered ring were attributed to H-1 and H-6 due to HMBC correlations of H-1/C-2 (δ_C 147.72), C-6a (δ_C 134.09) and C-10a (δ_C 133.11) and those of H-6/C-5 (δ_C

147.72), C-6a and C-10a. Furthermore, HMBC cross peaks of the methoxy protons (δ_H 3.95)/C-2 and C-5 established the linkage of the methoxyl groups at C-2 and C-5. According to the chemical-shift values of C-3 (δ_C 145.01) and C-4 (δ_C 134.09), these carbons carried hydroxyl substituents. Signal enhancement of H-7, H-10, 2-OCH_3 and 5-OCH_3 in the NOEDIFF experiment (**Figure 156**) upon irradiation of H-1 and H-6 supported above assignment. Thus, **GP10** was determined as 2,5,8-trimethoxy-3,4-dihydroxybenzocyclooctene, a new benzocyclooctene derivative.

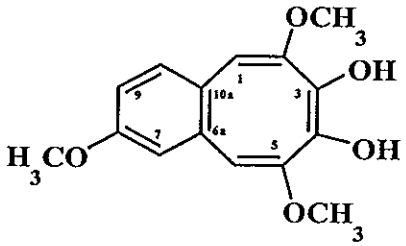

Table 60 The 300 MHz NMR data of compound GP10 in $CDCl_3$

Position	δ_H (*mult.*, J_{Hz})	δ_C (C-type)	HMBC correlations	NOE
1	6.72 (*s*)	104.02 (CH)	C-2, C-6a, C-10a	2-OCH_3, H-10
2		147.72 (C)		
2-OCH_3	3.95 (*s*)	56.44 (CH_3)	C-2	
3-OH		134.16 (C) *		
4-OH		145.01 (C)		
5		147.72 (C)		
5-OCH_3	3.95 (*s*)	56.44 (CH_3)	C-5	
6	6.72 (*s*)	104.02 (CH)	C-5, C-6a, C-10a	5-OCH_3, H-7
6a		134.09 (C)*		
7	7.00 (*d*, 2.1)	109.69 (CH)	C-6a, C-8, C-9, C-10a	
8		146.67 (C)		
8-OCH_3	3.96 (*s*)	56.08 (CH_3)	C-8	
9	7.04 (*dd*, 8.0, 2.1)	120.03 (CH)	C-7, C-10a	
10	6.97 (*d*, 8.0)	114.64 (CH)	C-6a, C-8, C-9, C-10a	
10a		133.11 (C)		

* interchangeable

3.6 Cyclohexanone derivative

3.6.1 Compound GP13

Compound **GP13** was isolated as a colorless gum. It exhibited UV (**Figure 157**) absorption bands at 205, 234 and 277 nm while the hydroxyl and conjugated carbonyl absorption bands were found at 3404 and 1655 cm^{-1}, respectively, in the IR spectrum (**Figure 158**). The ^1H NMR spectrum (**Figure 159**) (**Table 61**) contained signals of one olefinic proton δ_H 5.84 (*brq*, J = 1.2 Hz, 1H), two nonequivalent methylene protons [δ_H 2.54 (*brd*, J = 13.5 Hz, 1H) and 2.16 (*m*, 1H)], one oxymethine proton δ_H 4.15 (*brd*, J = 6.0 Hz, 1H), one methine proton δ_H 2.14 (*m*, 1H), one vinylic methyl group [δ_H 2.04 (*brt*, J = 1.2 Hz, 3H)] and one geranyl-geranyl unit [δ_H 5.20 (*mt*, J = 6.0 Hz, 1H), 5.09 (*m*, 3H), 2.36 (*m*, 1H), 2.17 (*m*, 1H), 2.13 (*m*, 6H), 2.06 (*m*, 2H), 2.00 (*m*, 2H), 1.95 (m, 2H), 1.68 (*brd*, J = 0.9 Hz, 3H), 1.64 (*brd*, J = 0.9 Hz, 3H), 1.62 (*s*, 3H) and 1.59 (*s*, 6H)]. The ^1H-^1H COSY (**Figure 162**) and HMBC correlations (**Figure 164**) supported the presence of the geranyl-geranyl unit. HMBC correlations of the olefinic proton (H-2, δ_H 5.84)/C-4 (δ_C 73.71) and C-6 (δ_C 41.37) and those of the methine proton H-5 (δ_H 2.16-2.11)/C-1 (δ_C 196.45) and C-4 established a cyclohexenone moiety. The vinylic methyl was located at C-3 due to its ^3J HMBC correlations with C-2 and C-4. The geranyl-geranyl unit was linked at C-5 on the basis of HMBC correlations of nonequivalent methylene protons, H_2-8 (δ_H 2.36 and 2.17)/C-1, C-4, C-5 (δ_C 43.62) and C-6 (δ_C 41.37). The relative configuration of C-4 and C-5 was assigned as *cis* since irradiation of H-4 enhanced the signal intensity of H-5 in the NOEDIFF experiment (**Figure 165**). The coupling-constant value of 6.0 Hz between H-4 and H-5 supported this orientation. Therefore, **GP13** was determined as (2*E*,6*E*,10*E*)-(+)-4β-hydroxy-3-methyl-5β-(3,7,11,15-tetramethylhexadeca-2,6,10,14-tetraenyl)cyclohex-2-en-1-one, previously isolated form *Garcinia cowa* (Wahyuni, 2004). GP13 had the same relative configuration as the previously isolated compound since they gave similar specific rotation [GP13: $[\alpha]_D$ = +60.01 (c = 0.01, $CHCl_3$) and the previously isolated compound: $[\alpha]_D$ = +50 (c = 0.01, $CHCl_3$)]

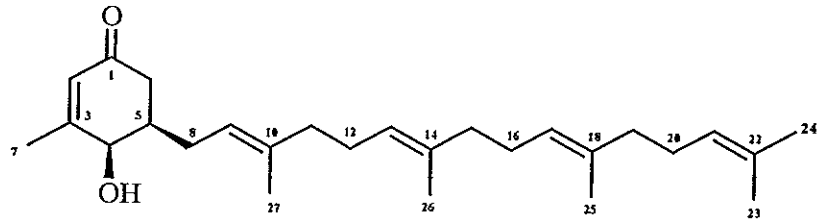

Table 61 The 300 MHz NMR data of compound GP13 in $CDCl_3$

Position	δ_H (*mult.*, J_{Hz})	δ_C (C-type)	HMBC correlations	NOE
1		196.45 (C=O)		
2	5.84 (*brq*, 1.2)	126.85 (CH)	C-4, C-6, C-7	H-7
3		162.96 (C)		
4	4.15 (*brd*, 6.0)	73.71 (CH)		H-5, H-7, H-8
5	2.14 (*m*)	43.62 (CH)	C-1, C-4, C-8, C-9	H-4, H-6
6	2.54 (*brd*, 13.5)	41.37 (CH_2)	C-1, C-4, C-5, C-8	
	2.16 (*m*)			
7	2.04 (*brt*, 1.2)	20.32 (CH_3)	C-2, C-3, C-4	
8	2.36 (*m*)	31.01 (CH_2)	C-1, C-4, C-5, C-6,	H-5, H-9,
	2.17 (*m*)		C-9	H-27
9	5.20 (*mt*, 6.0)	120.73 (CH)	C-8, C-11, C-27	H-11
10		138.54 (C)		
11	2.06 (*m*)	39.85 (CH_2)[a]	C-12, C-13	H-9, H-13
12	2.13 (*m*)	26.47 (CH_2)[b]	C-10, C-11, C-13, C-14, C-26	
13	5.09 (*m*)	123.81 (CH)[c]	C-12, C-15, C-26	
14		135.47 (C)[d]		
15	1.95(*m*)	39.73 (CH_2)[a]	C-13, C-14, C-16, C-26	H-13, H-17
16	2.13 (*m*)	26.77 (CH_2)[b]	C-14, C-15, C-18	
17	5.09 (*m*)	124.17 (CH)[c]	C-15, C-16, C-19, C-25	

Table 61 (Continued)

Position	δ_H (*mult.*, J_{Hz})	δ_C (C-type)	HMBC correlations	NOE
18		134.98 (C) [d]		
19	2.00 (*m*)	39.69 (CH_2) [a]	C-18, C-20, C-25	
20	2.13 (*m*)	26.61 (CH_2) [b]	C-18, C-19, C-22	
21	5.09 (*m*)	124.39 (CH) [c]	C-19, C-20, C-23,	H-24
22		131.29 (C)	C-24	
23	1.62 (*s*)	17.69 (CH_3)	C-21, C-22, C-24	
24	1.68 (*brd*, 0.9)	25.70 (CH_3)	C-21, C-22, C-23	
25	1.59 (s)	16.01 (CH_3) [e]	C-17, C-18, C-19	
26	1.59 (s)	16.07 (CH_3) [e]	C-13, C-14, C-15	
27	1.64 (*brd*, 0.9)	16.29 (CH_3)	C-9, C-10, C-11	

[a,b,c,d,e] Chemical shifts with the same index may be interchanged

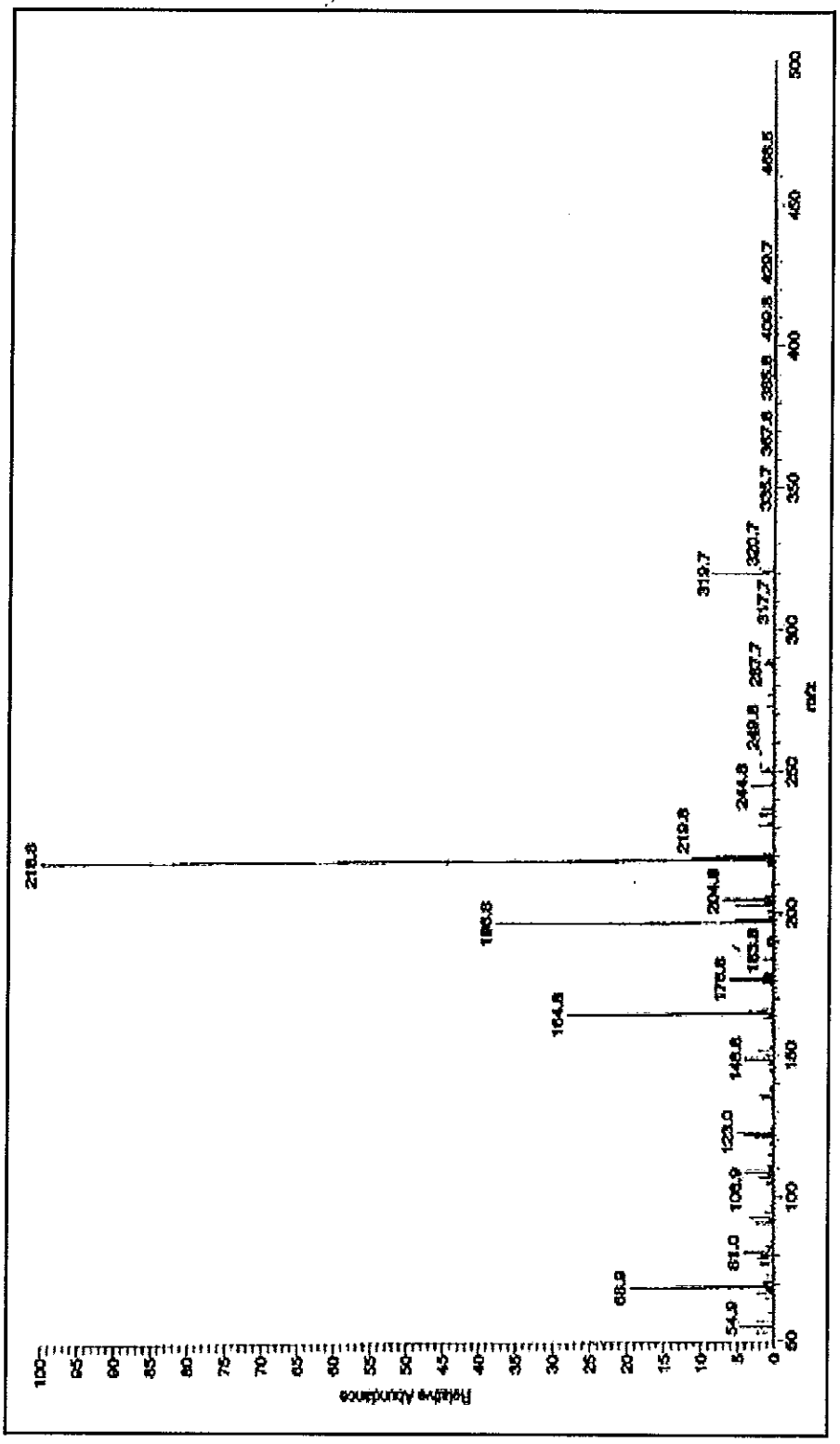

Figure 1 Mass spectrum of compound GP7

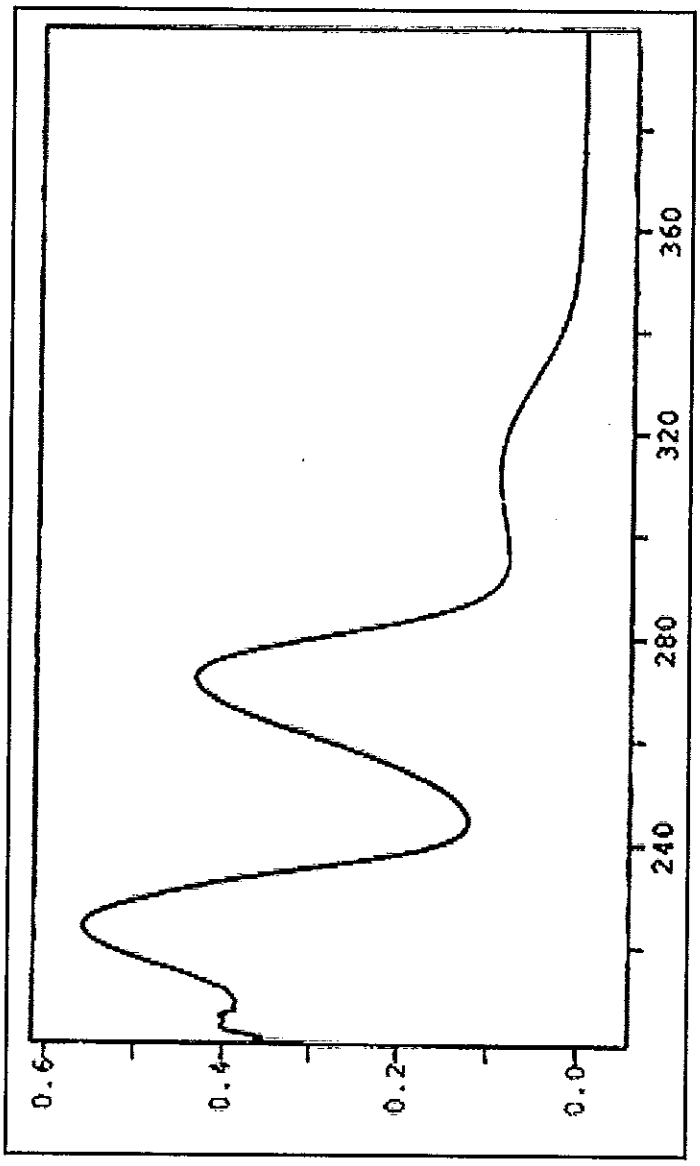

Figure 2 UV (MeOH) spectrum of compound GP7

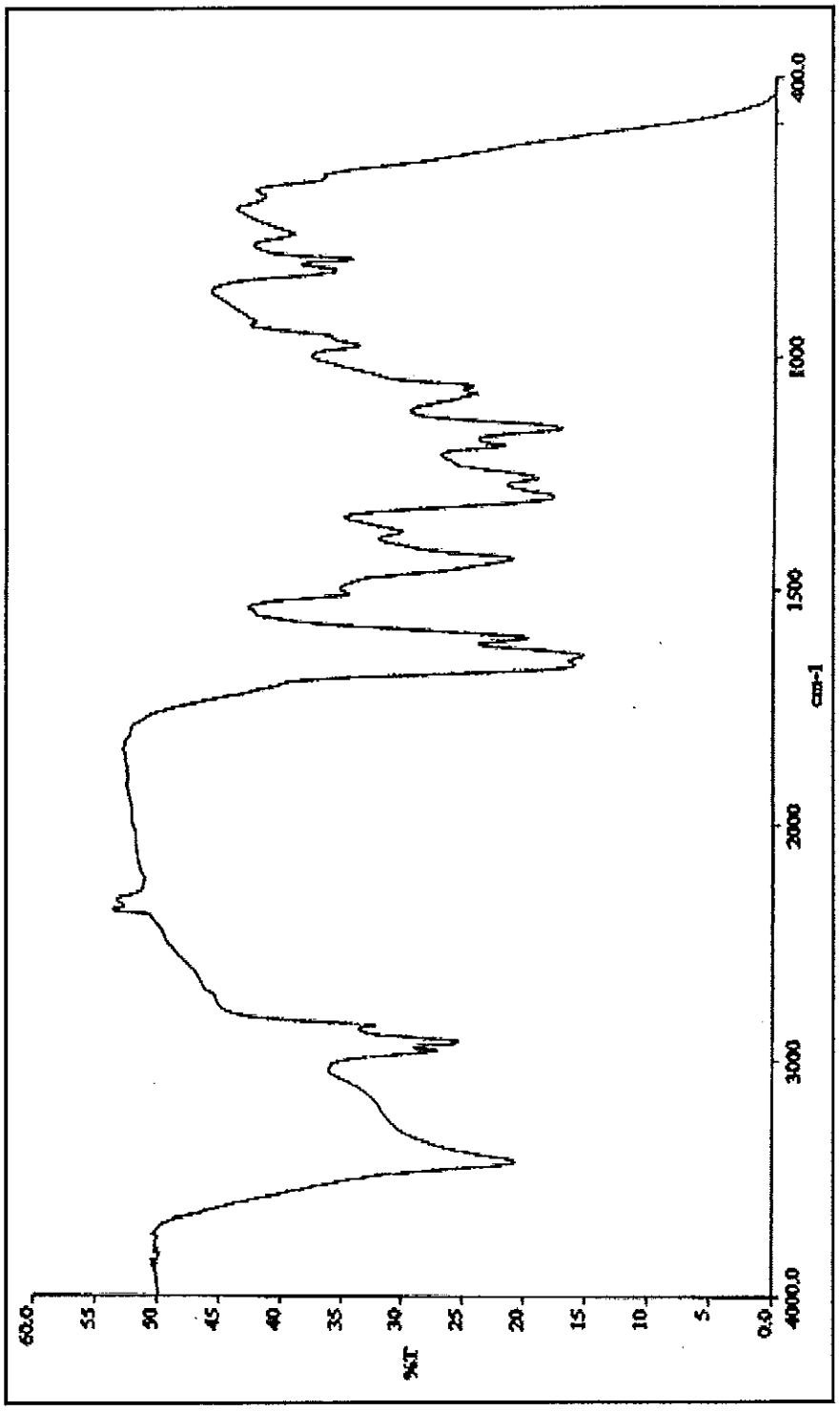

Figure 3 FT-IR (neat) spectrum of compound GP7

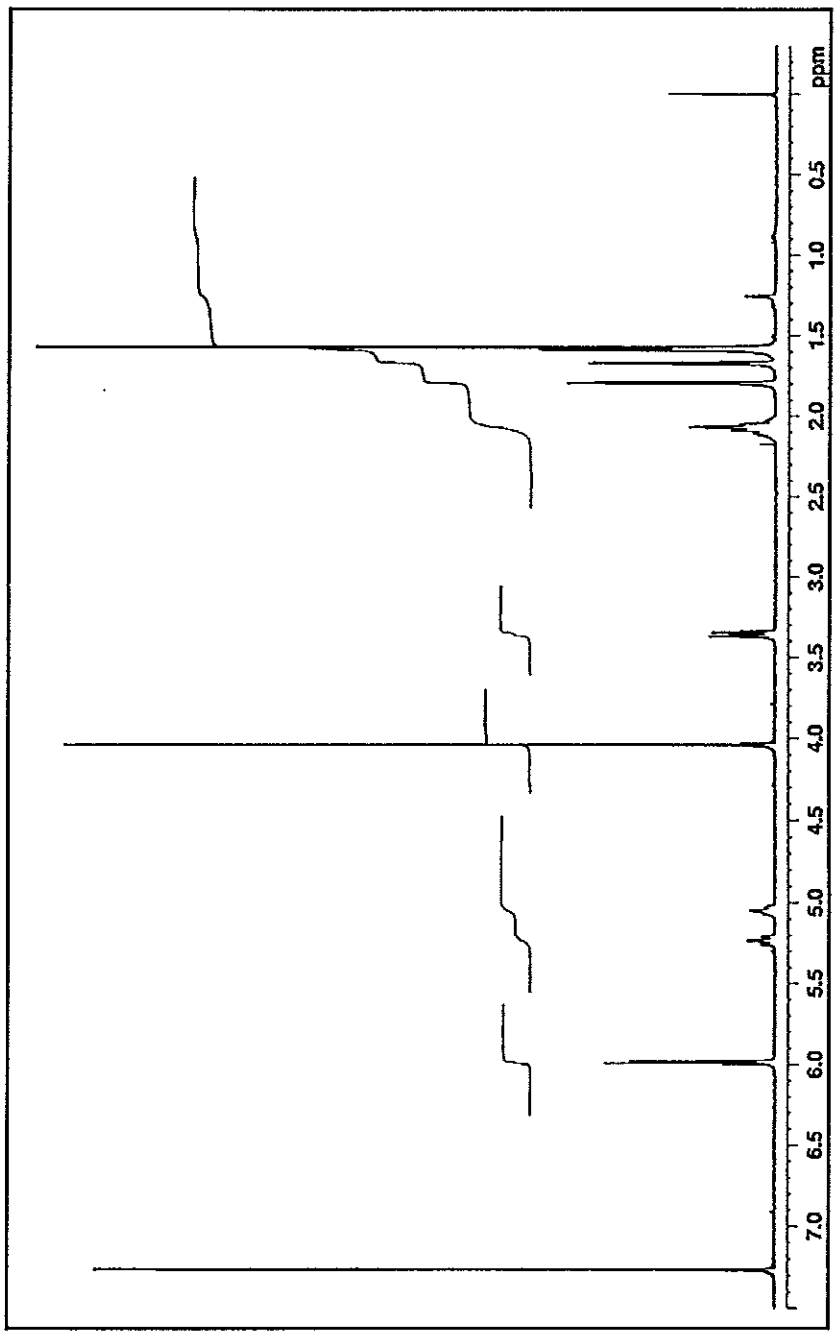

Figure 4 ^{1}H NMR (300 MHz) ($CDCl_3$) spectrum of compound GP7

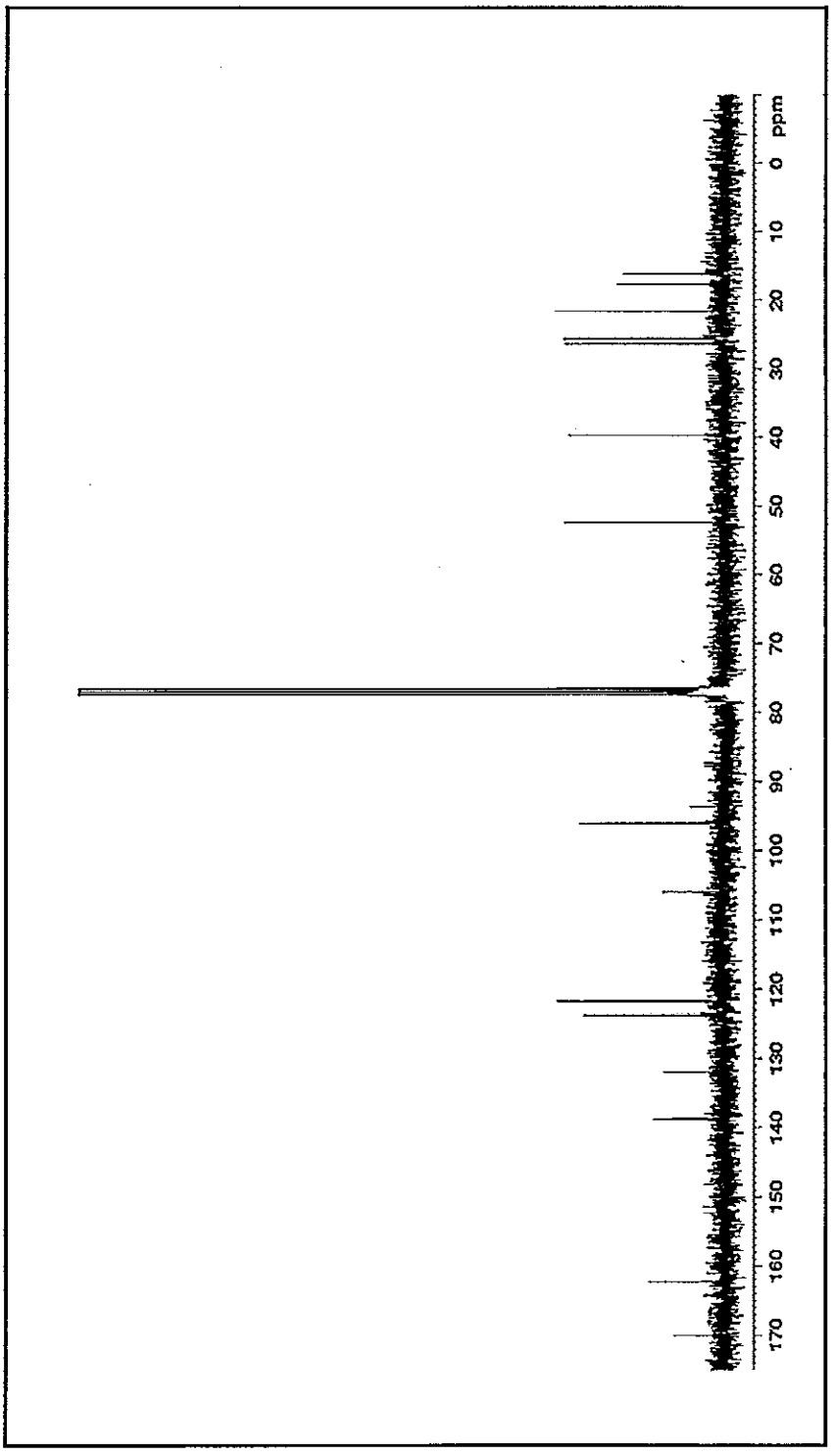

Figure 5 ^{13}C NMR (75 MHz) ($CDCl_3$) spectrum of compound GP7

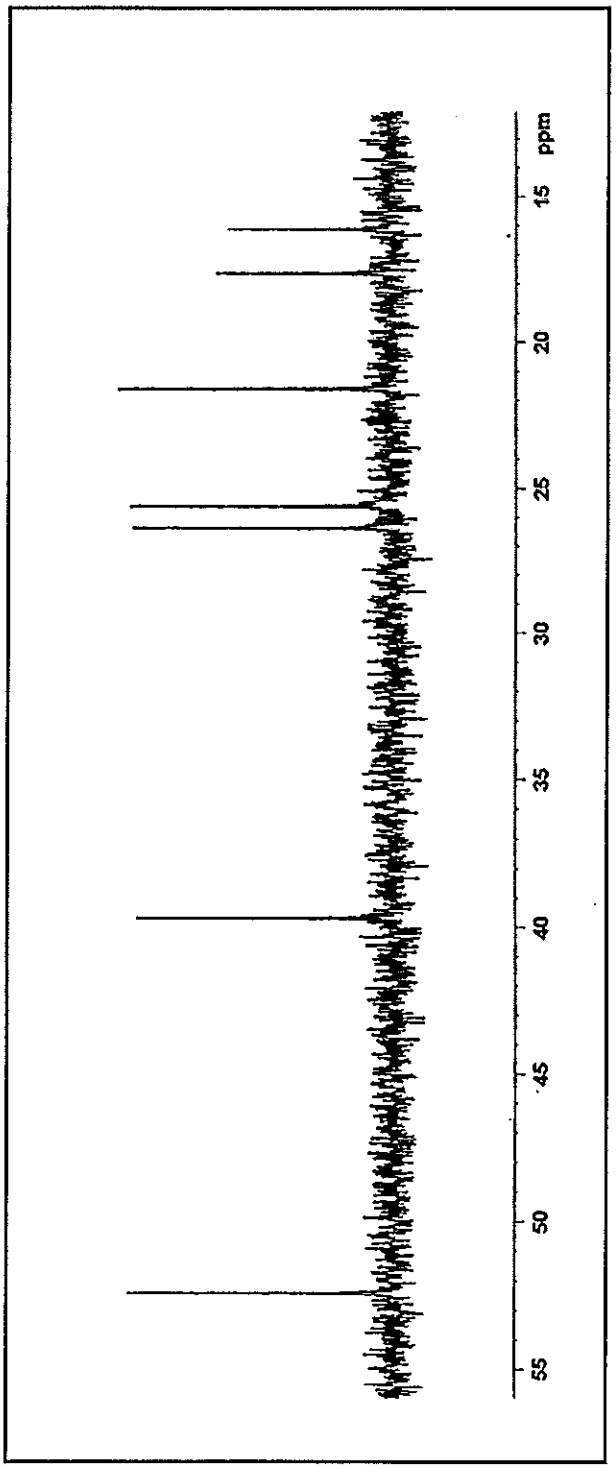

Figure 6 DEPT 90° spectra of compound GP7

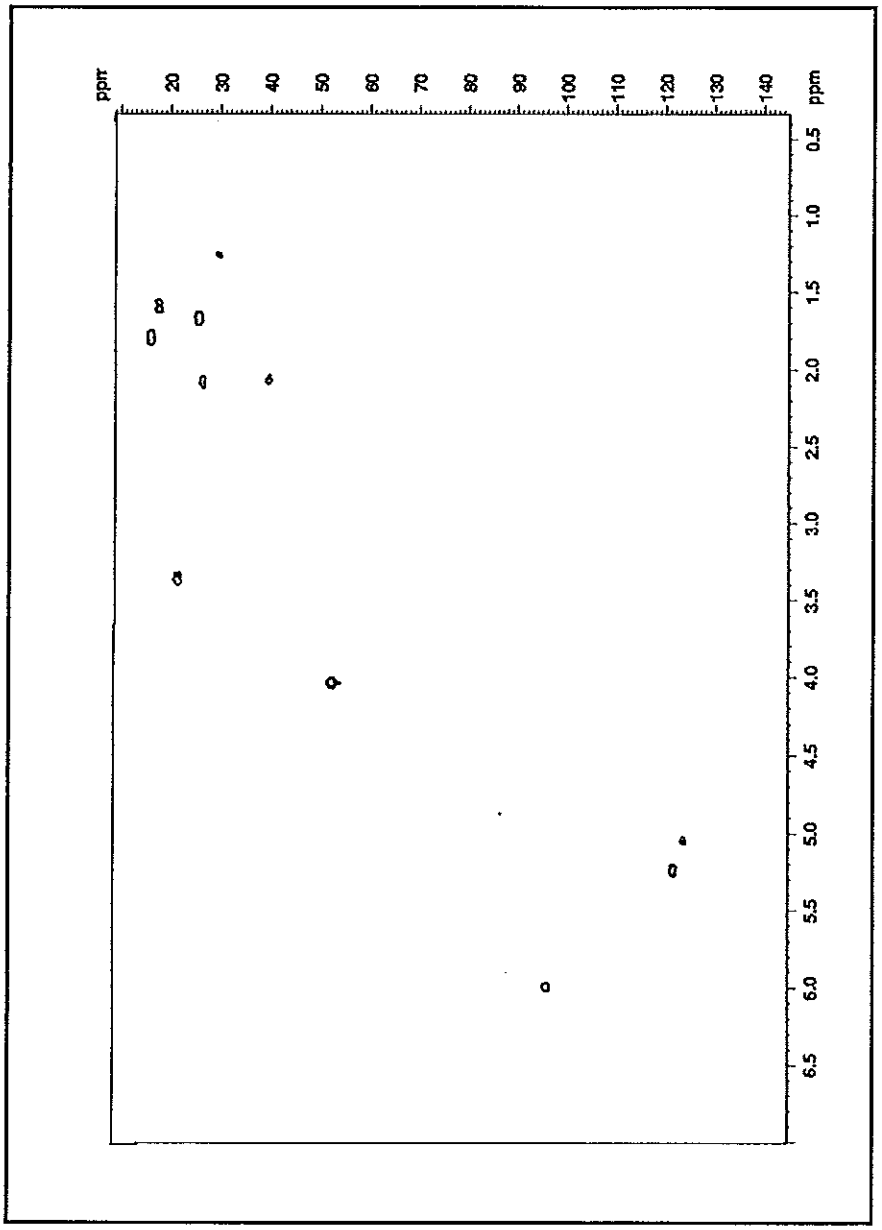

Figure 7 2D HMQC spectrum of compound GP7

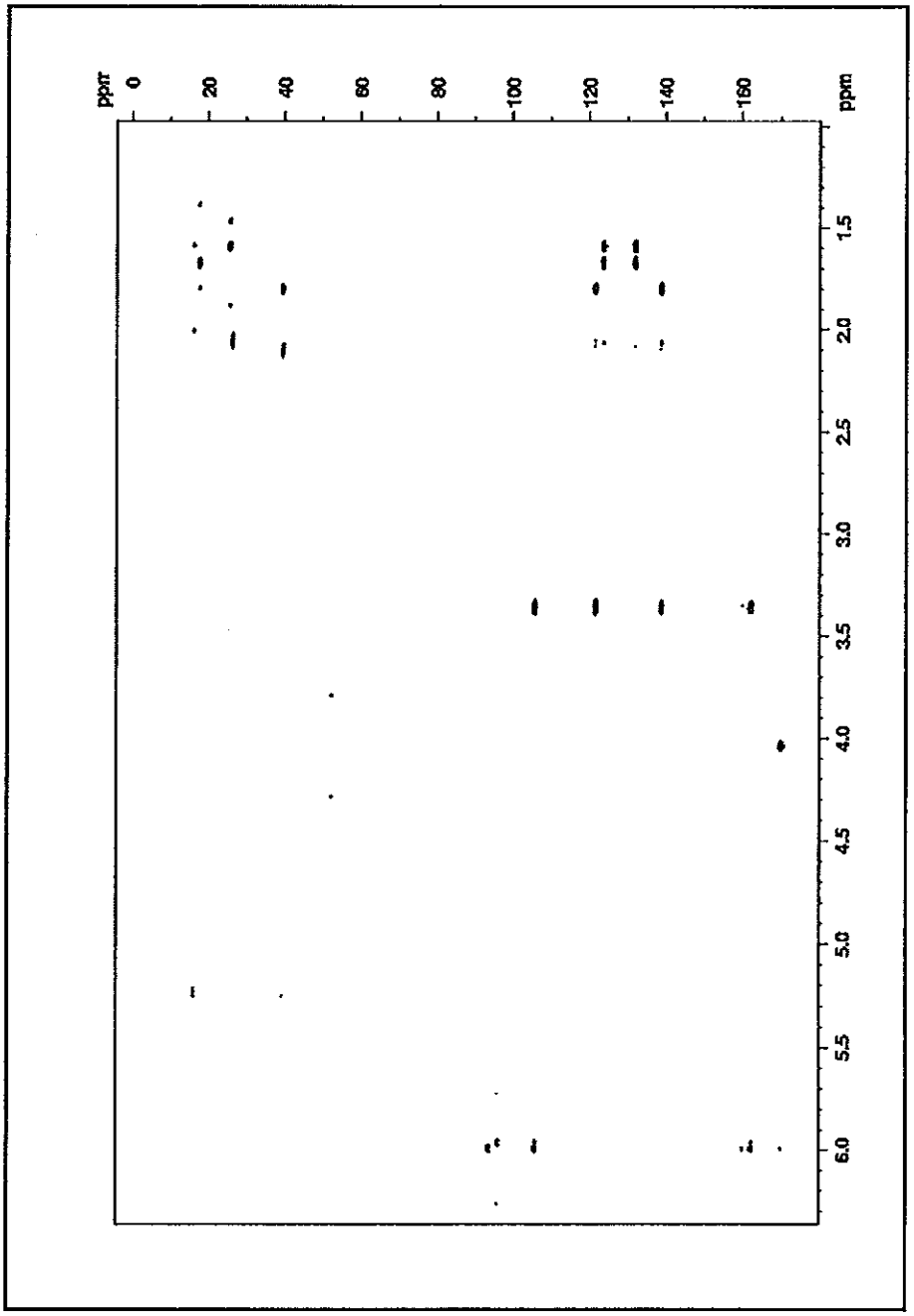

Figure 8 2D HMBC spectrum of compound GP7

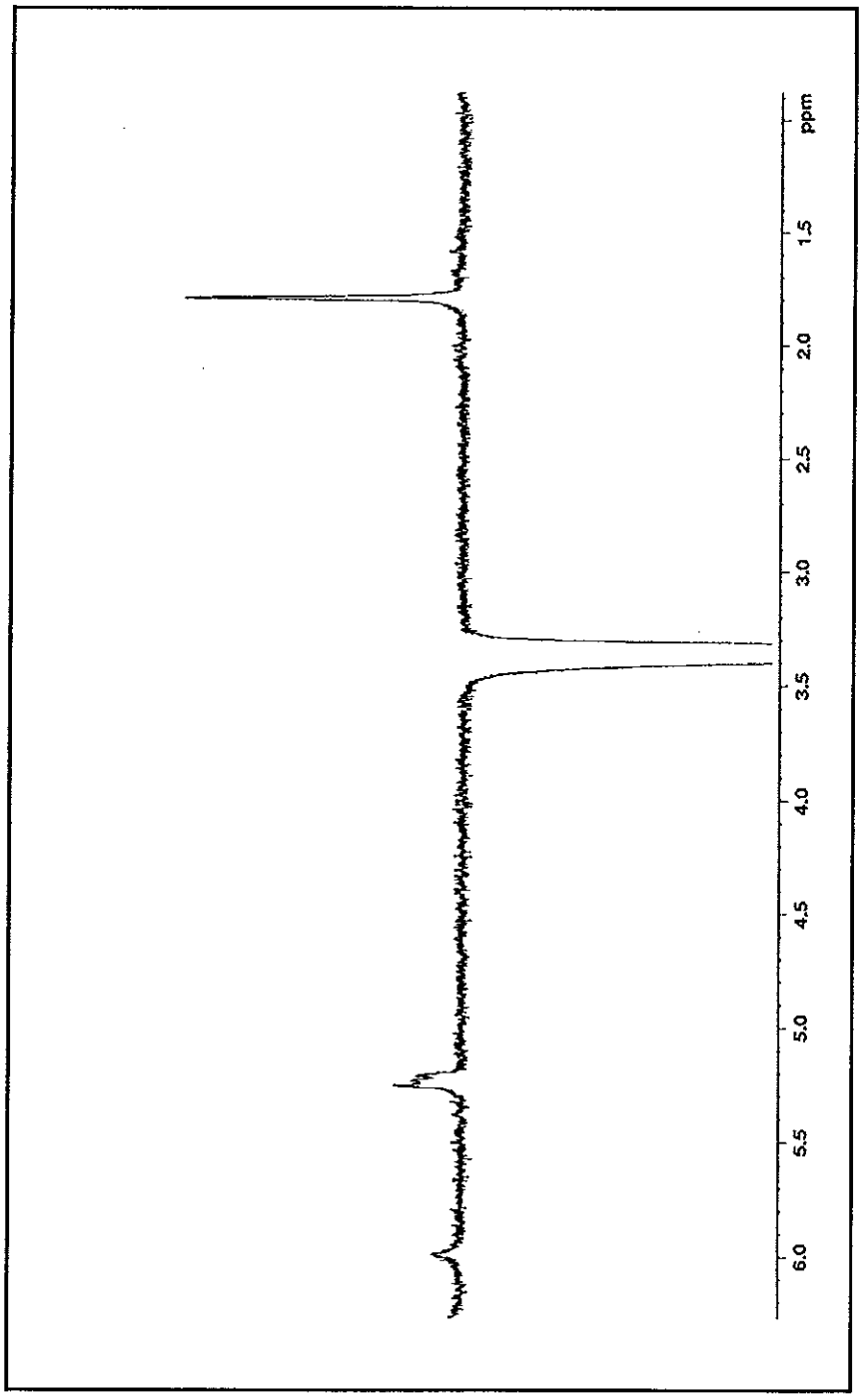

Figure 9 NOE difference spectrum of compound GP7 after irradiation at δ_H 3.35 (H_2-7)

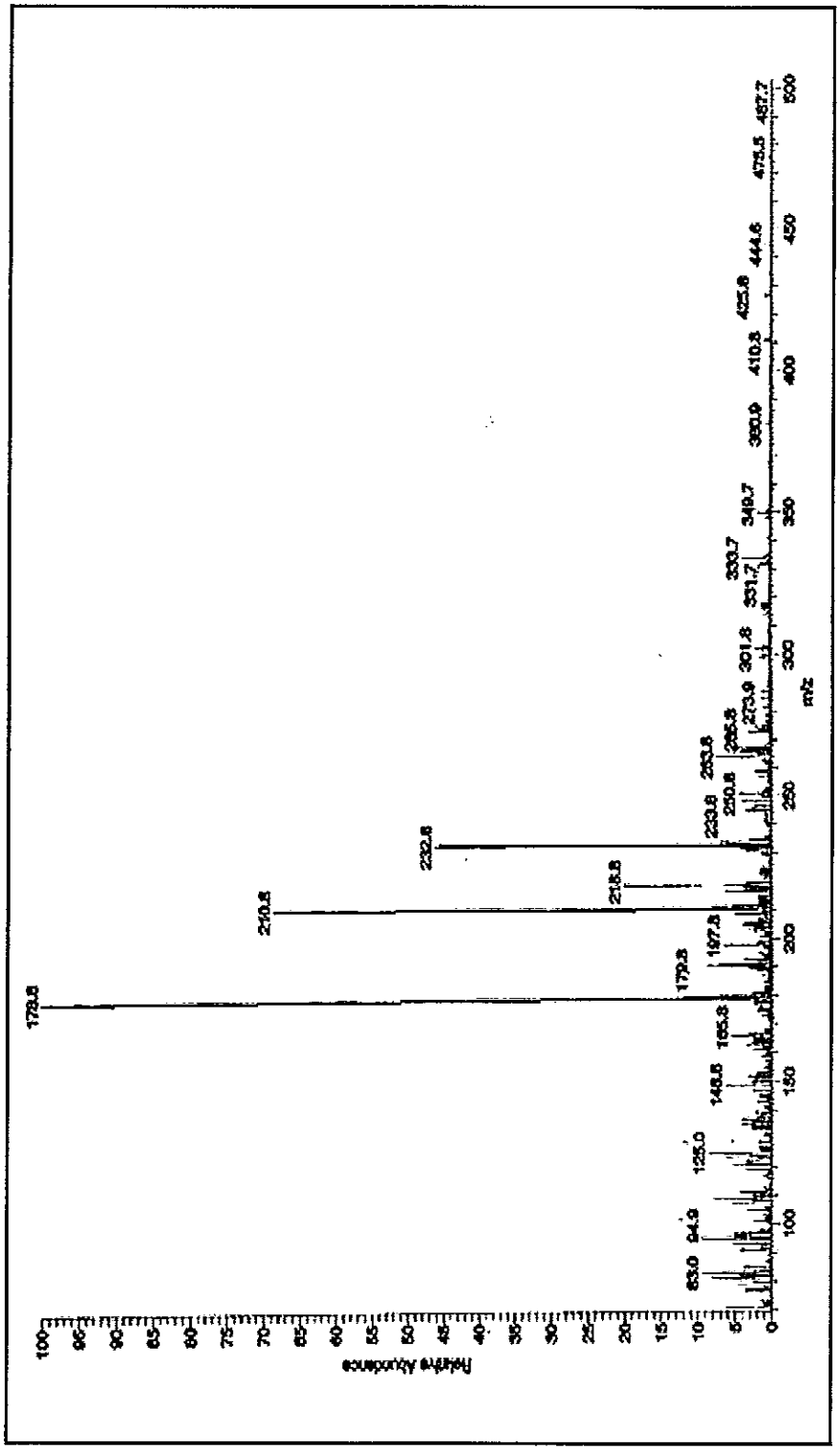

Figure 10 Mass spectrum of compound GP2

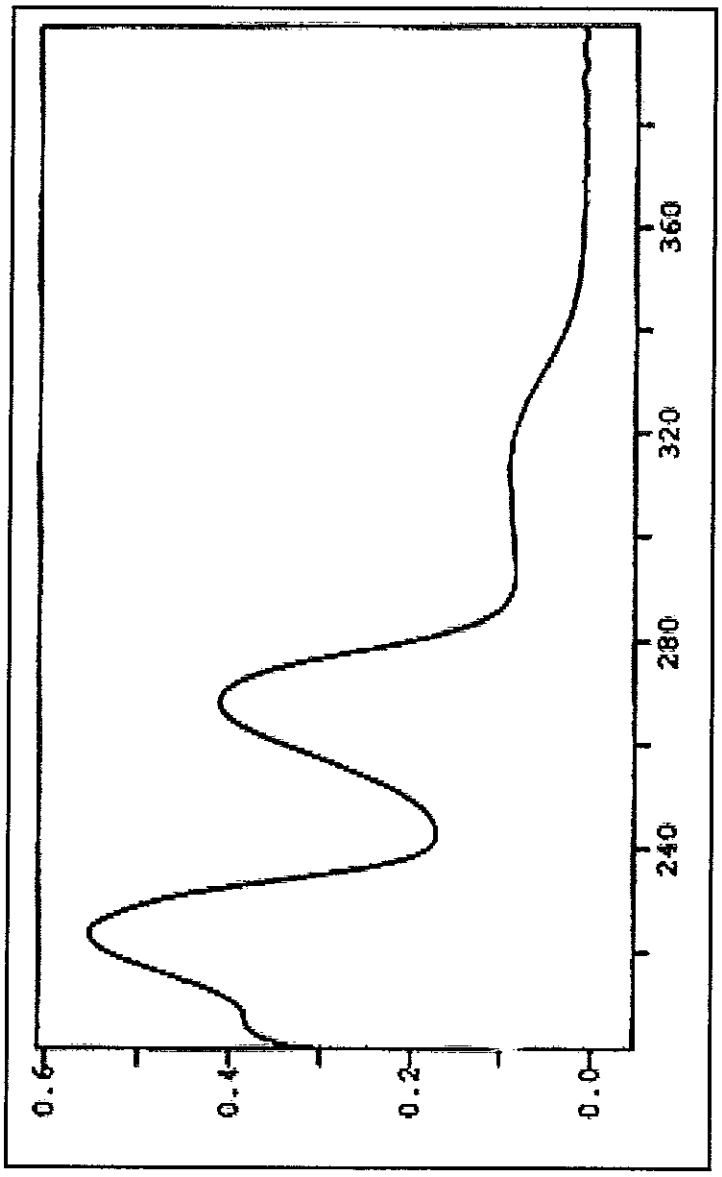

Figure 11 UV (MeOH) spectrum of compound GP2

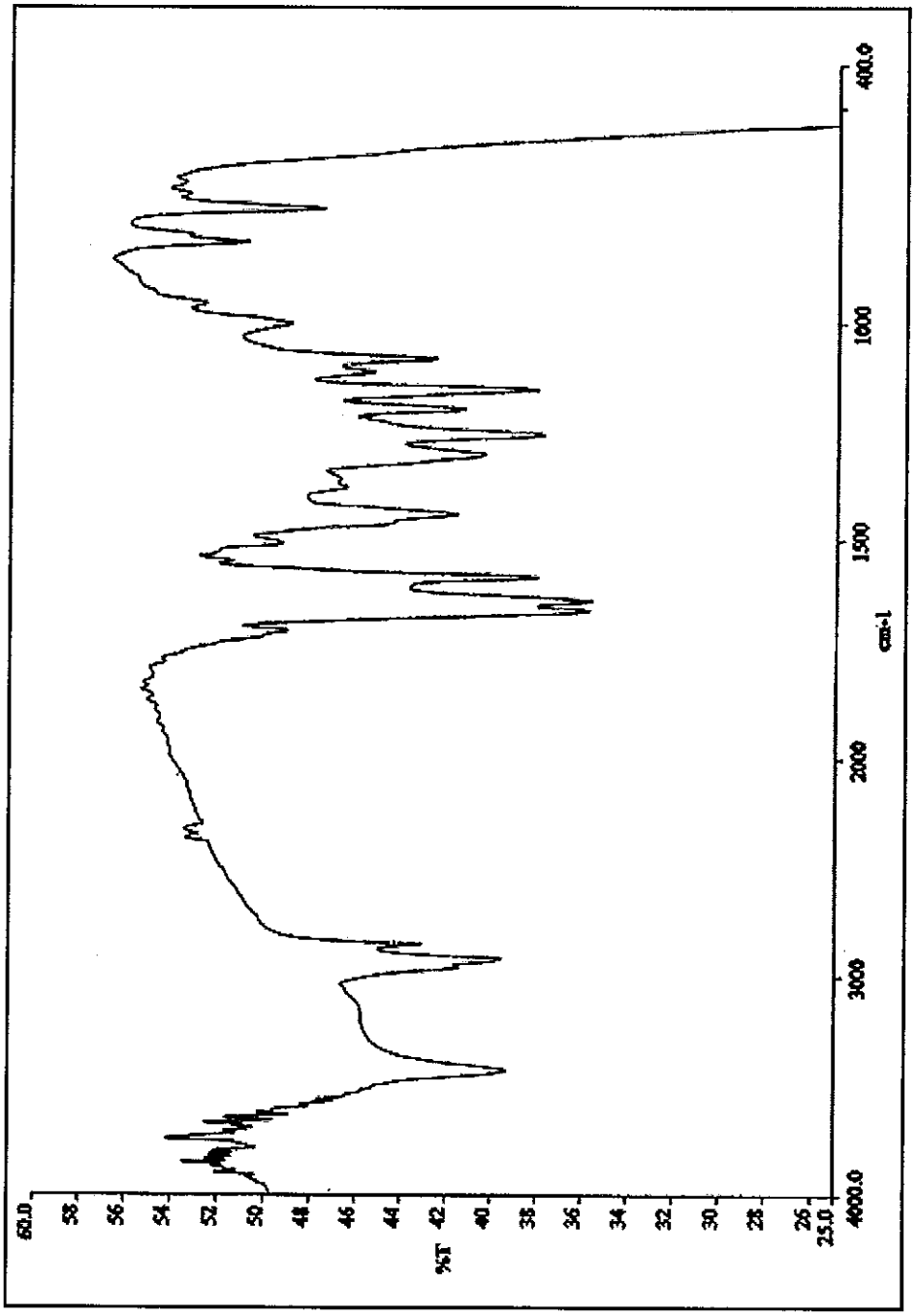

Figure 12 FT-IR (neat) spectrum of compound GP2

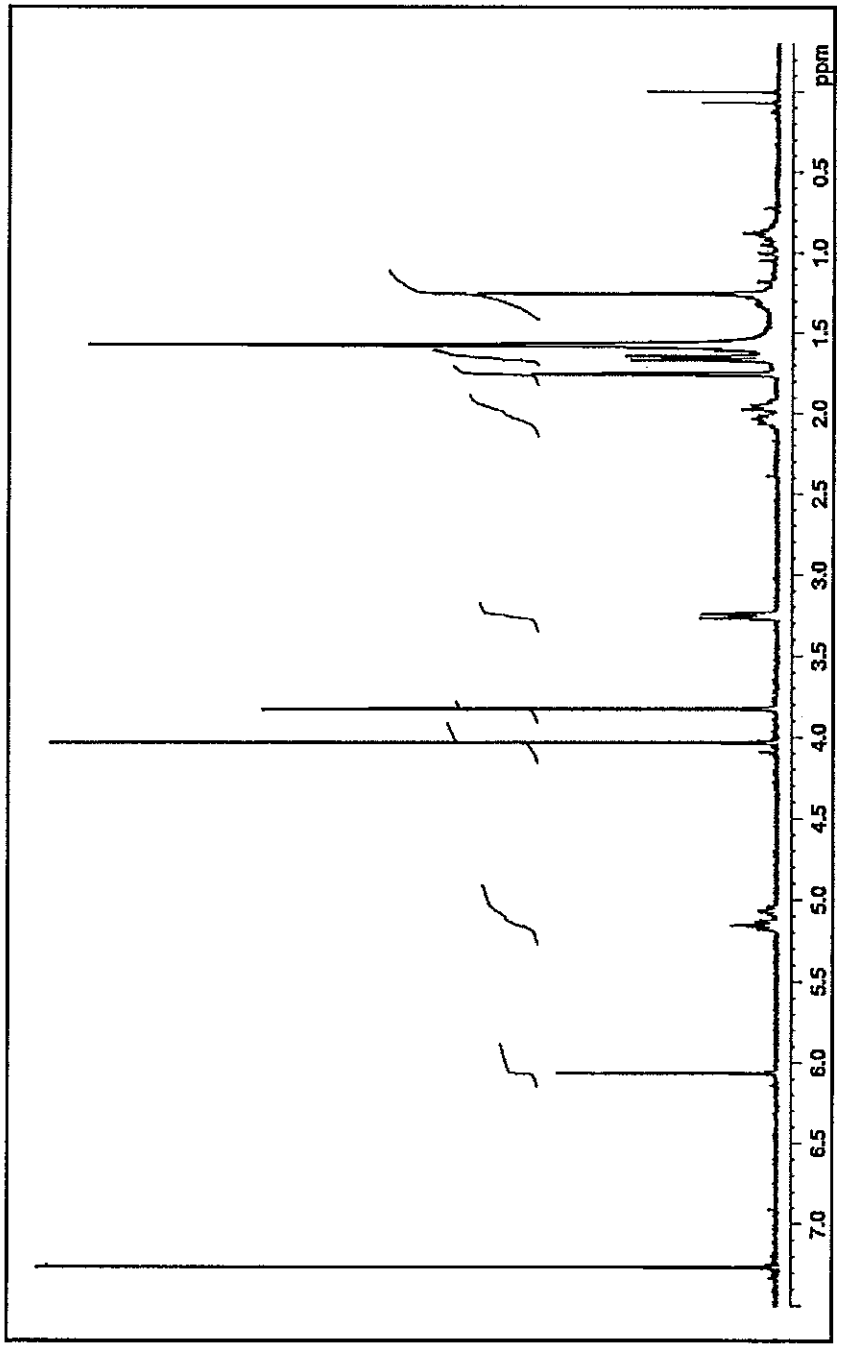

Figure 13 ^{1}H NMR (300 MHz) ($CDCl_3$) spectrum of compound GP2

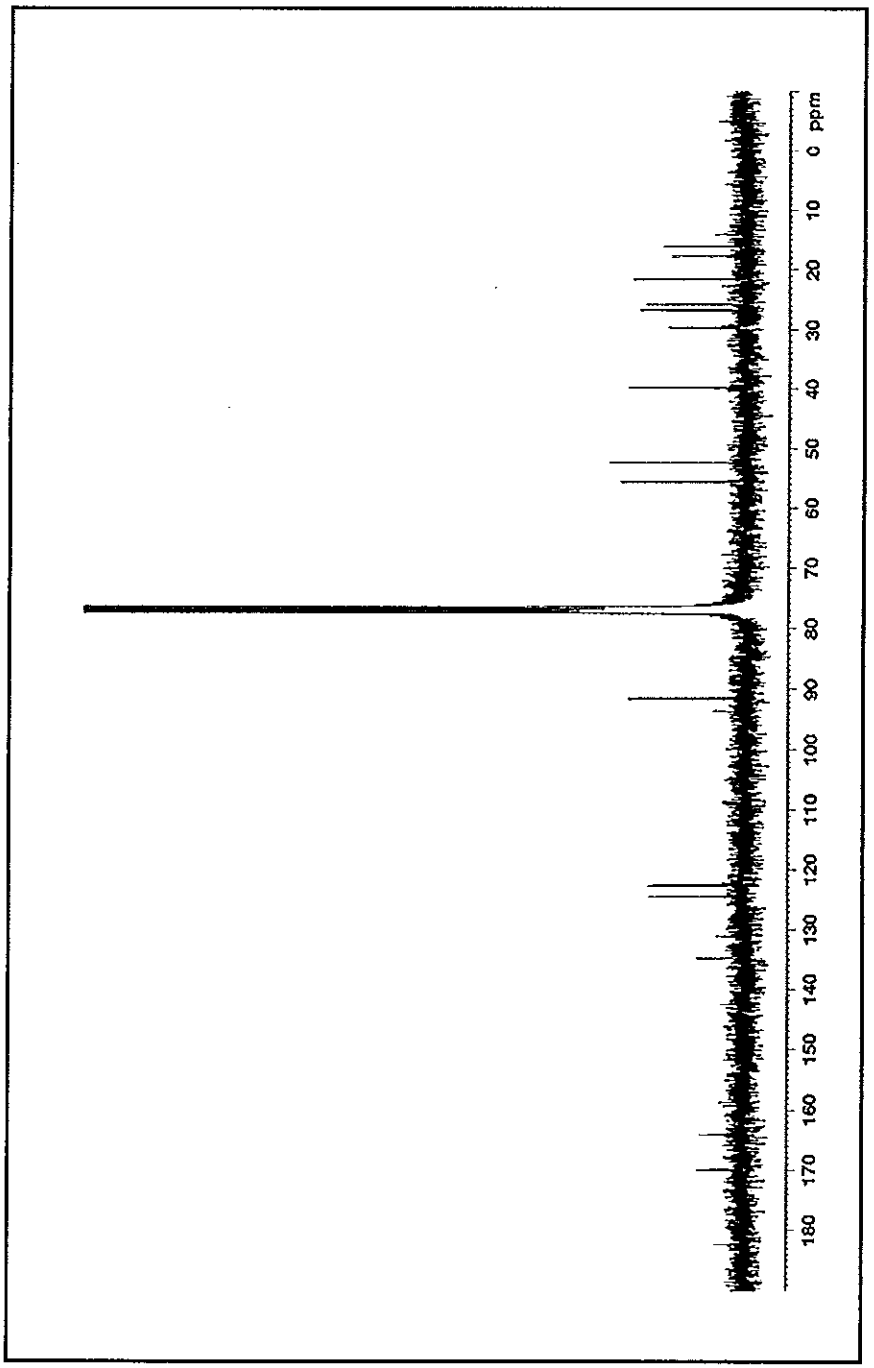

Figure 14 ^{13}C NMR (75 MHz) ($CDCl_3$) spectrum of compound GP2

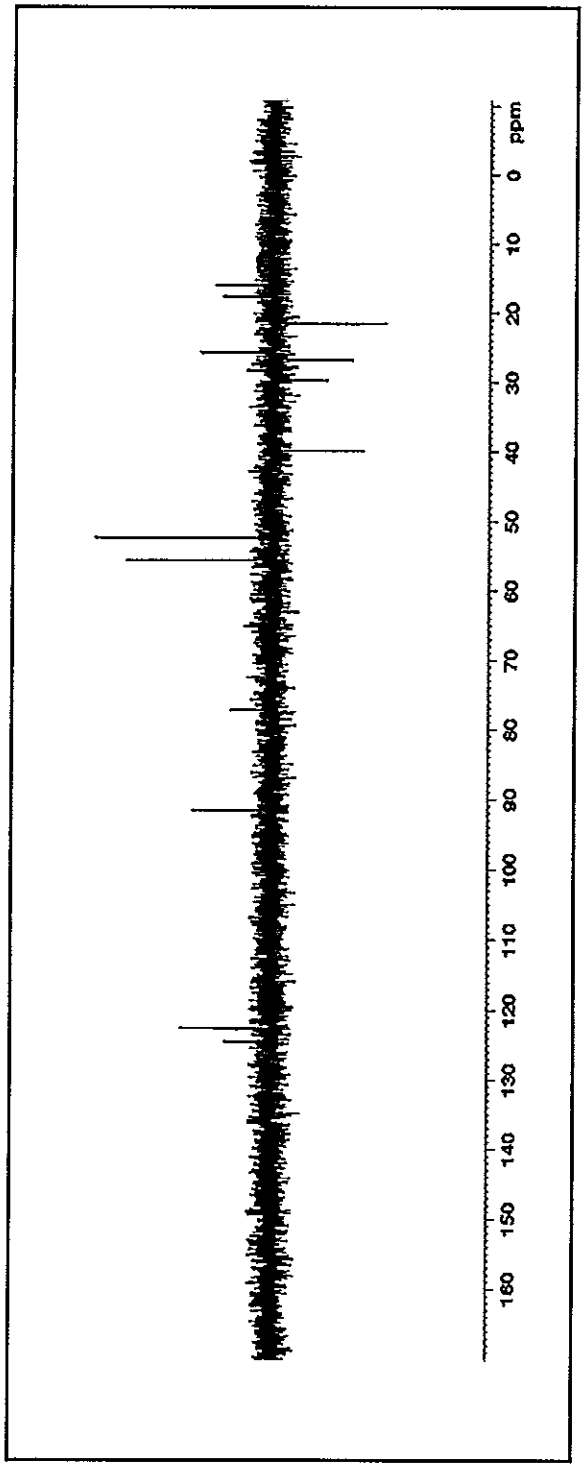

Figure 15 DEPT 135° spectra of compound GP2

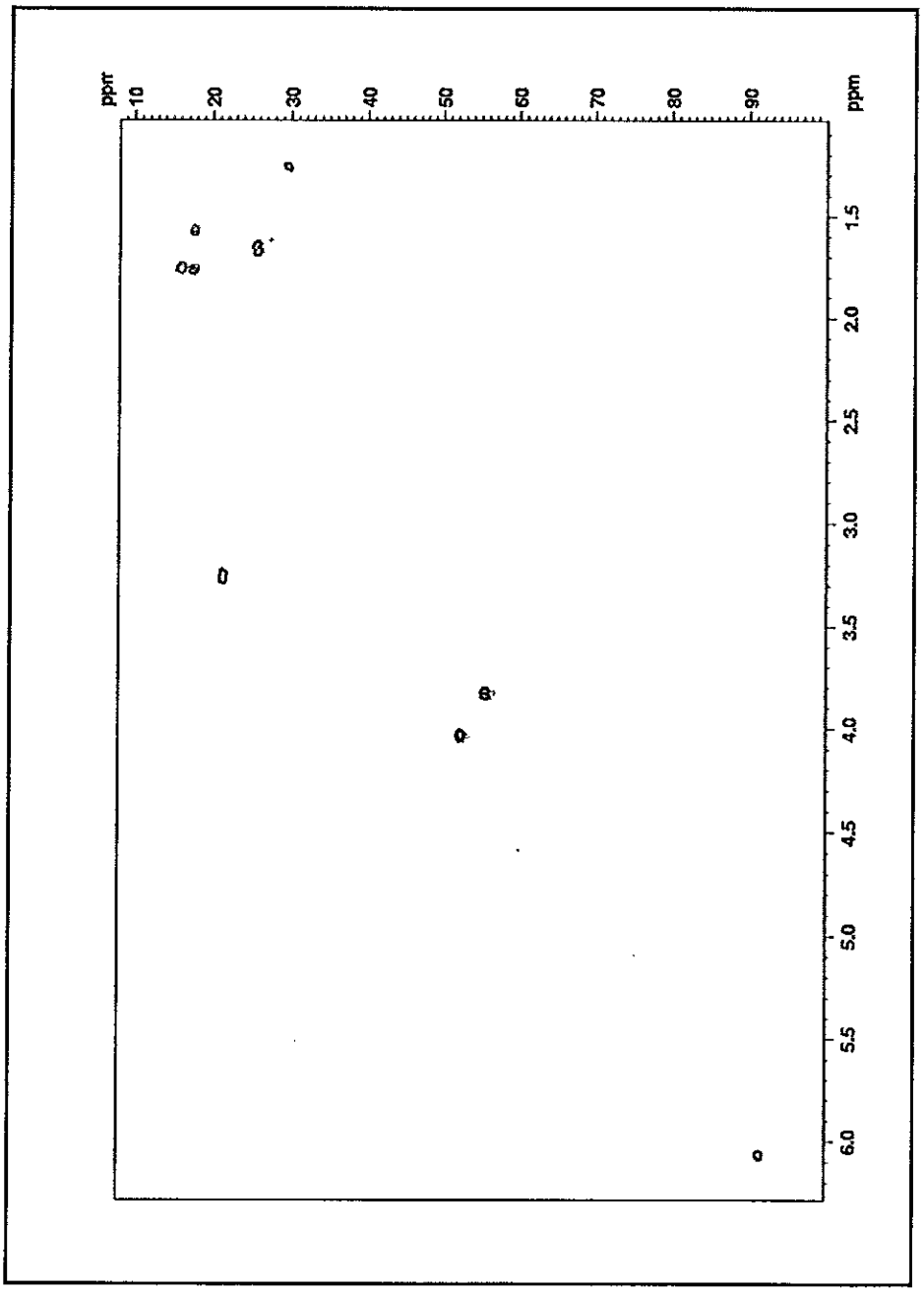

Figure 16 2D HMQC spectrum of compound GP2

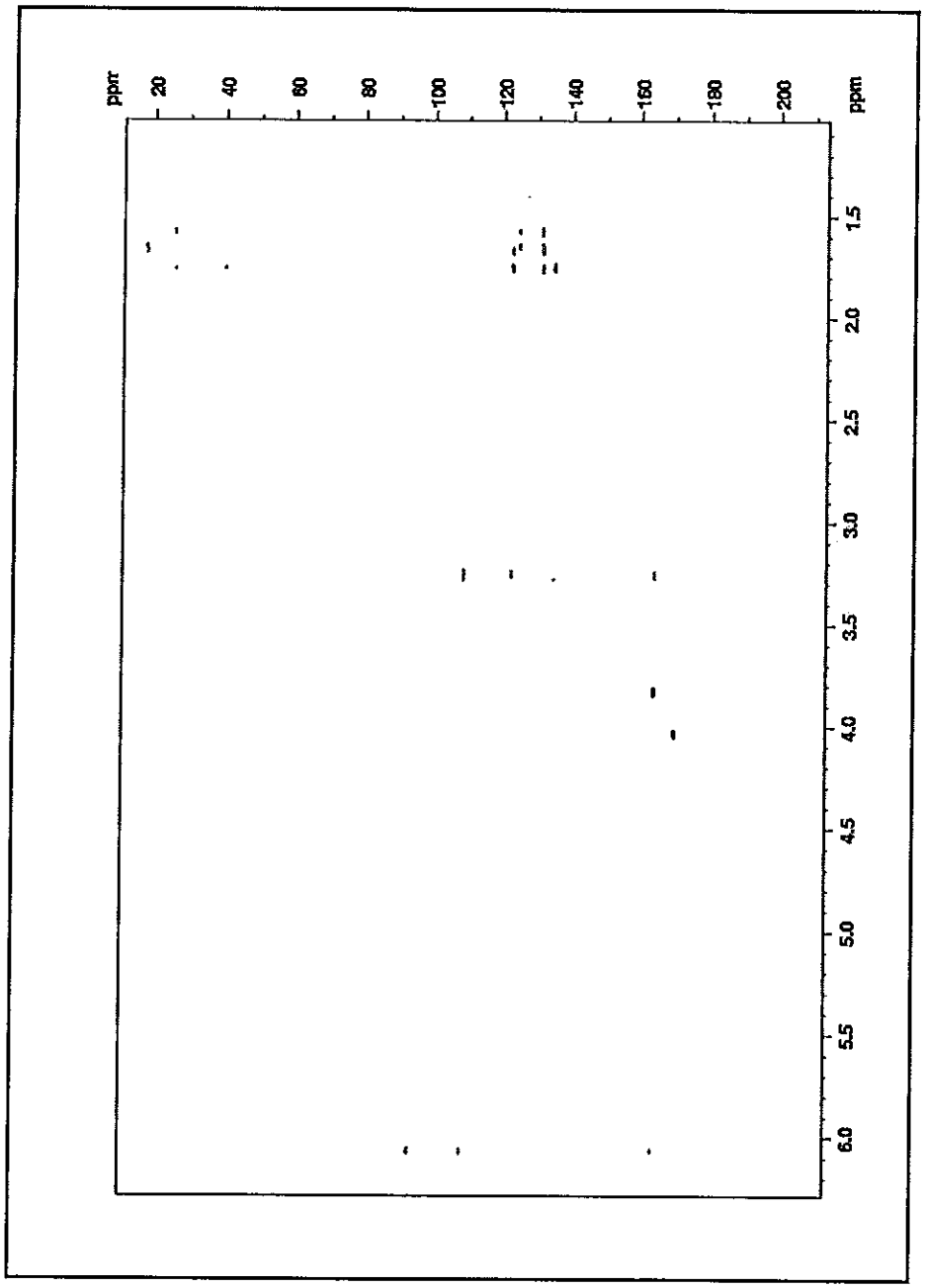

Figure 17 2D HMBC spectrum of compound GP2

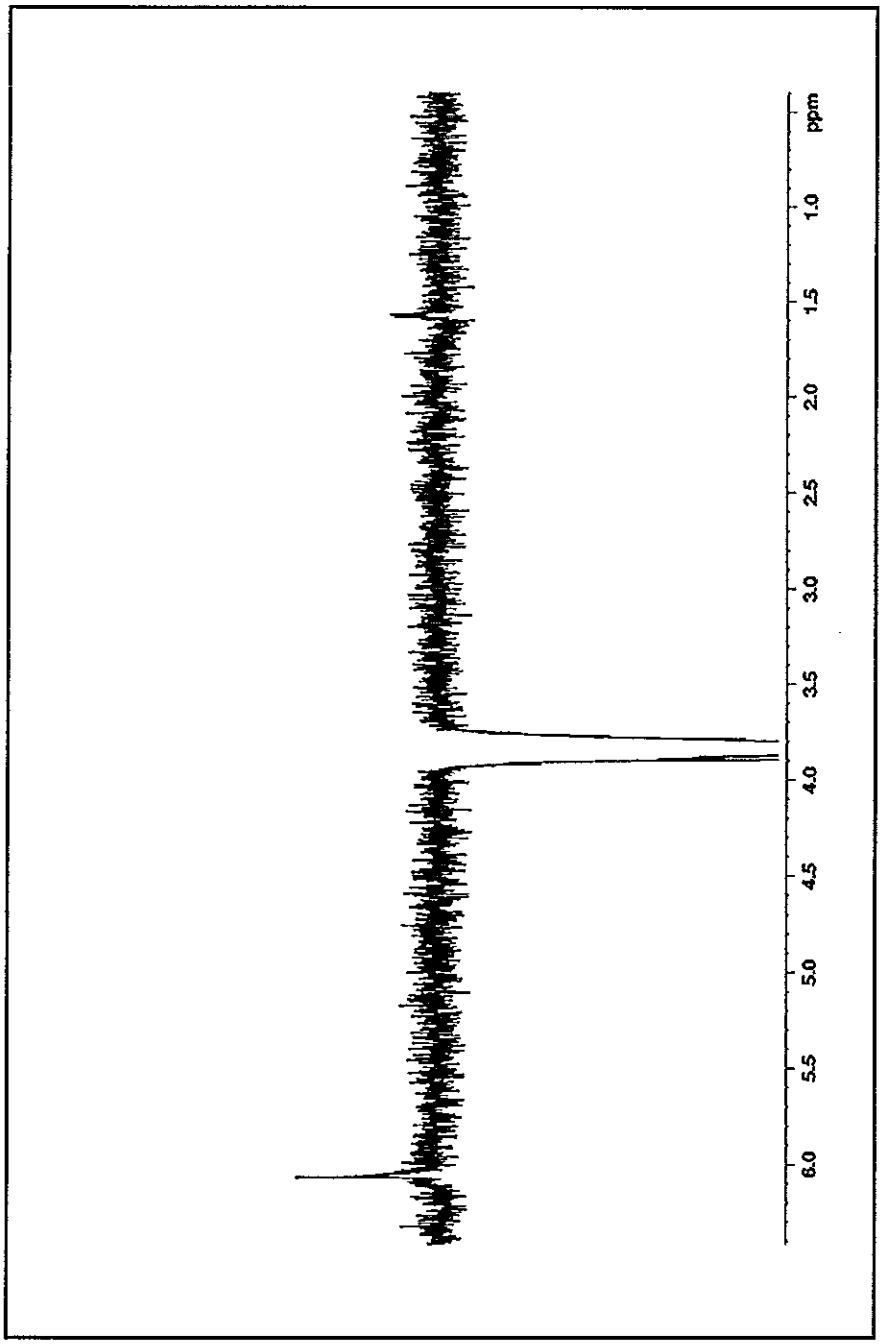

Figure 18 NOE difference spectrum of compound GP2 after irradiation at δ_H 3.83 (4-OCH_3)

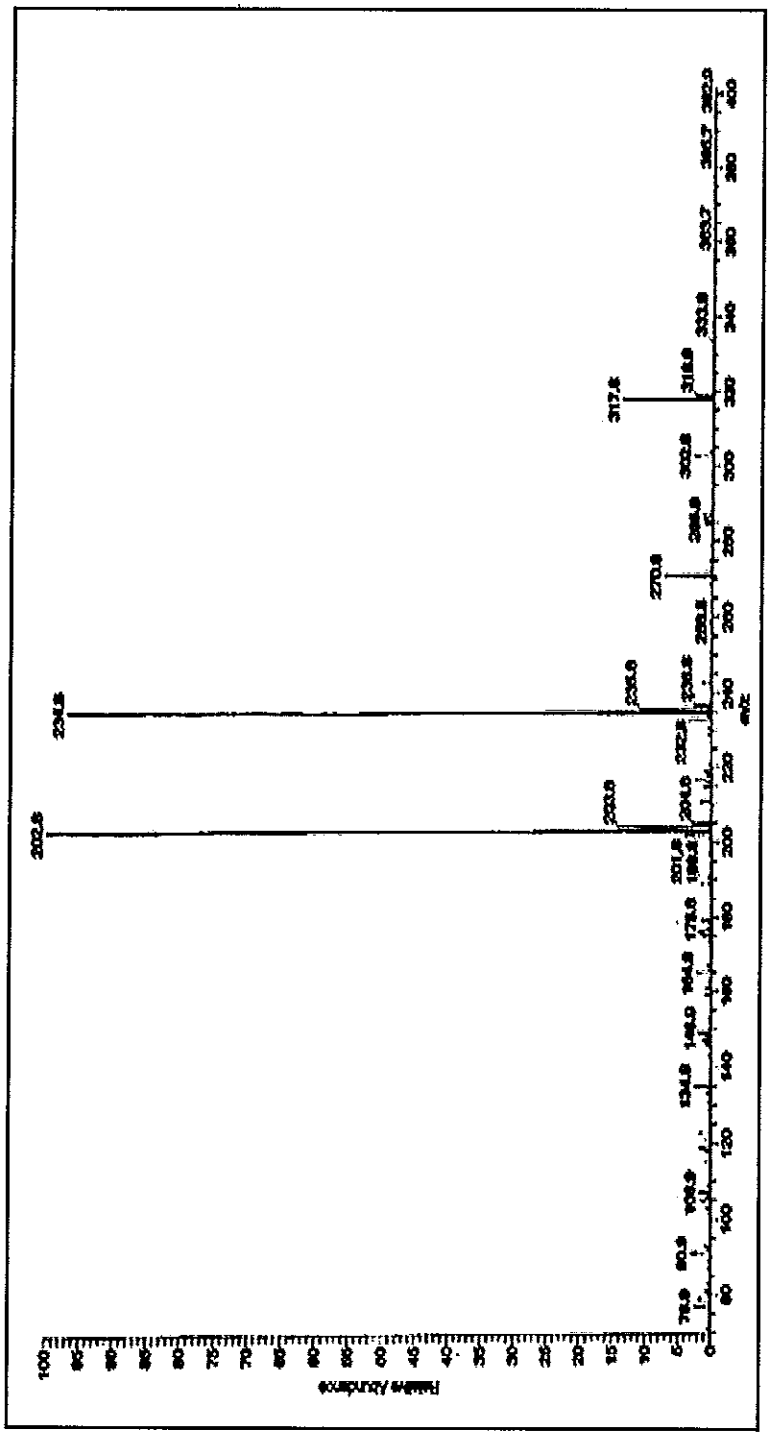

Figure 19 Mass spectrum of compound GP1

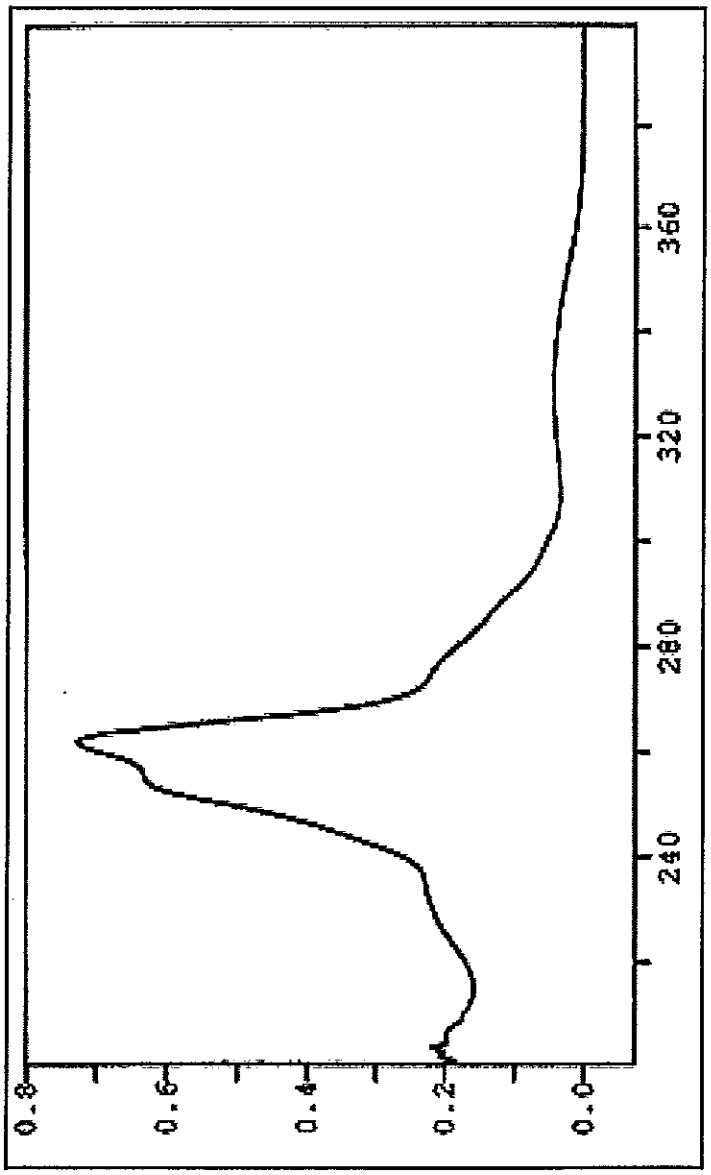

Figure 20 UV (MeOH) spectrum of compound GP1

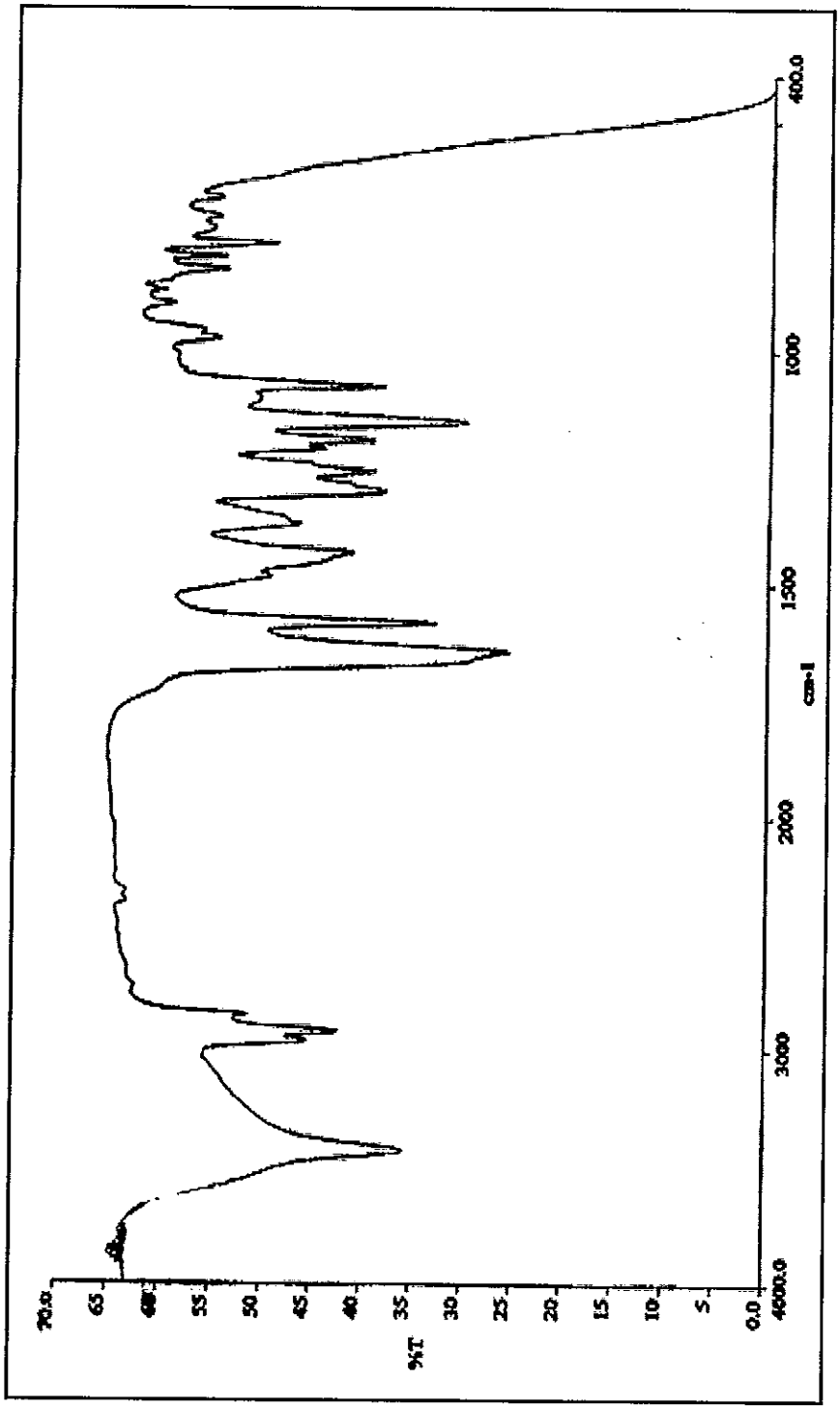

Figure 21 FT-IR (neat) spectrum of compound GP1

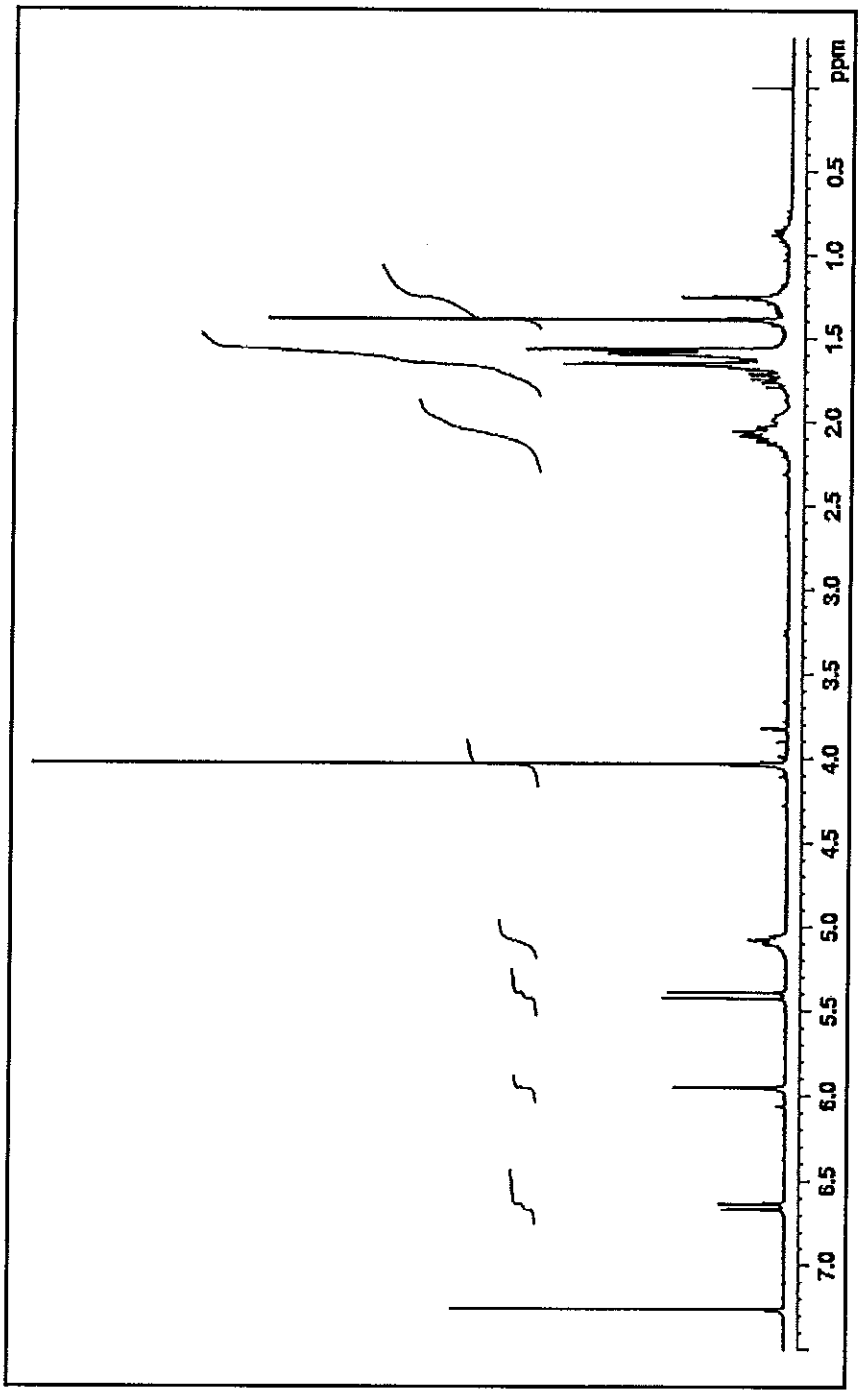

Figure 22 ^{1}H NMR (300 MHz) ($CDCl_3$) spectrum of compound GP1

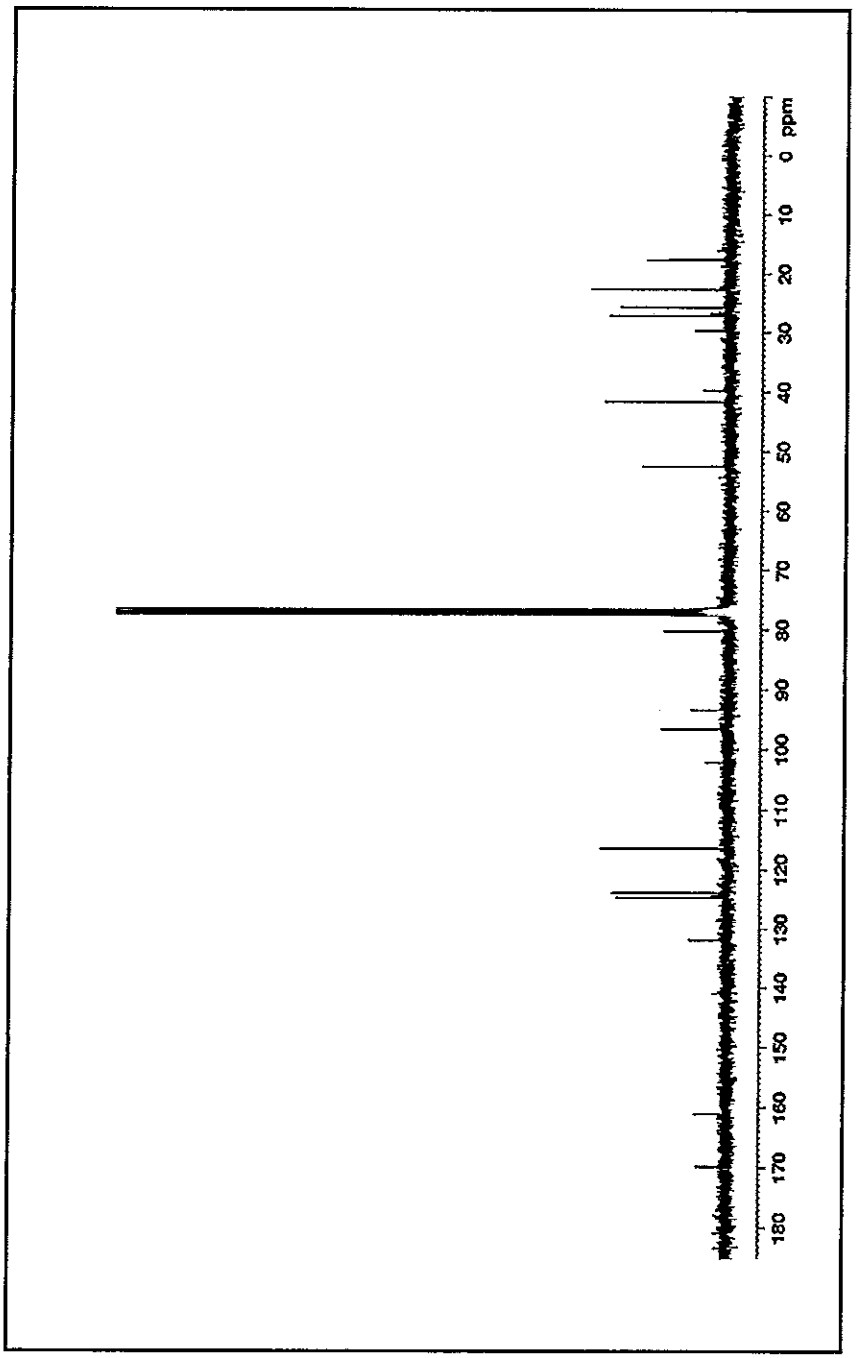

Figure 23 ^{13}C NMR (75 MHz) ($CDCl_3$) spectrum of compound GP1

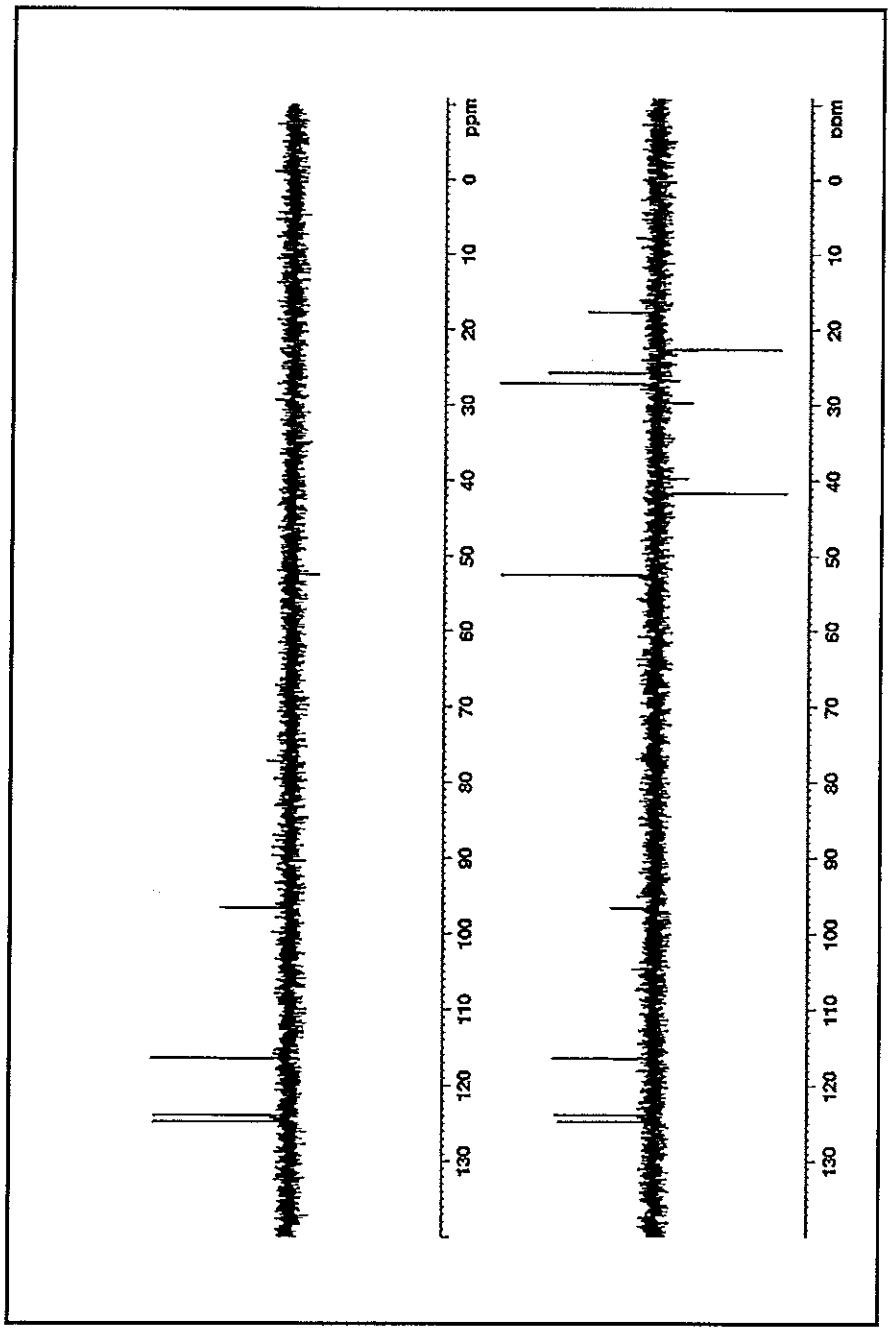

Figure 24 DEPT 90° and 135° spectra of compound GP1

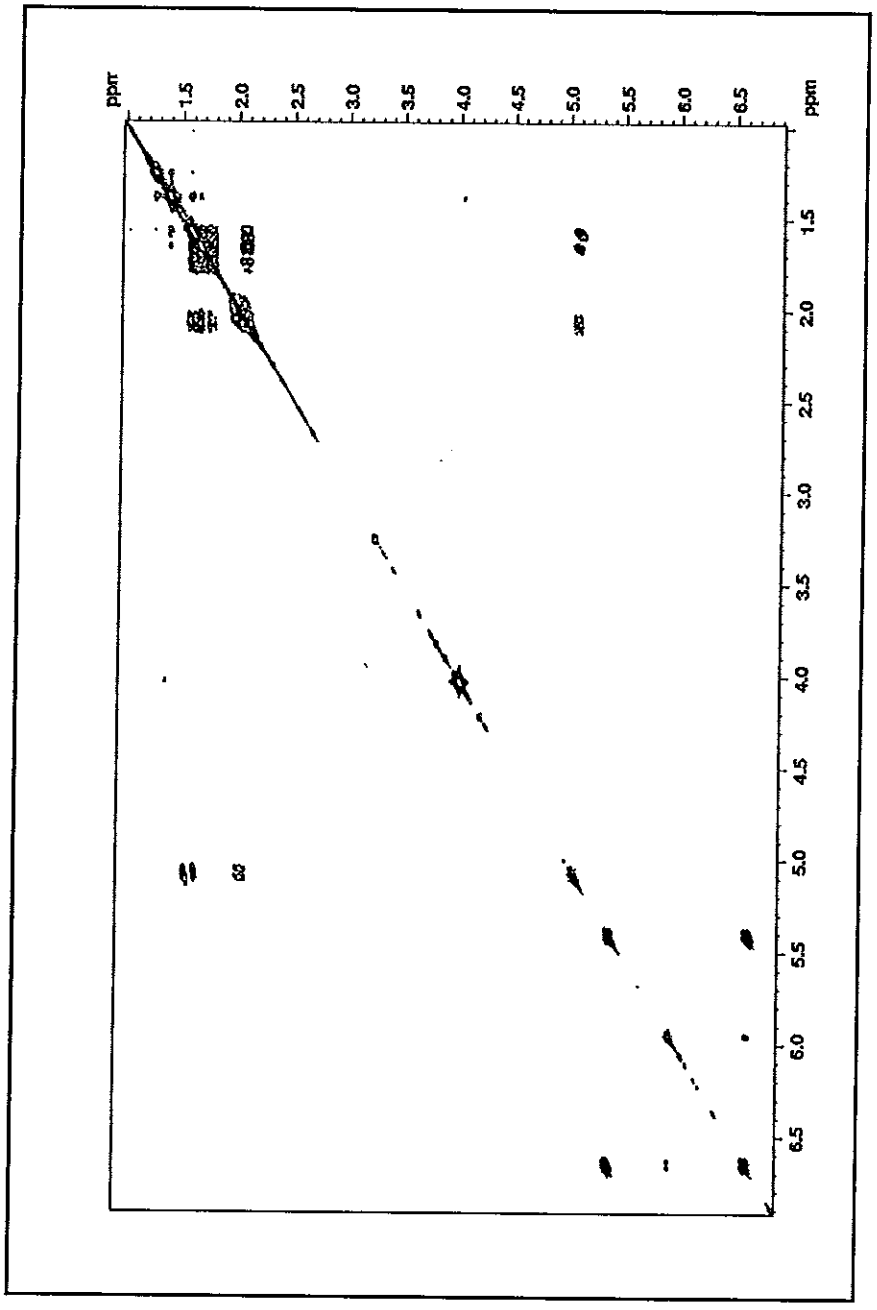

Figure 25 ^{1}H-^{1}H COSY spectrum of compound GP1

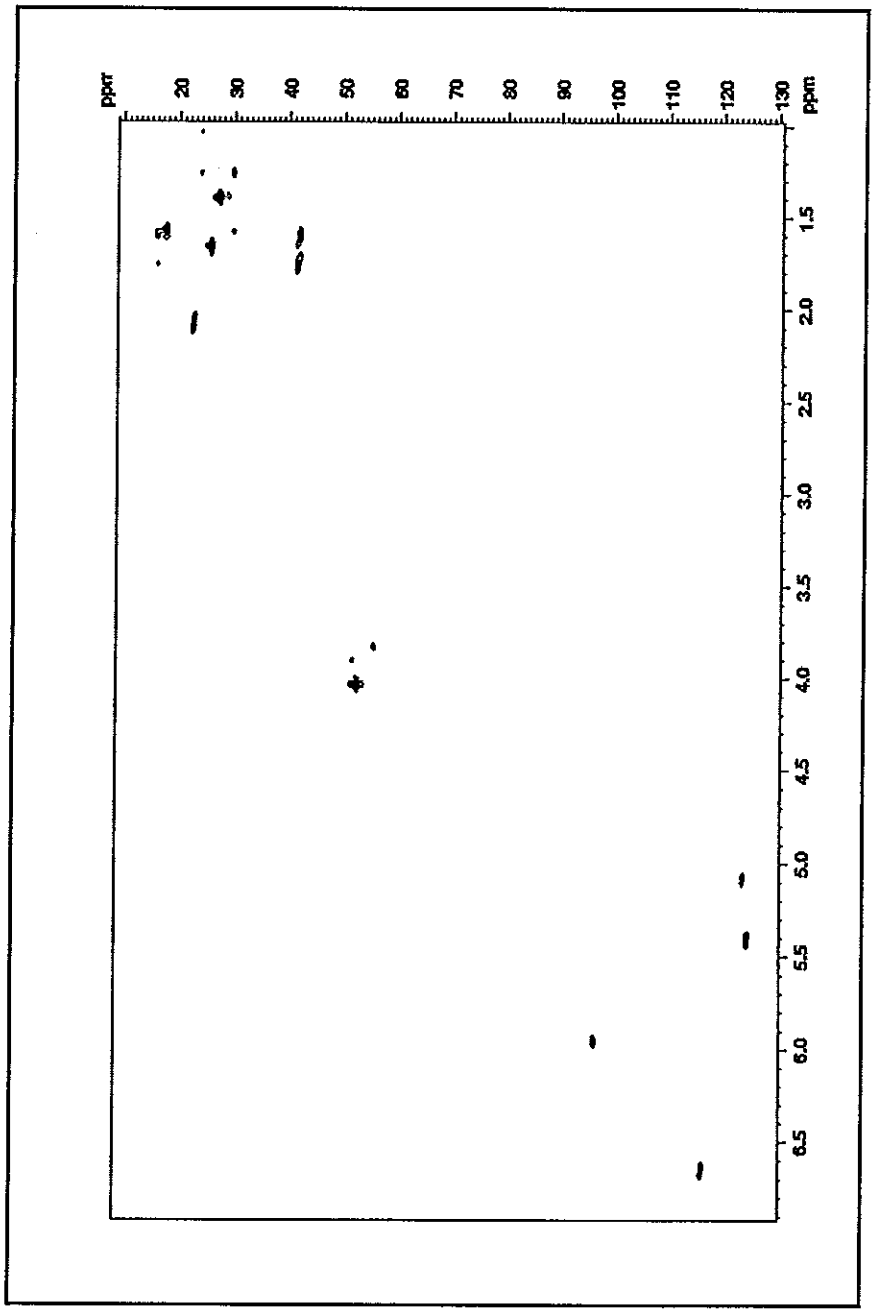

Figure 26 2D HMQC spectrum of compound GP1

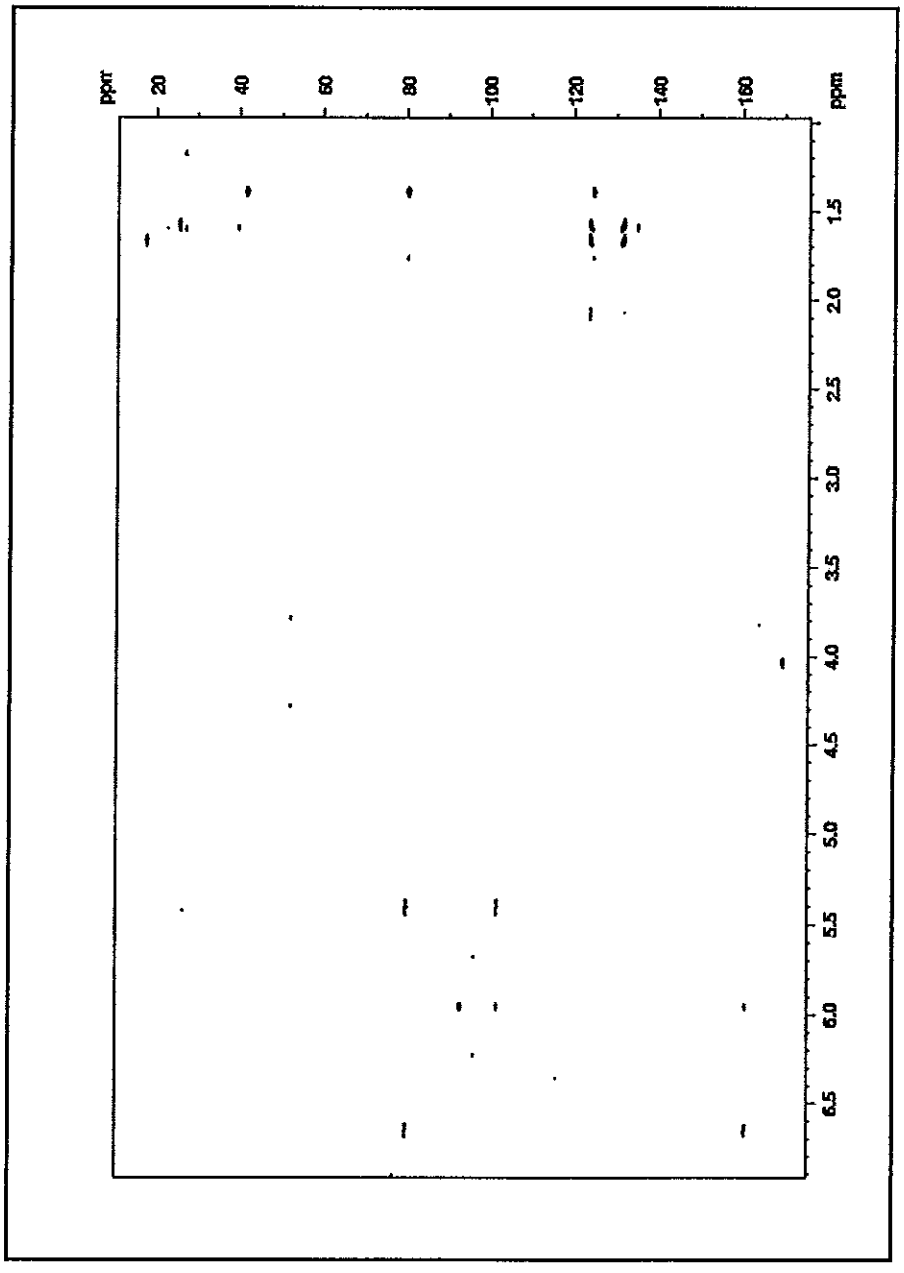

Figure 27 2D HMBC spectrum of compound GP1

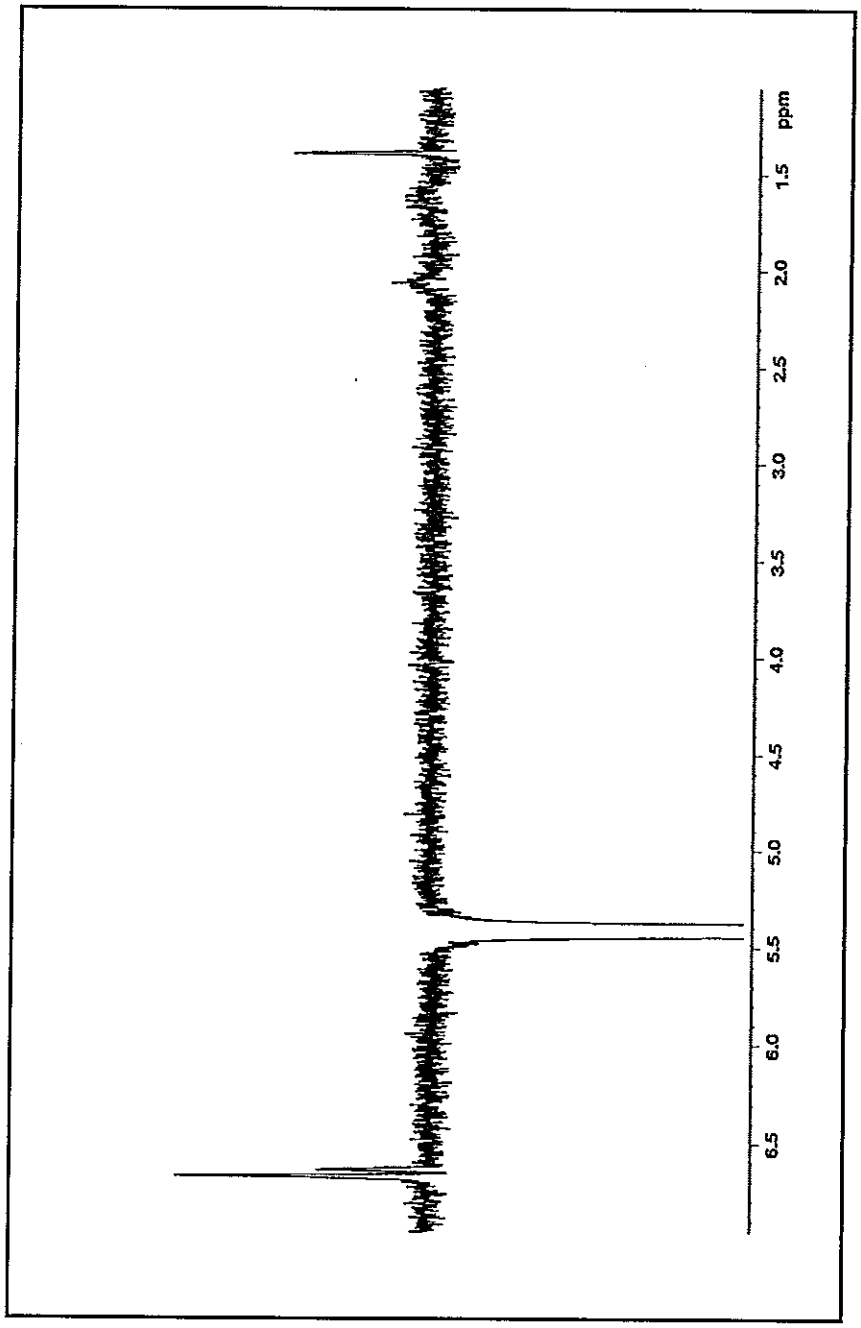

Figure 28 NOE difference spectrum of compound GP1 after irradiation at δ_H 5.41 (H-3)

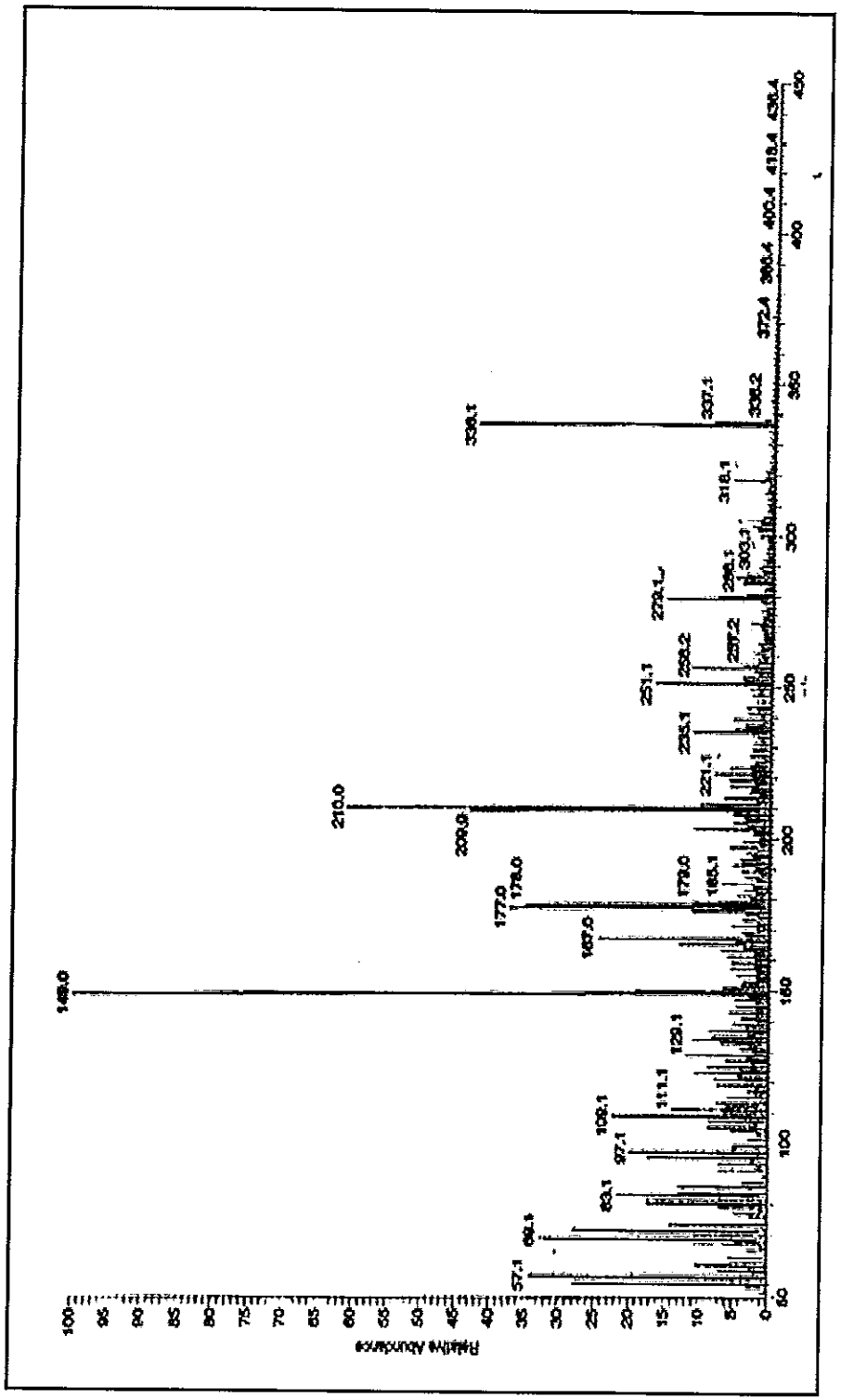

Figure 29 Mass spectrum of compound GP6

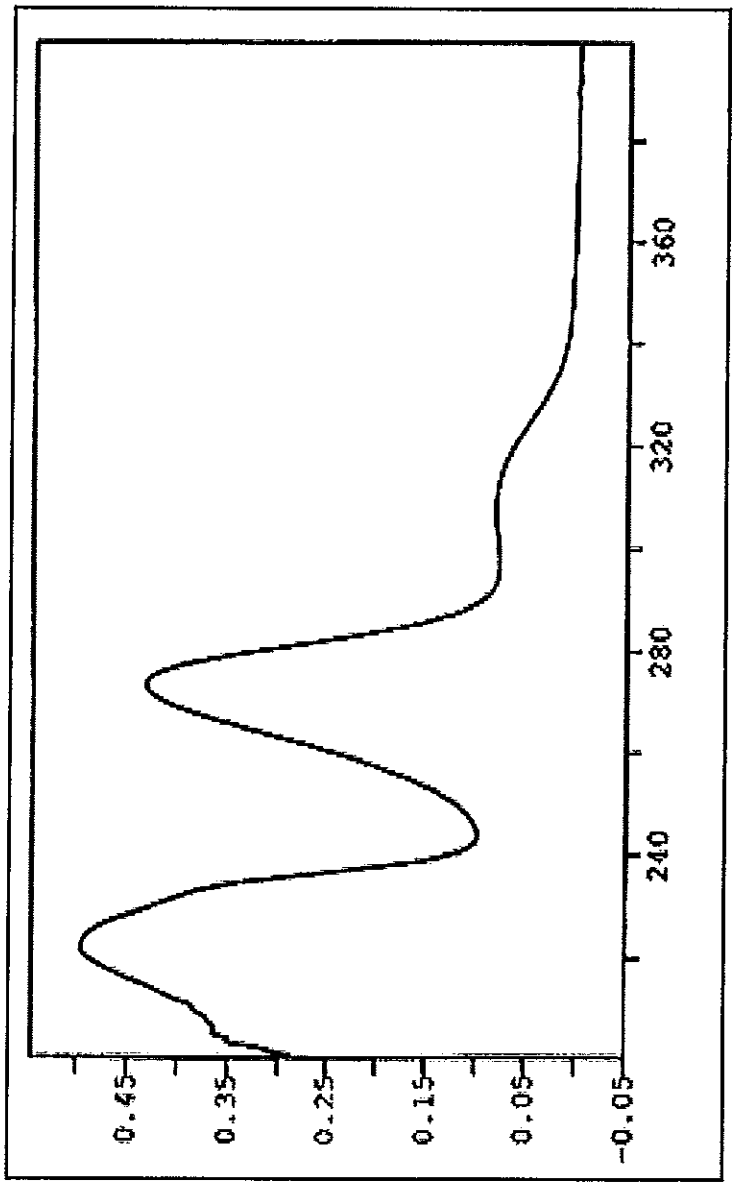

Figure 30 UV (MeOH) spectrum of compound GP6

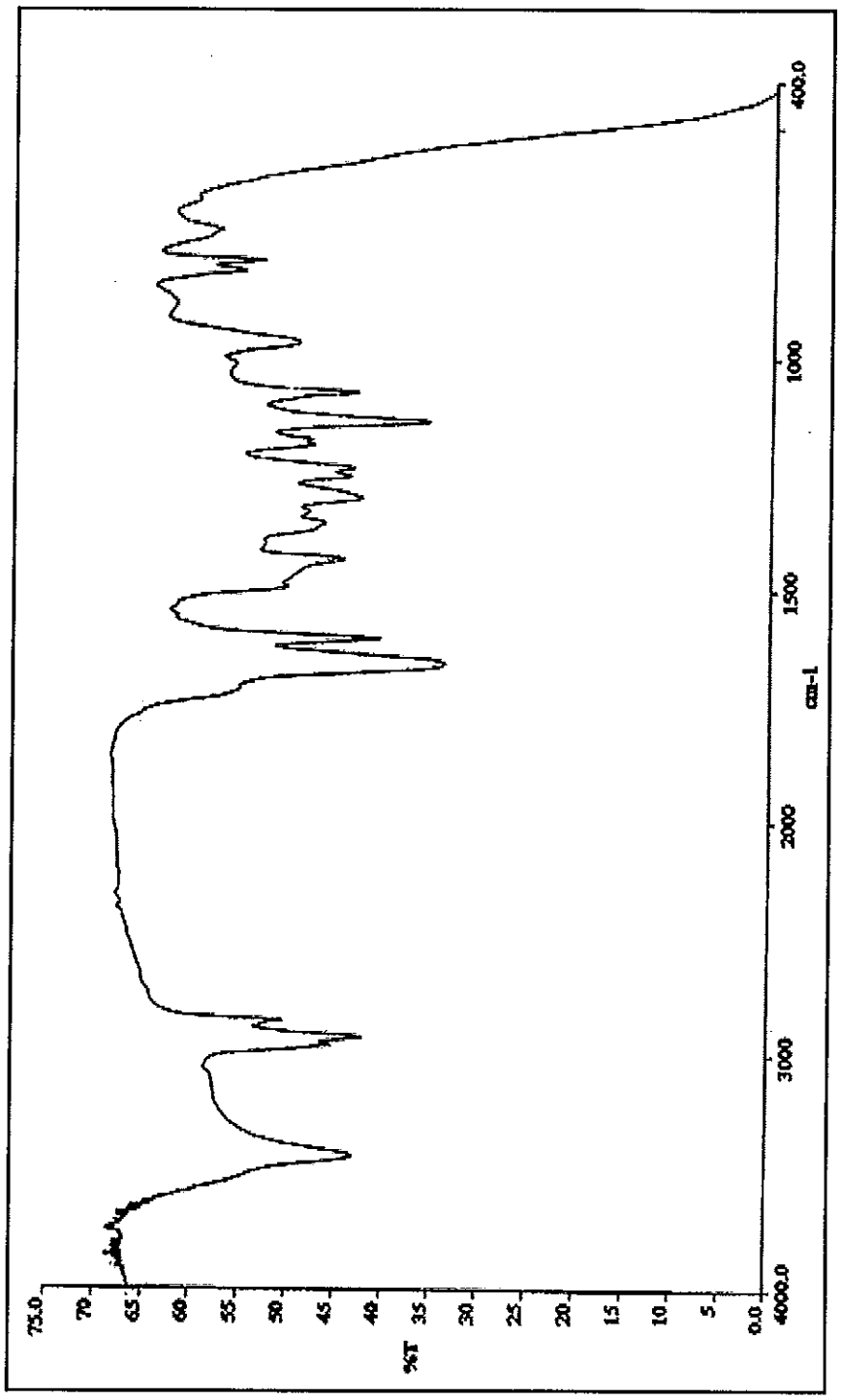

Figure 31 FT-IR (neat) spectrum of compound GP6

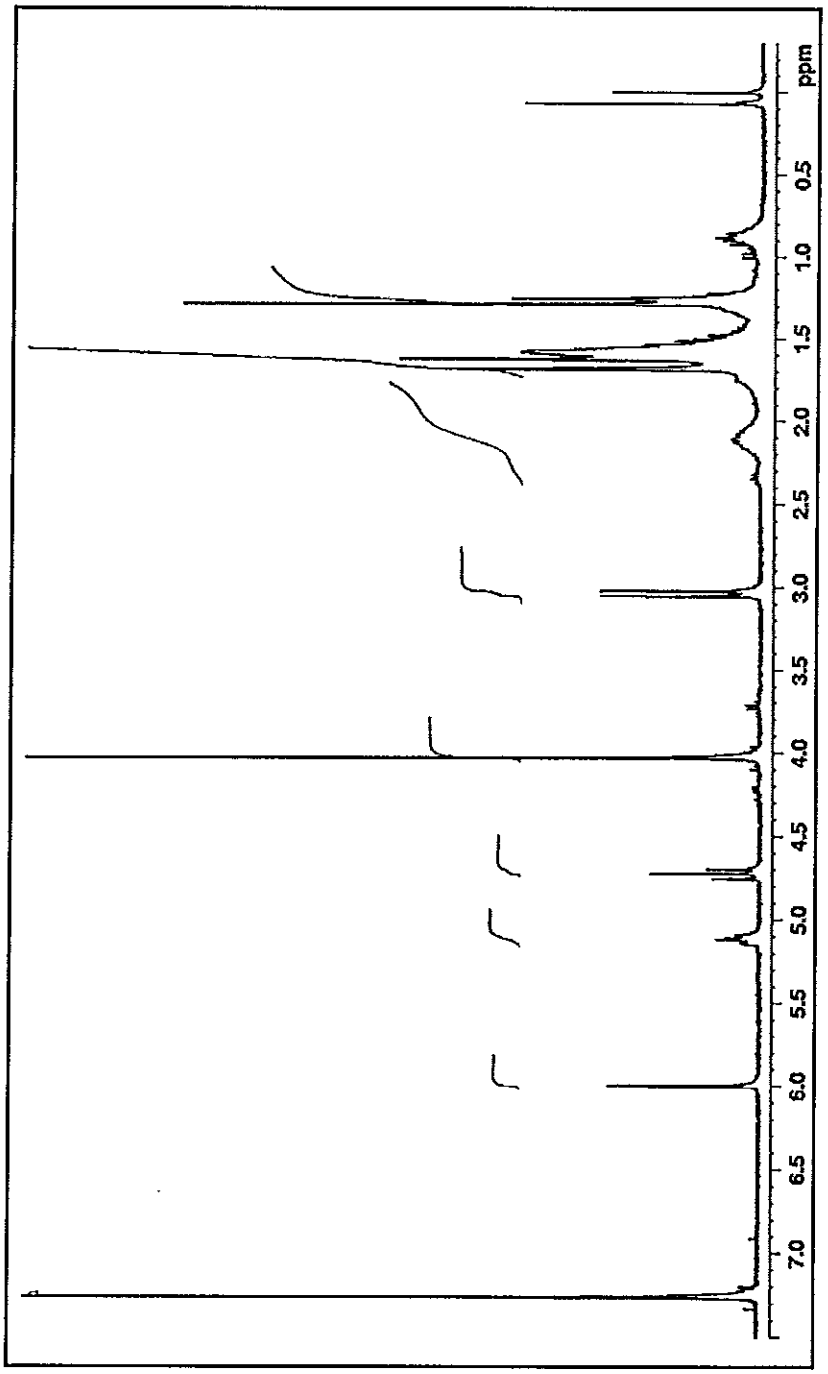

Figure 32 ^{1}H NMR (300 MHz) ($CDCl_3$) spectrum of compound GP6

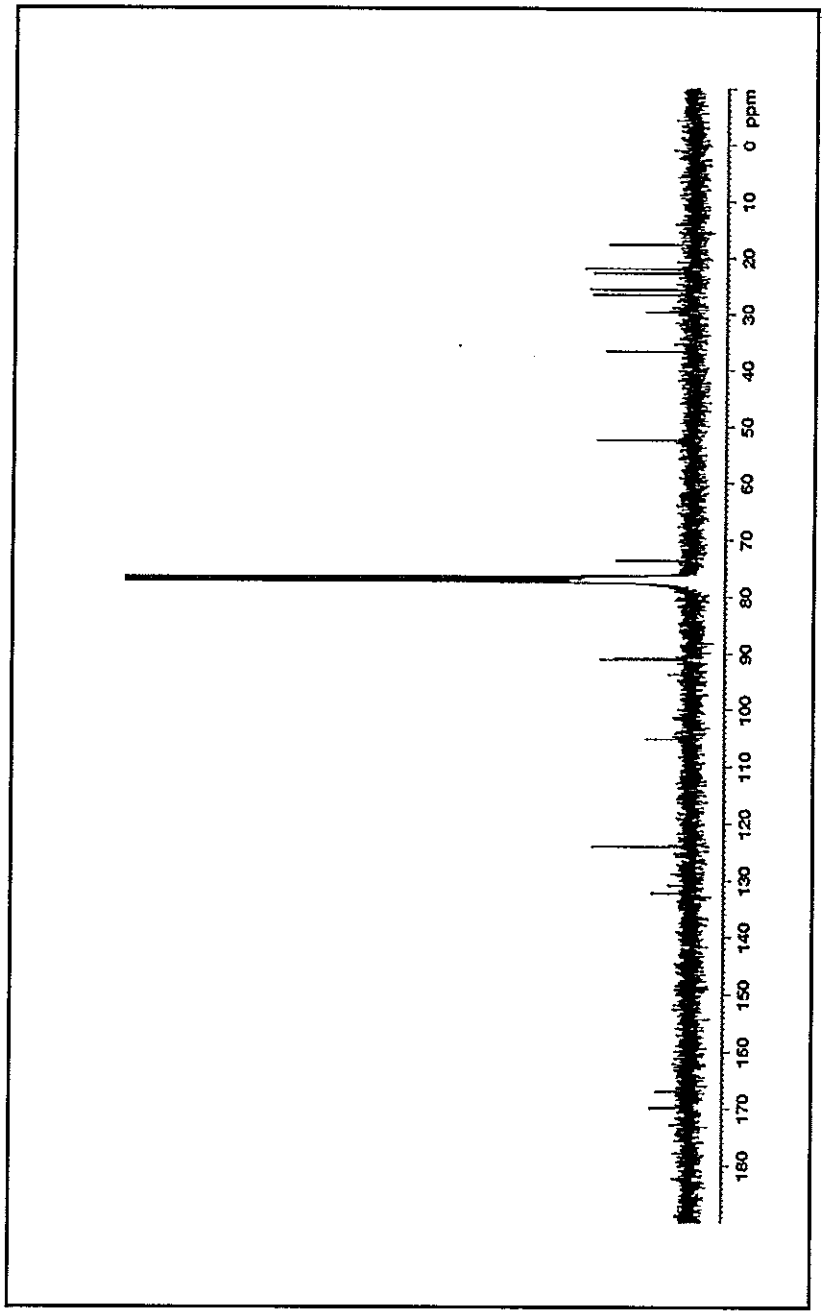

Figure 33 ^{13}C NMR (75 MHz) ($CDCl_3$) spectrum of compound GP6

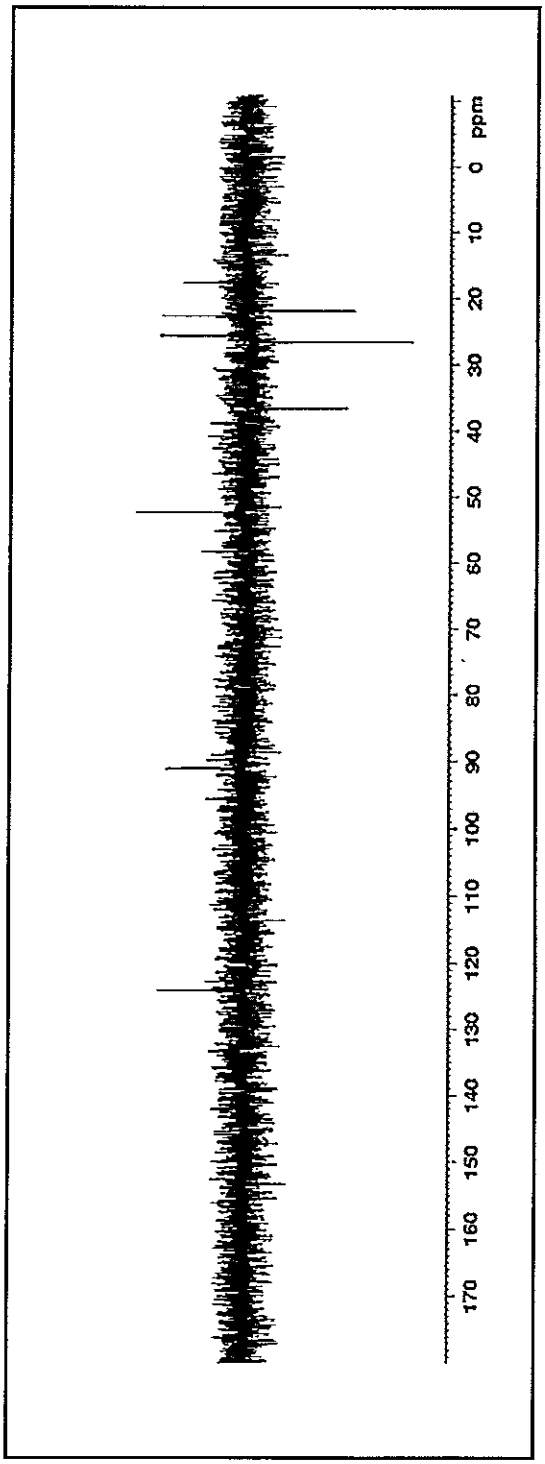

Figure 34 DEPT 135° spectra of compound GP6

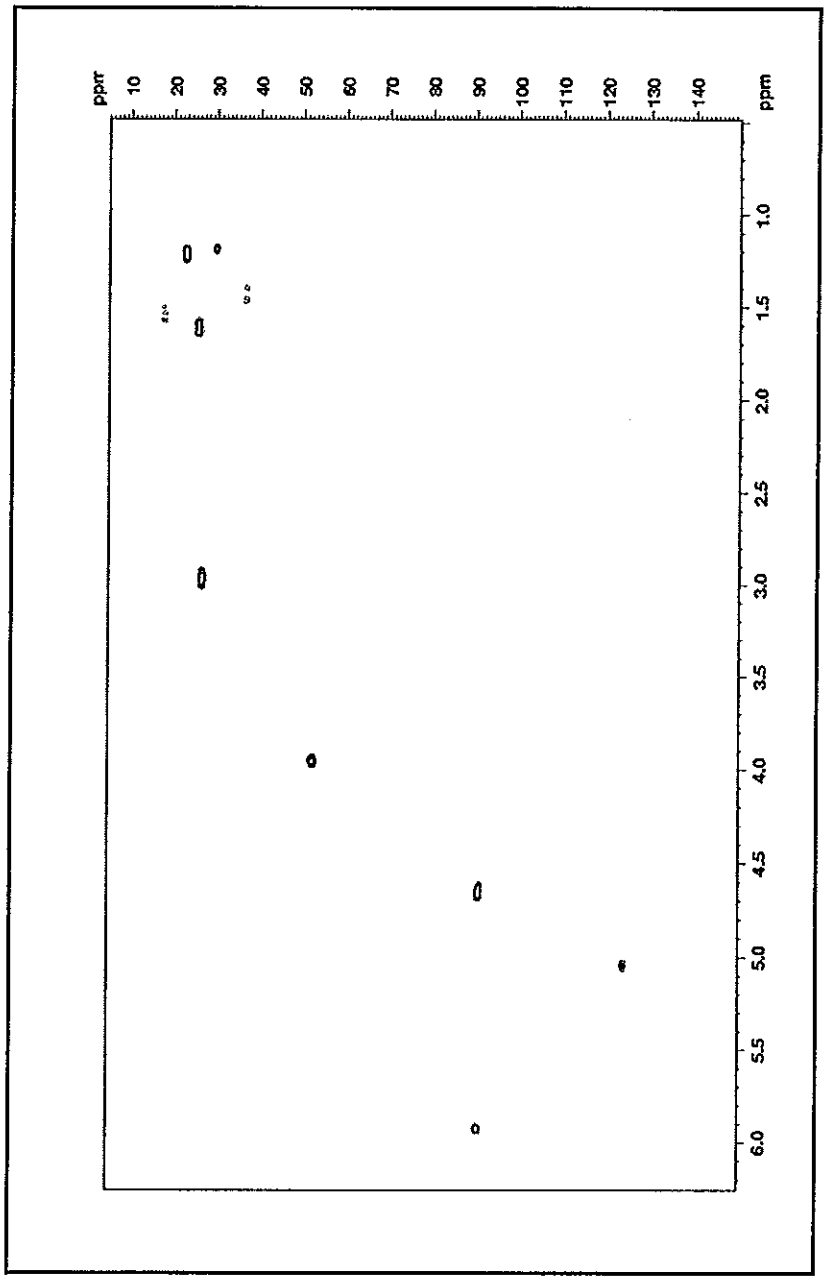

Figure 35 2D HMQC spectrum of compound GP6

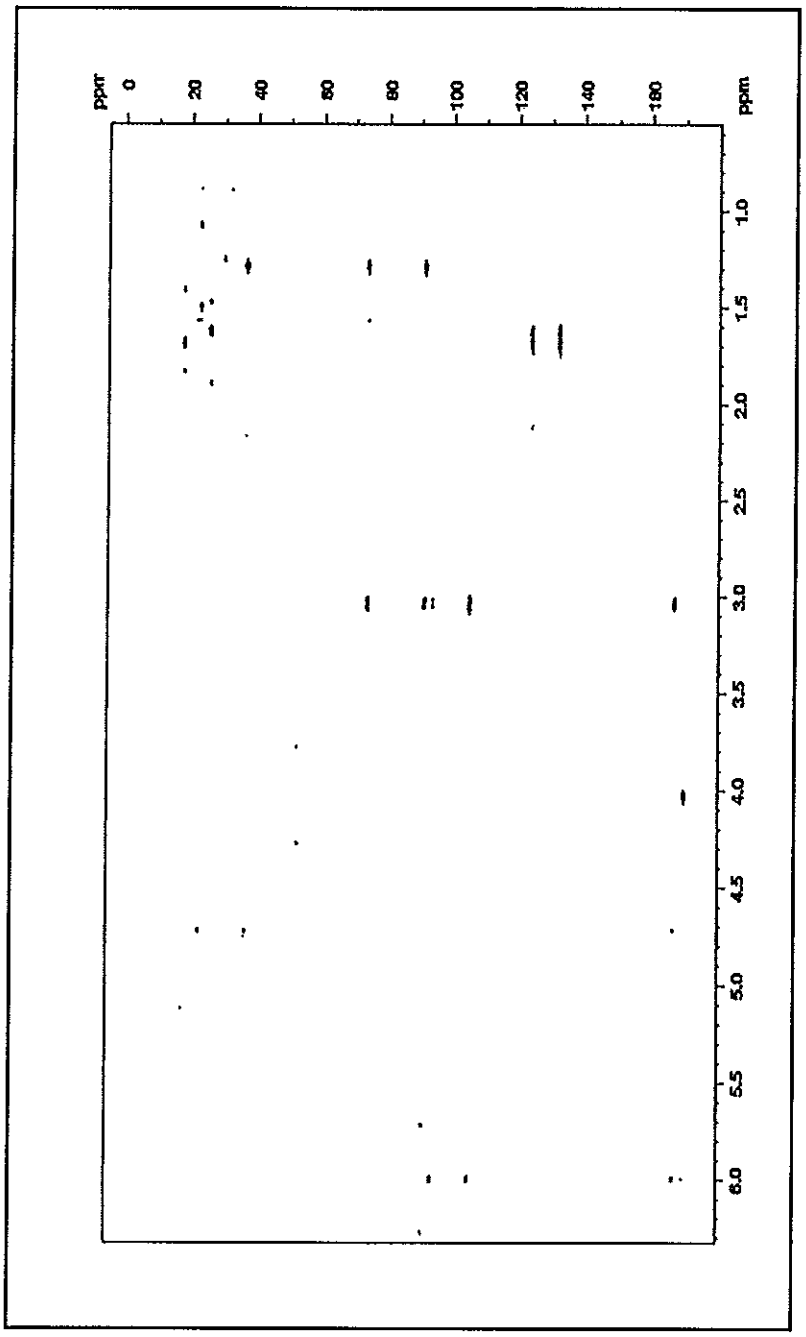

Figure 36 2D HMBC spectrum of compound GP6

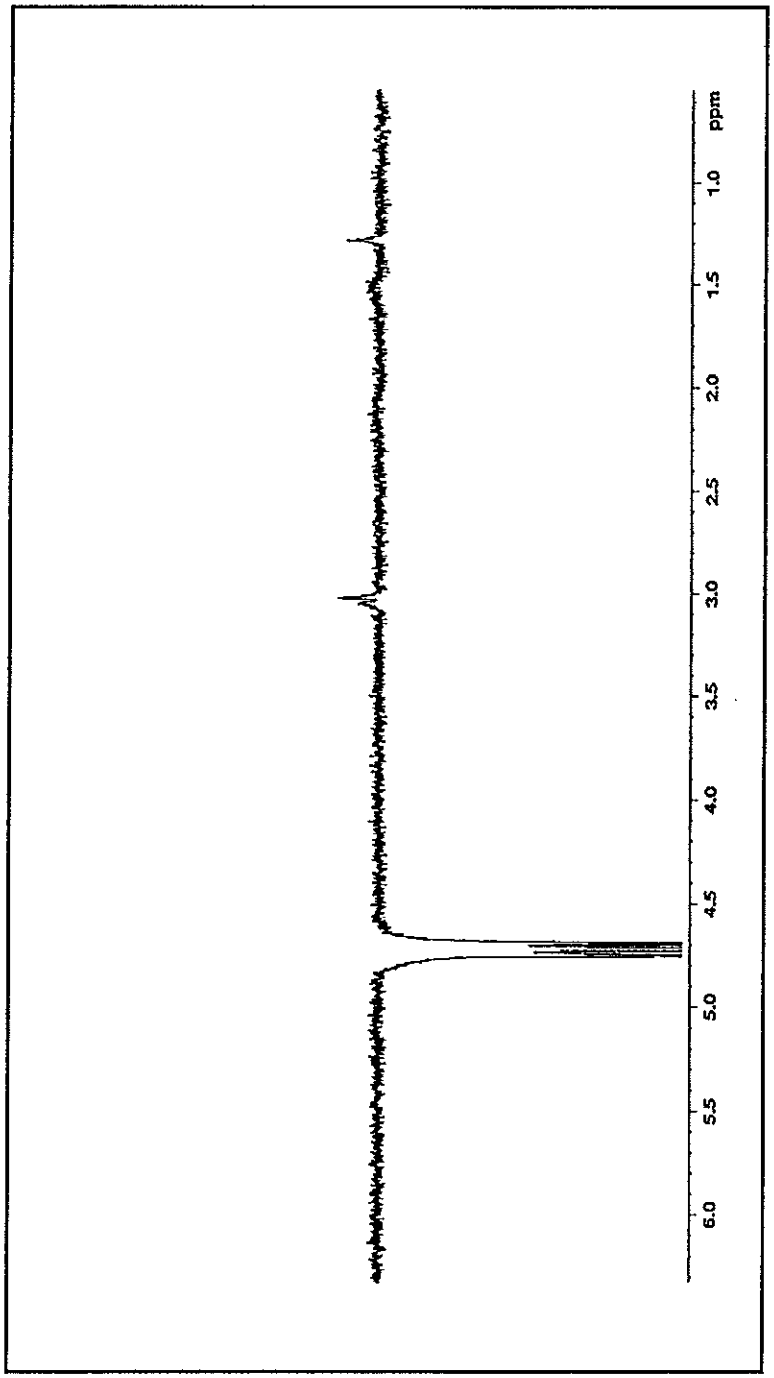

Figure 37 NOE difference spectrum of compound GP6 after irradiation at δ_H 4.73 (H-3)

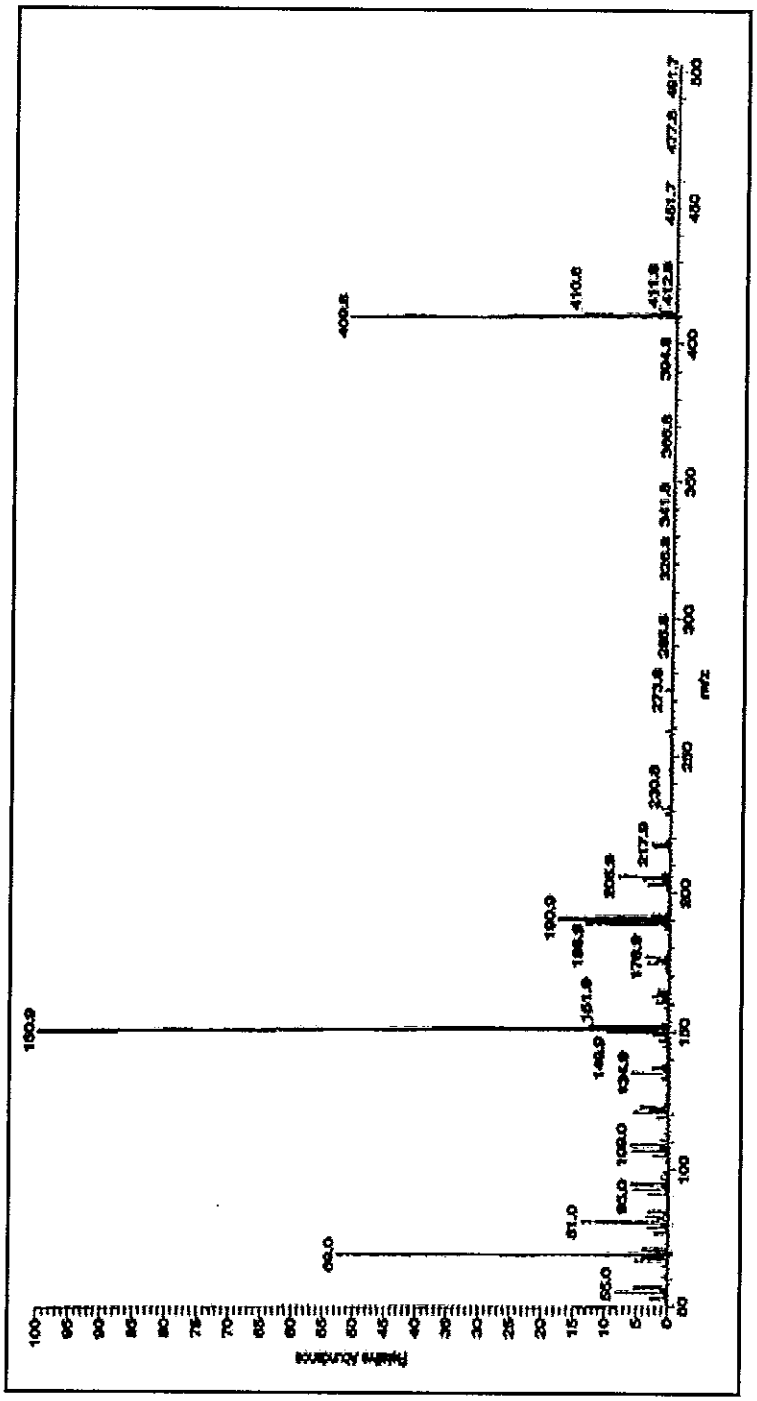

Figure 38 Mass spectrum of compound GP3

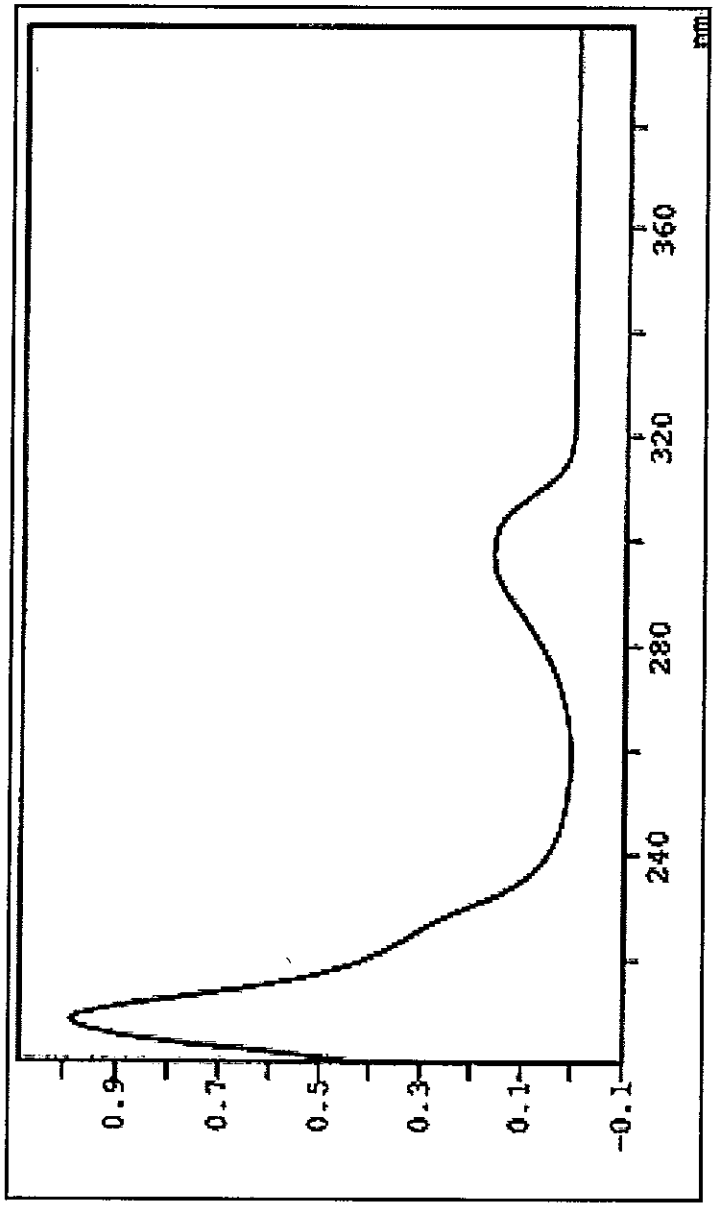

Figure 39 UV (MeOH) spectrum of compound GP3

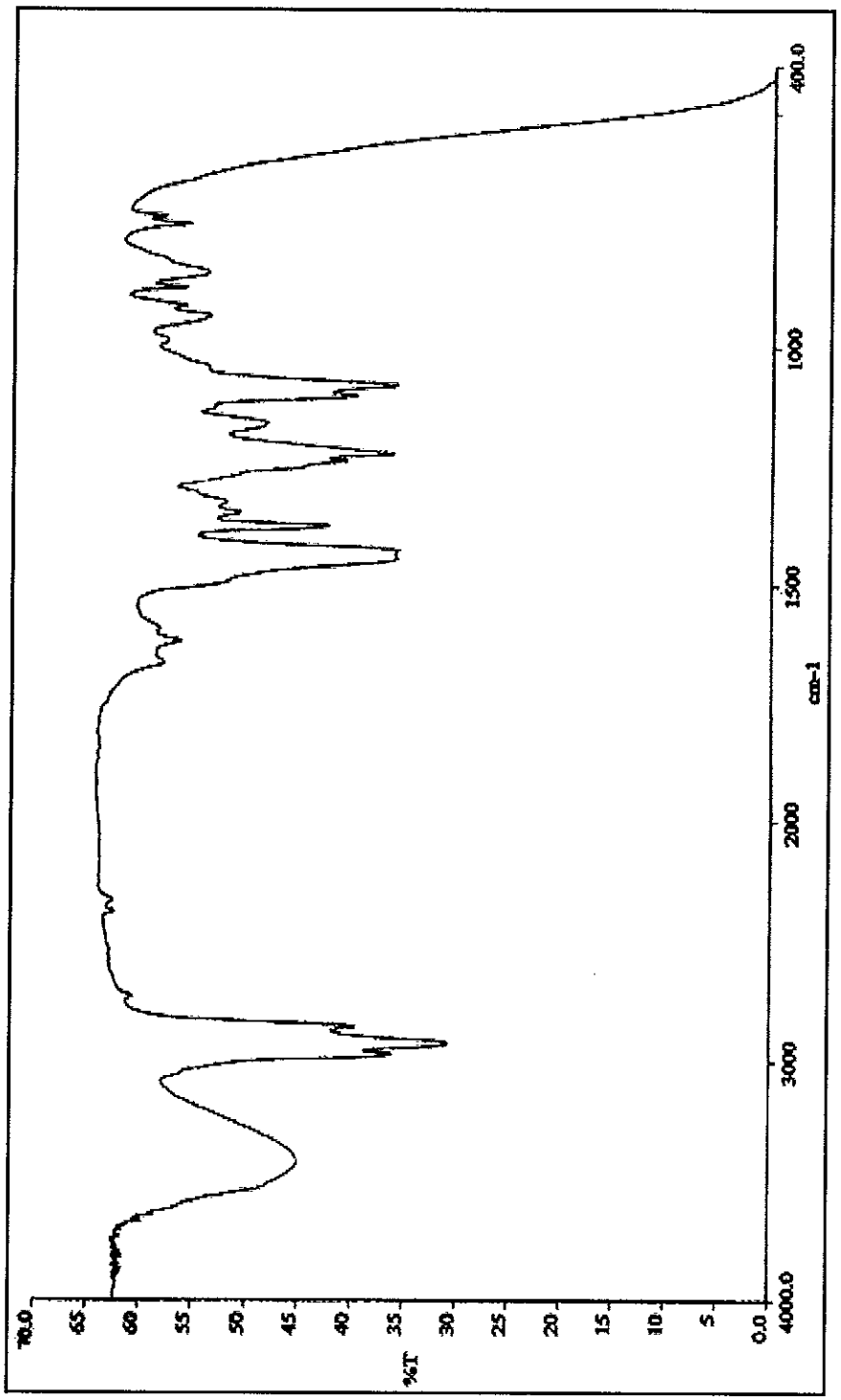

Figure 40 FT-IR (neat) spectrum of compound GP3

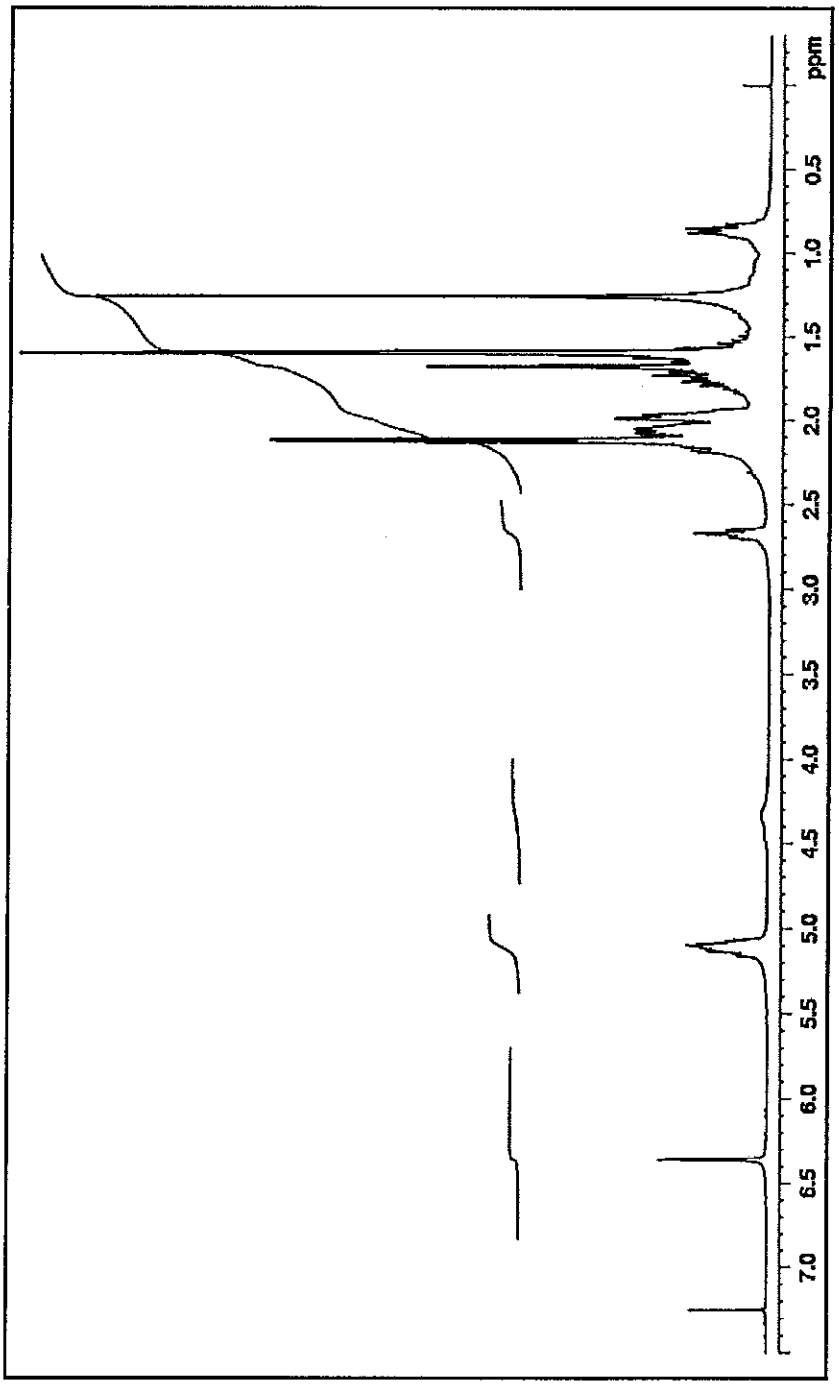

Figure 41 ^{1}H NMR (300 MHz) ($CDCl_3$) spectrum of compound GP3

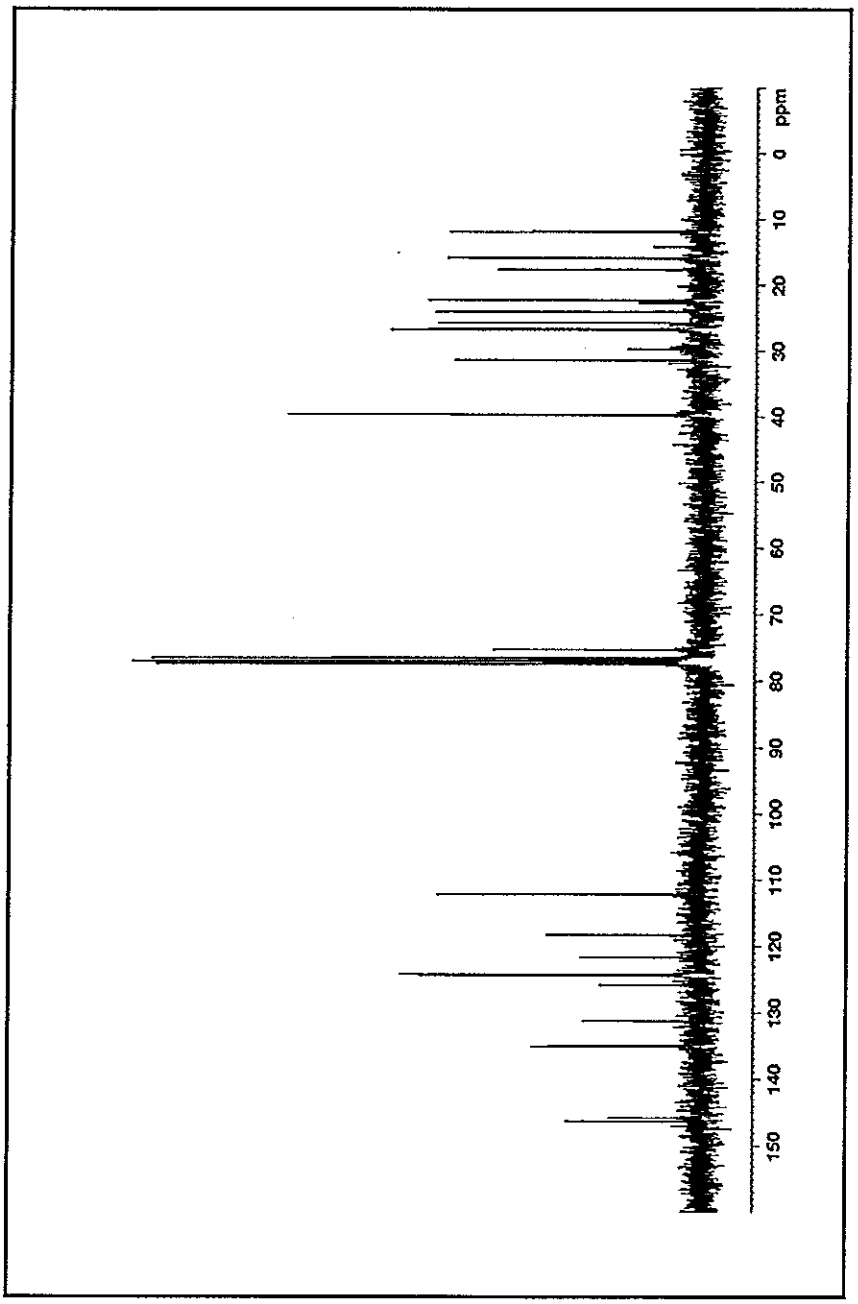

Figure 42 ^{13}C NMR (75 MHz) ($CDCl_3$) spectrum of compound GP3

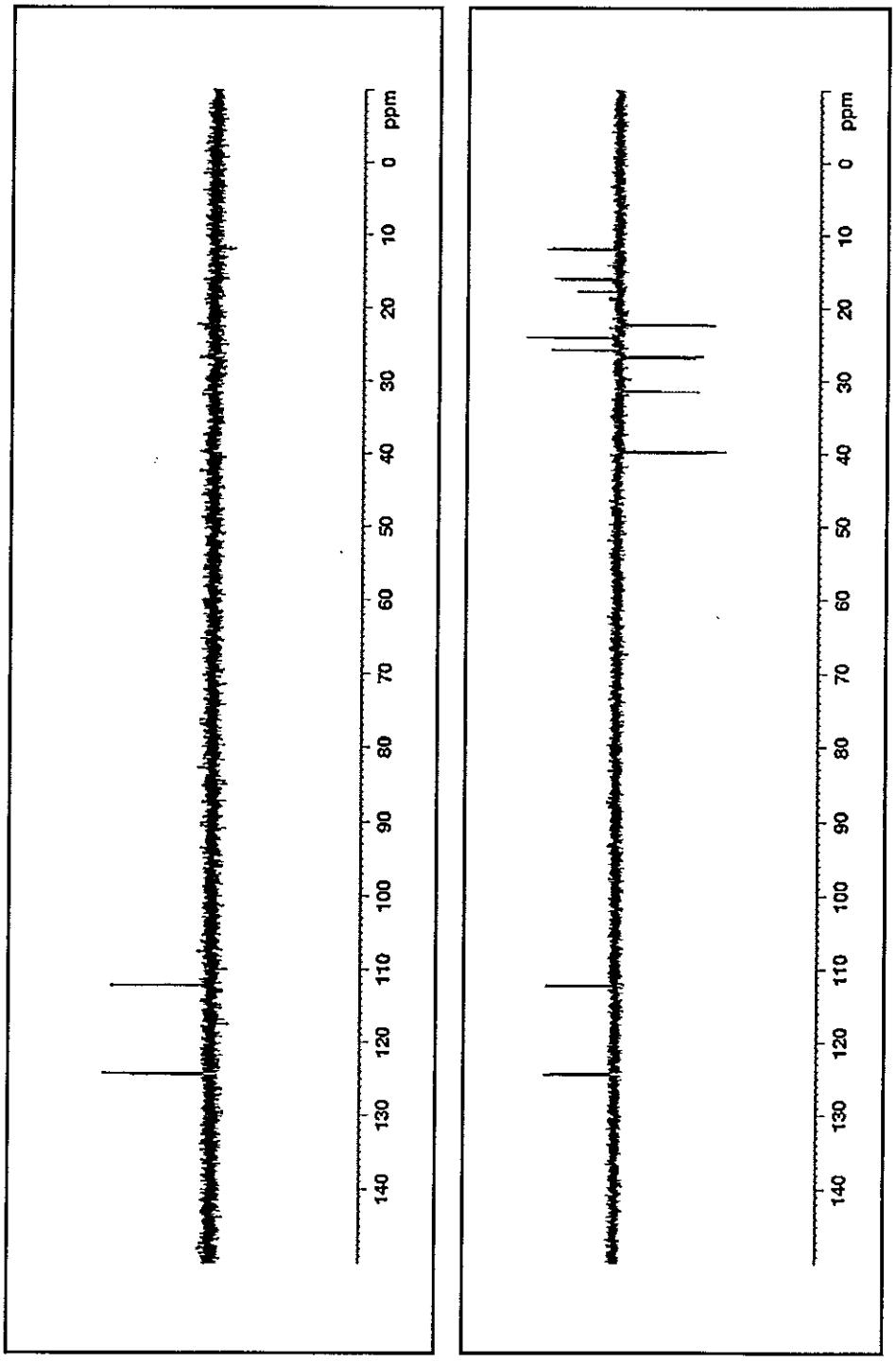

Figure 43 DEPT 90° and 135° spectra of compound GP3

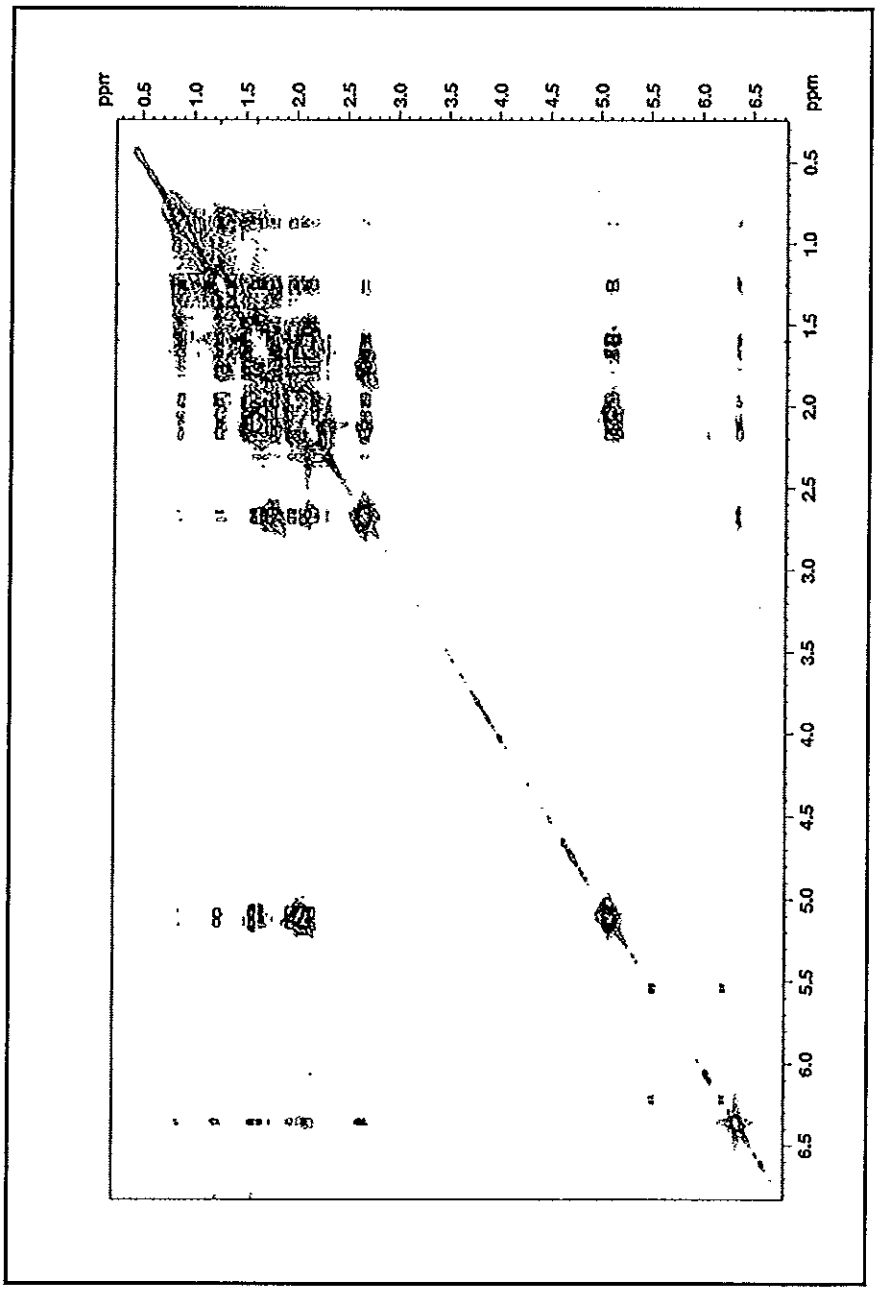

Figure 44 ^{1}H-^{1}H COSY spectrum of compound GP3

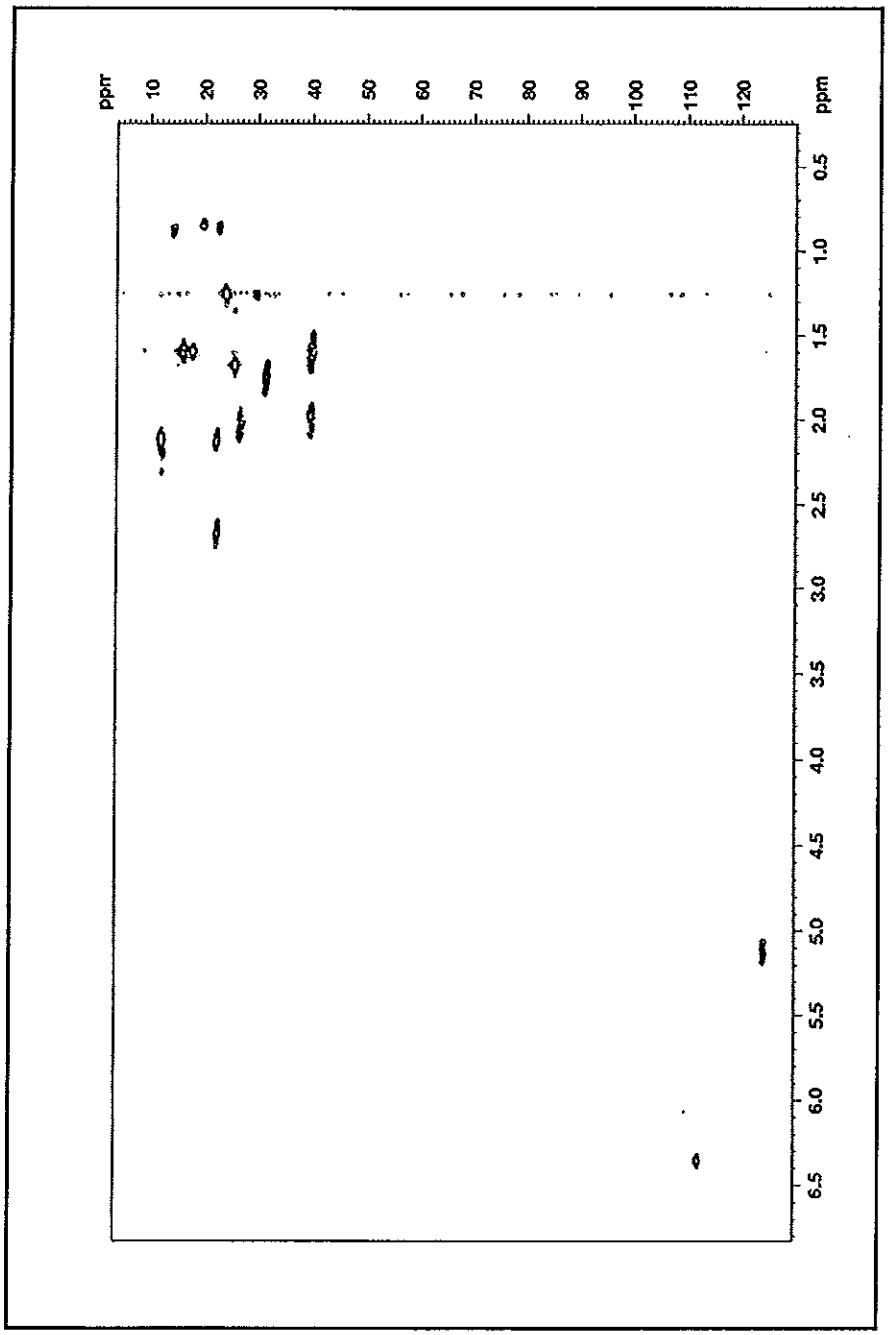

Figure 45 2D HMQC spectrum of compound GP3

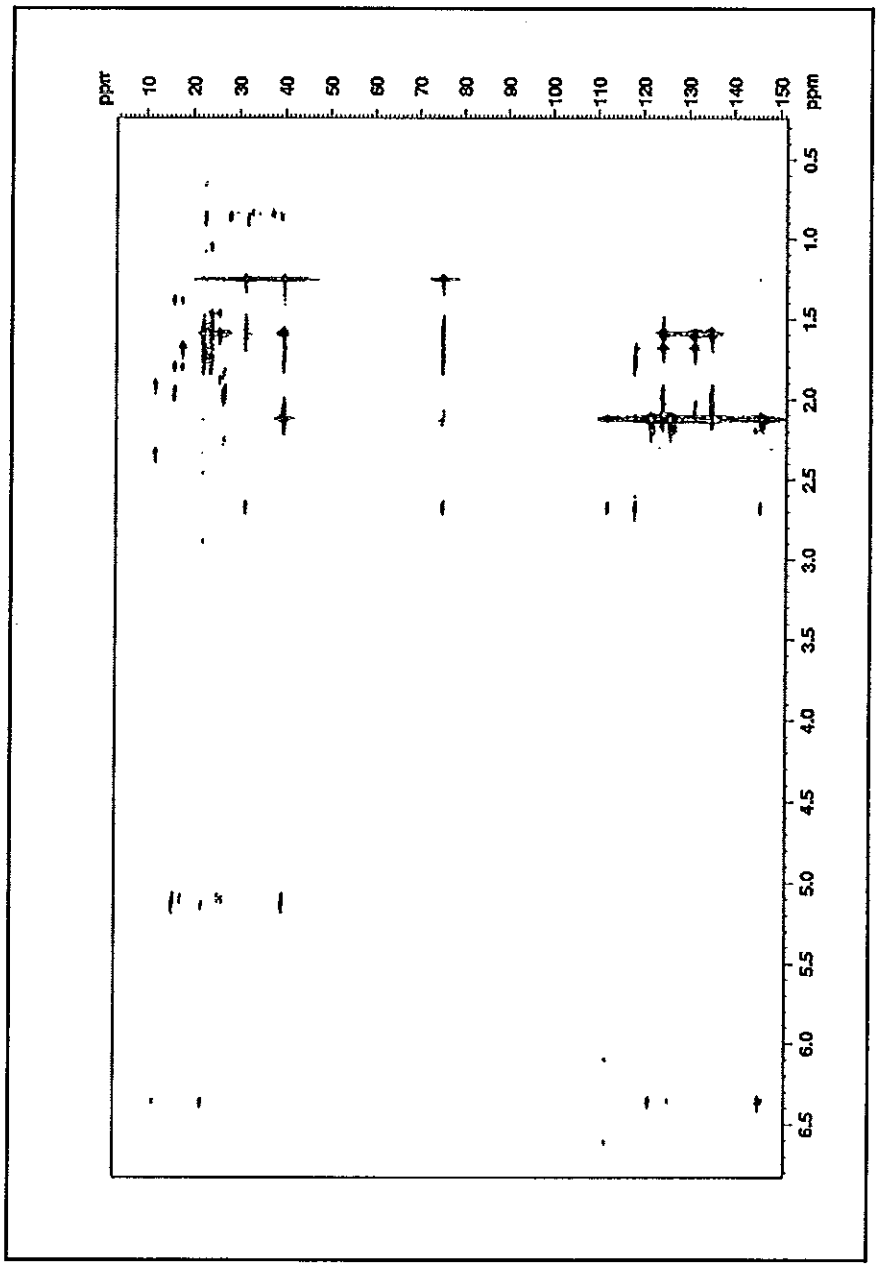

Figure 46 2D HMBC spectrum of compound GP3

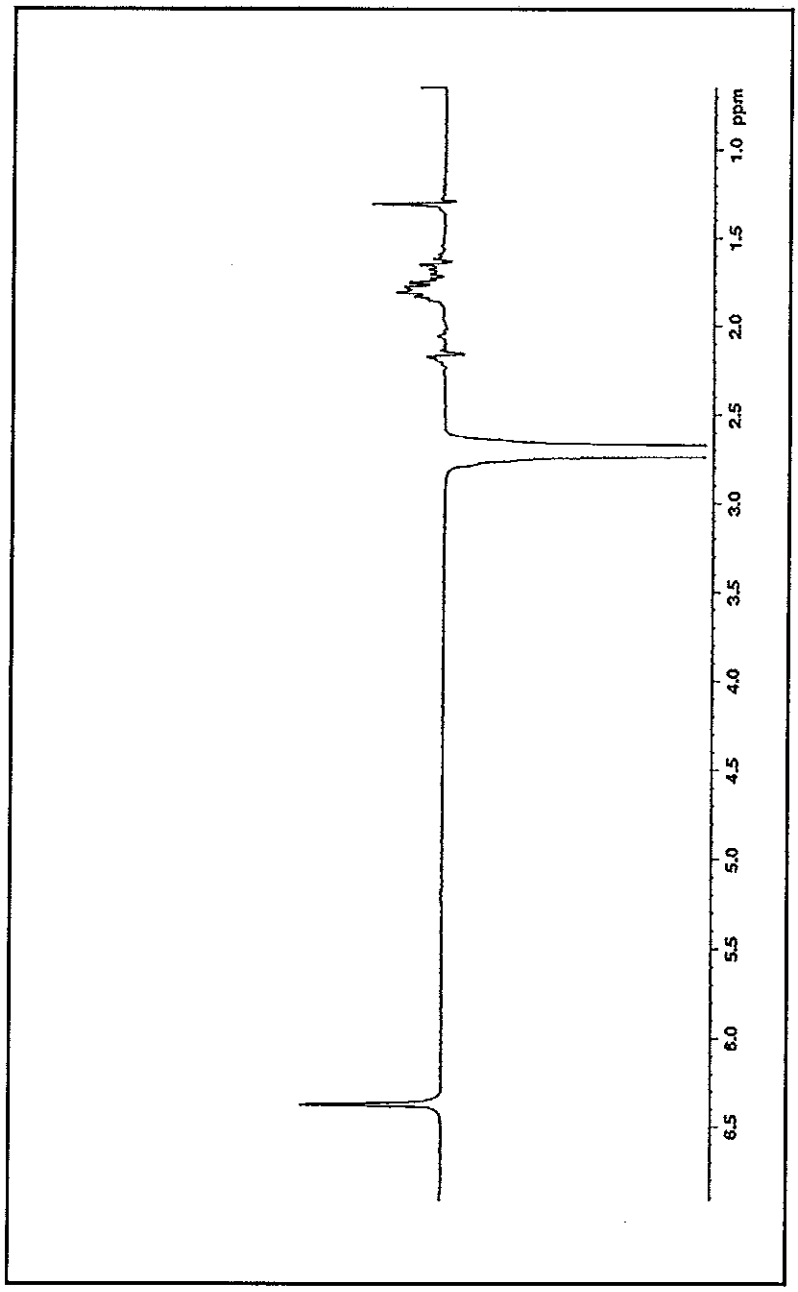

Figure 47 NOE difference spectrum of compound GP3 after irradiation at δ_H 2.67 (H-4)

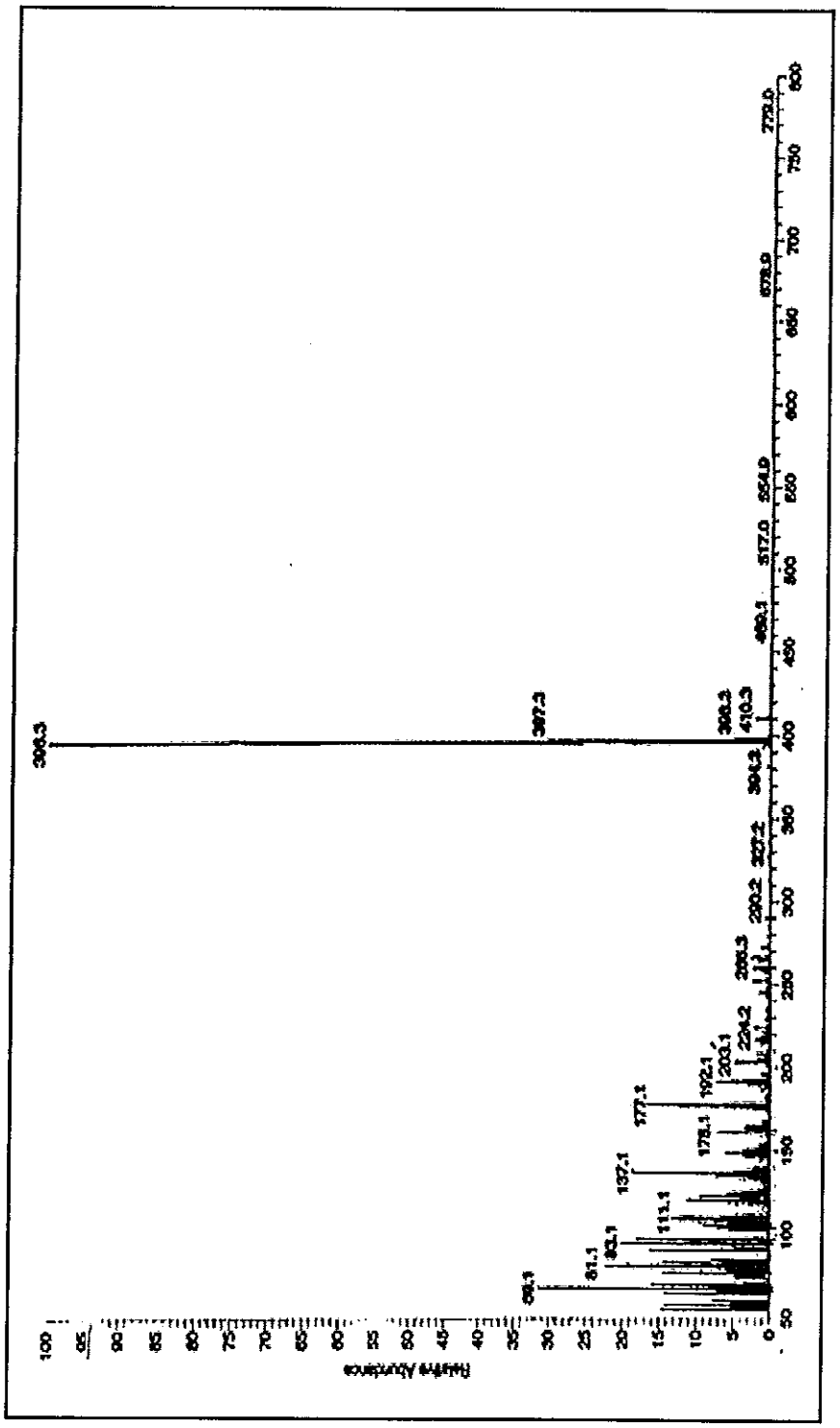

Figure 48 Mass spectrum of compound GP5

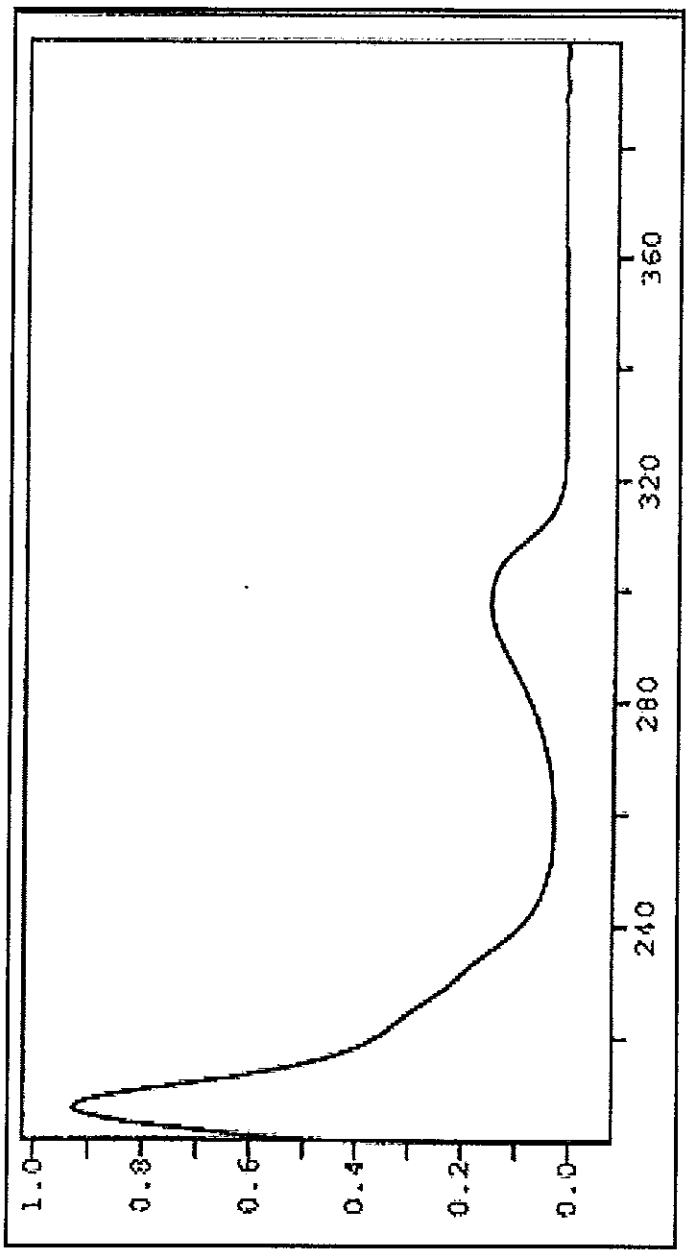

Figure 49 UV (MeOH) spectrum of compound GP5

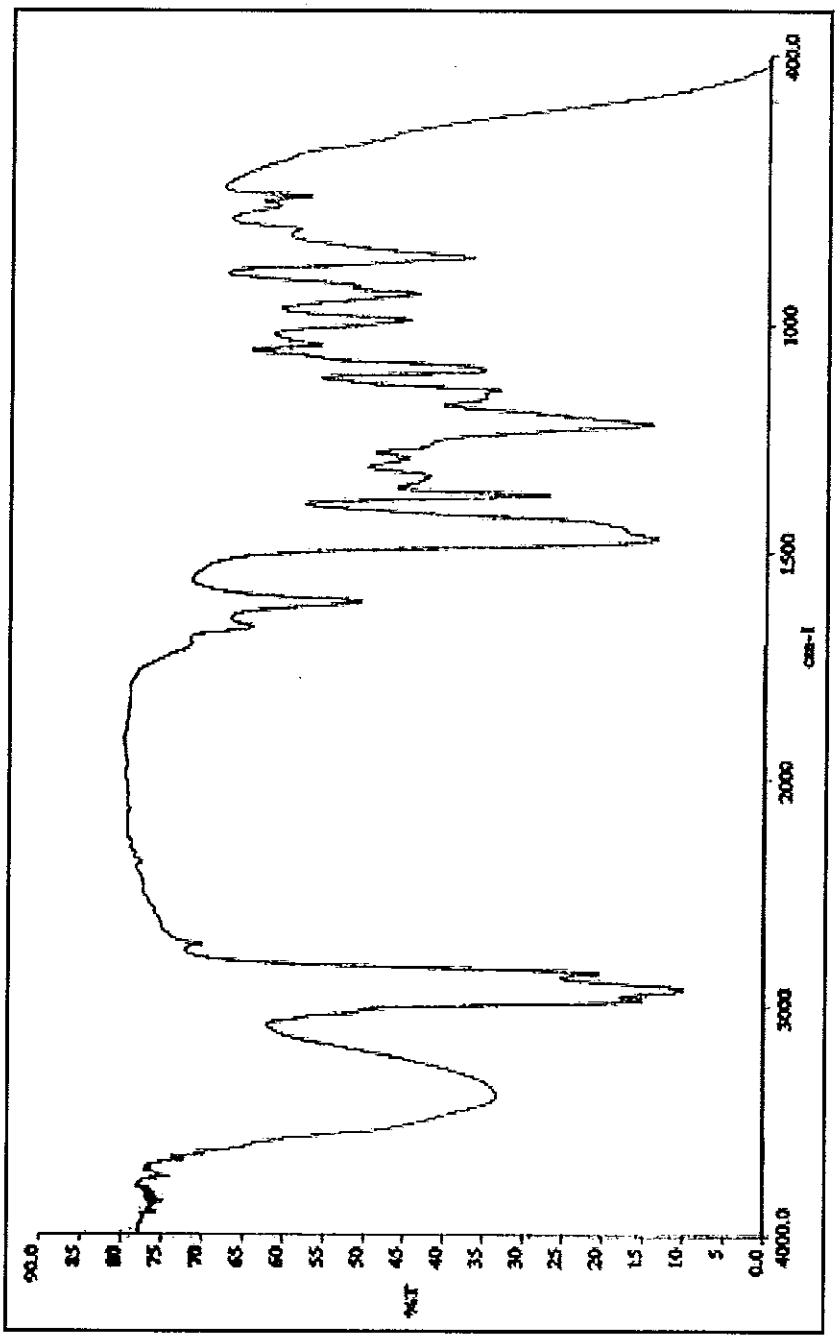

Figure 50 FT-IR (neat) spectrum of compound GP5

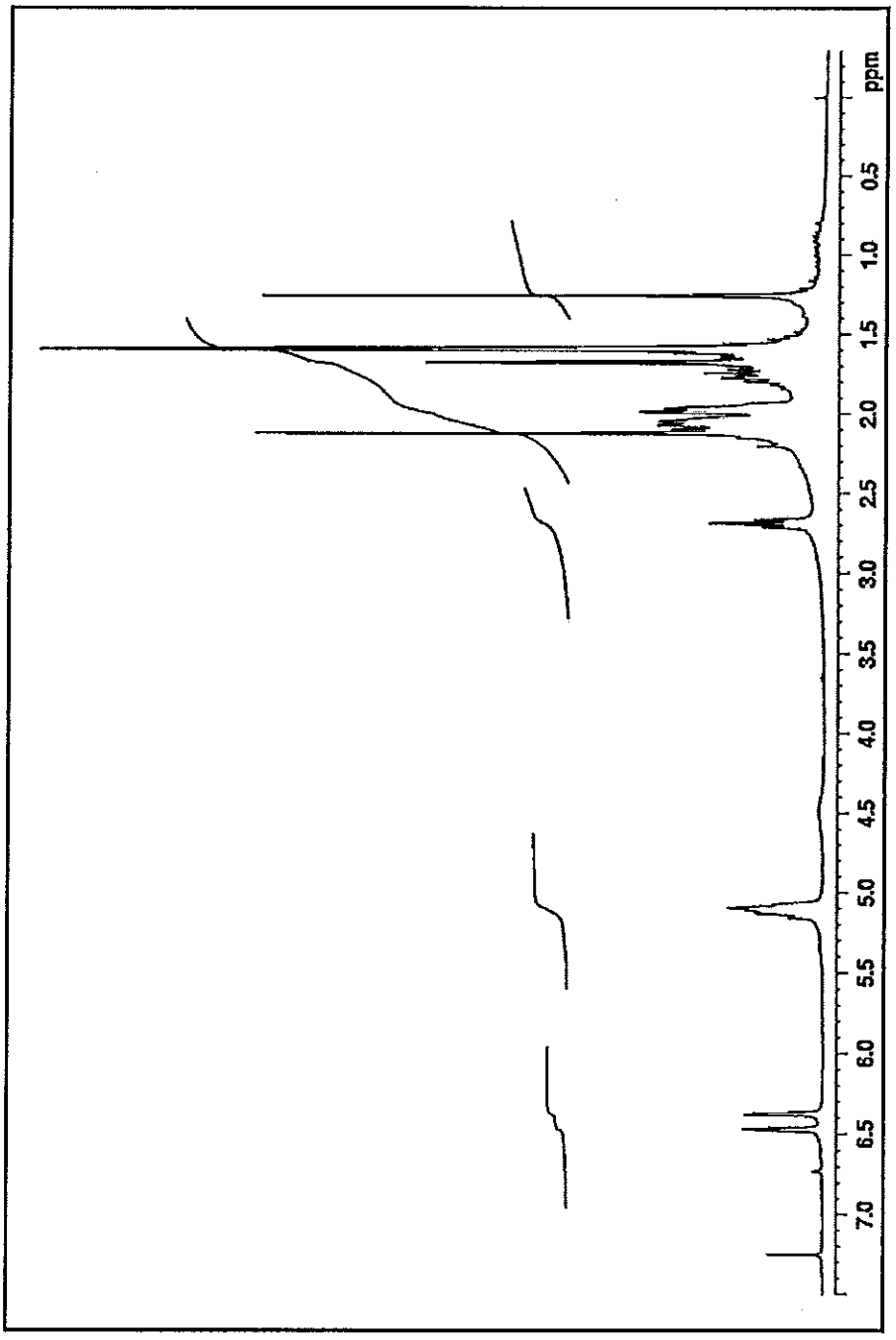

Figure 51 ^{1}H NMR (300 MHz) ($CDCl_3$) spectrum of compound GP5

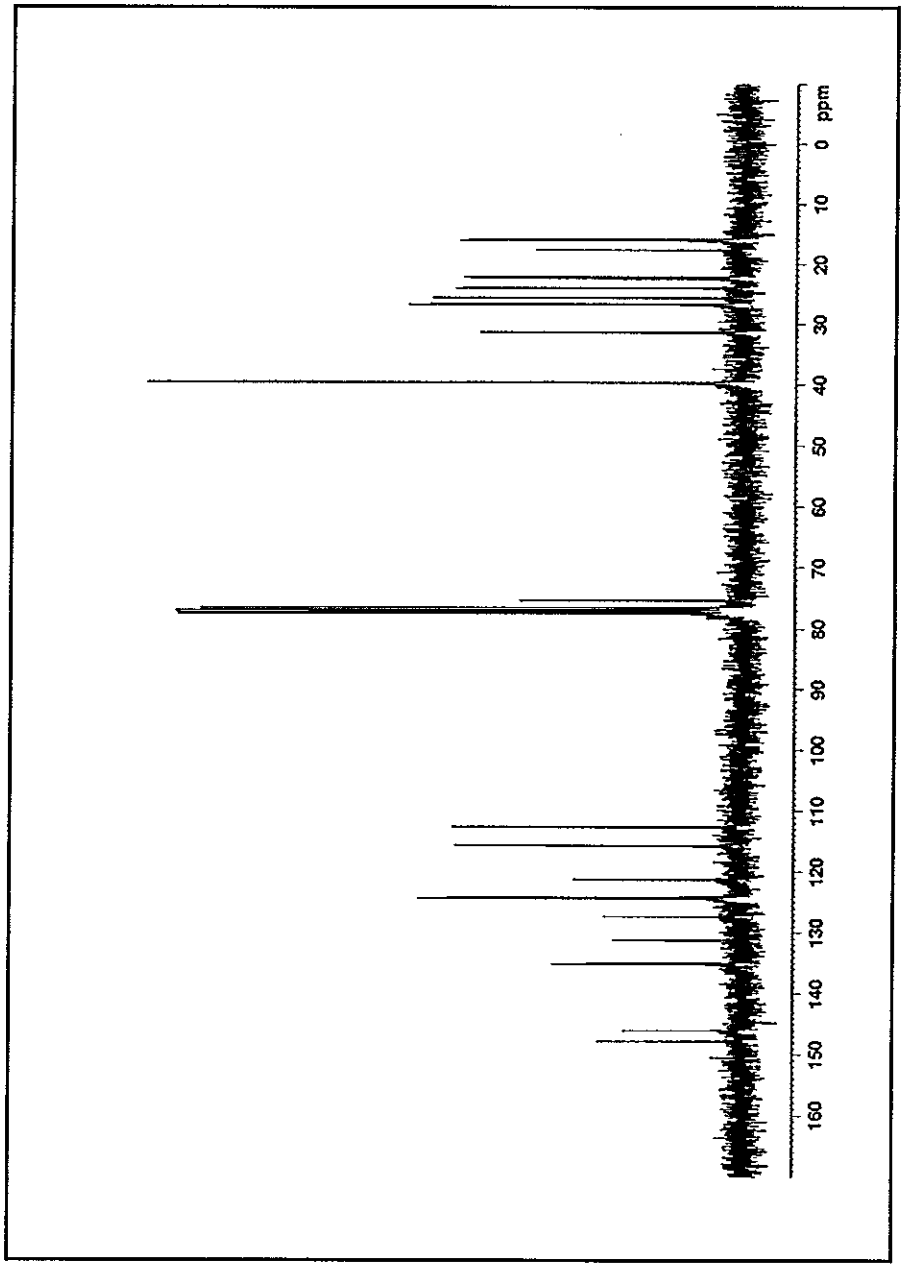

Figure 52 ^{13}C NMR (75 MHz) ($CDCl_3$) spectrum of compound GP5

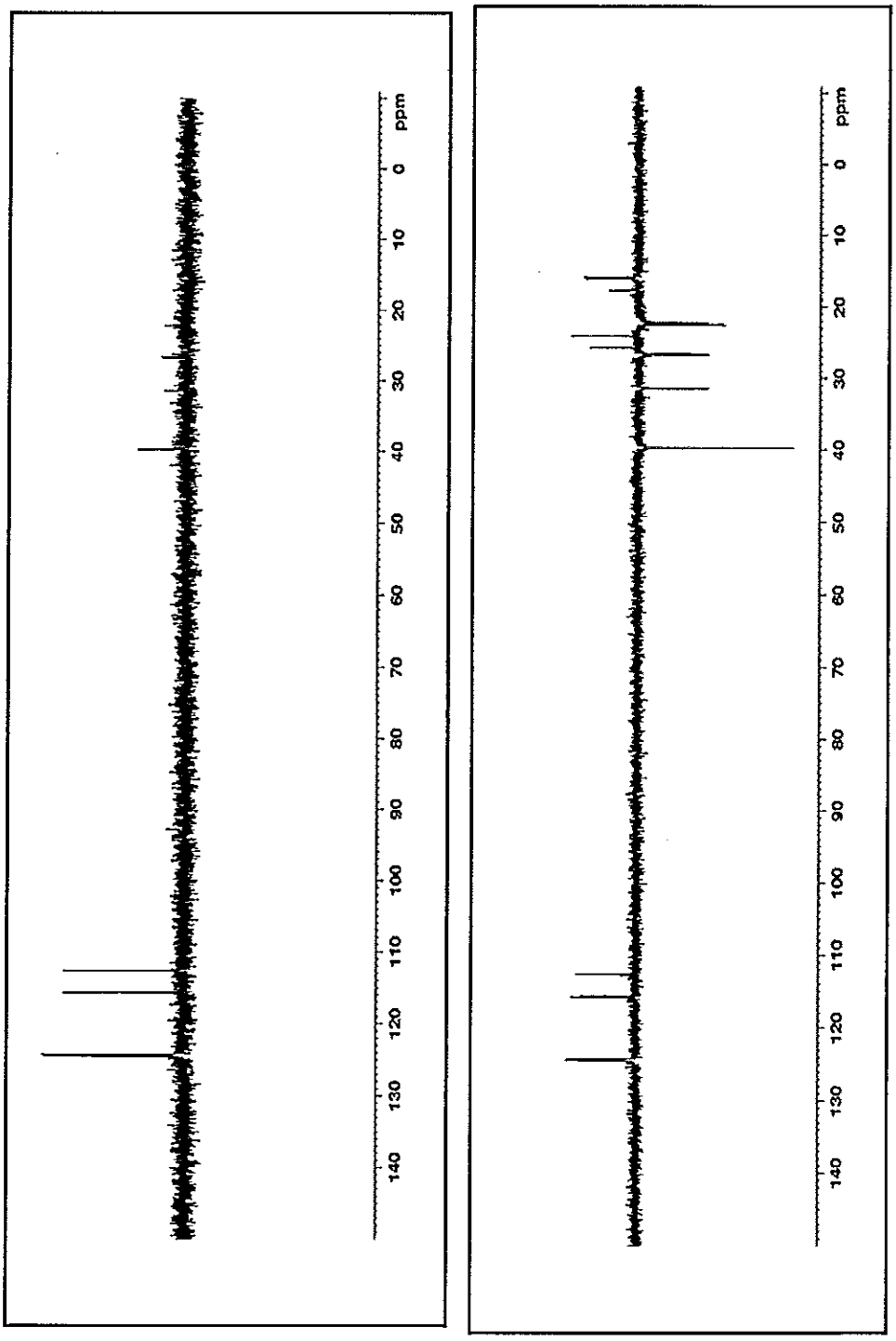

Figure 53 DEPT 90° and 135° spectra of compound GP5

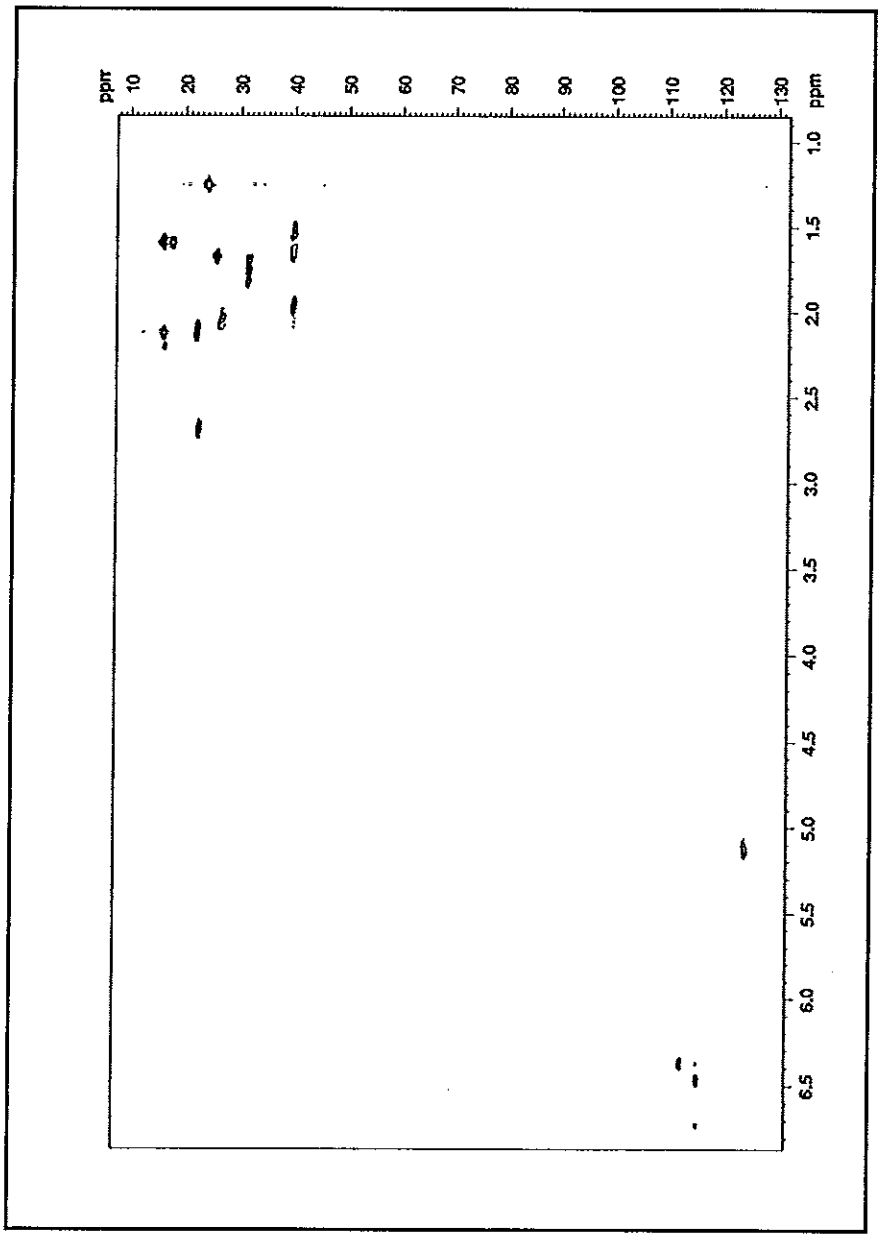

Figure 54 2D HMQC spectrum of compound GP5

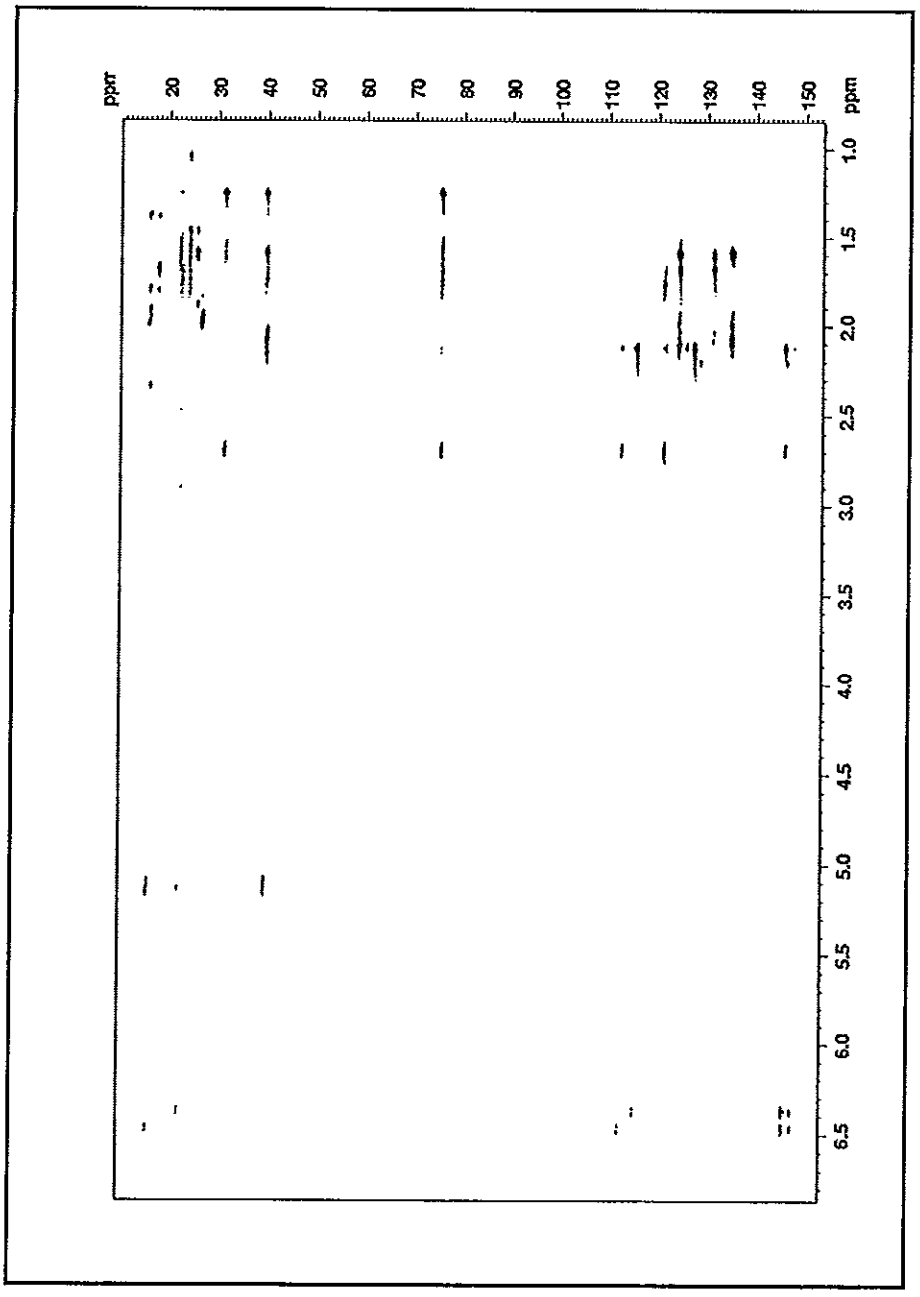

Figure 55 2D HMBC spectrum of compound GP5

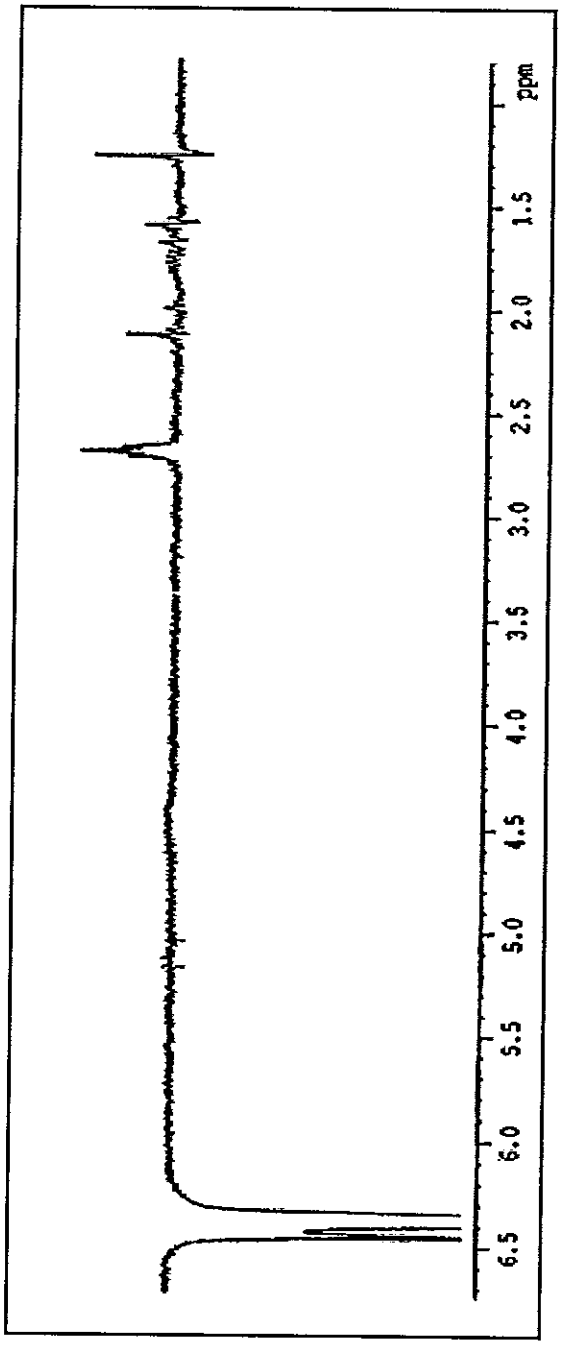

Figure 56 NOE difference spectrum of compound GP5 after irradiation at δ_H 6.37 (H-5)

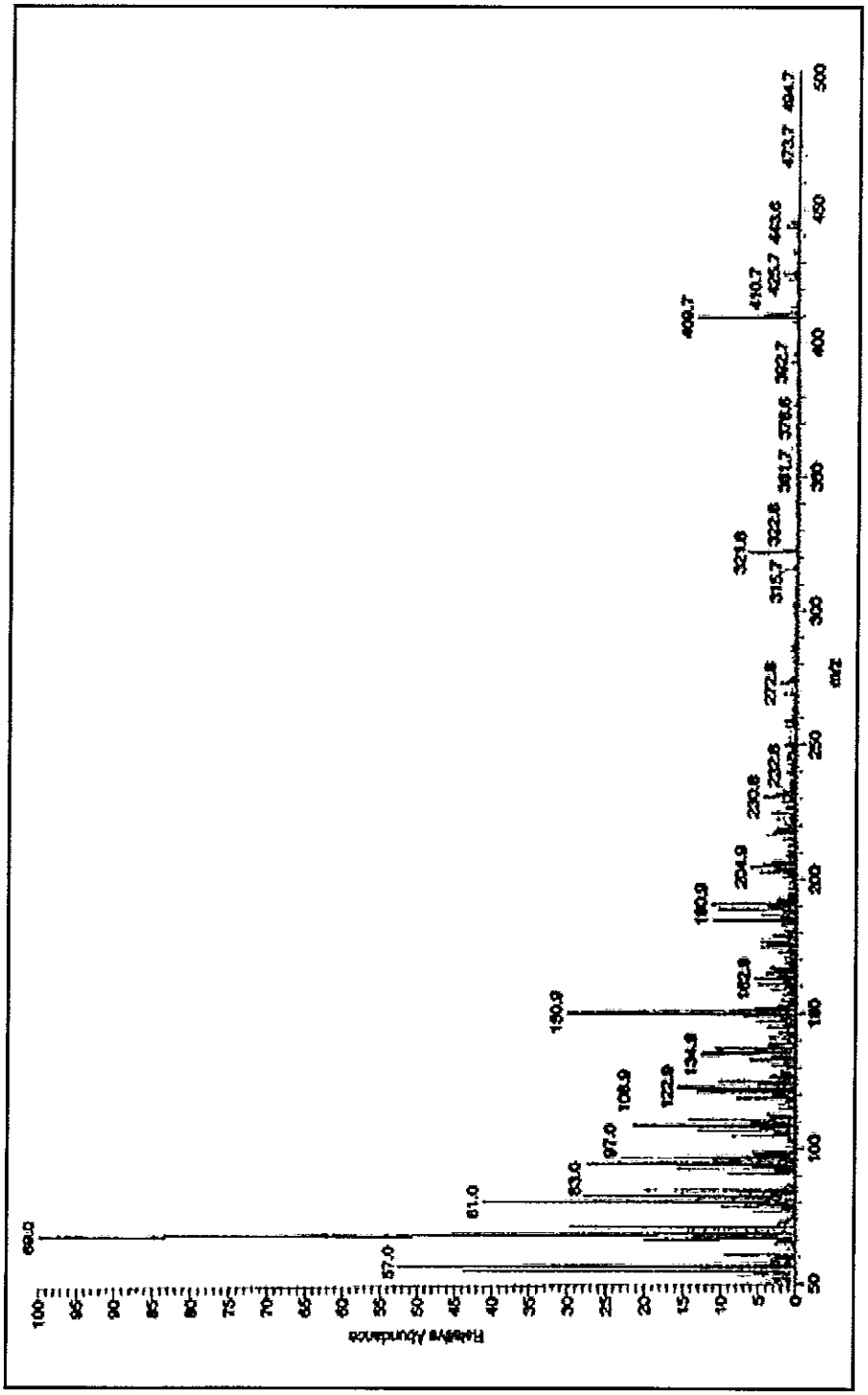

Figure 57 Mass spectrum of compound GP4

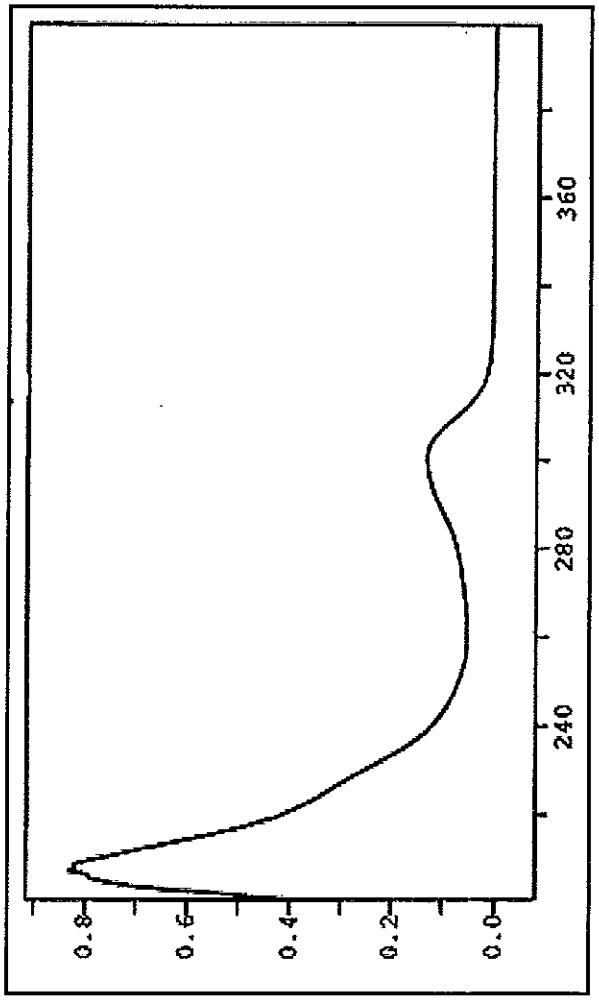

Figure 58 UV (MeOH) spectrum of compound GP4

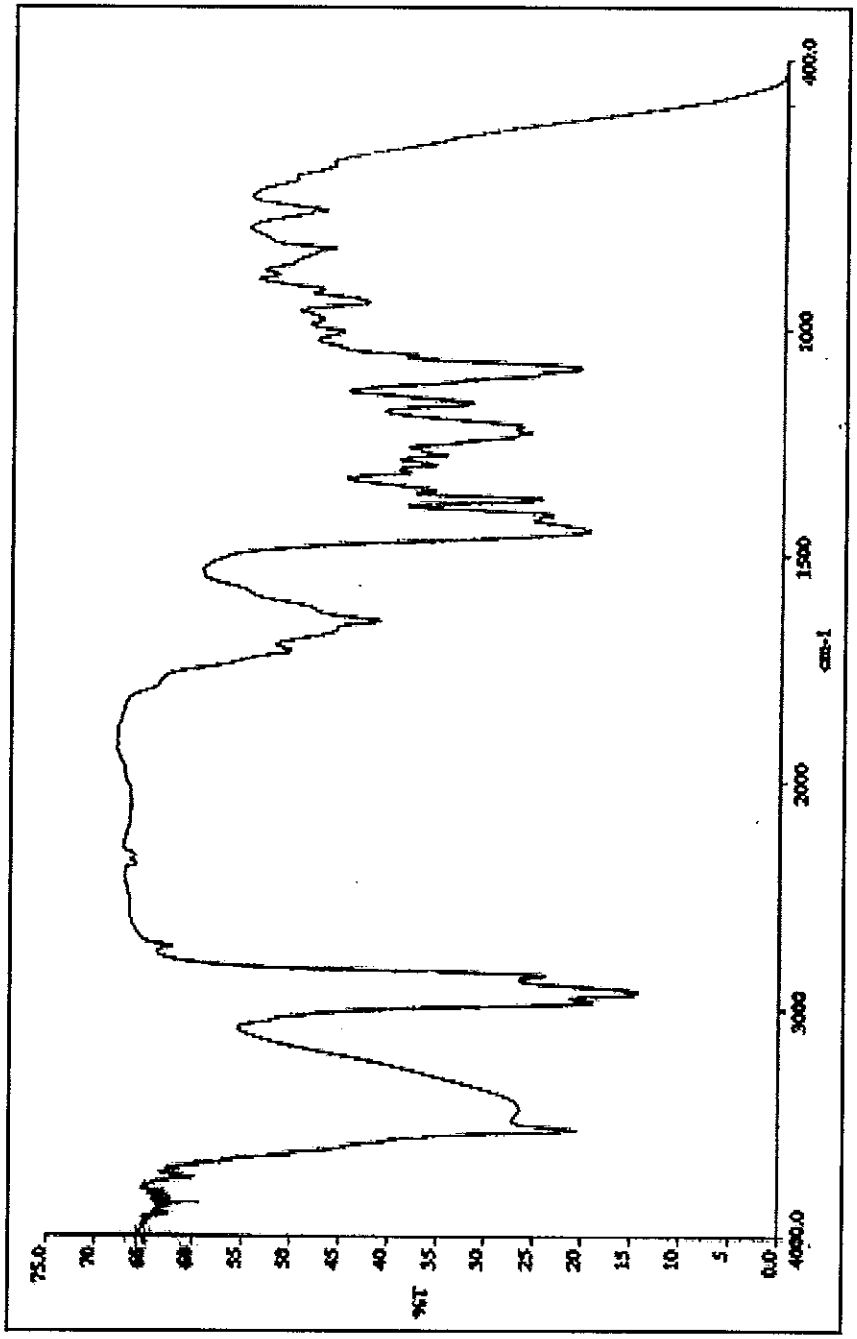

Figure 59 FT-IR (neat) spectrum of compound GP4

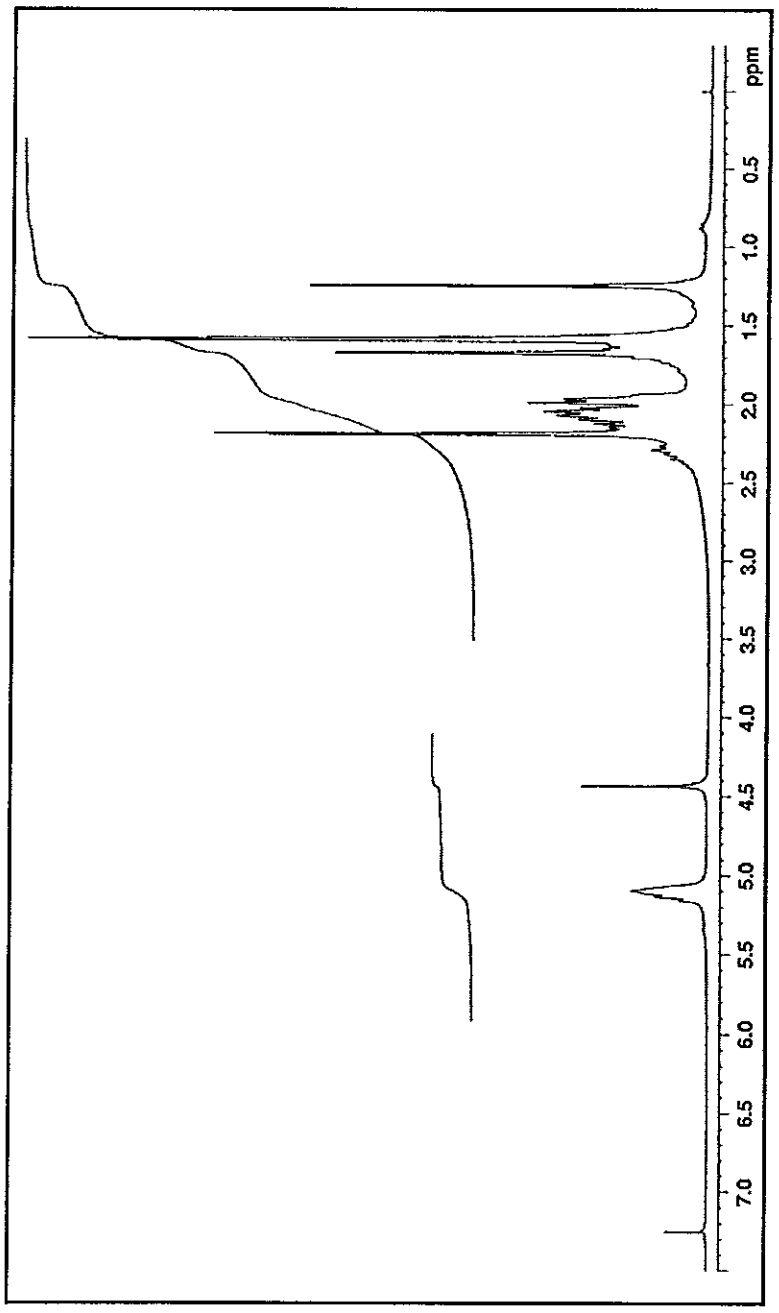

Figure 60 ^{1}H NMR (300 MHz) ($CDCl_3$) spectrum of compound GP4

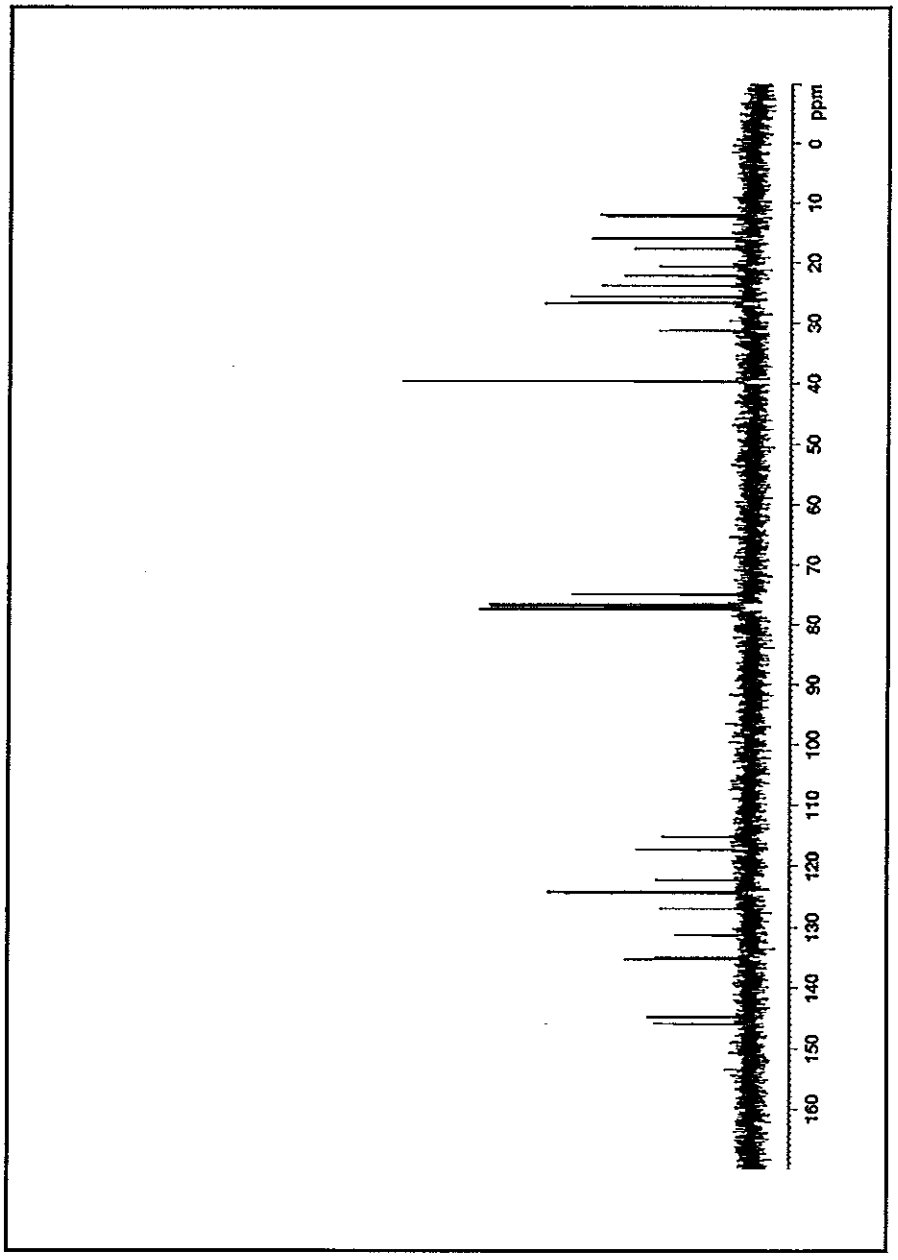

Figure 61 ^{13}C NMR (75 MHz) ($CDCl_3$) spectrum of compound GP4

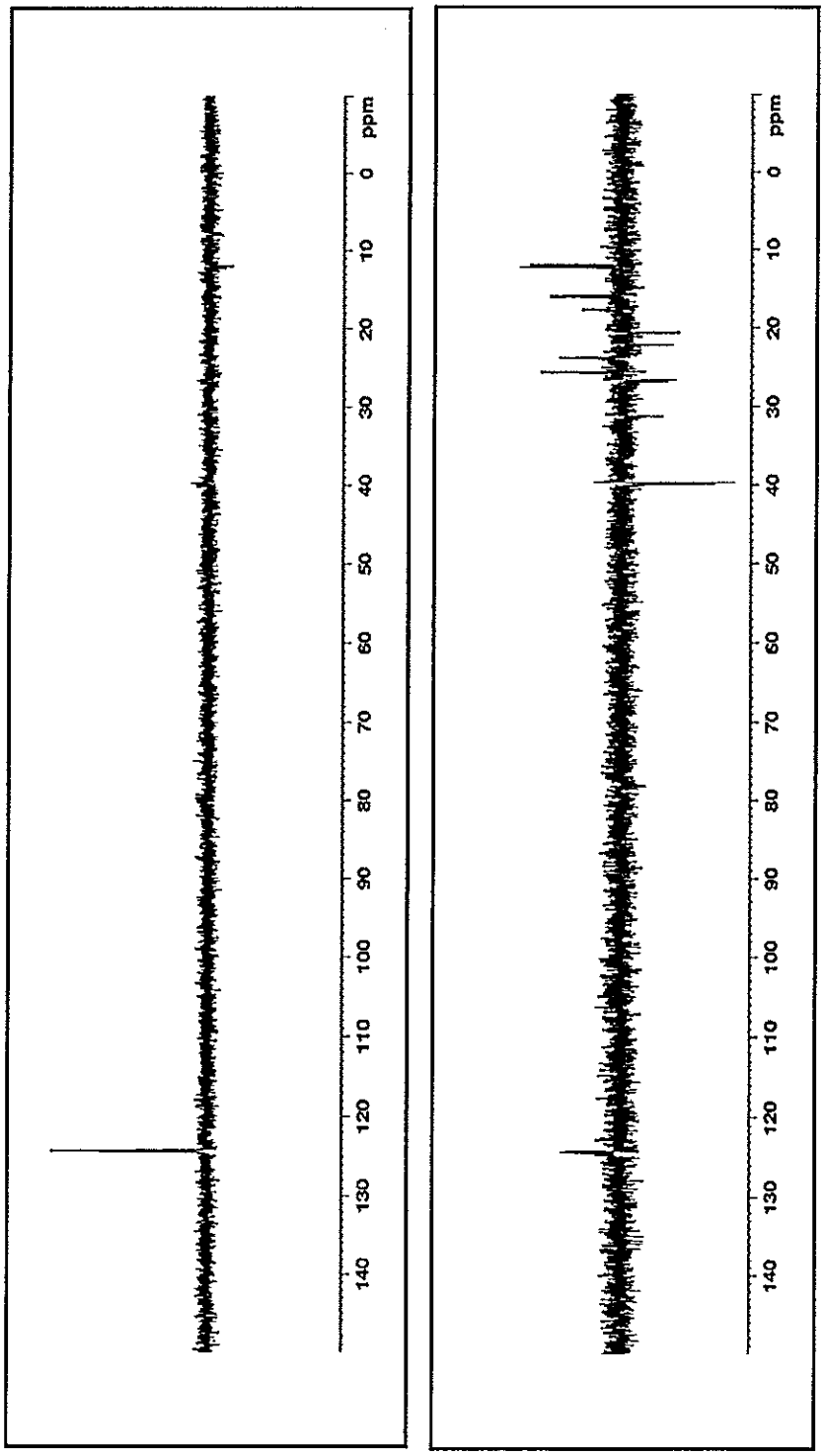

Figure 62 DEPT 90° and 135° spectra of compound GP4

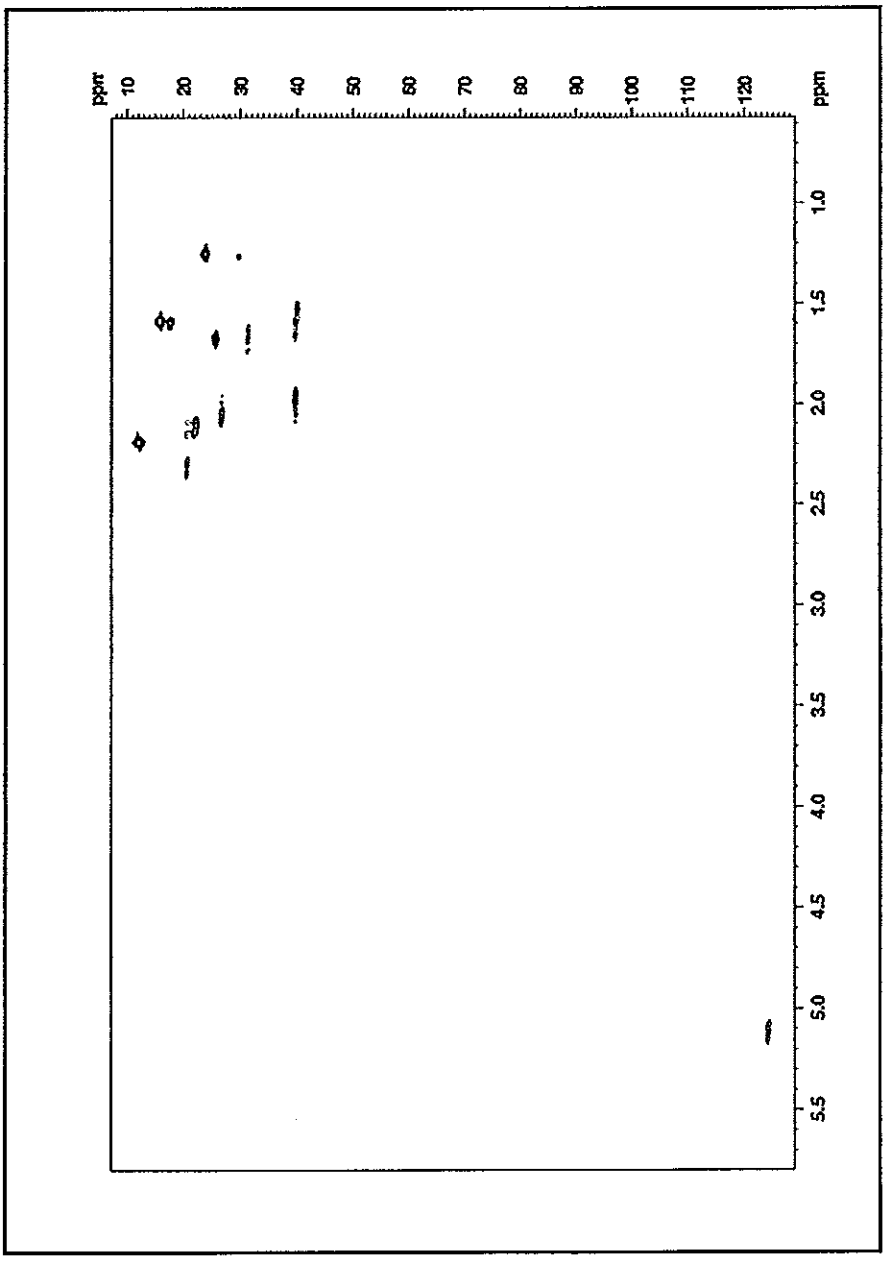

Figure 63 2D HMQC spectrum of compound GP4

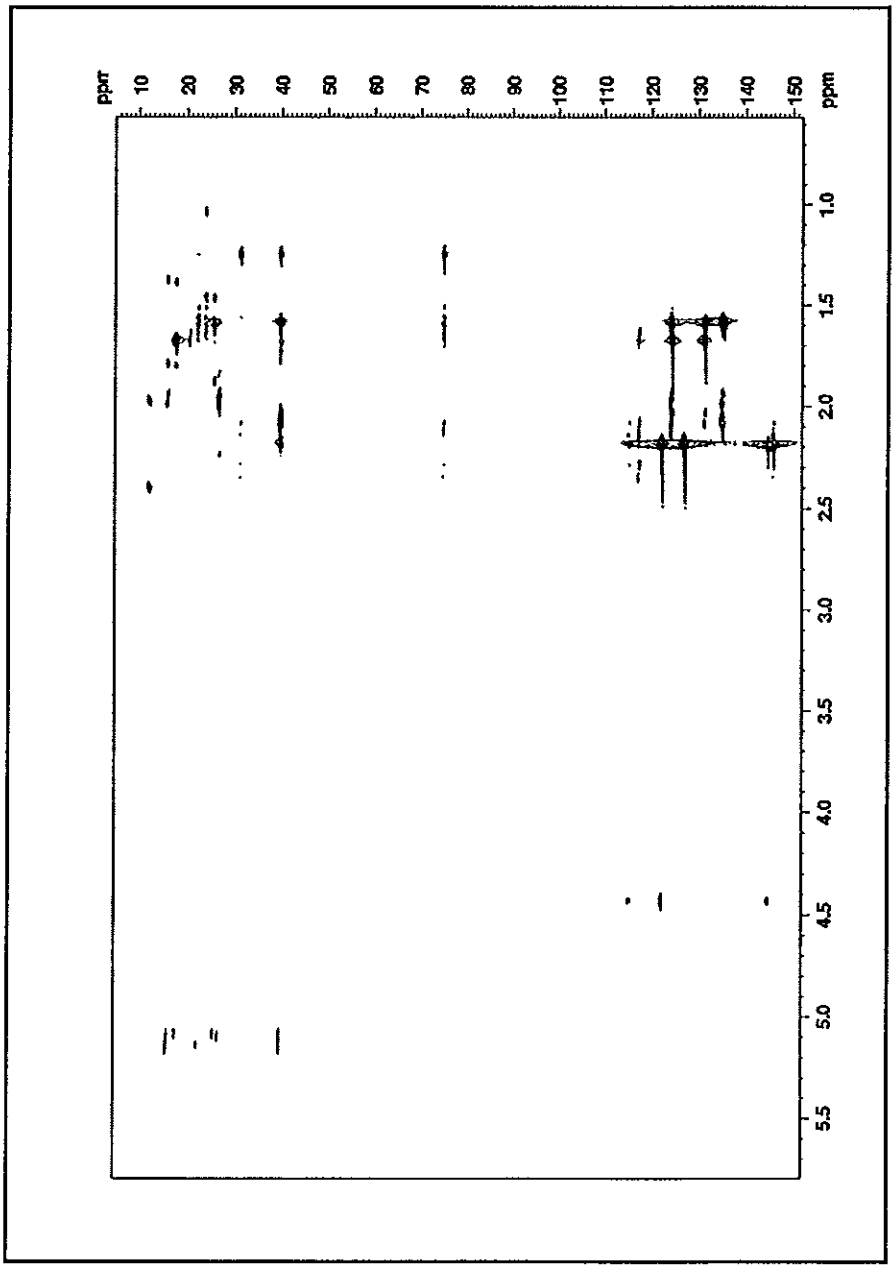

Figure 64 2D HMBC spectrum of compound GP4

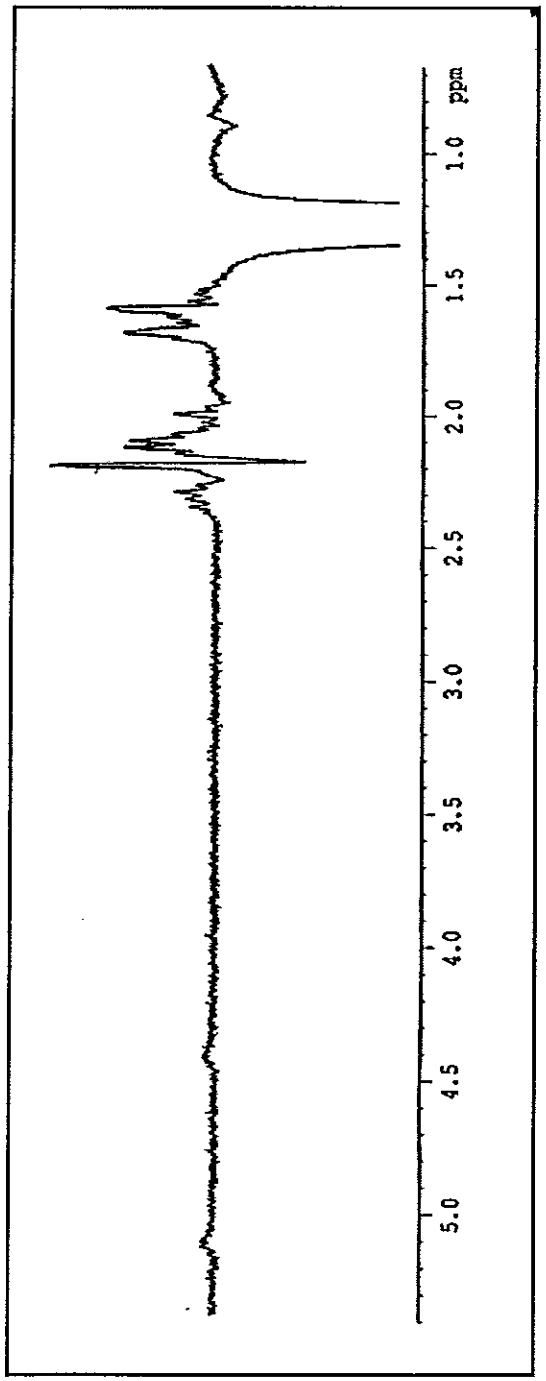

Figure 65 NOE difference spectrum of compound GP4 after irradiation at δ_H 1.26 (H_3-25)

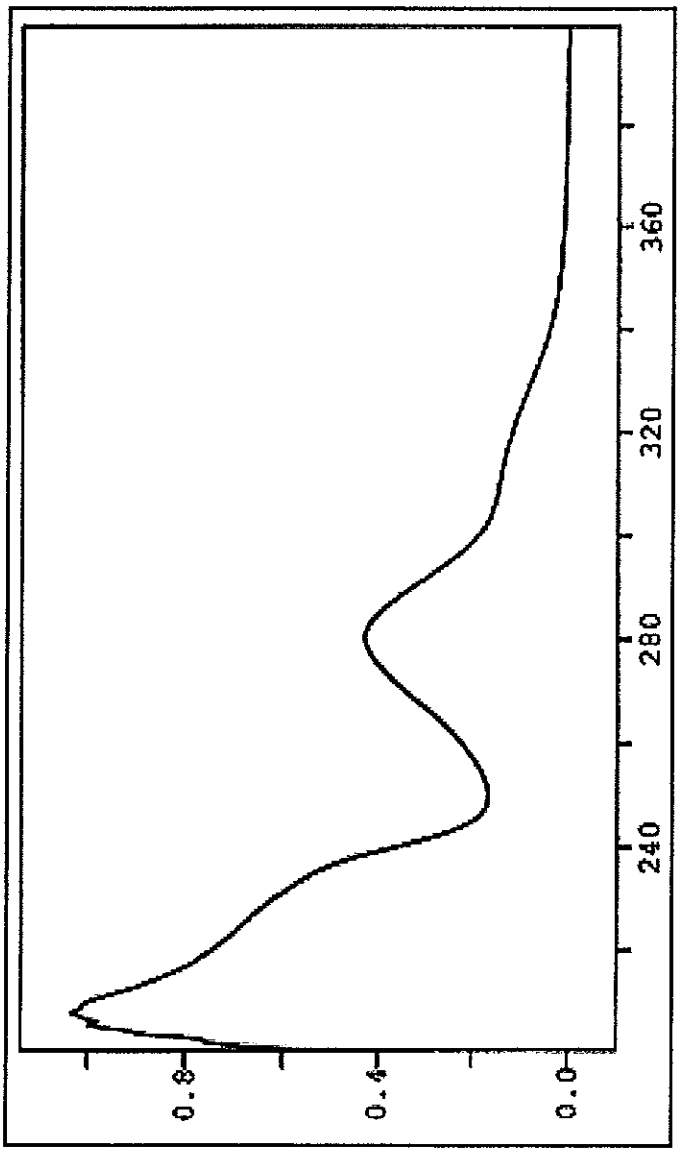

Figure 66 UV (MeOH) spectrum of compound GP18

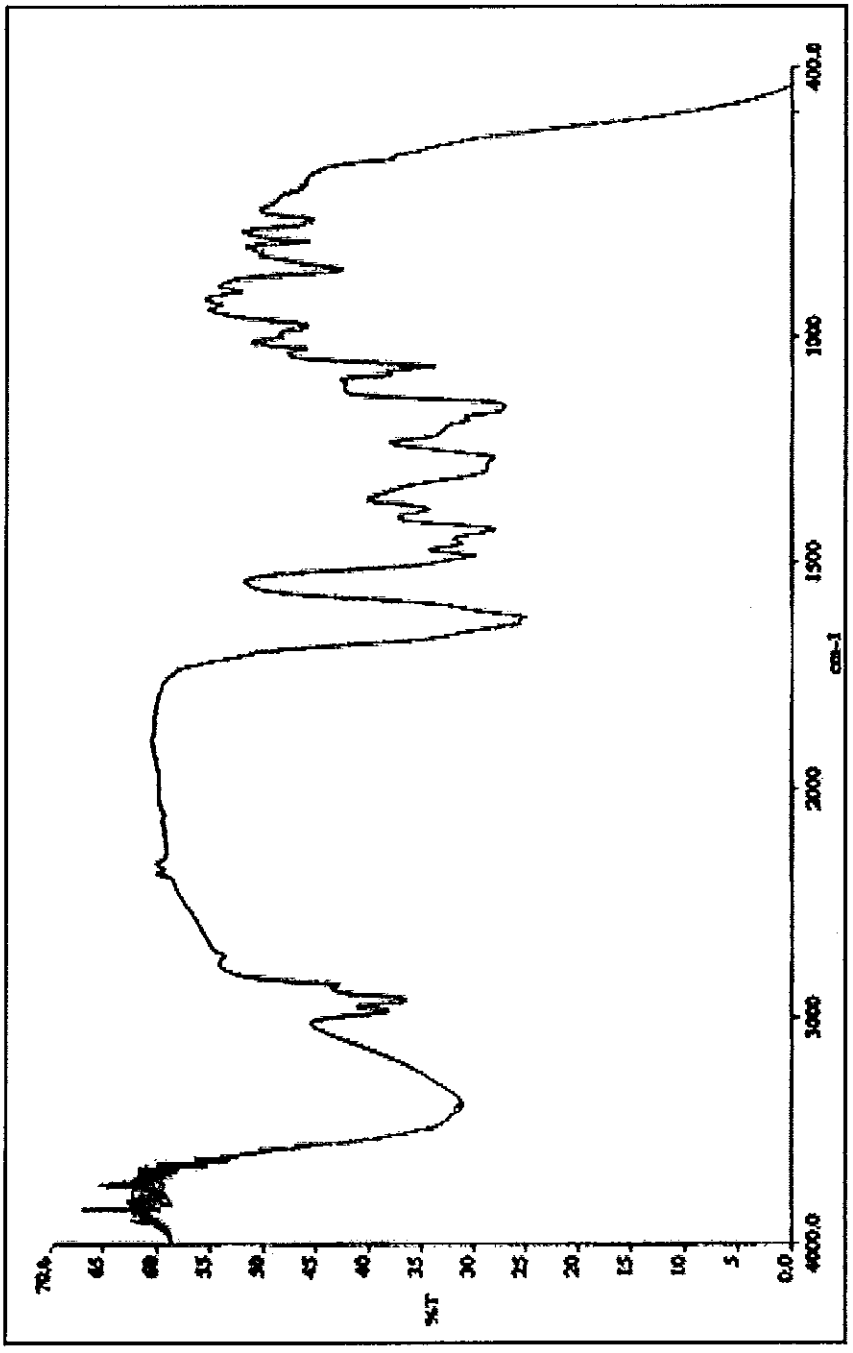

Figure 67 FT-IR (neat) spectrum of compound GP18

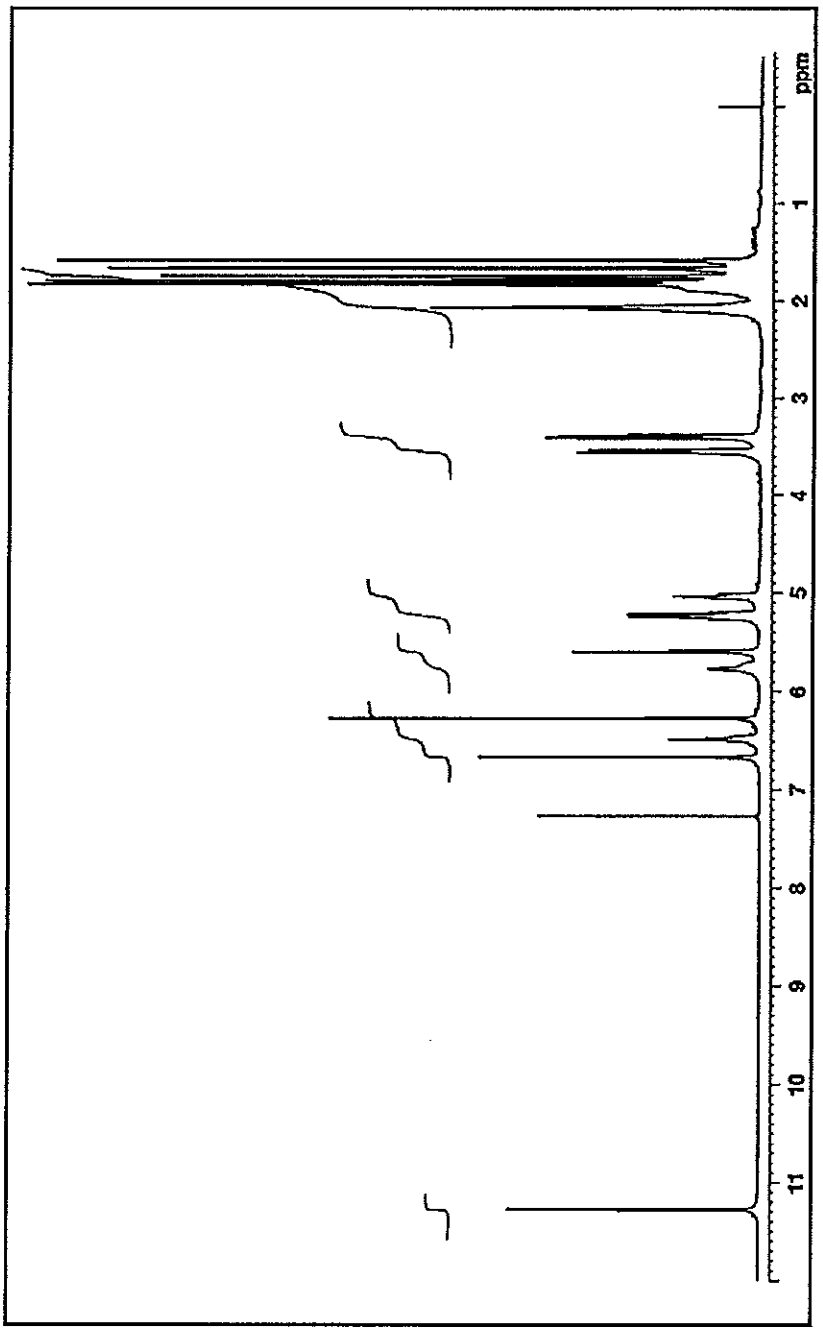

Figure 68 ^{1}H NMR (300 MHz) ($CDCl_3$) spectrum of compound GP18

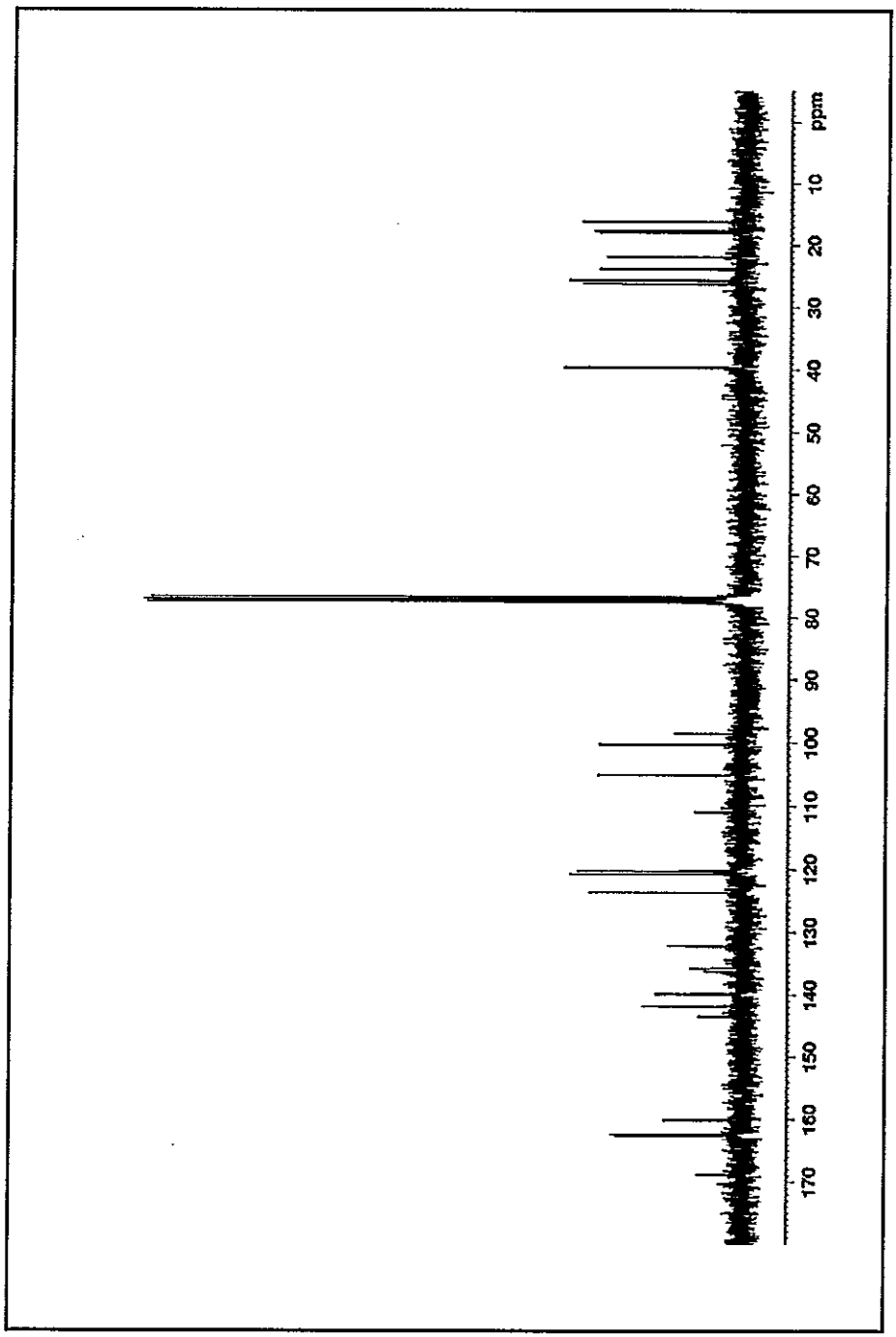

Figure 69 ^{13}C NMR (75 MHz) ($CDCl_3$) spectrum of compound GP18

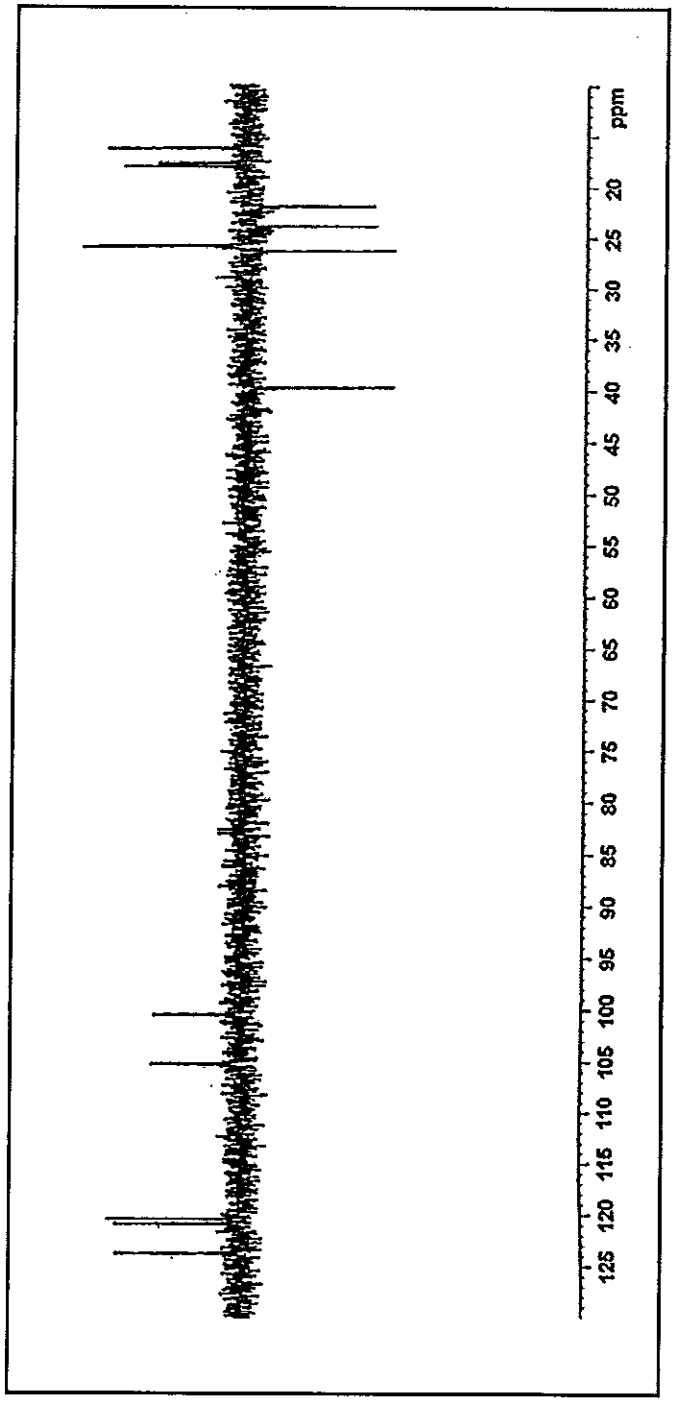

Figure 70 DEPT 135° spectra of compound GP18

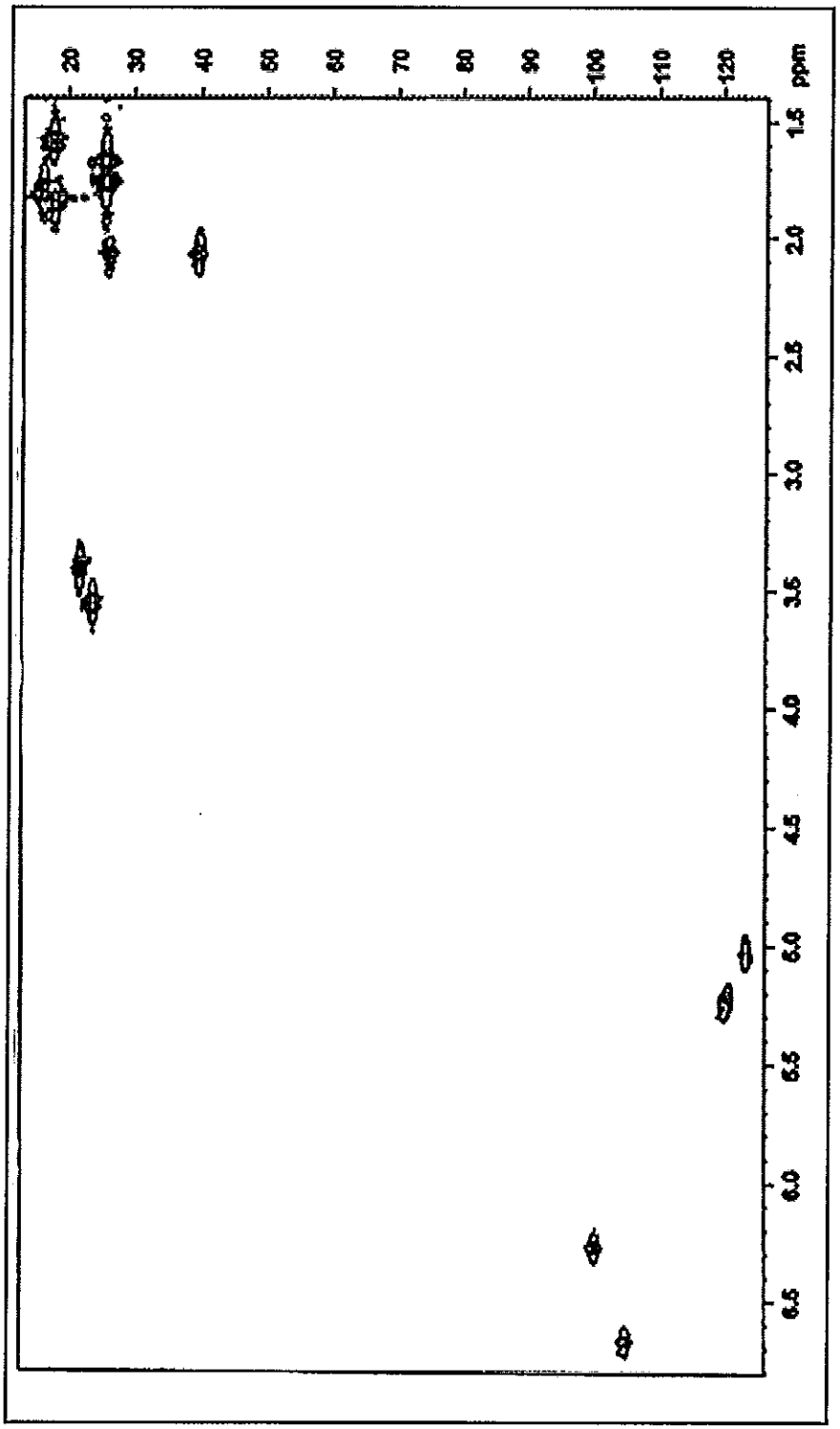

Figure 71 2D HMQC spectrum of compound GP18

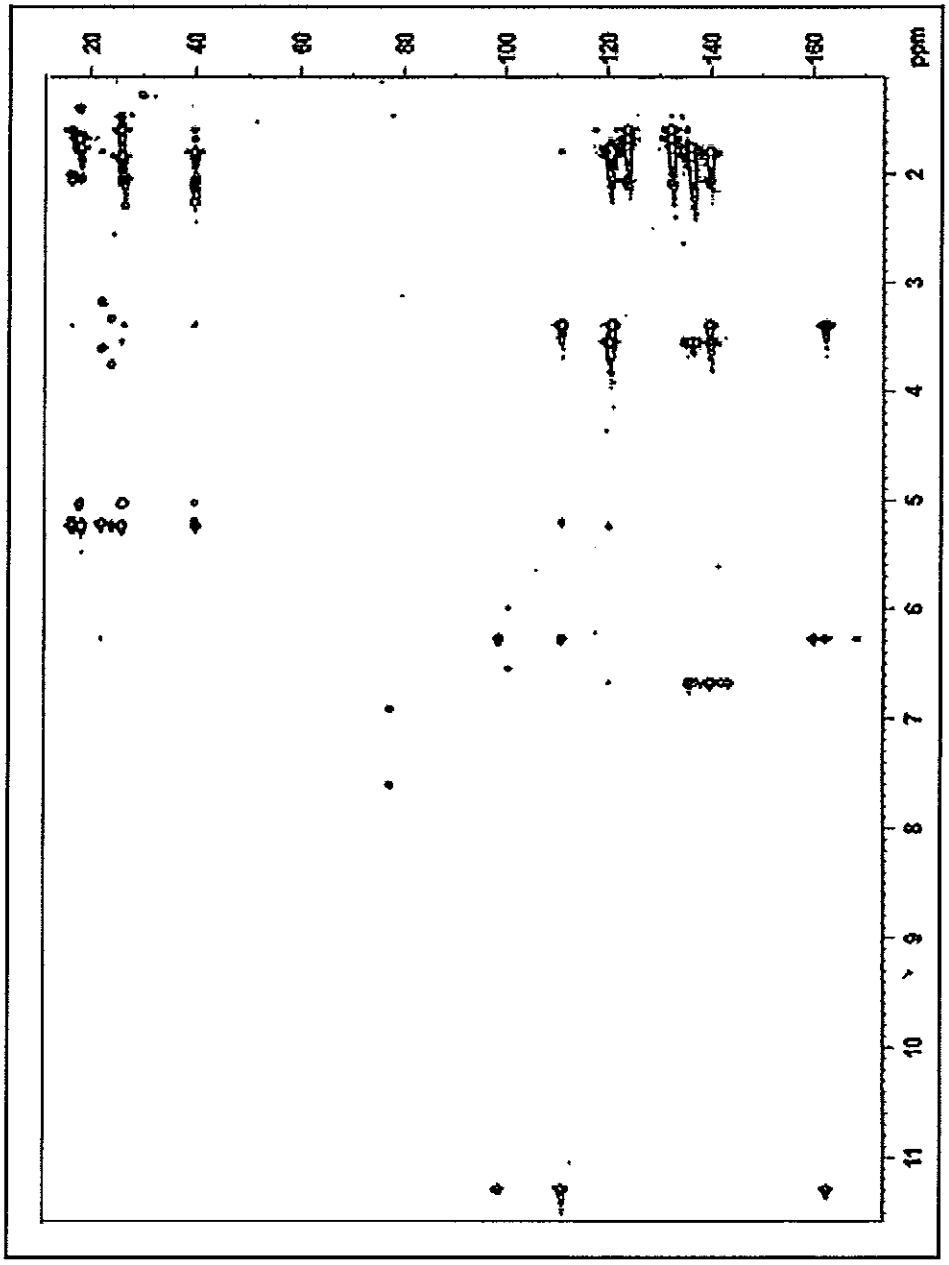

Figure 72 2D HMBC spectrum of compound GP18

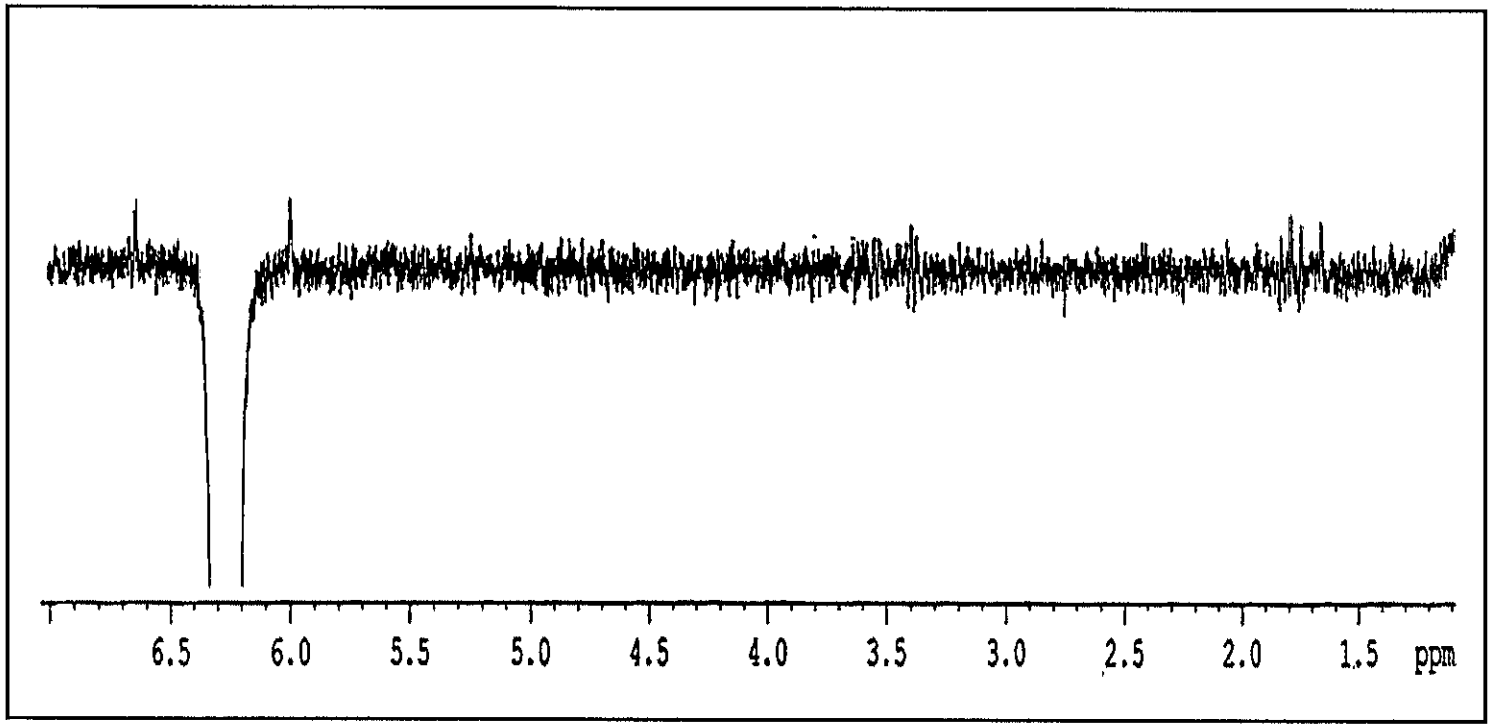

Figure 73 NOE difference spectrum of compound GP18 after irradiation at δ_H 6.27 (H-4)

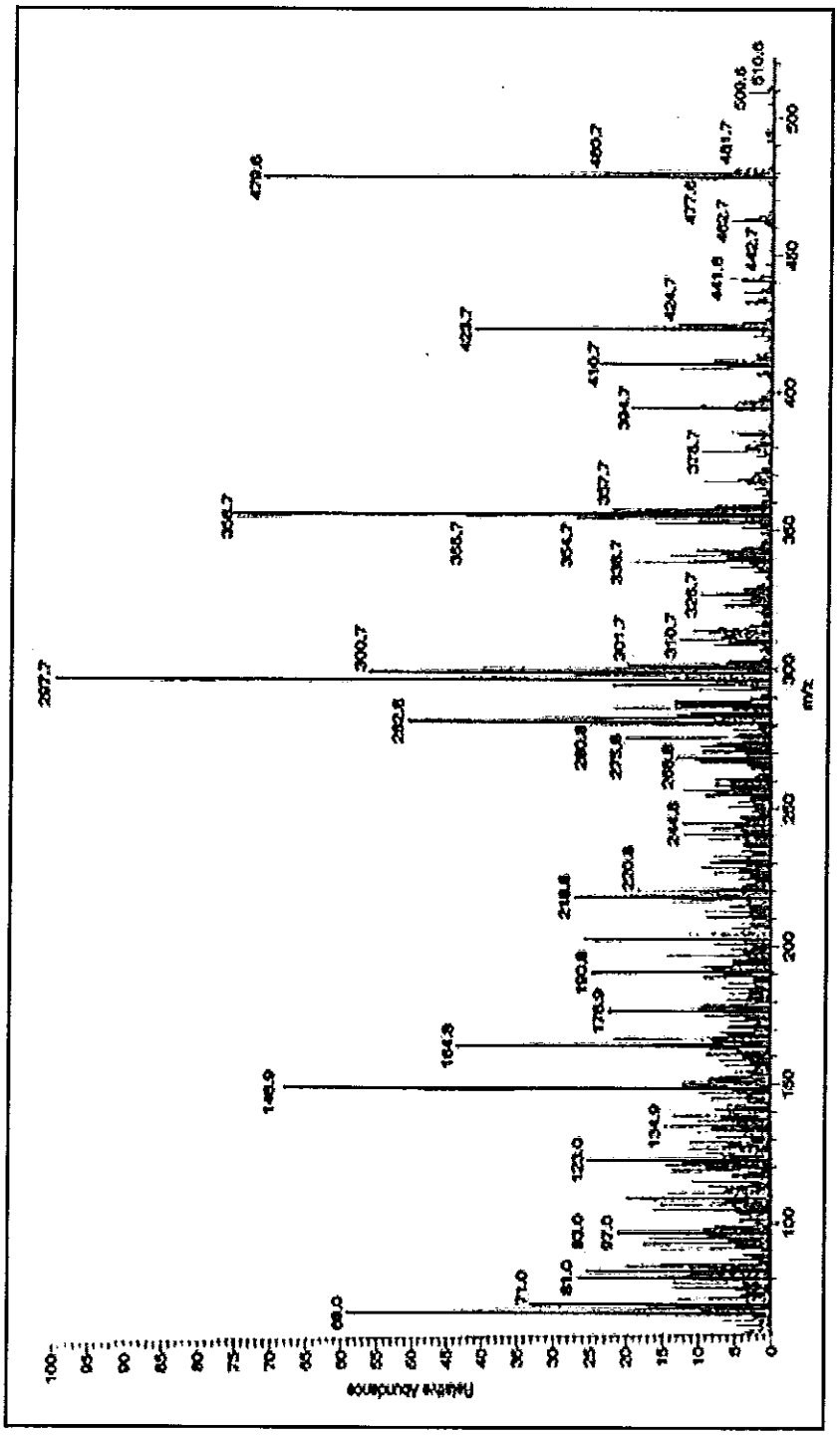

Figure 74 Mass spectrum of compound GP14

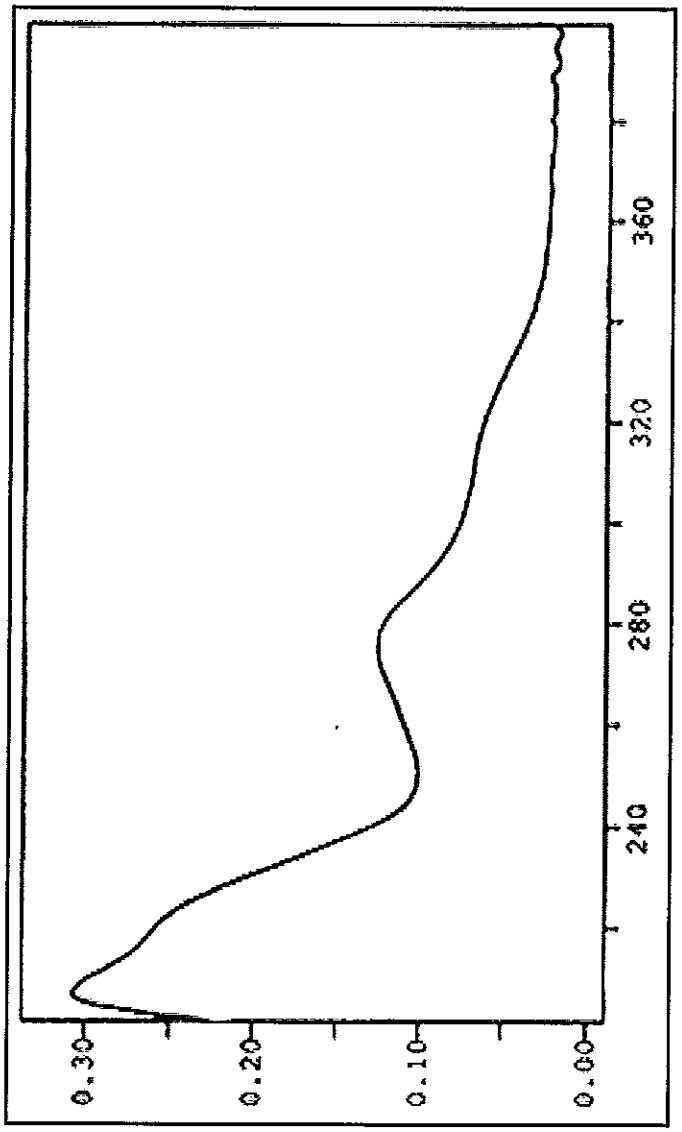

Figure 75 UV (MeOH) spectrum of compound GP14

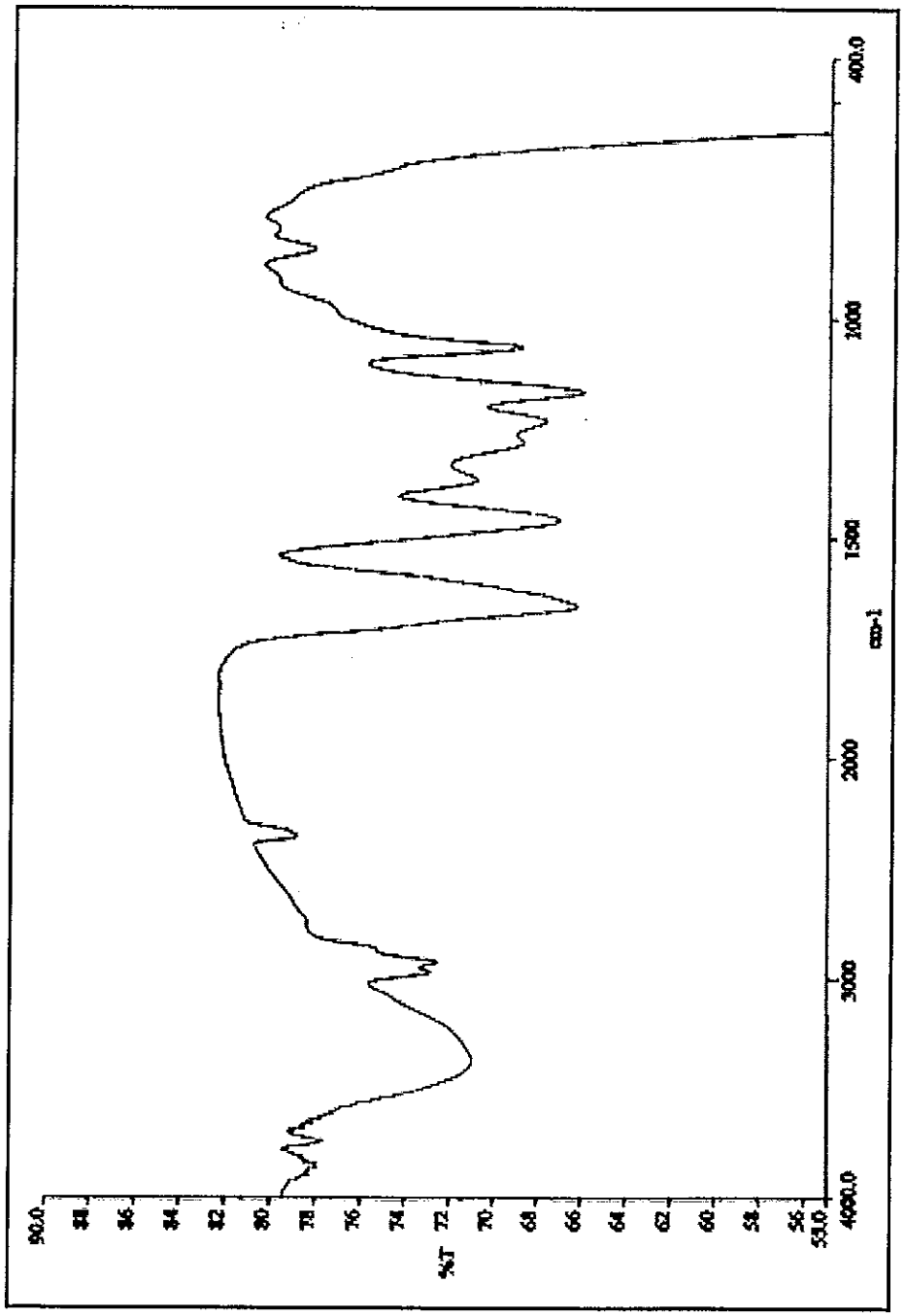

Figure 76 FT-IR (neat) spectrum of compound GP14

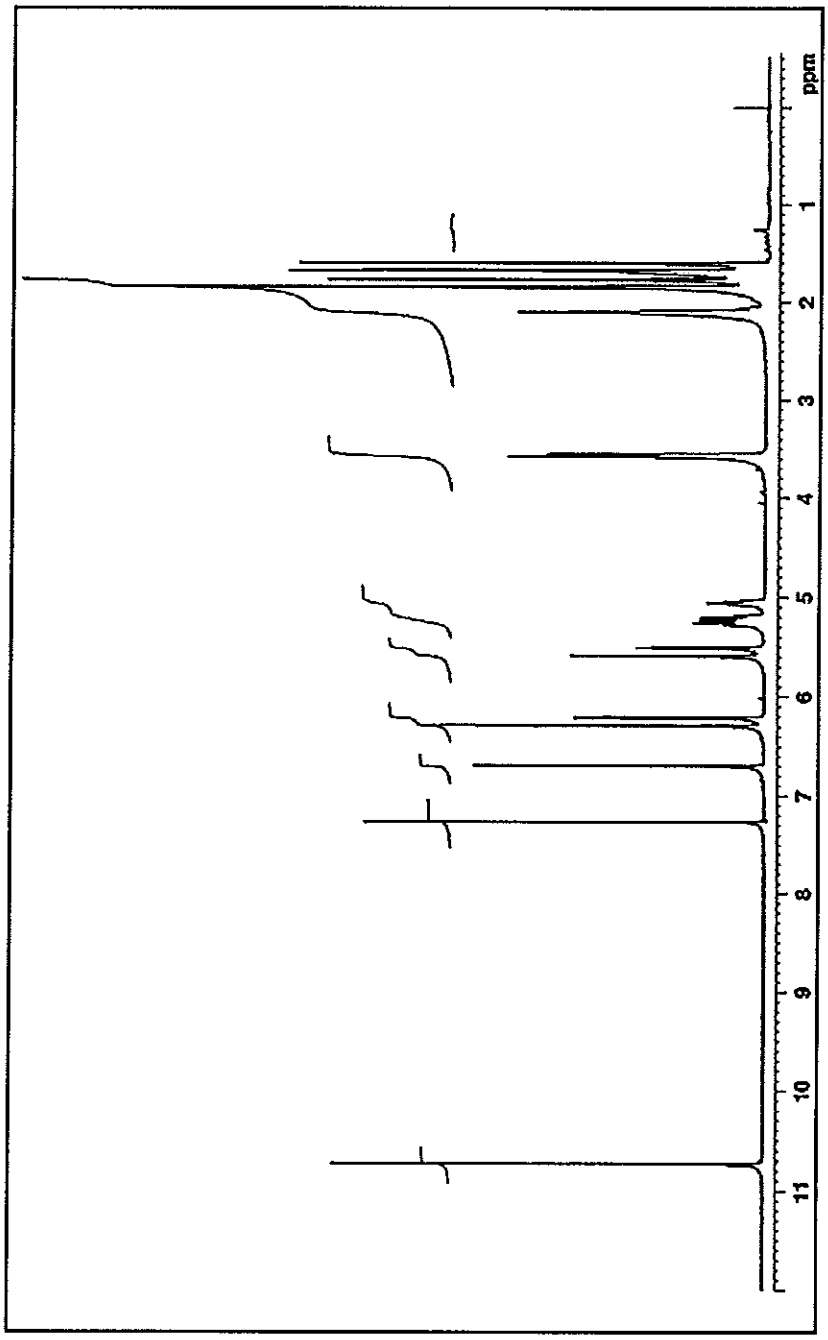

Figure 77 ^{1}H NMR (300 MHz) ($CDCl_3$) spectrum of compound GP14

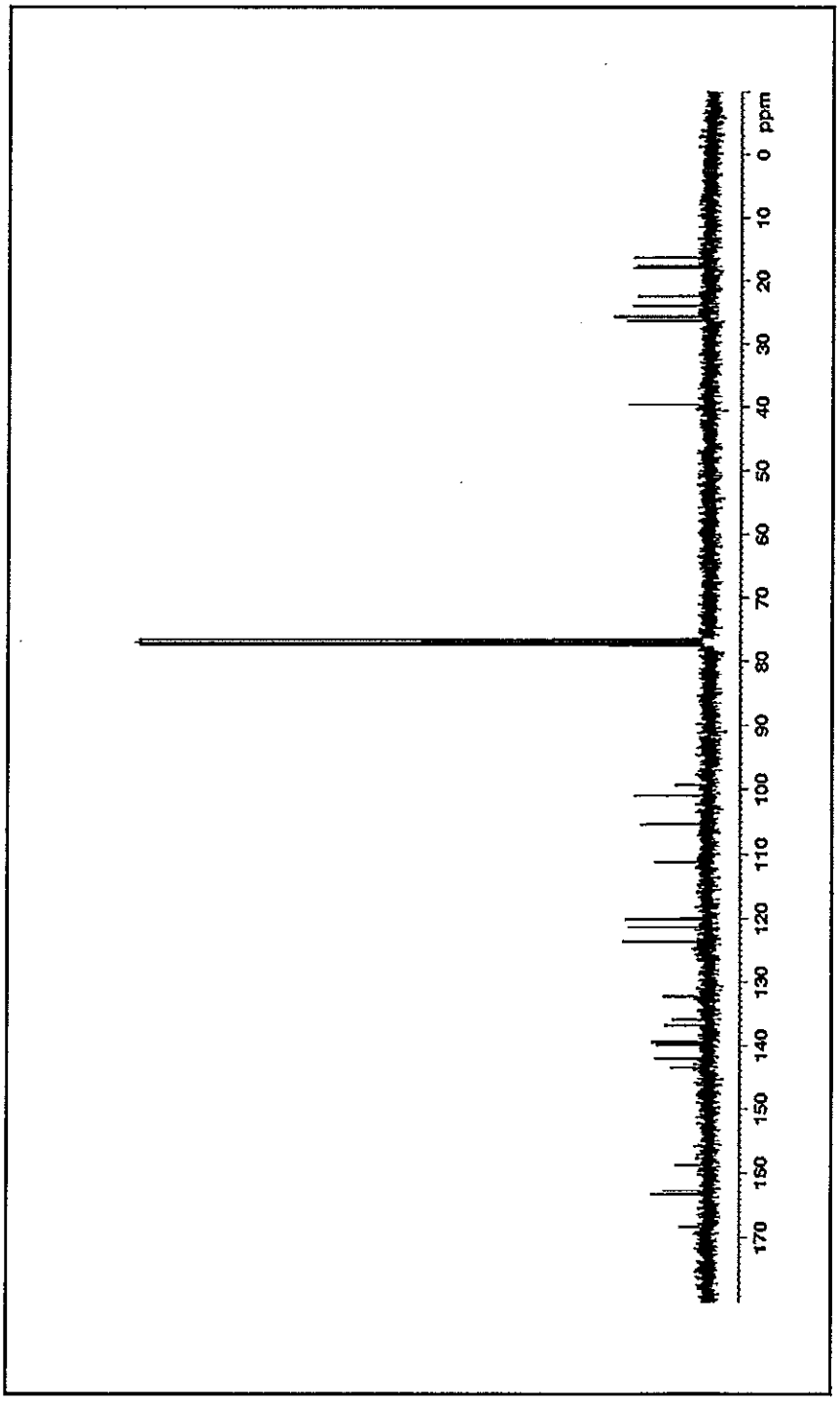

Figure 78 ^{13}C NMR (75 MHz) ($CDCl_3$) spectrum of compound GP14

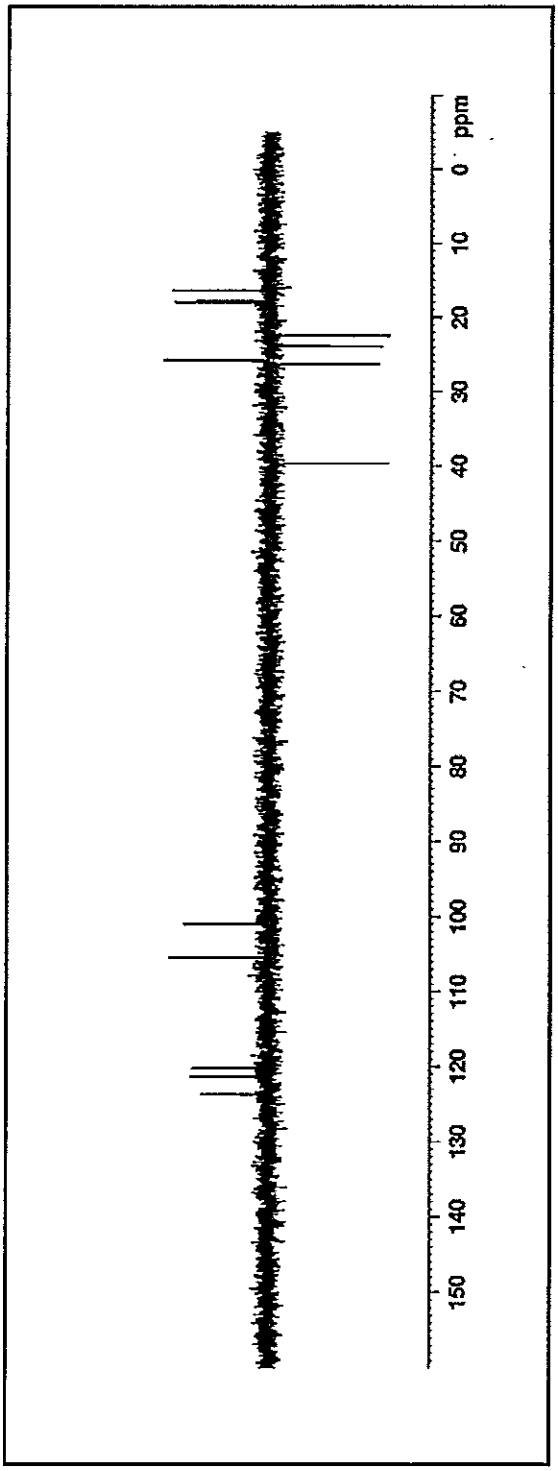

Figure 79 DEPT 135° spectra of compound GP14

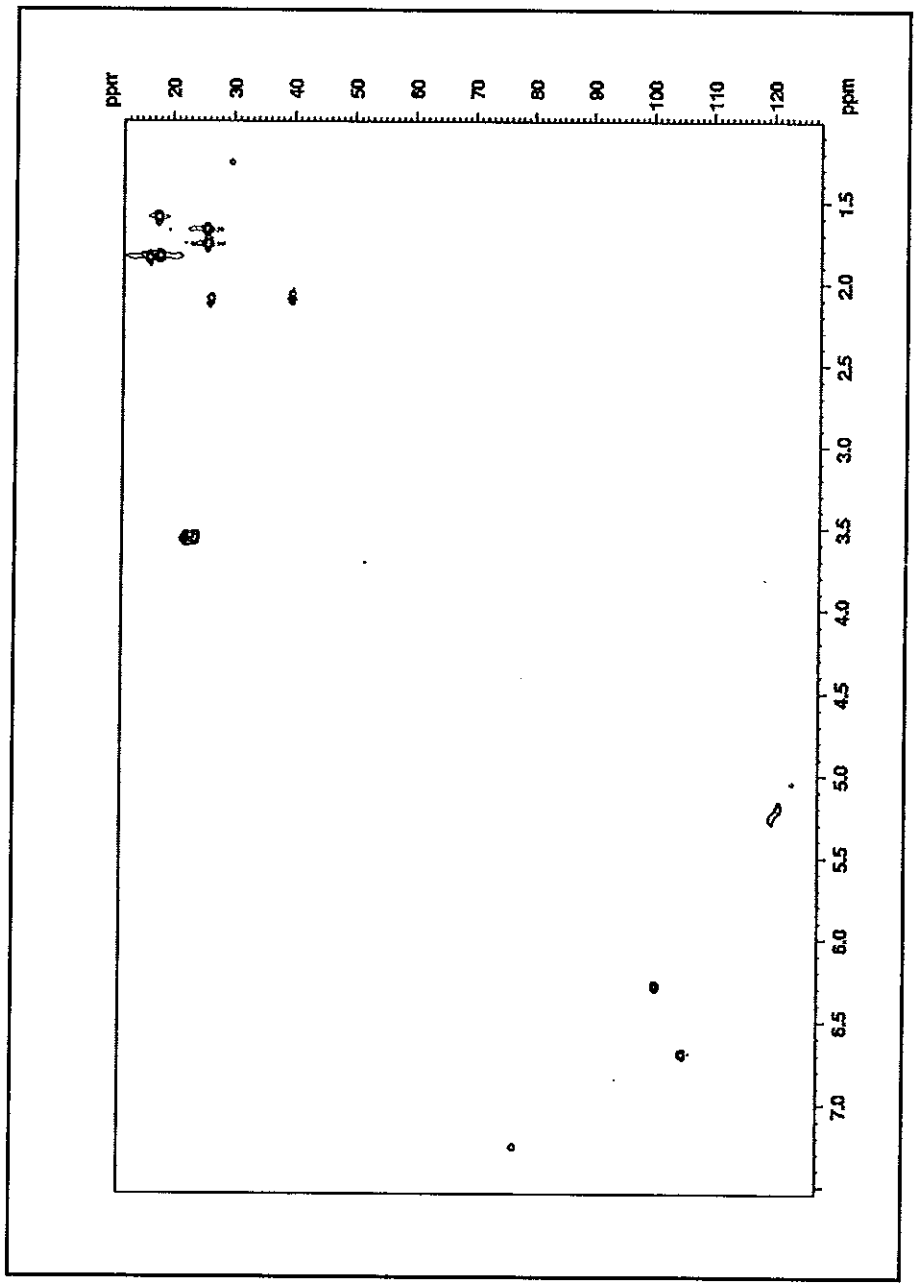

Figure 80 2D HMQC spectrum of compound GP14

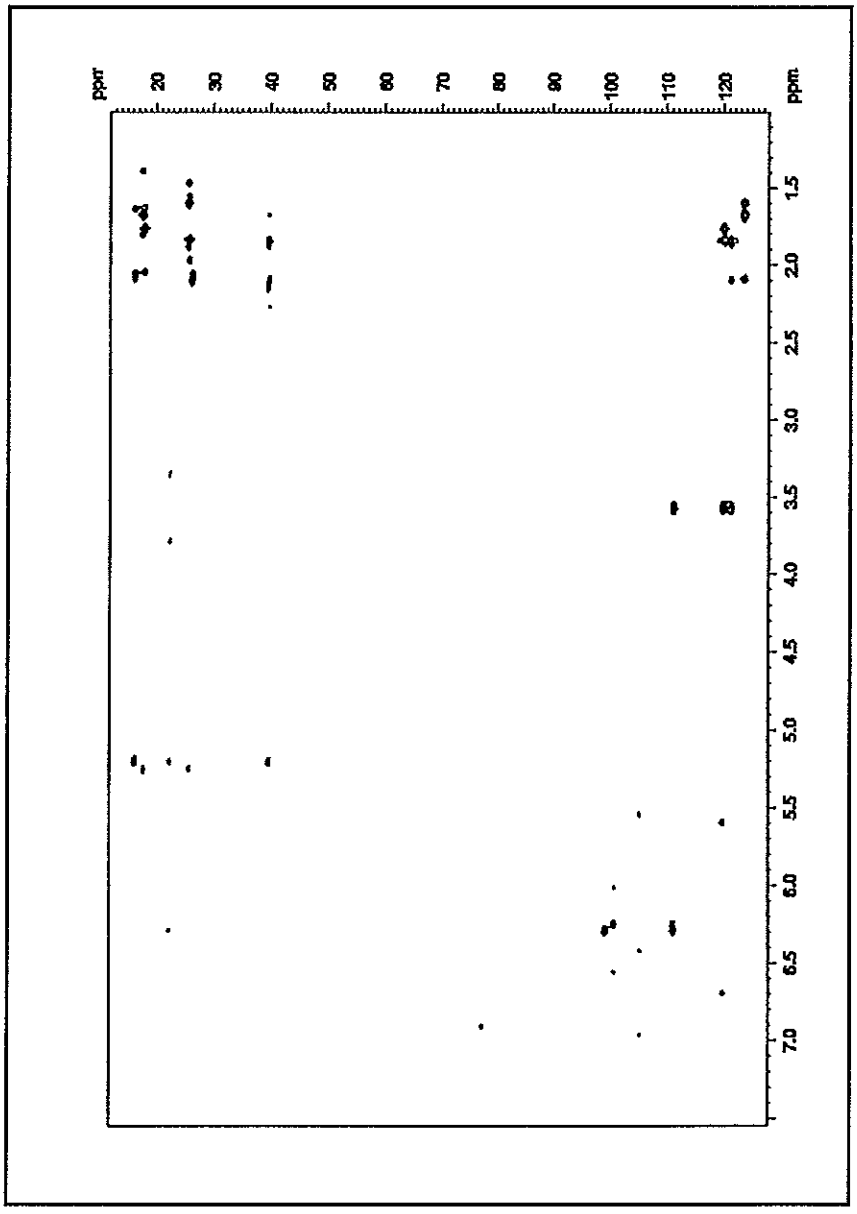

Figure 81 2D HMBC spectrum of compound GP14

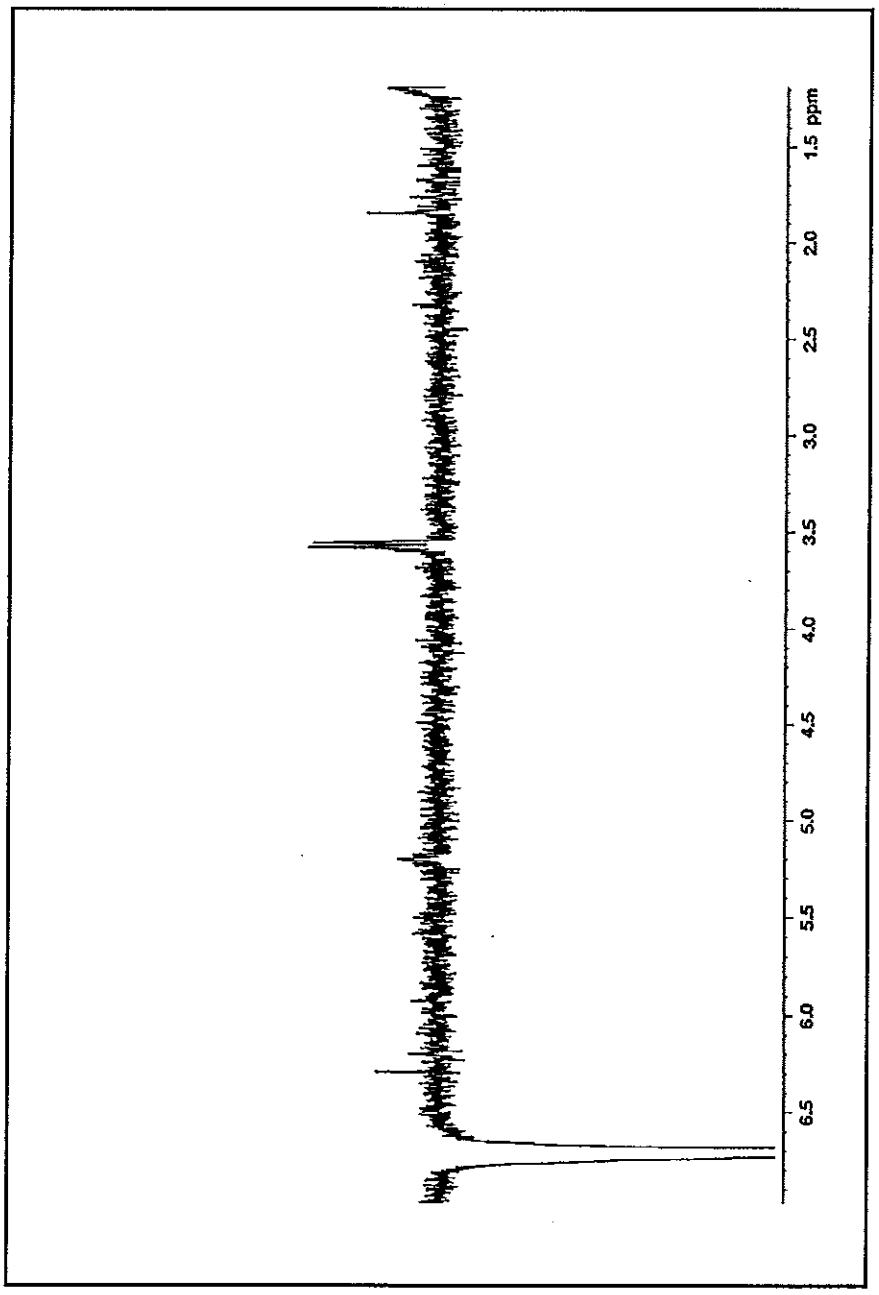

Figure 82 NOE difference spectrum of compound GP14 after irradiation at δ_H 6.67 (H-6)

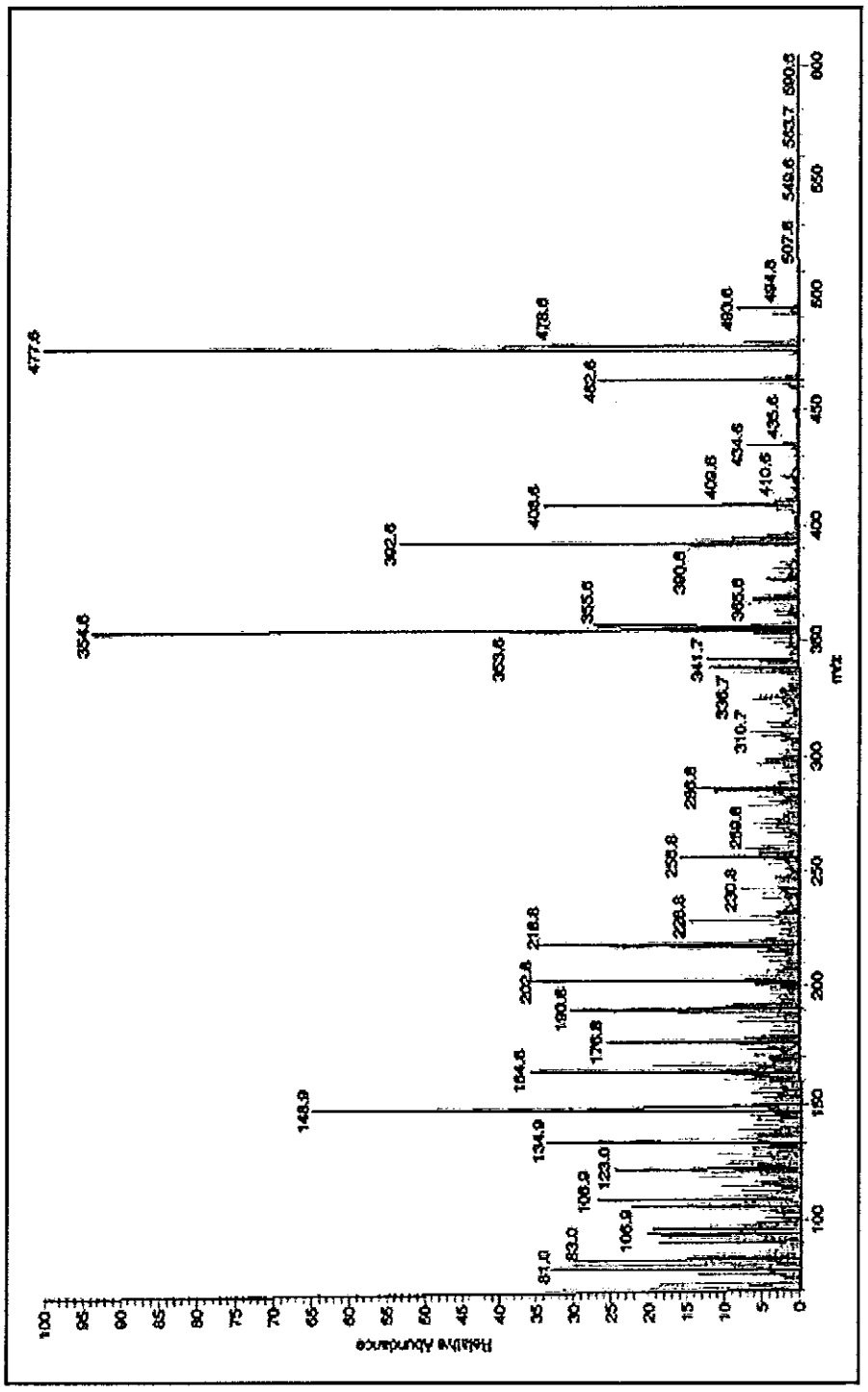

Figure 83 Mass spectrum of compound GP12

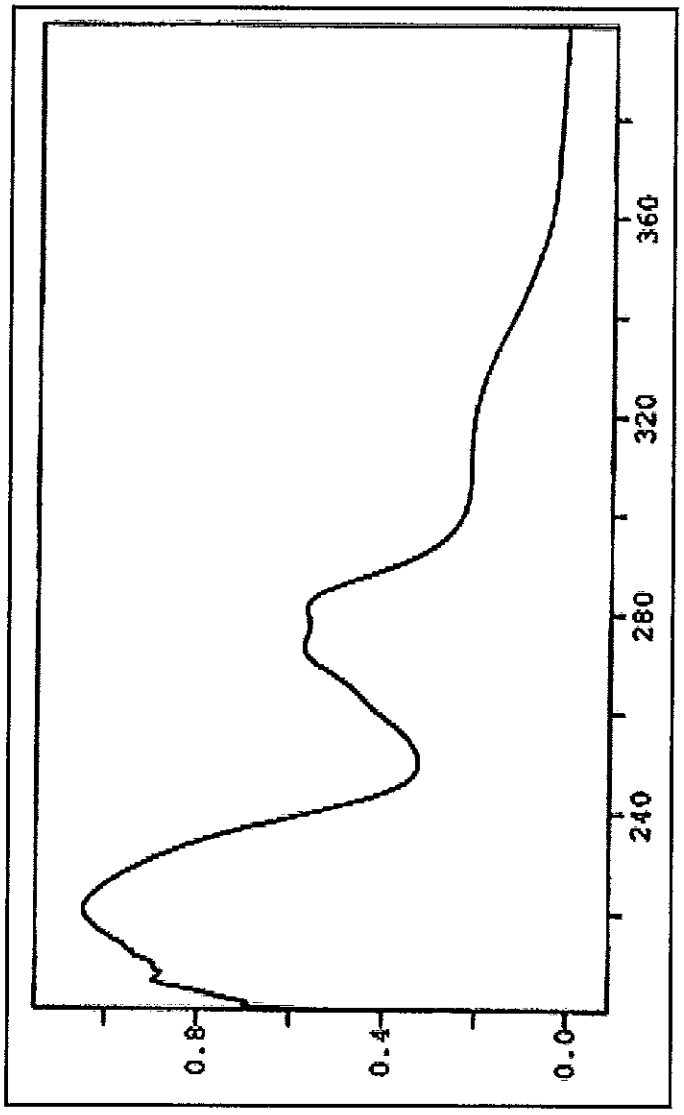

Figure 84 UV (MeOH) spectrum of compound GP12

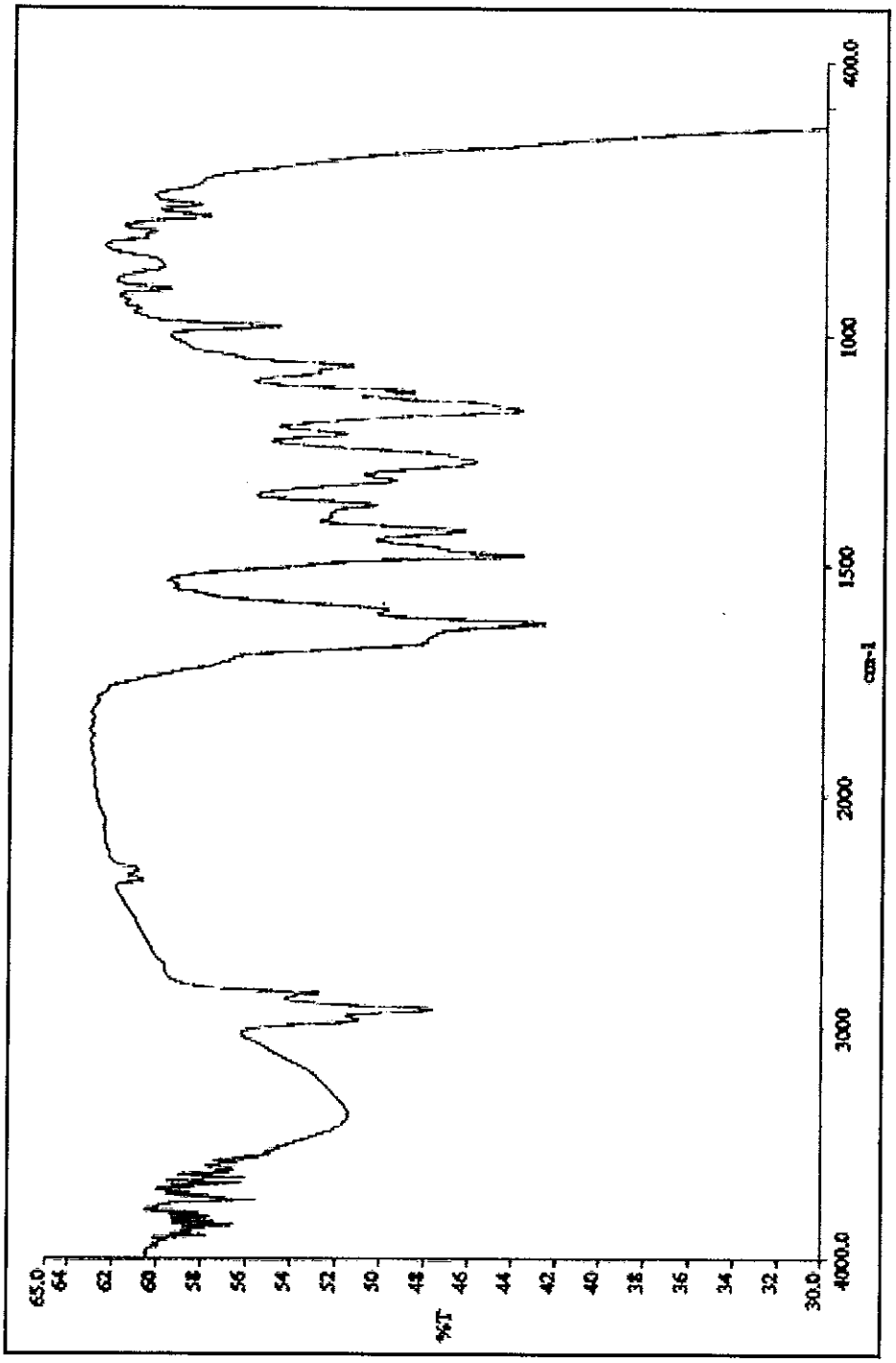

Figure 85 FT-IR (neat) spectrum of compound GP12

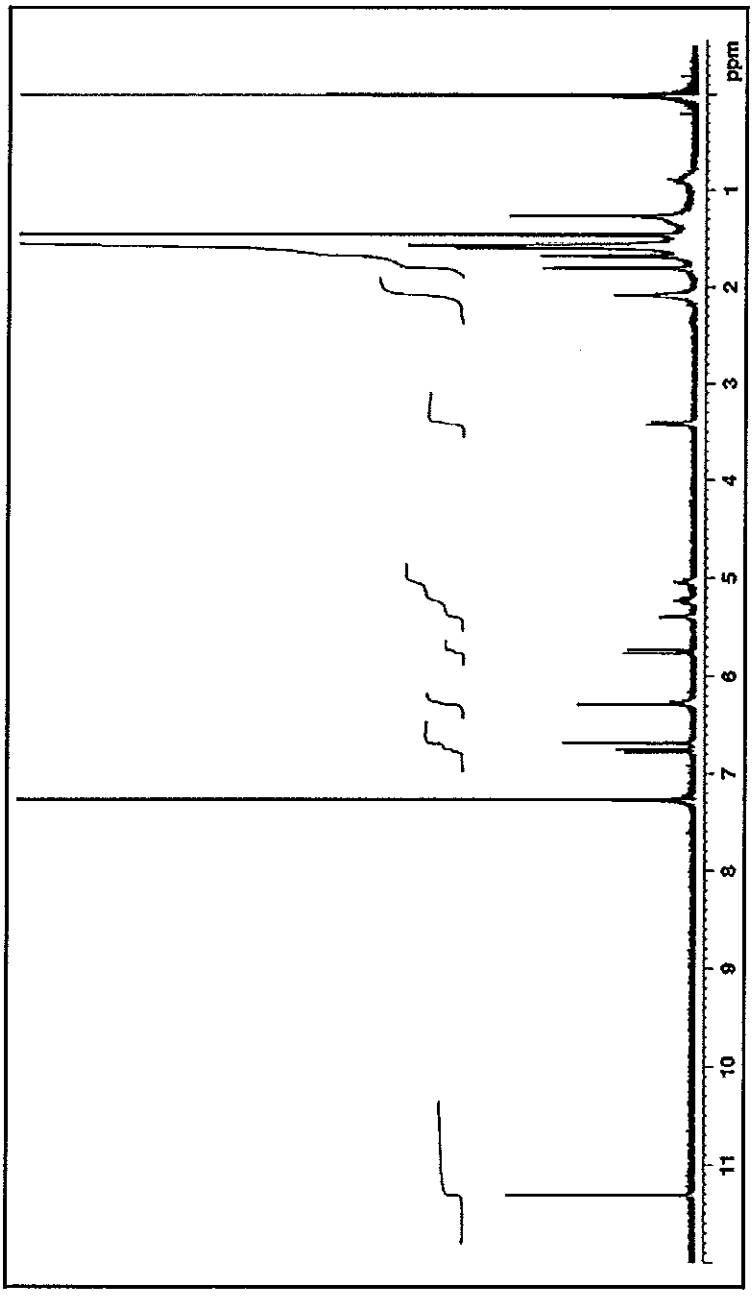

Figure 86 ^{1}H NMR (300 MHz) ($CDCl_3$) spectrum of compound GP12

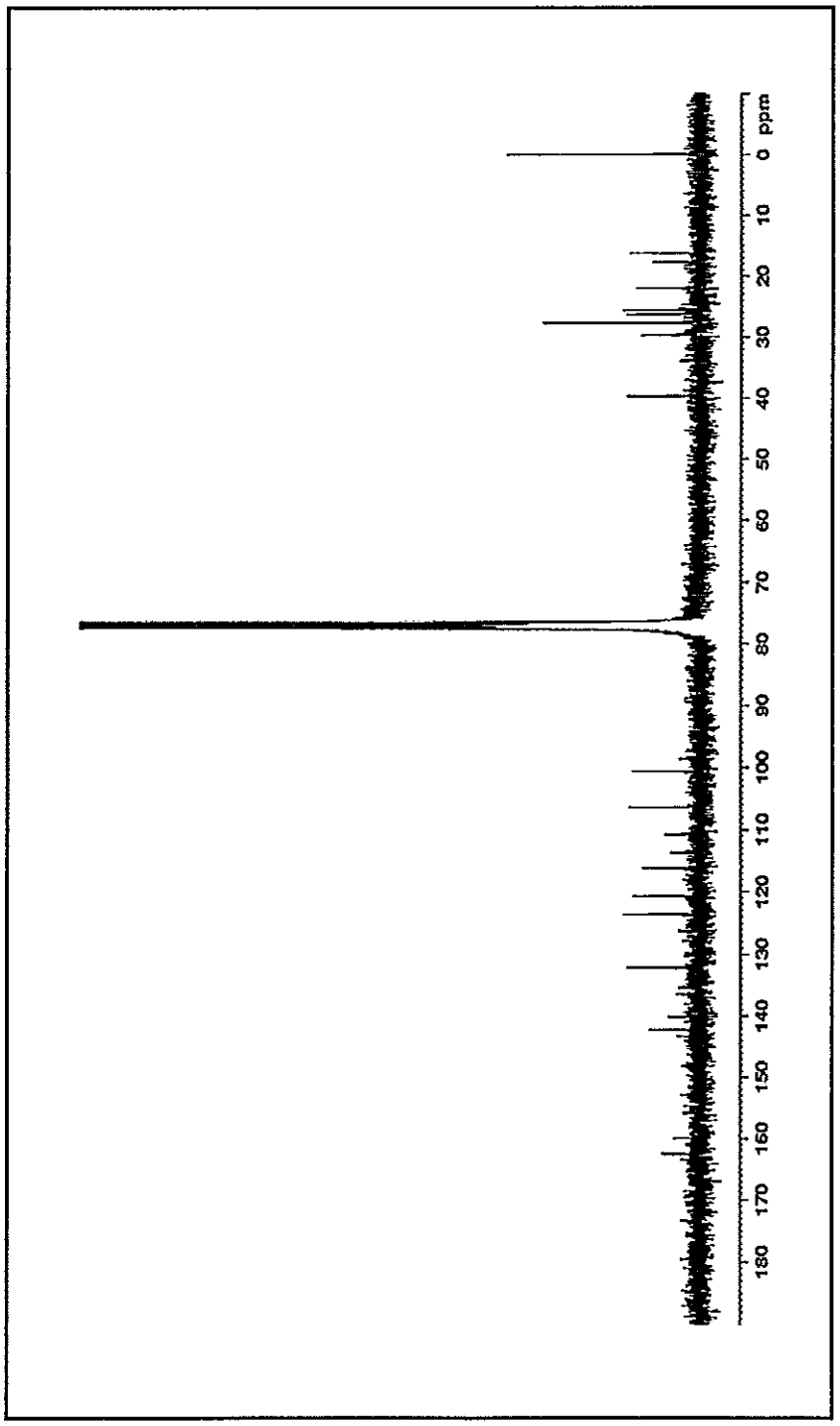

Figure 87 ^{13}C NMR (75 MHz) ($CDCl_3$) spectrum of compound GP12

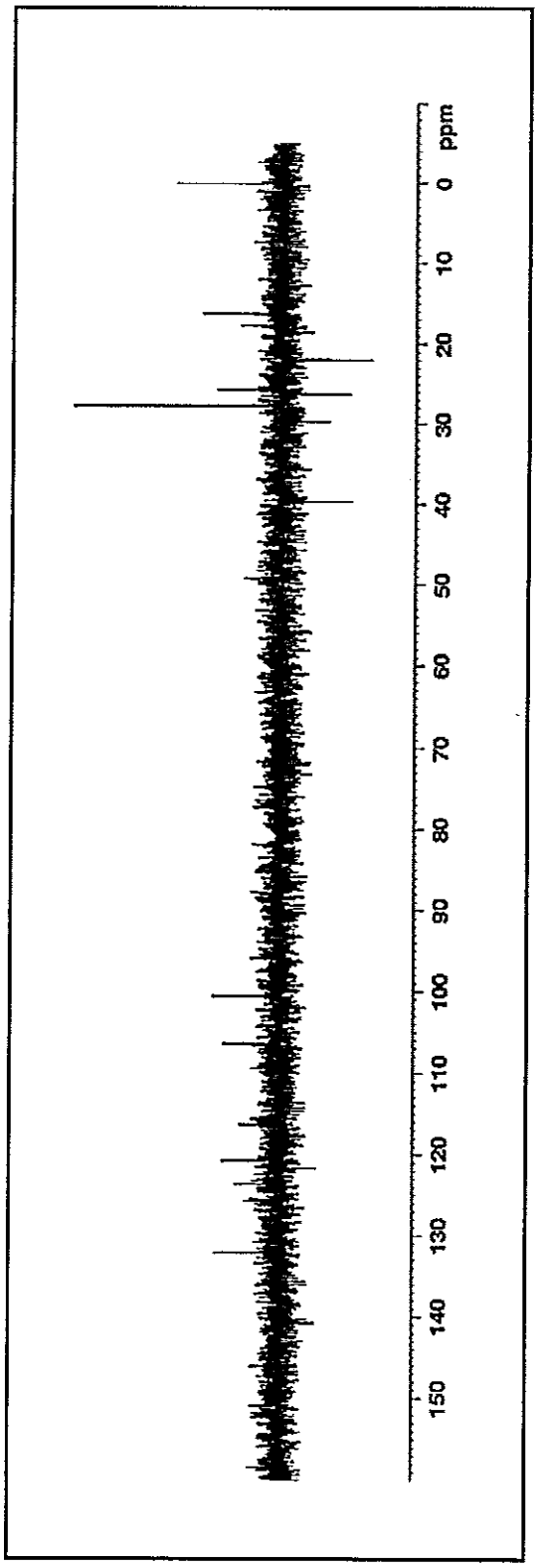

Figure 88 DEPT 135° spectra of compound GP12

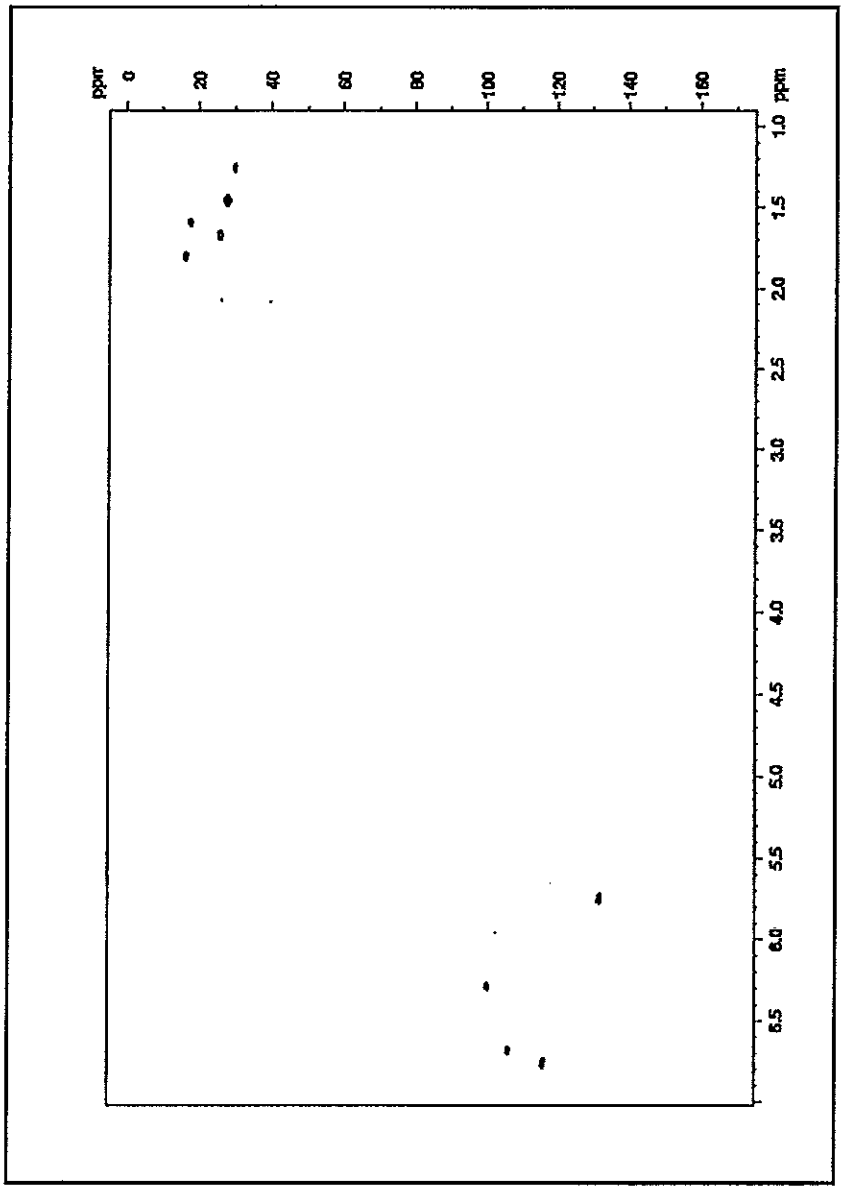

Figure 89 2D HMQC spectrum of compound GP12

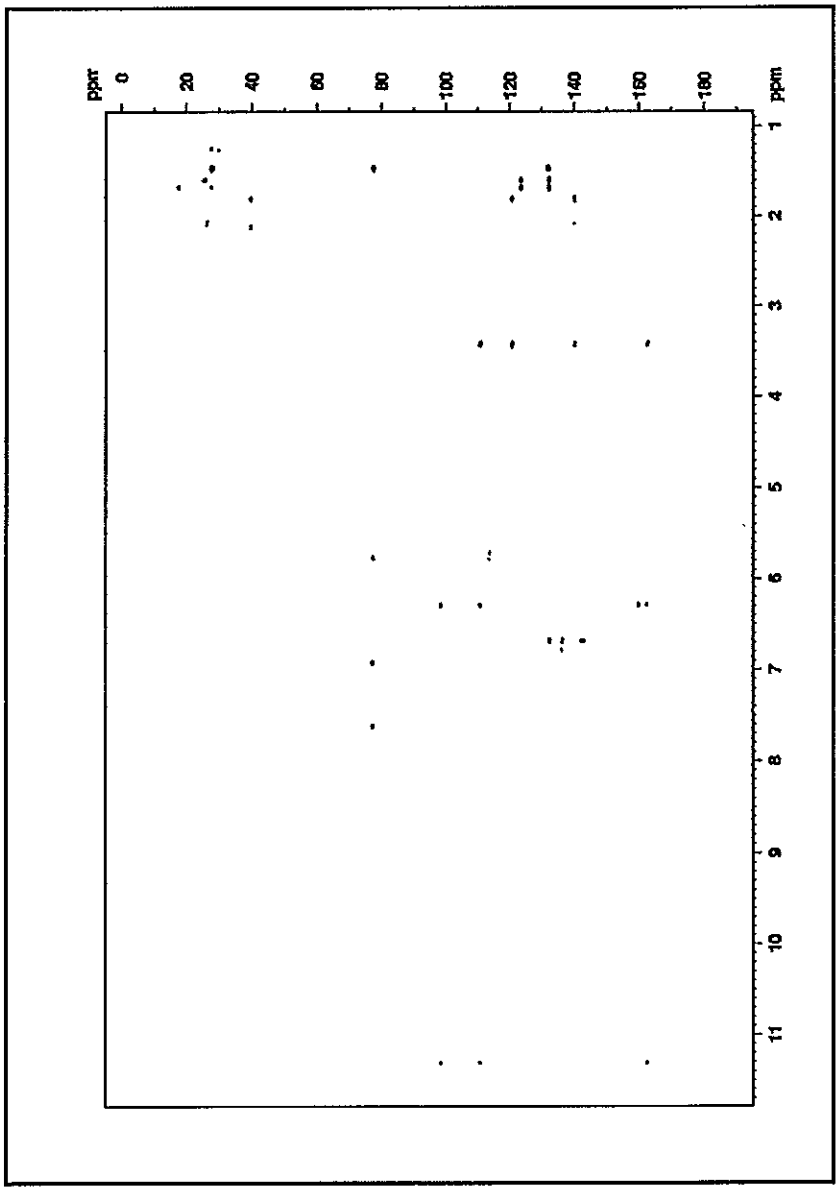

Figure 90 2D HMBC spectrum of compound GP12

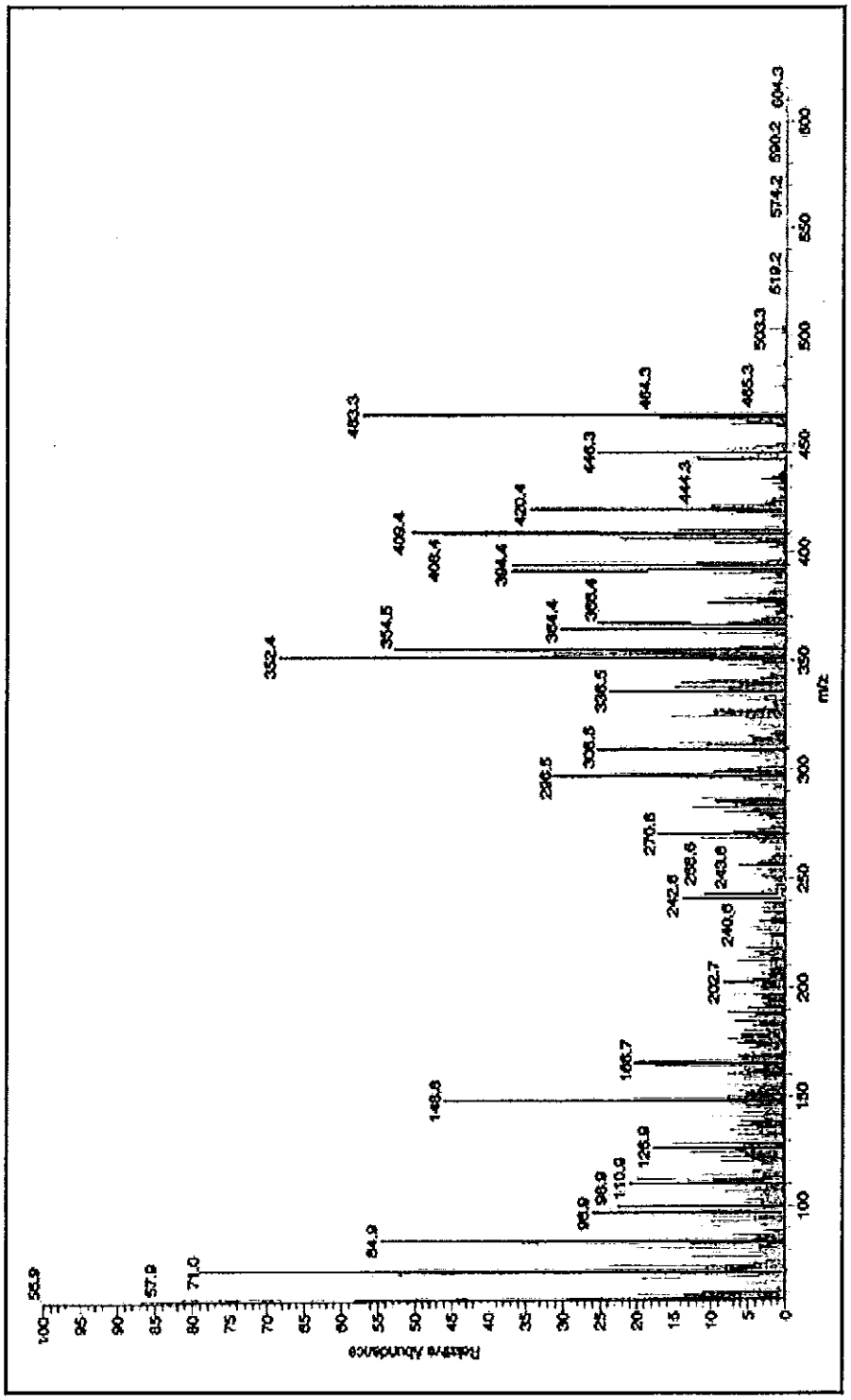

Figure 91 Mass spectrum of compound GP9

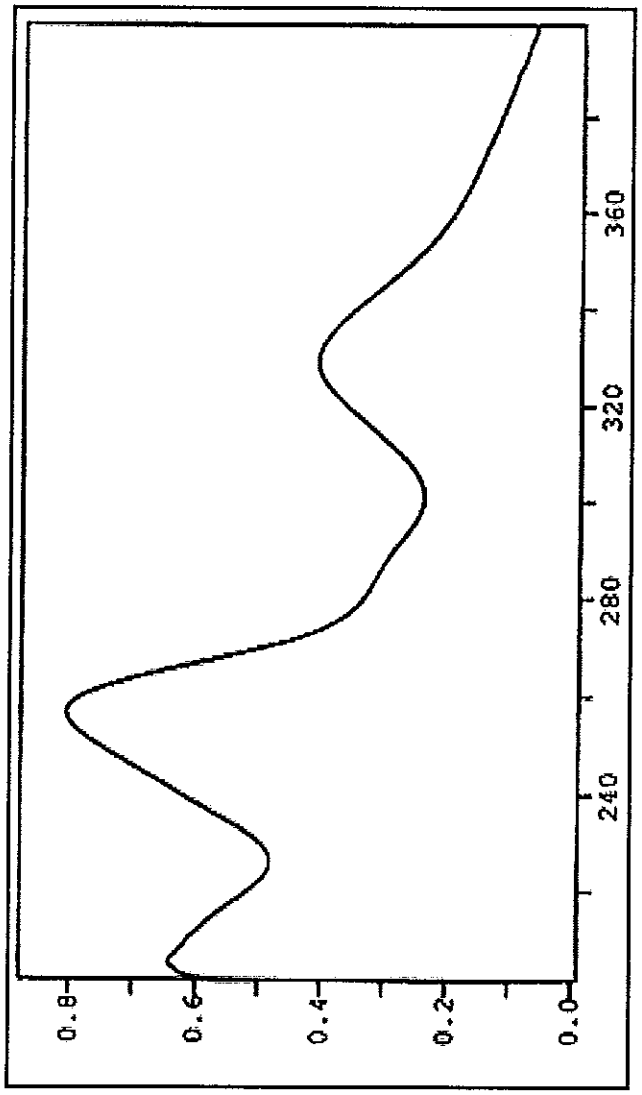

Figure 92 UV (MeOH) spectrum of compound GP9

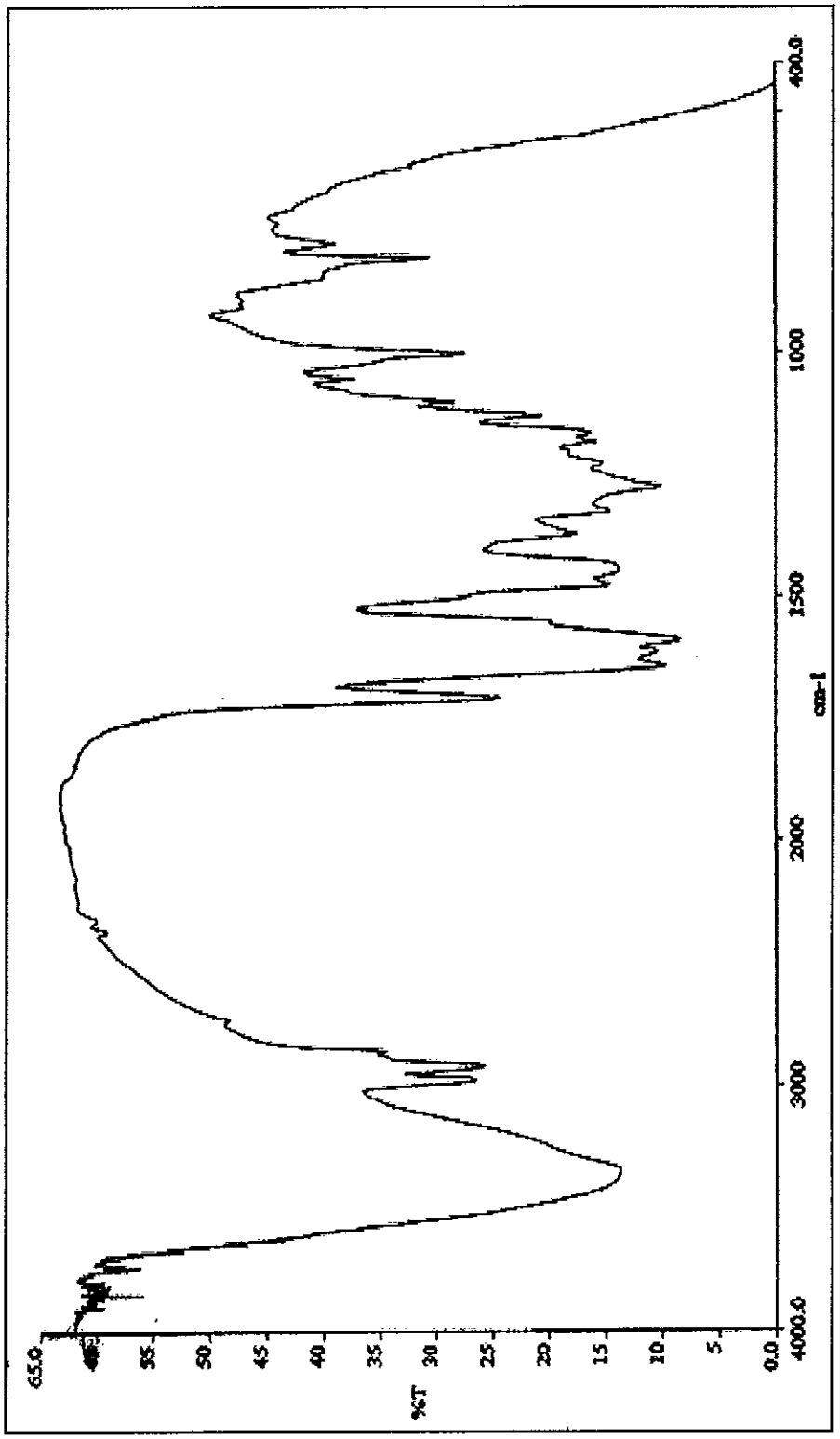

Figure 93 FT-IR (neat) spectrum of compound GP9

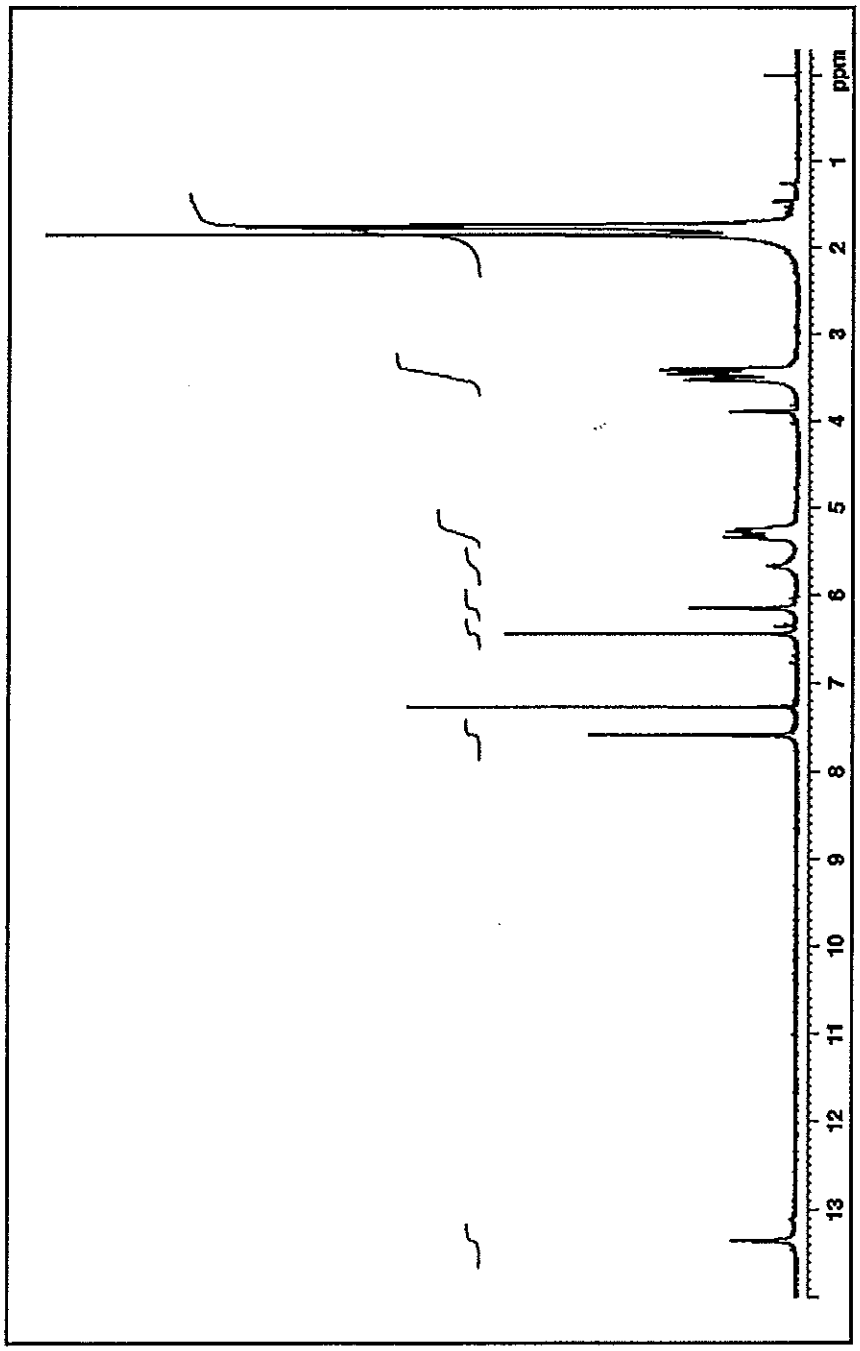

Figure 94 ^{1}H NMR (300 MHz) ($CDCl_3$) spectrum of compound GP9

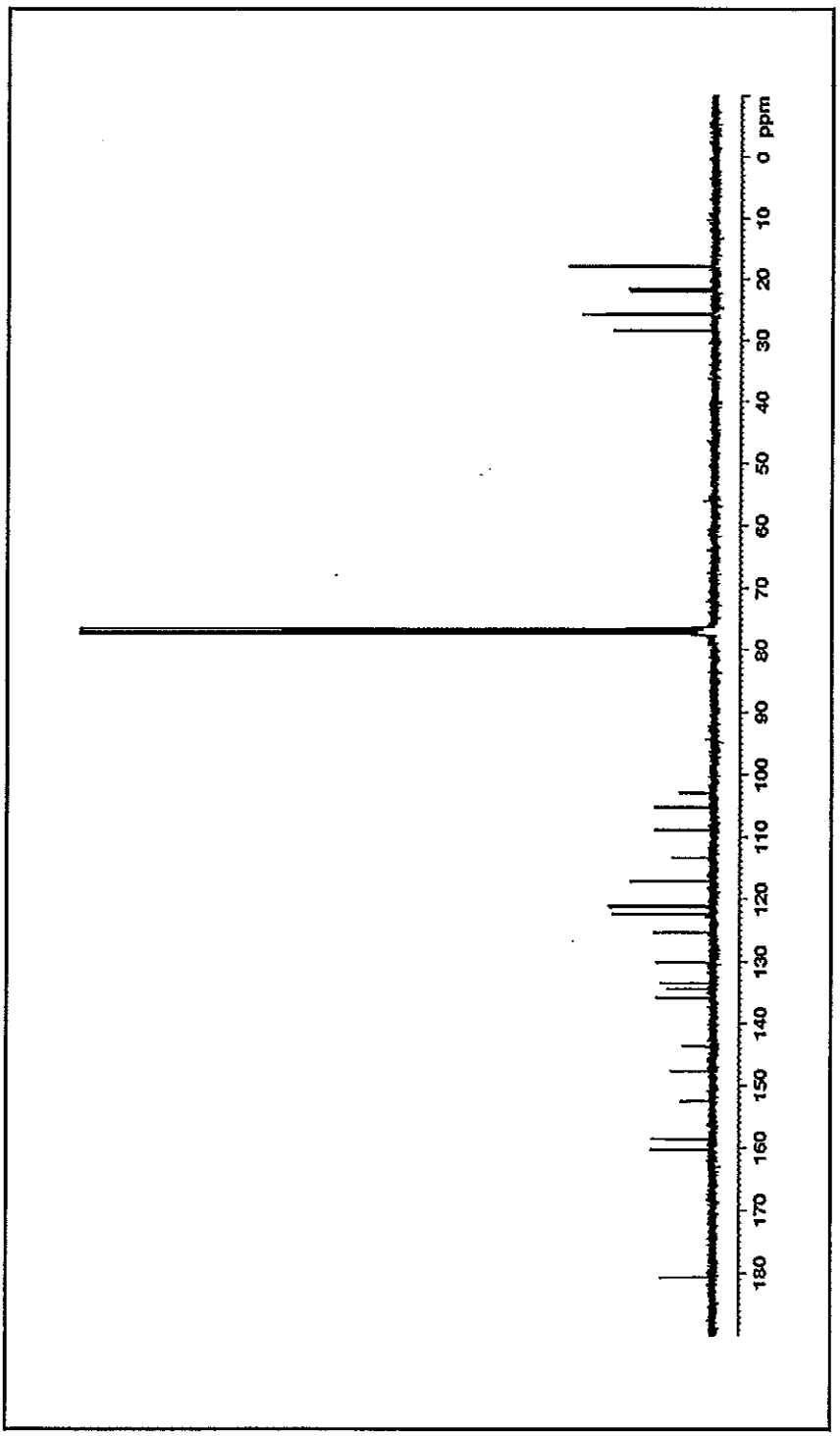

Figure 95 ^{13}C NMR (75 MHz) ($CDCl_3$) spectrum of compound GP9

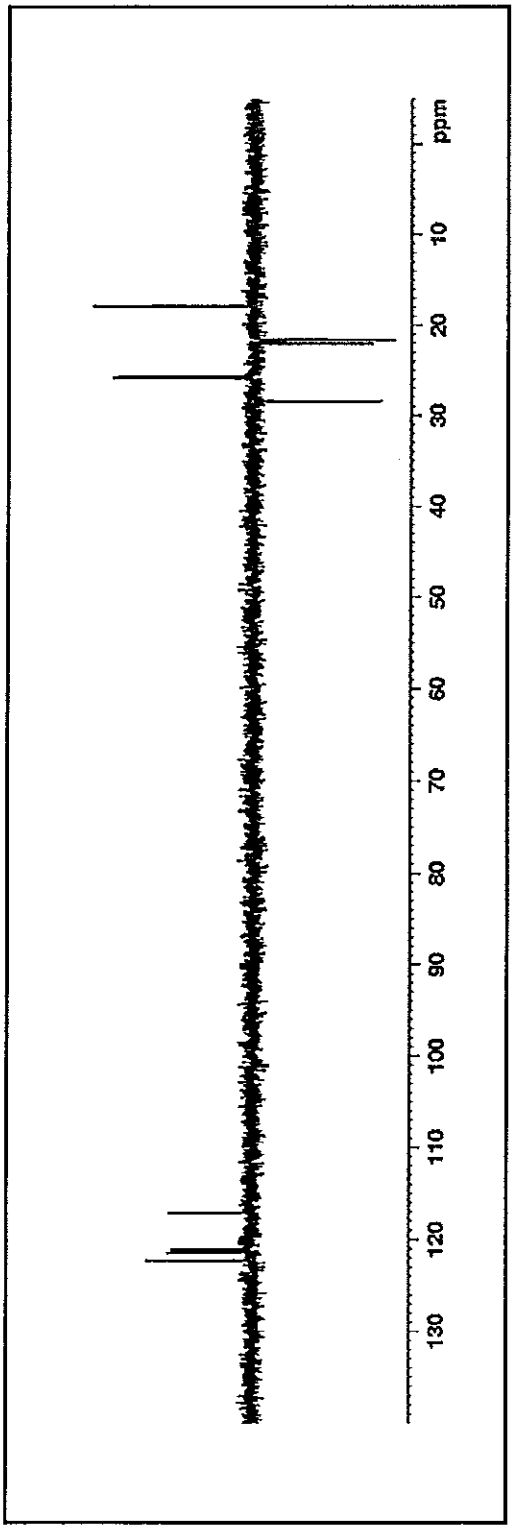

Figure 96 DEPT 135° spectra of compound GP9

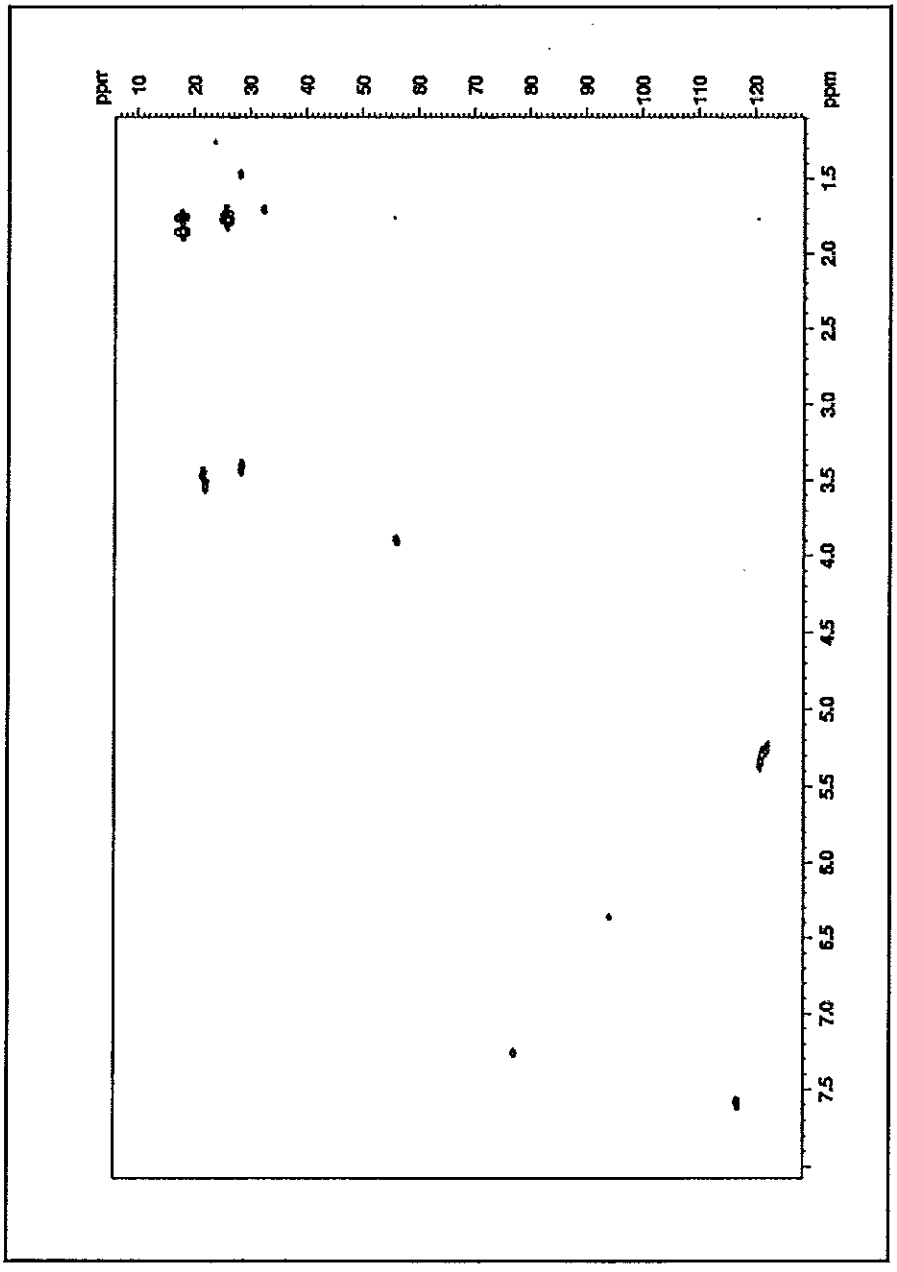

Figure 97 2D HMQC spectrum of compound GP9

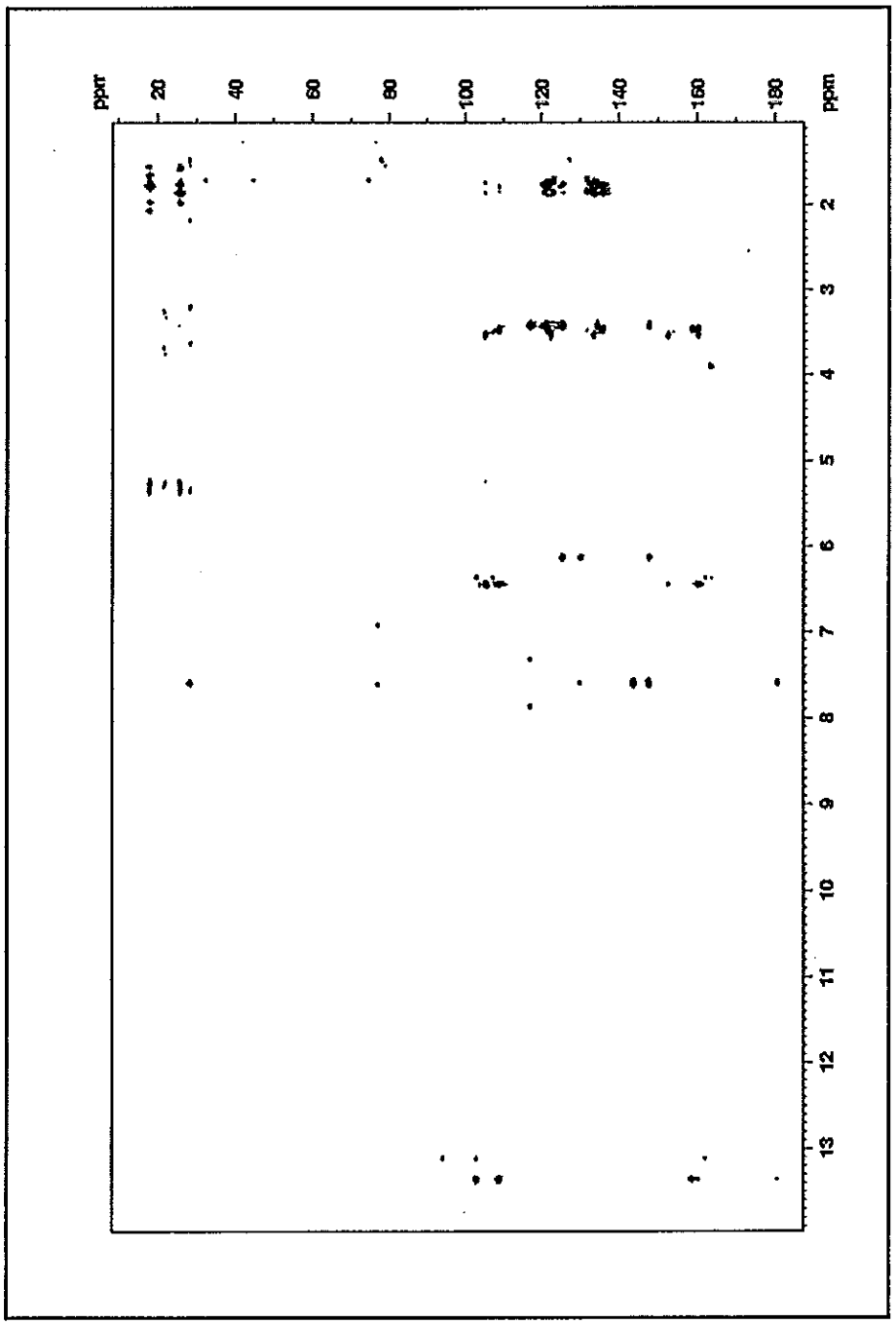

Figure 98 2D HMBC spectrum of compound GP9

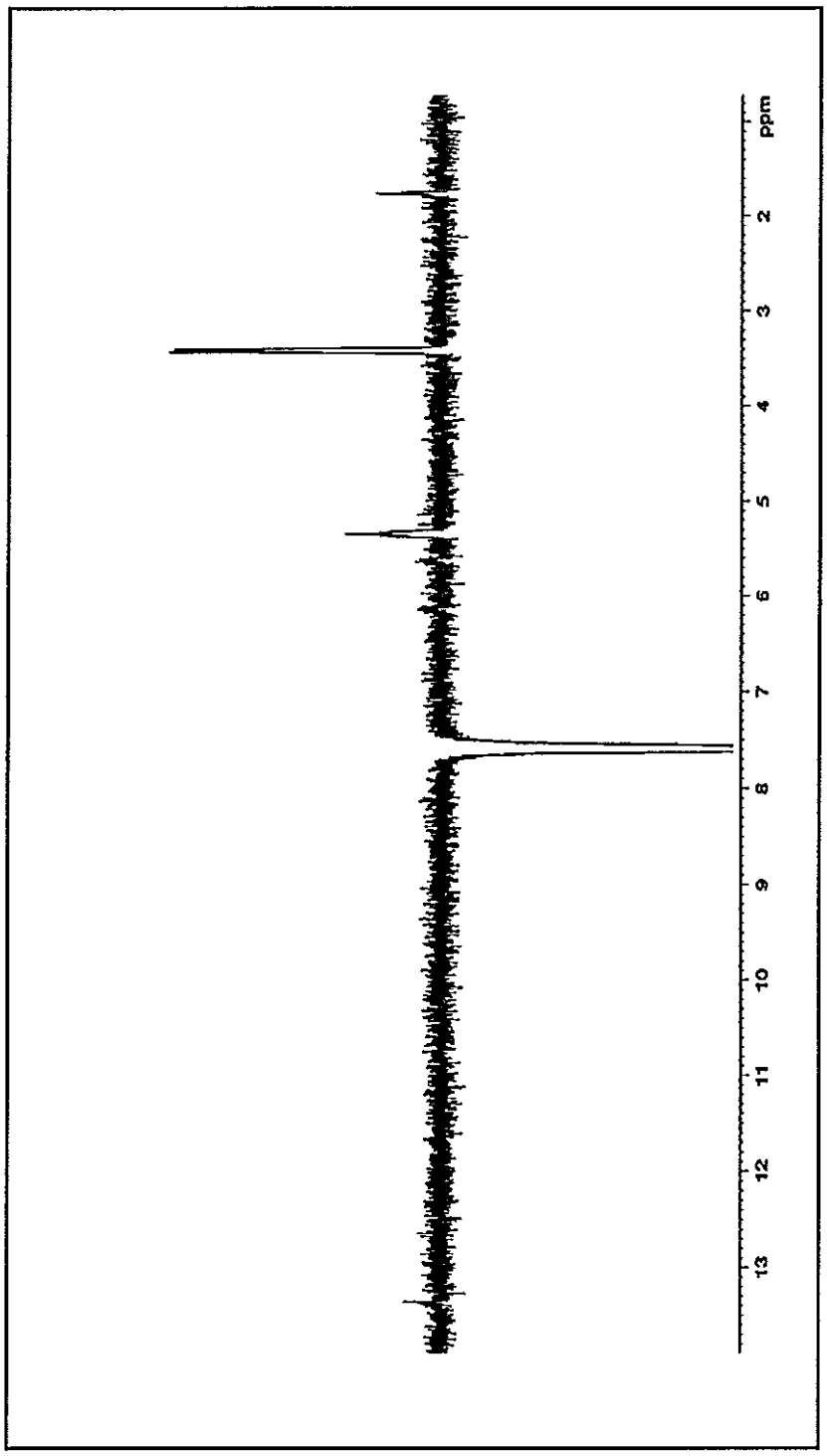

Figure 99 NOE difference spectrum of compound GP9 after irradiation at δ_H 7.58 (H-8)

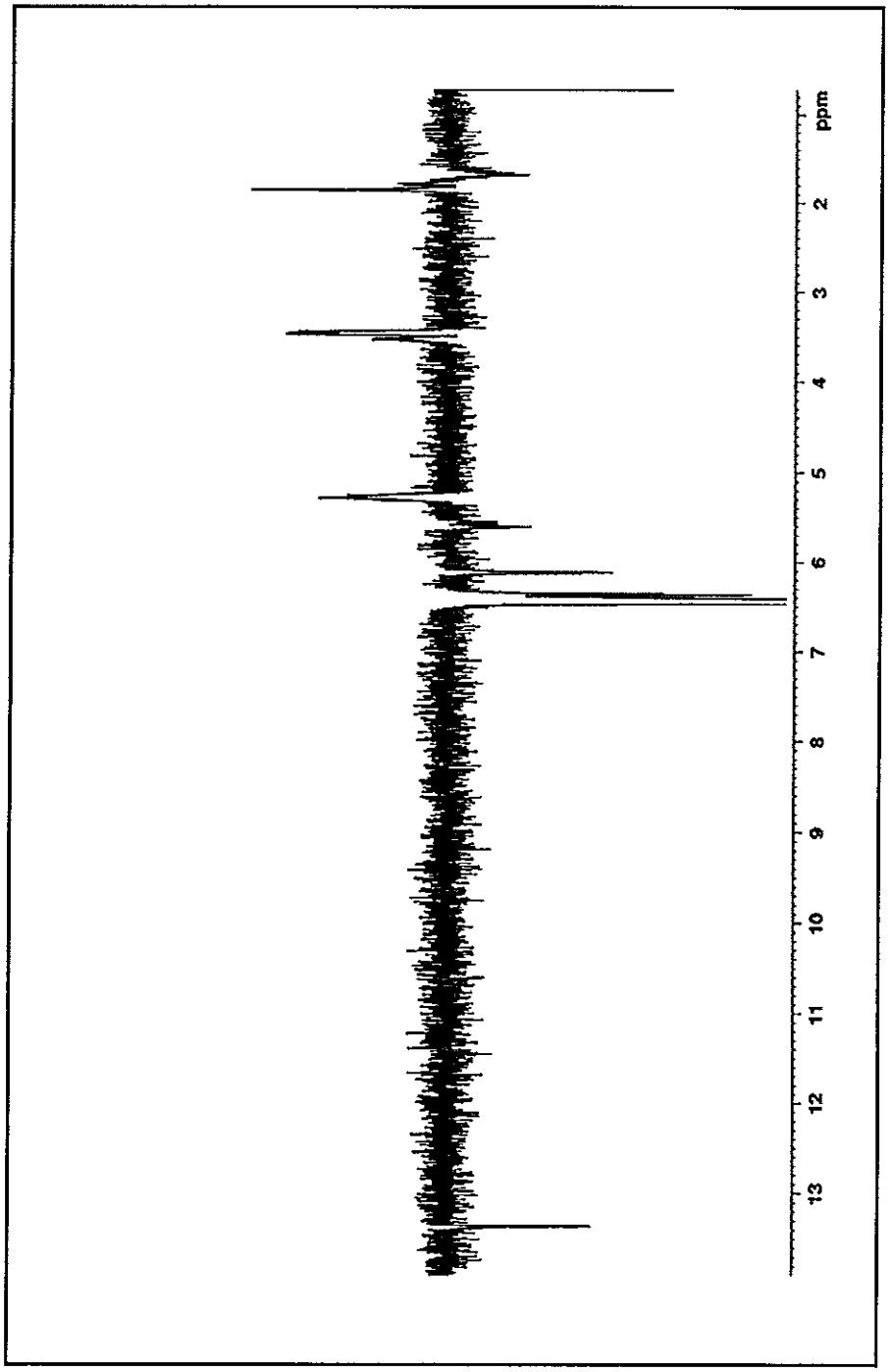

Figure 100 NOE difference spectrum of compound GP9 after irradiation at δ_H 6.43 (3-OH)

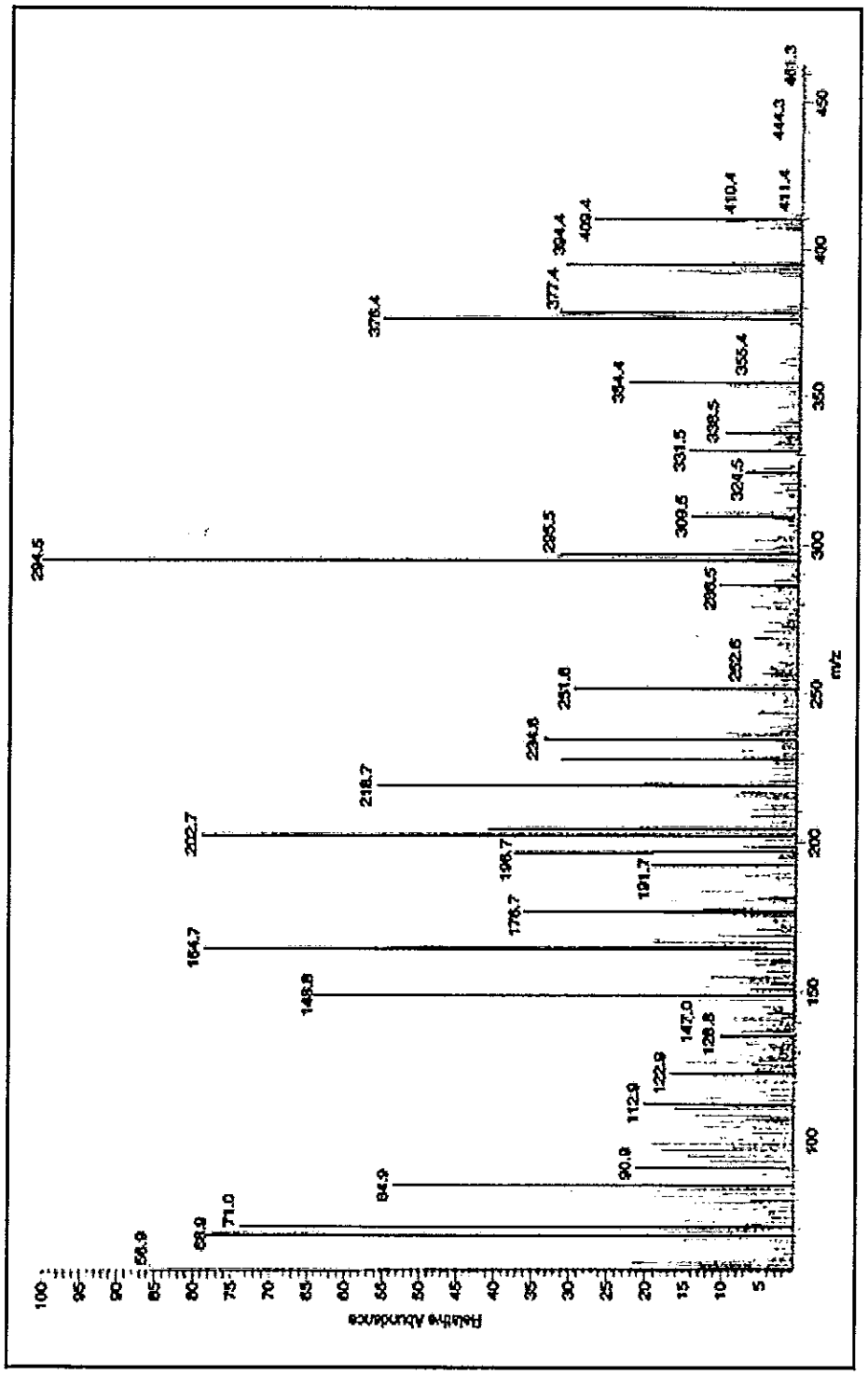

Figure 101 Mass spectrum of compound GP8

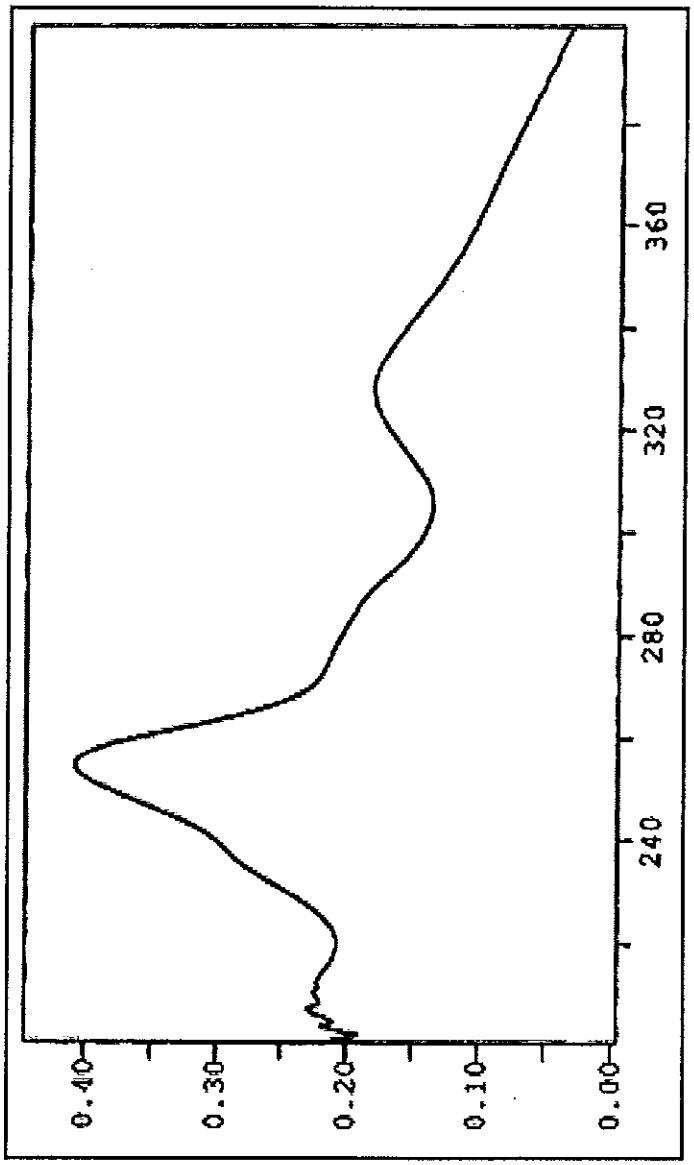

Figure 102 UV (MeOH) spectrum of compound GP8

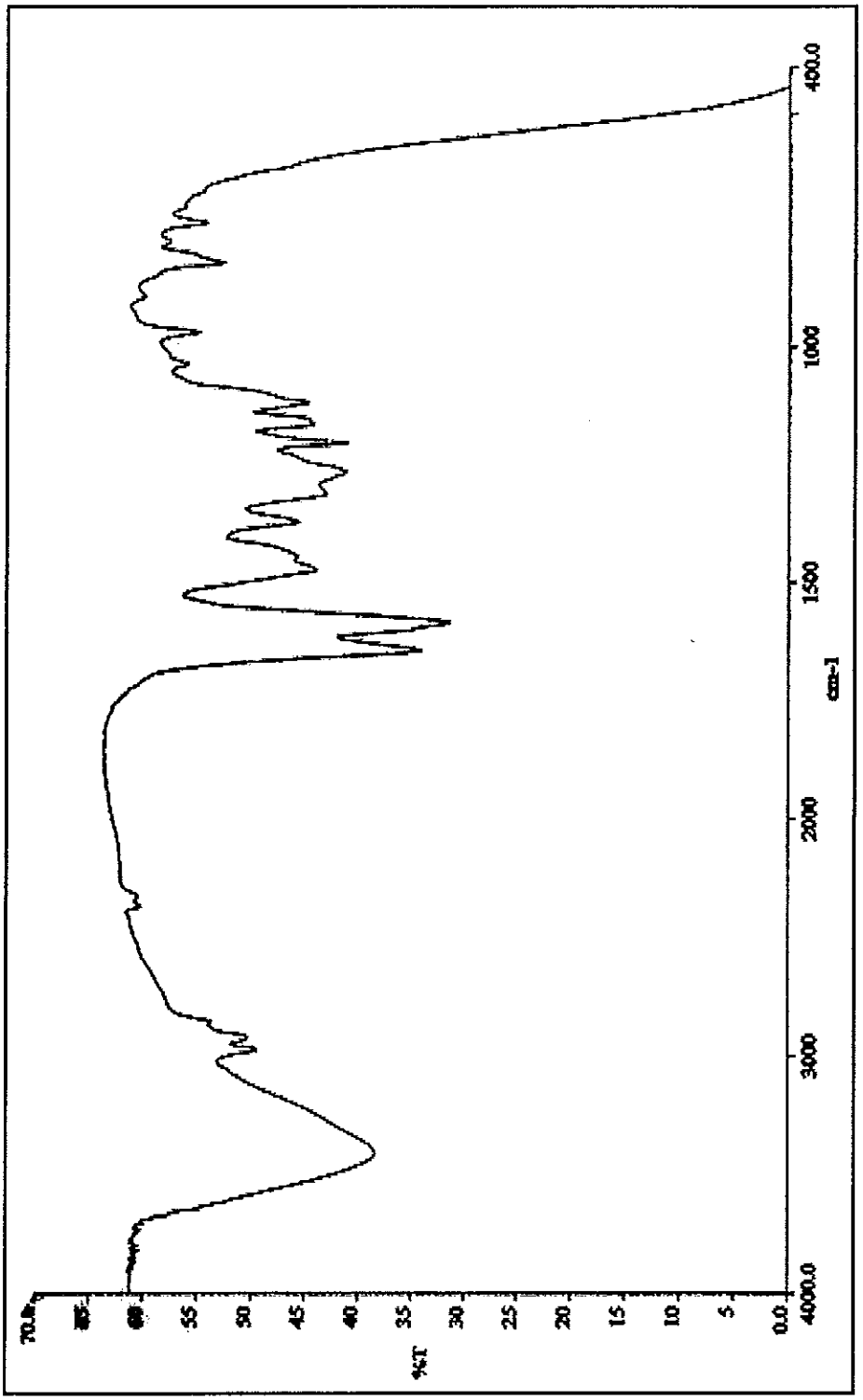

Figure 103 FT-IR (neat) spectrum of compound GP8

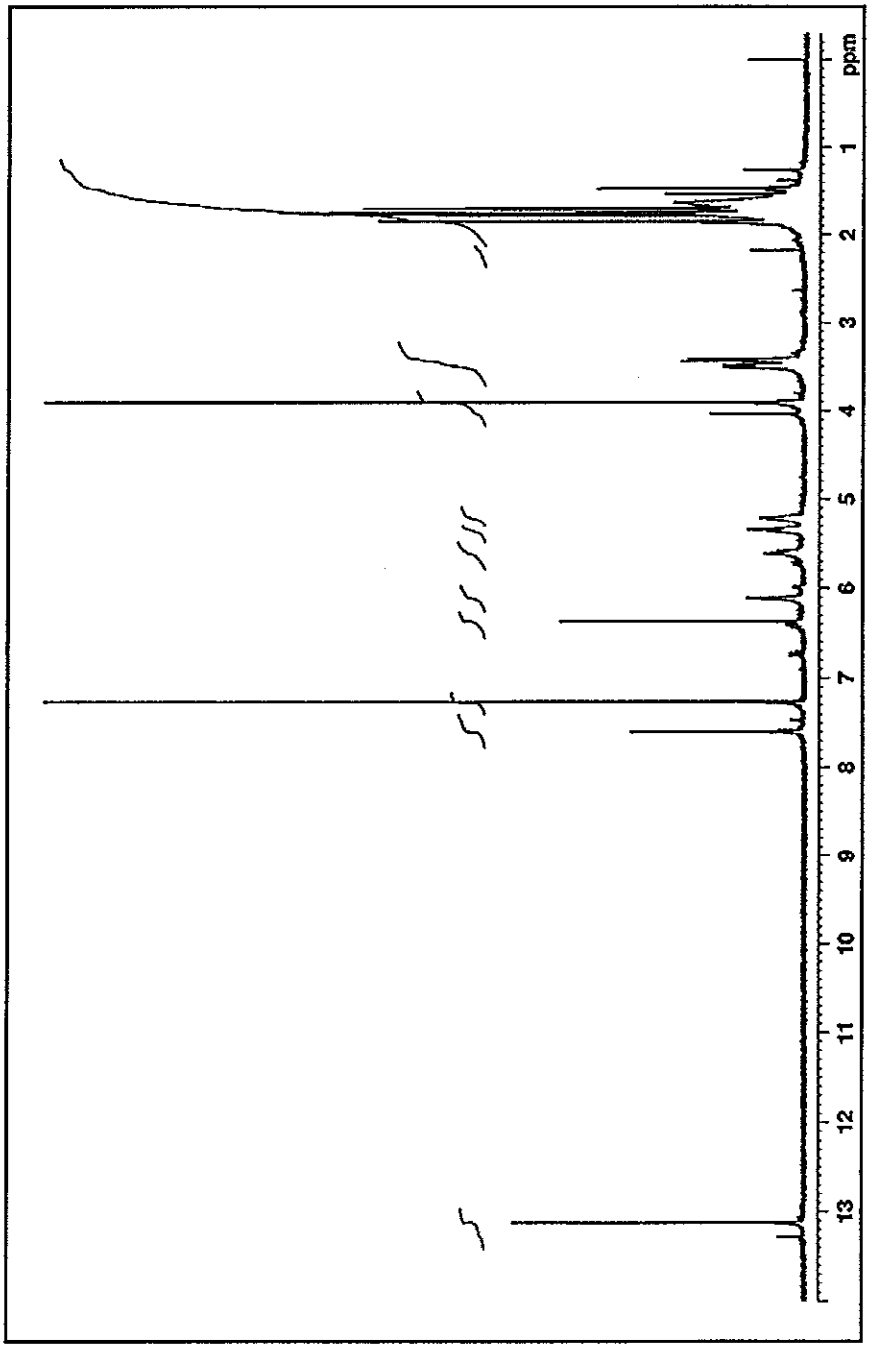

Figure 104 ^{1}H NMR (300 MHz) ($CDCl_3$) spectrum of compound GP8

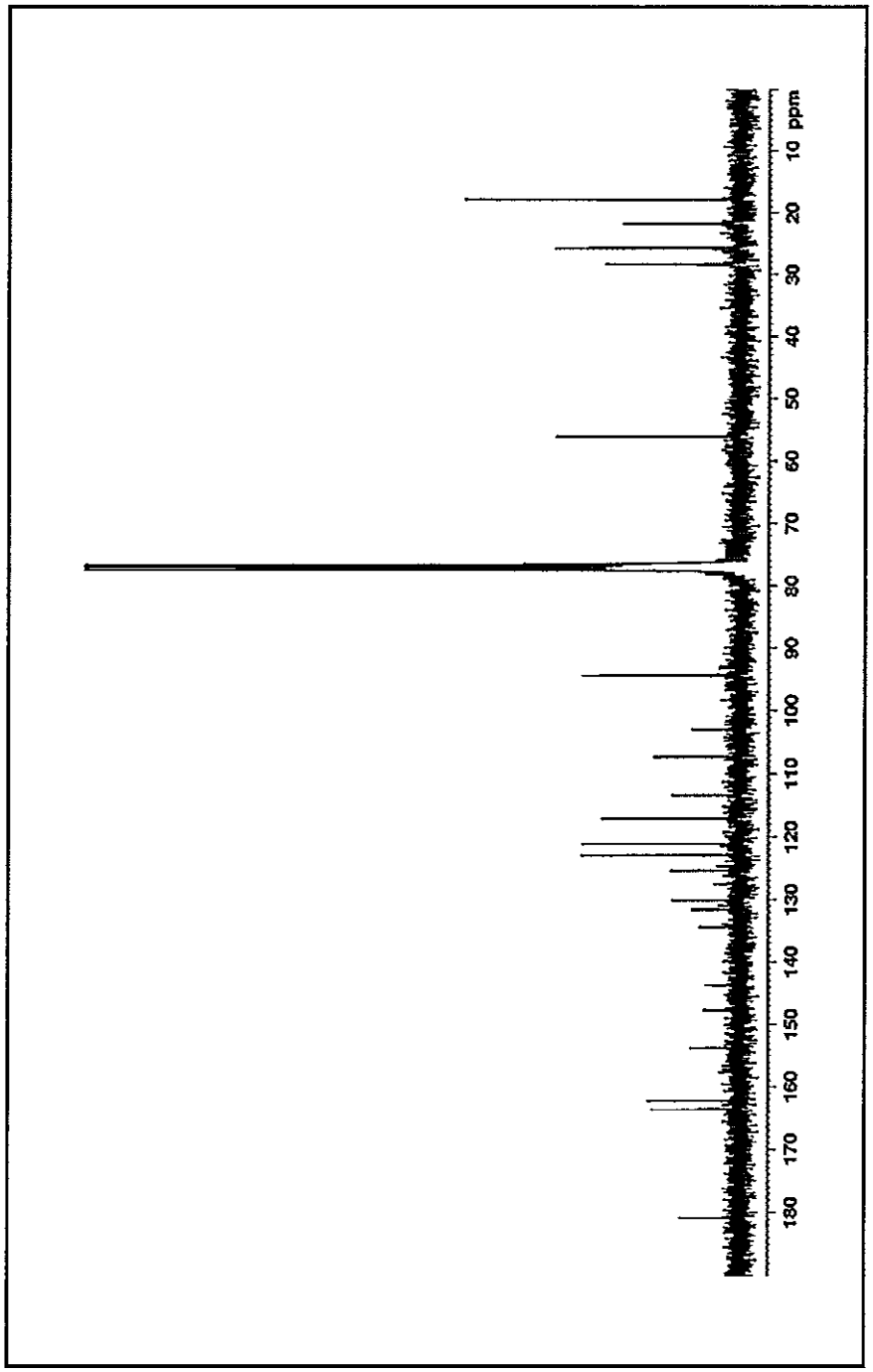

Figure 105 ^{13}C NMR (75 MHz) ($CDCl_3$) spectrum of compound GP8

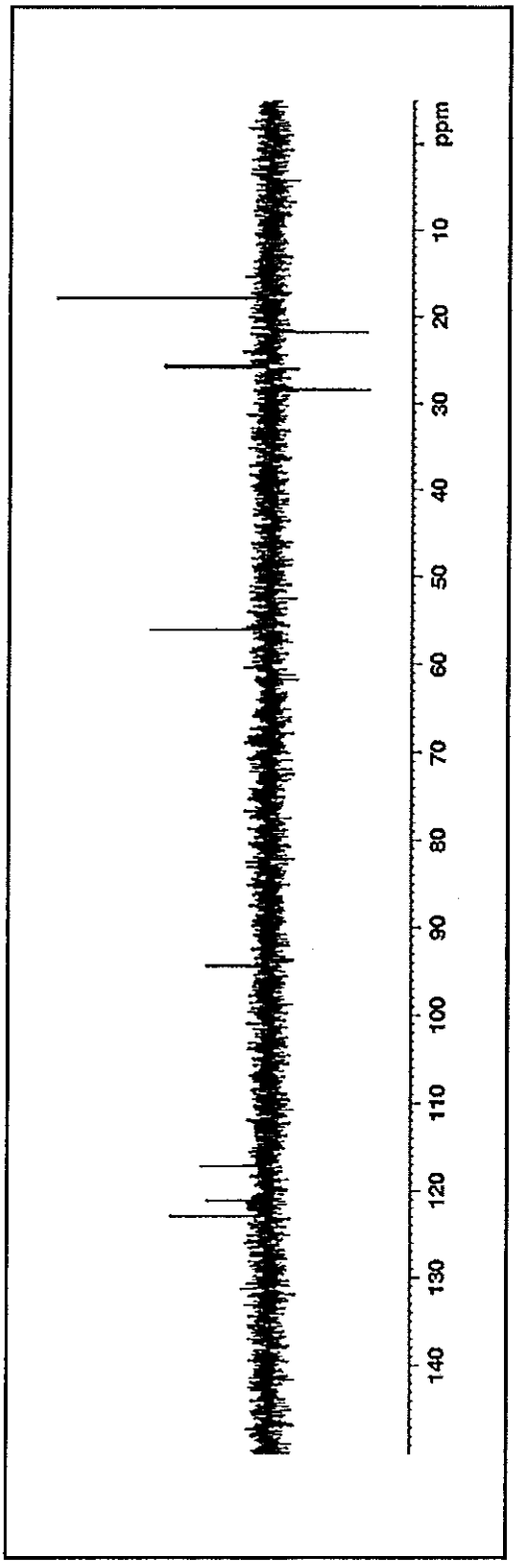

Figure 106 DEPT 135° spectra of compound GP8

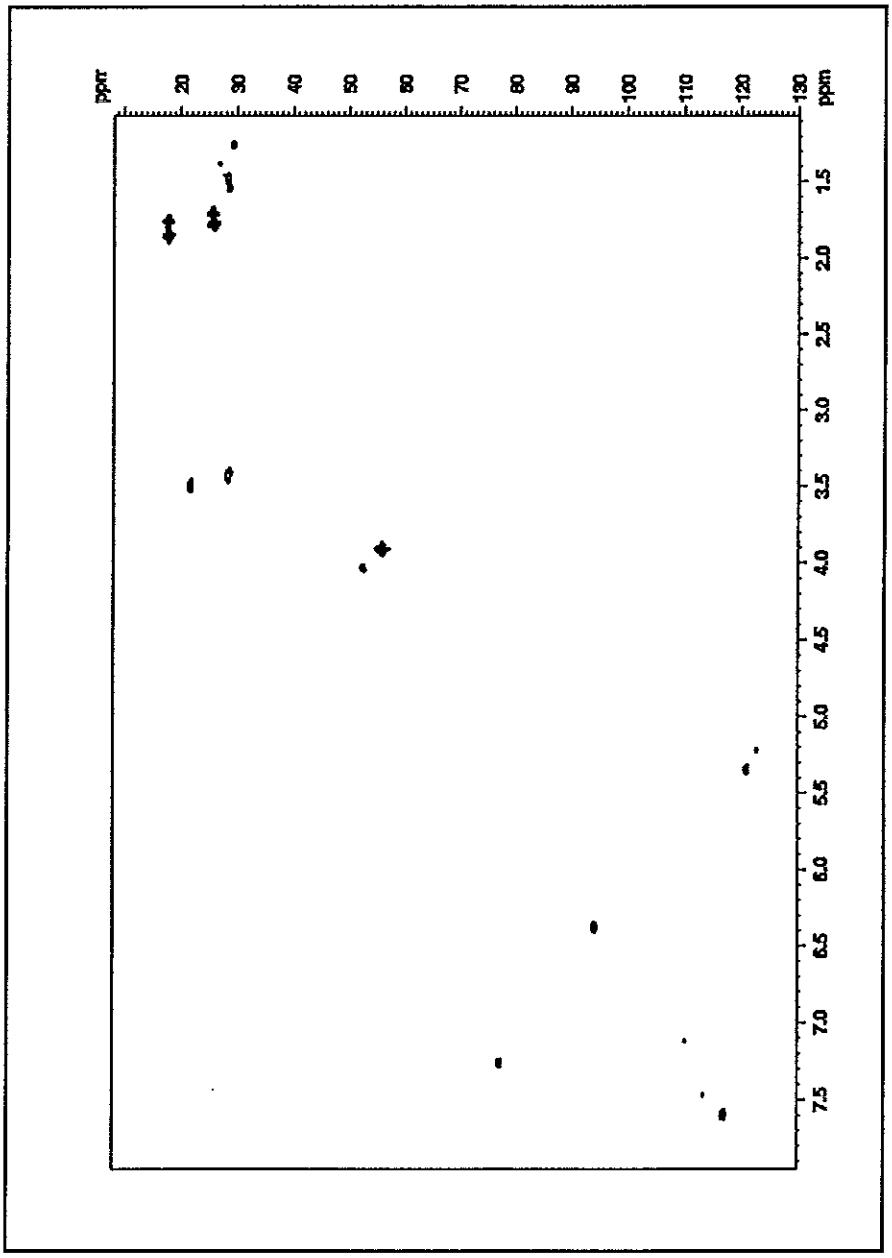

Figure 107 2D HMQC spectrum of compound GP8

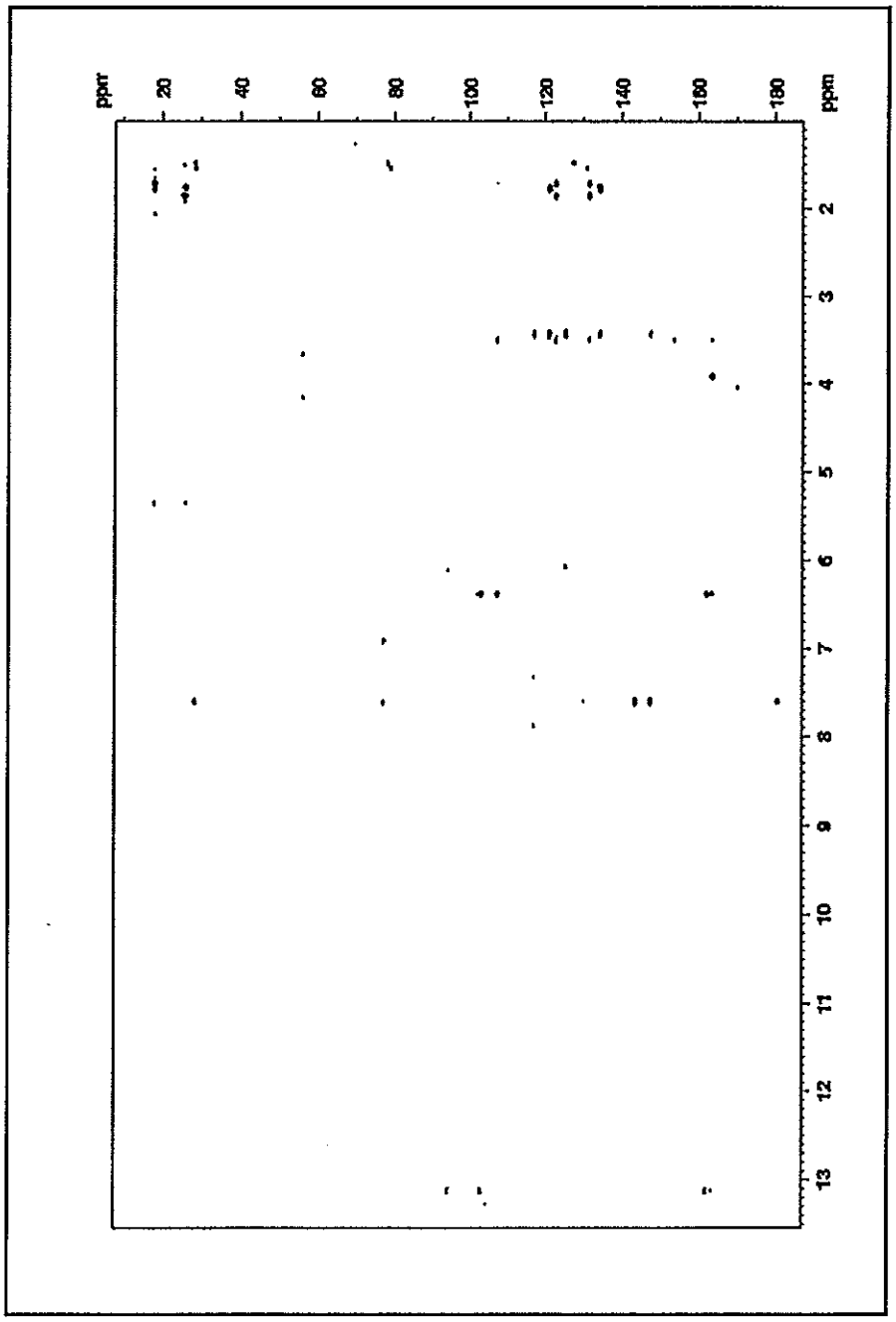

Figure 108 2D HMBC spectrum of compound GP8

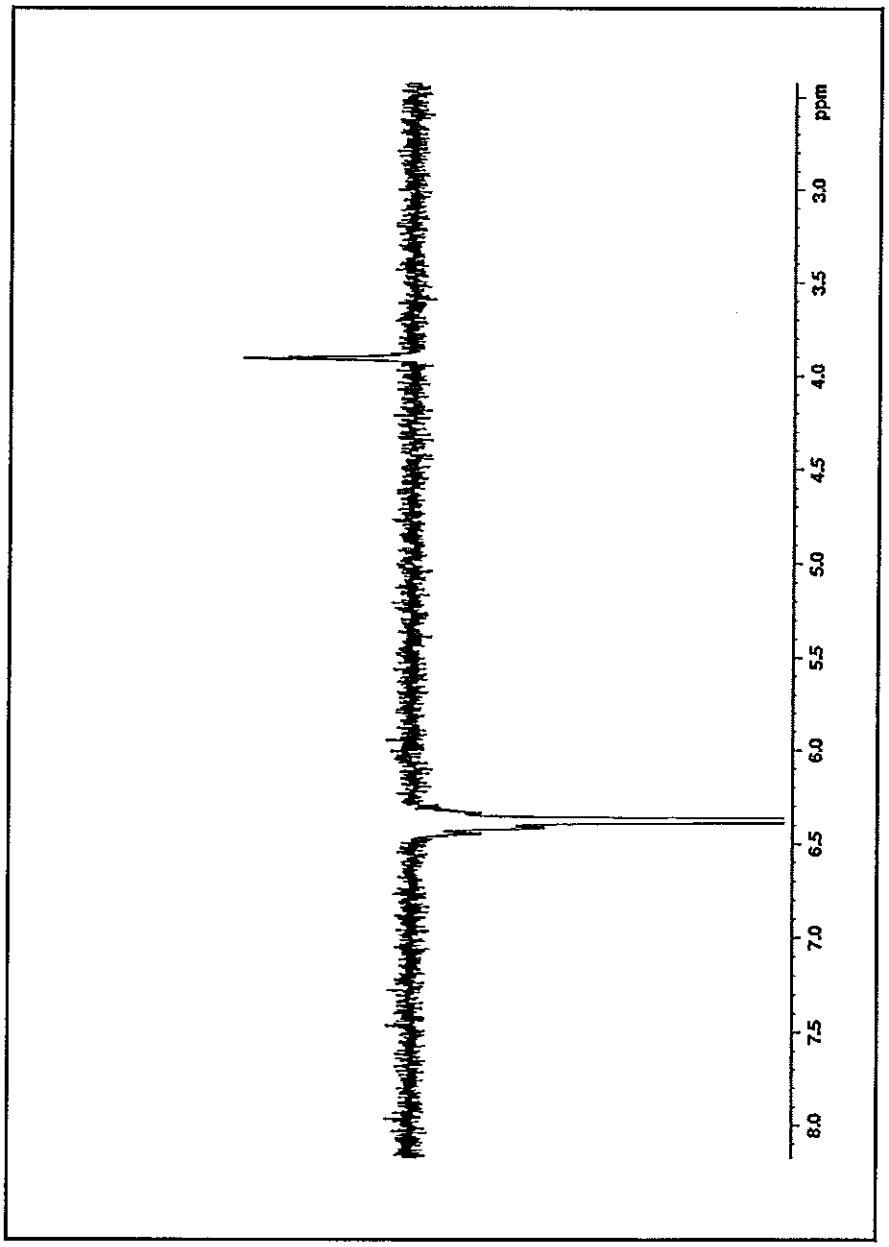

Figure 109 NOE difference spectrum of compound GP8 after irradiation at δ_H 6.37 (H-2)

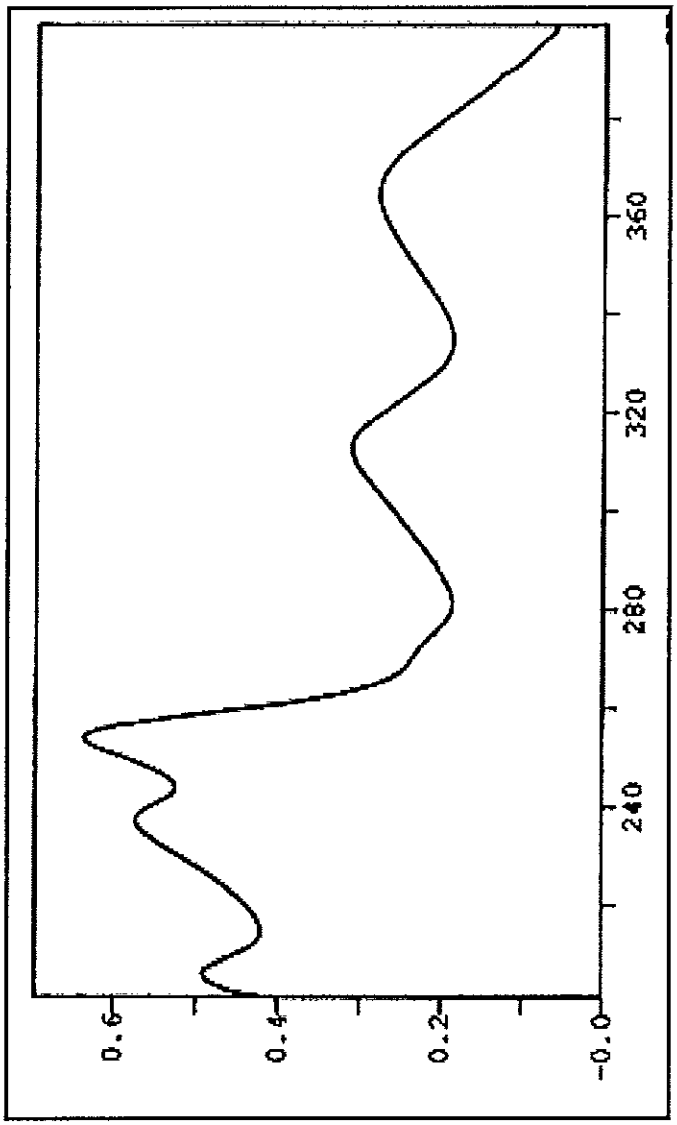

Figure 110 UV (MeOH) spectrum of compound GP20

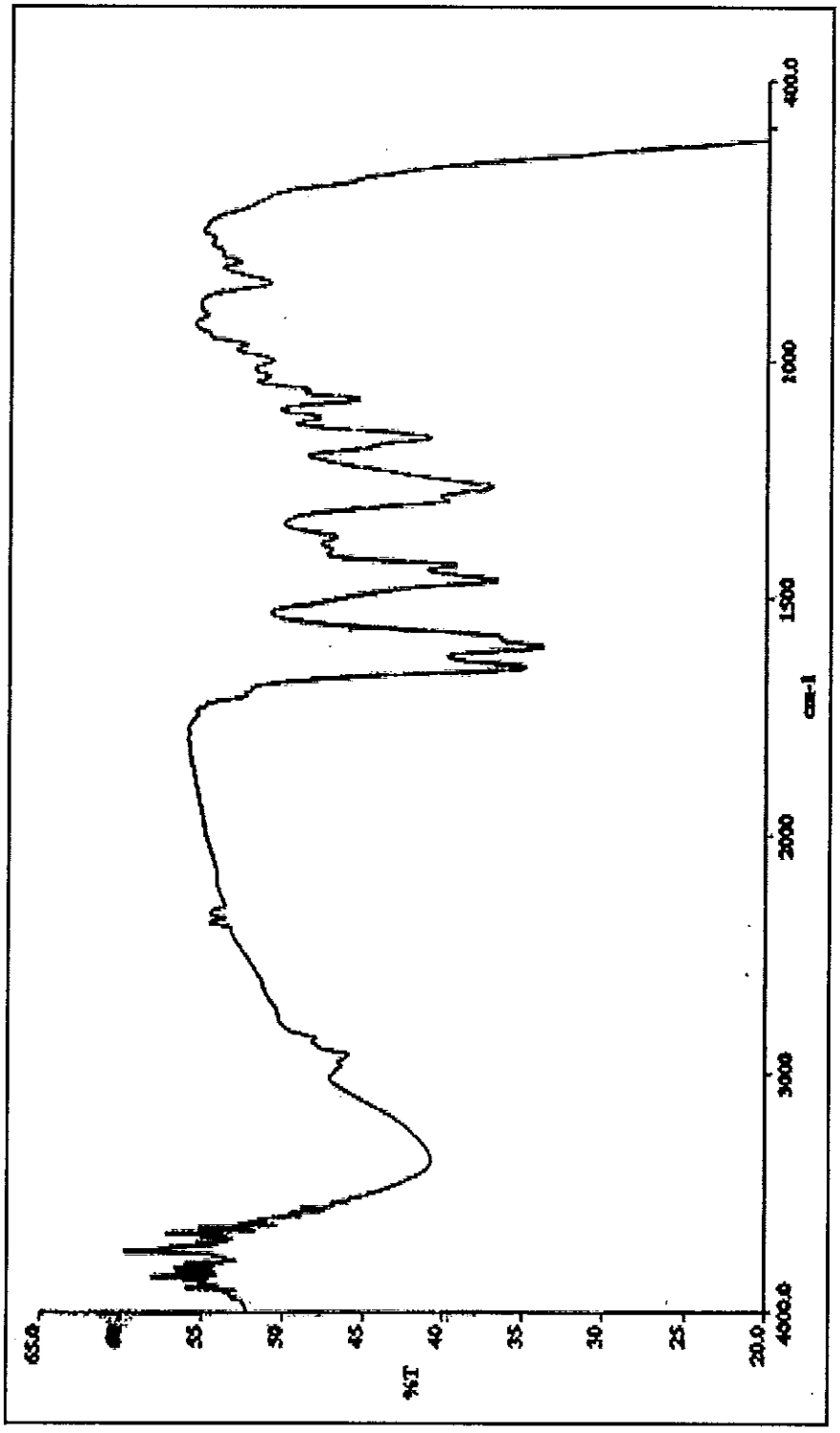

Figure 111 FT-IR (neat) spectrum of compound GP20

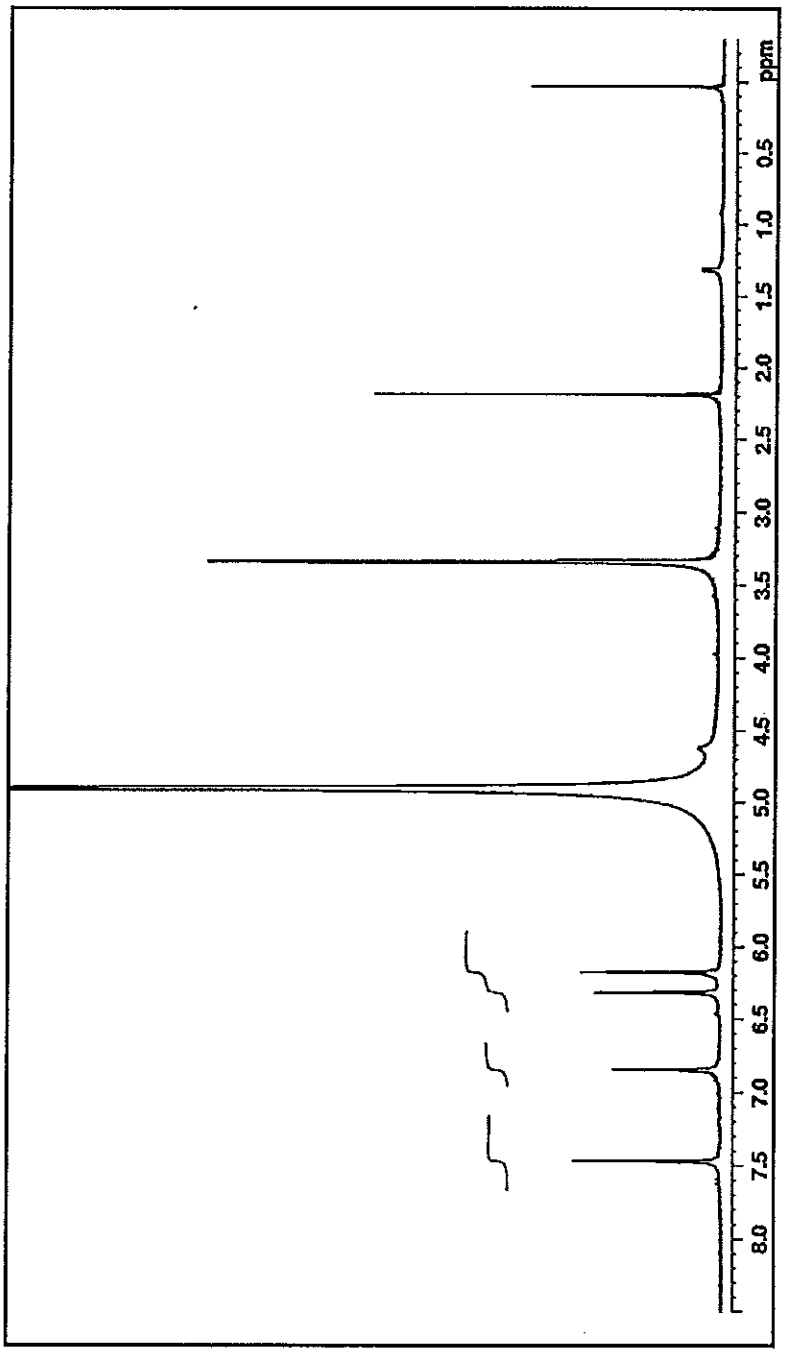

Figure 112 ^{1}H NMR (300 MHz) (CD_3OD) spectrum of compound GP20

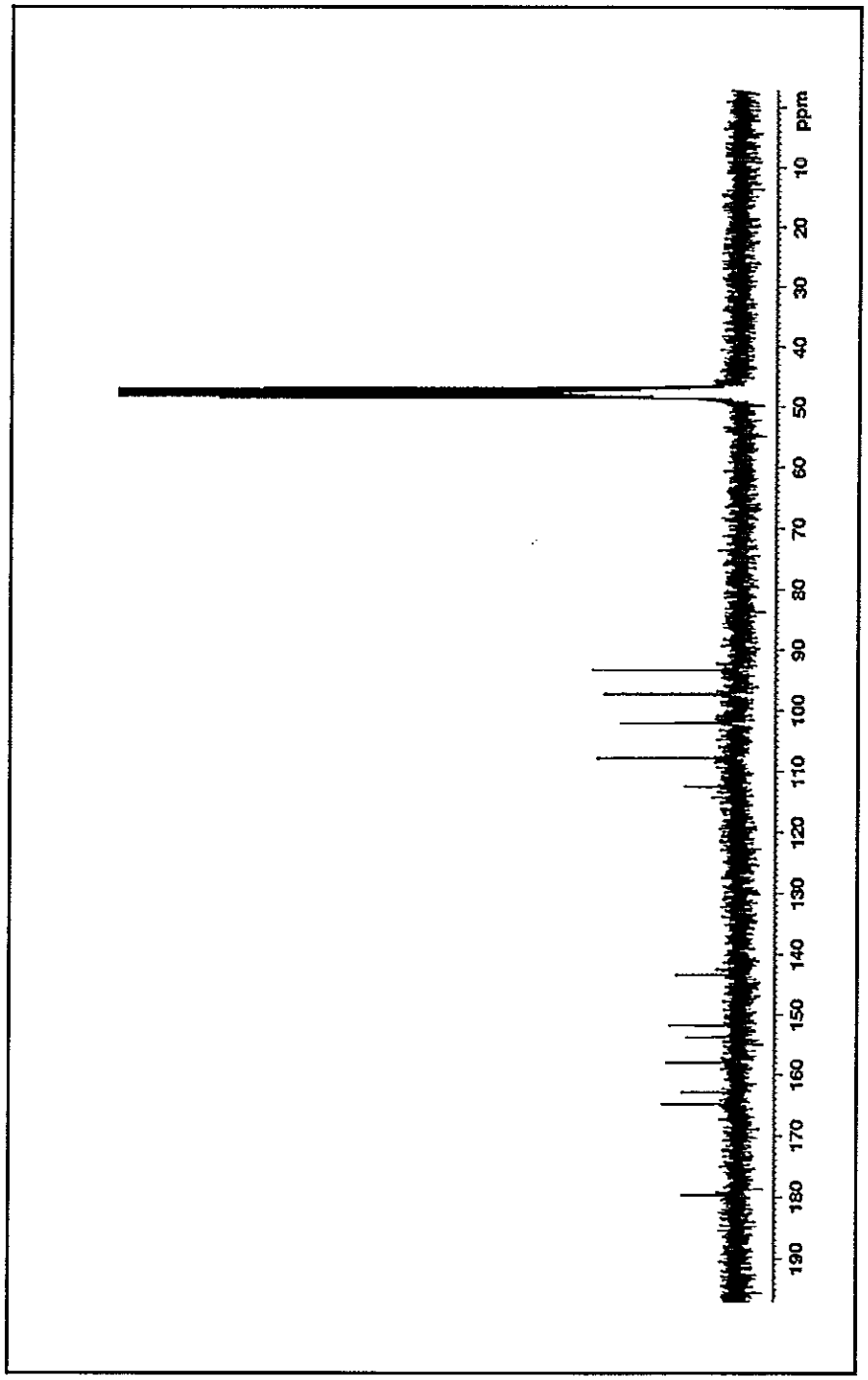

Figure 113 ^{13}C NMR (75 MHz) (CD_3OD) spectrum of compound GP20

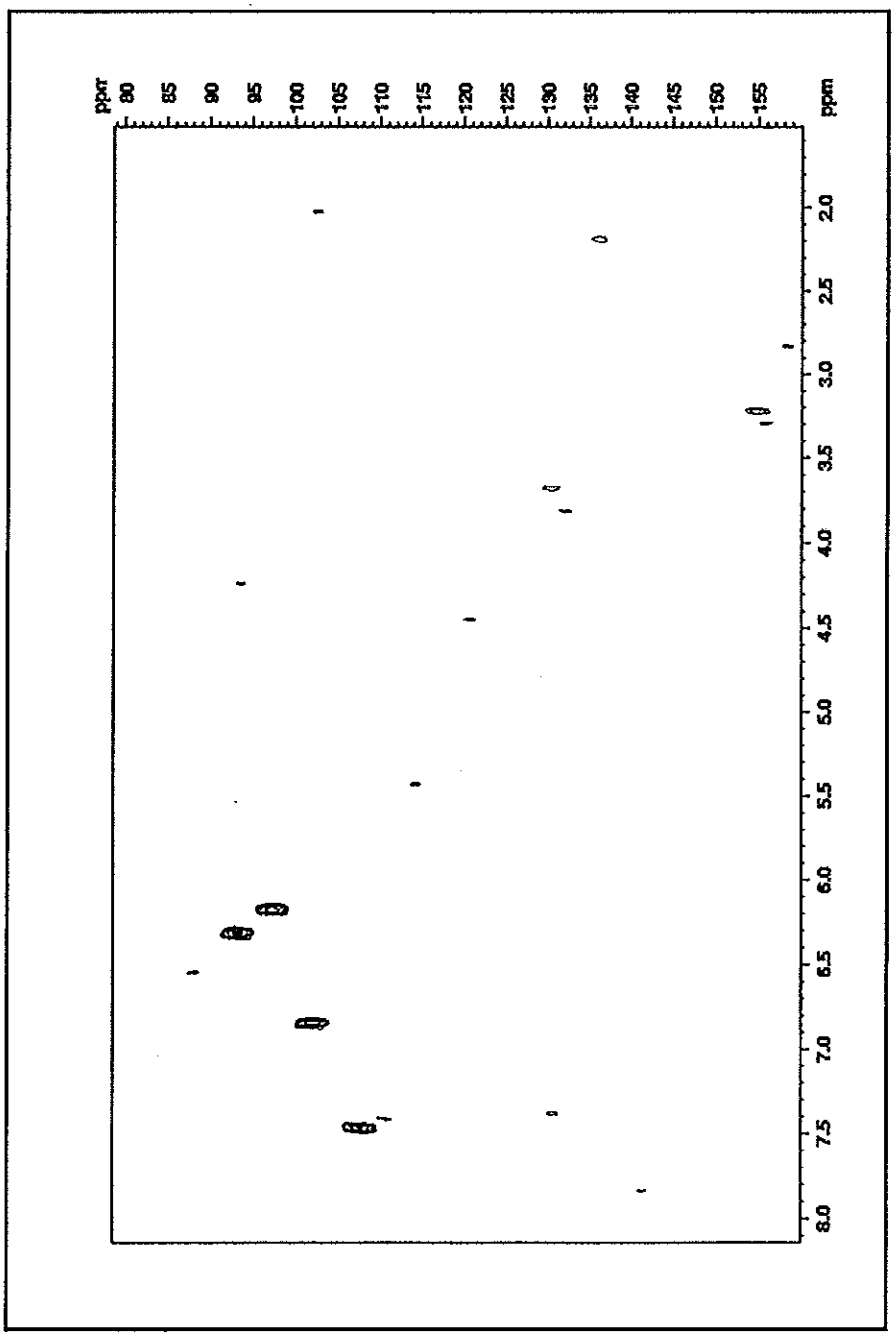

Figure 114 2D HMQC spectrum of compound GP20

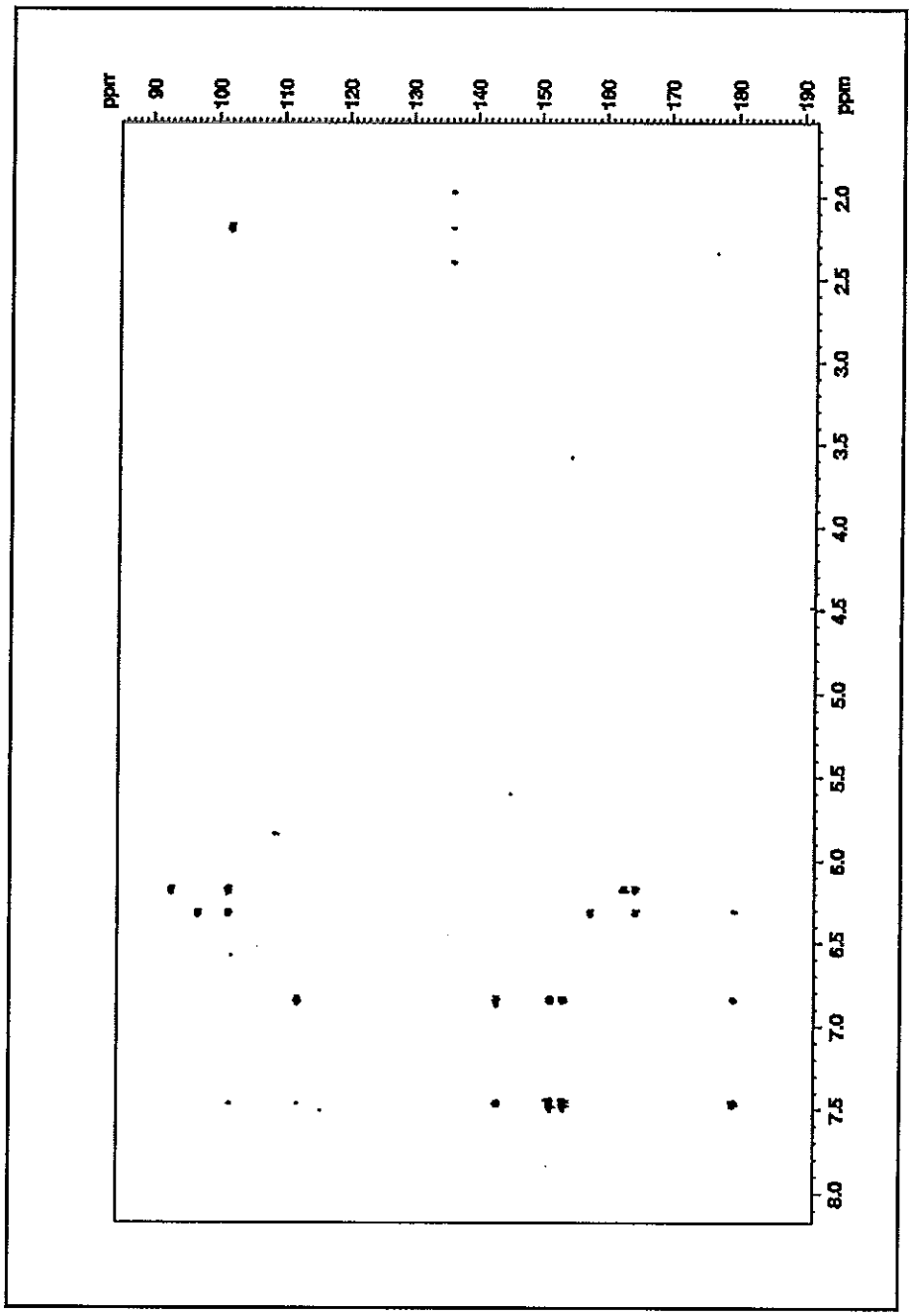

Figure 115 2D HMBC spectrum of compound GP20

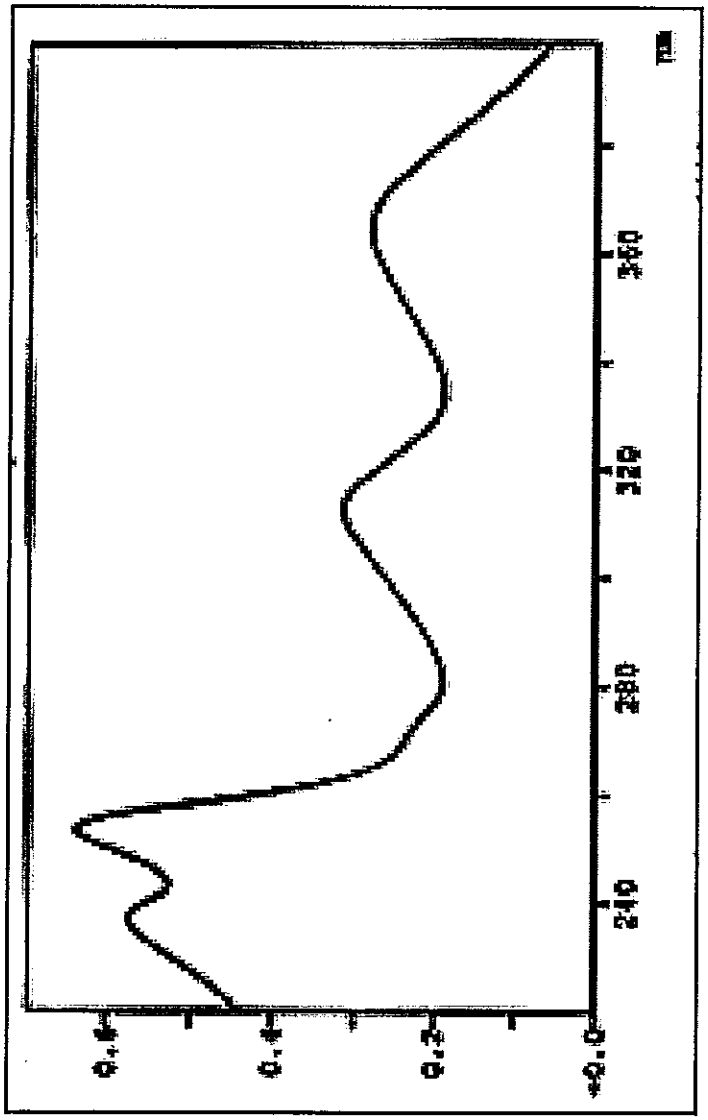

Figure 116 UV (MeOH) spectrum of compound GP19

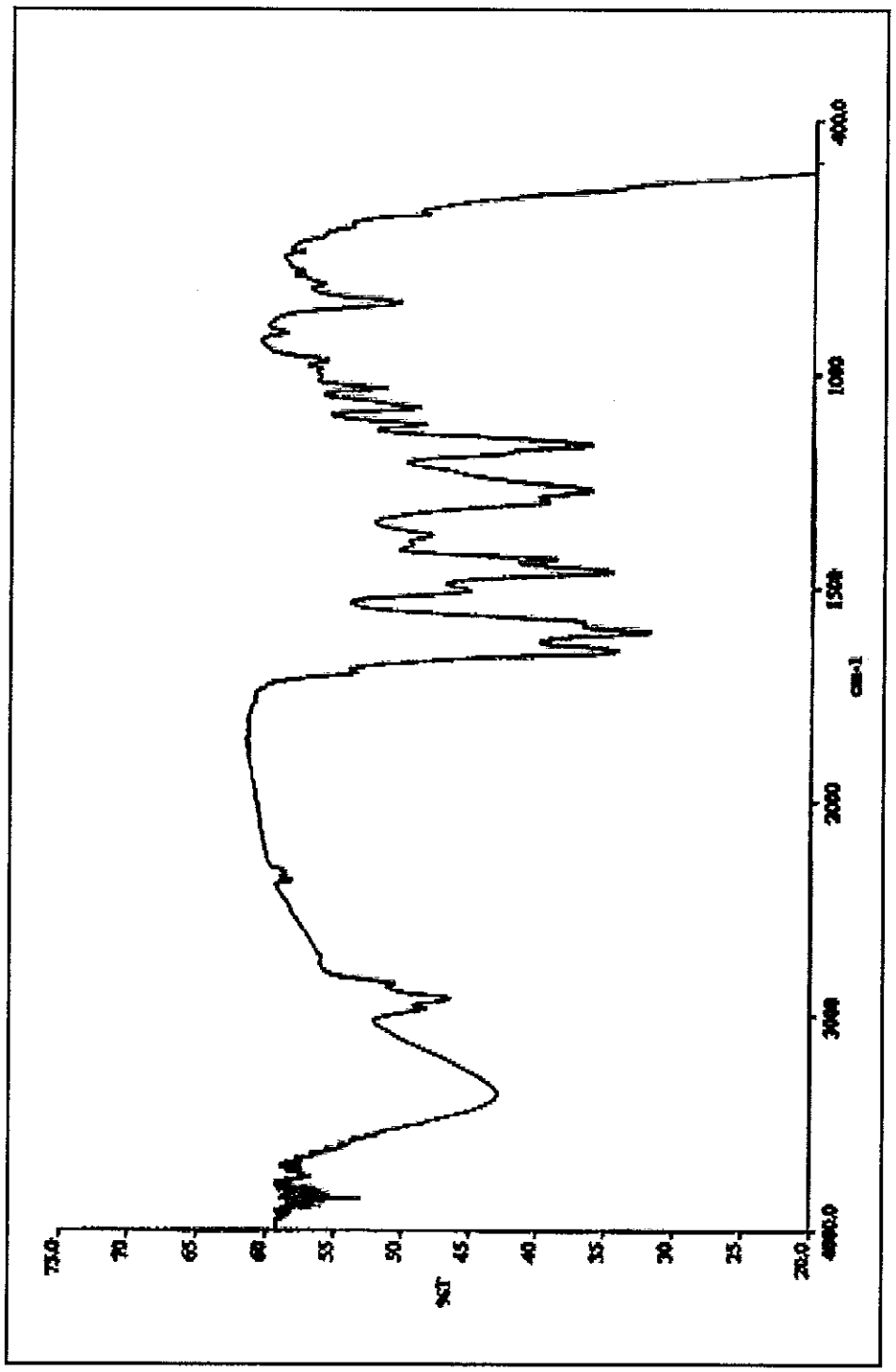

Figure 117 FT-IR (neat) spectrum of compound GP19

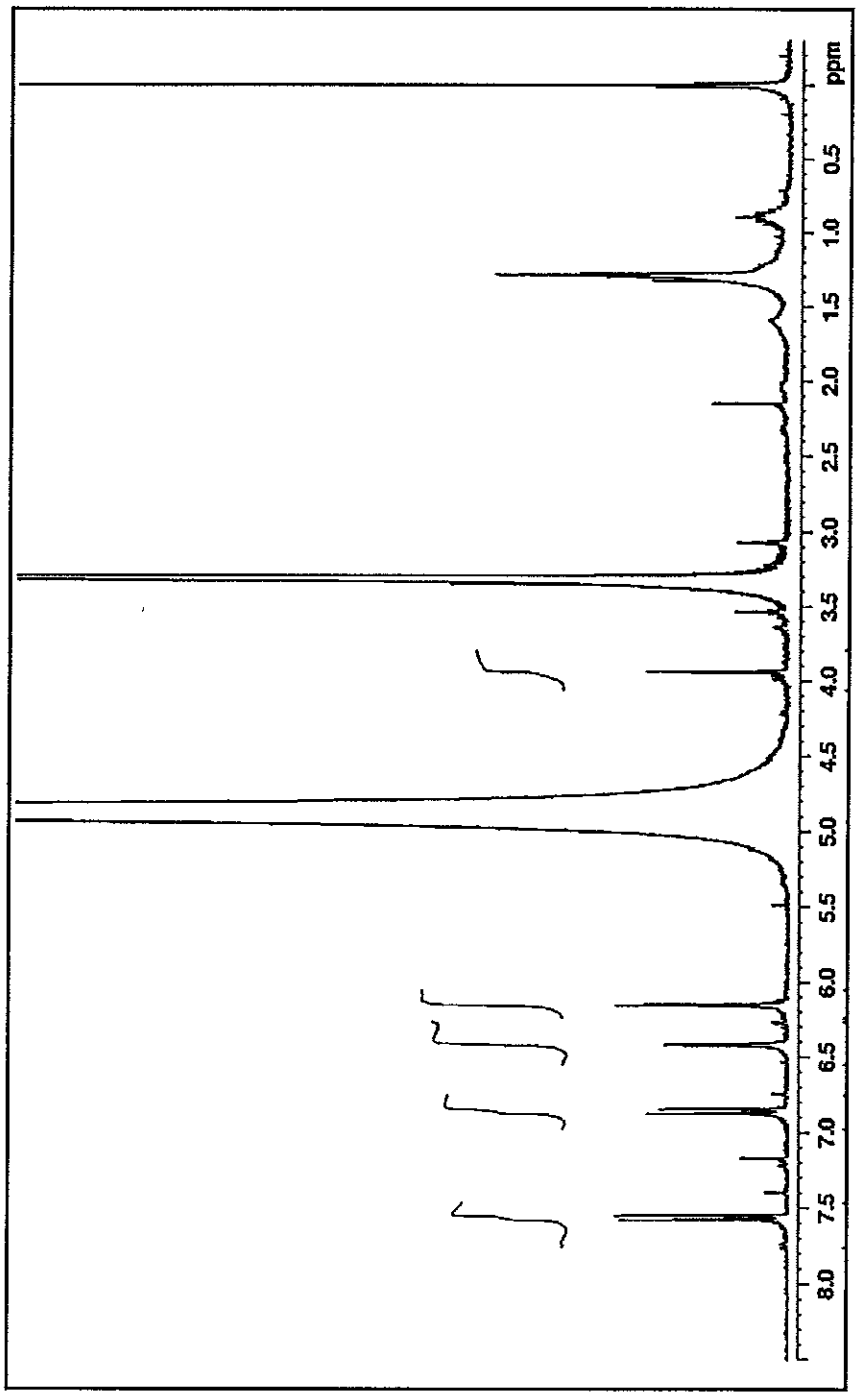

Figure 118 ^{1}H NMR (300 MHz) (CD_3OD) spectrum of compound GP19

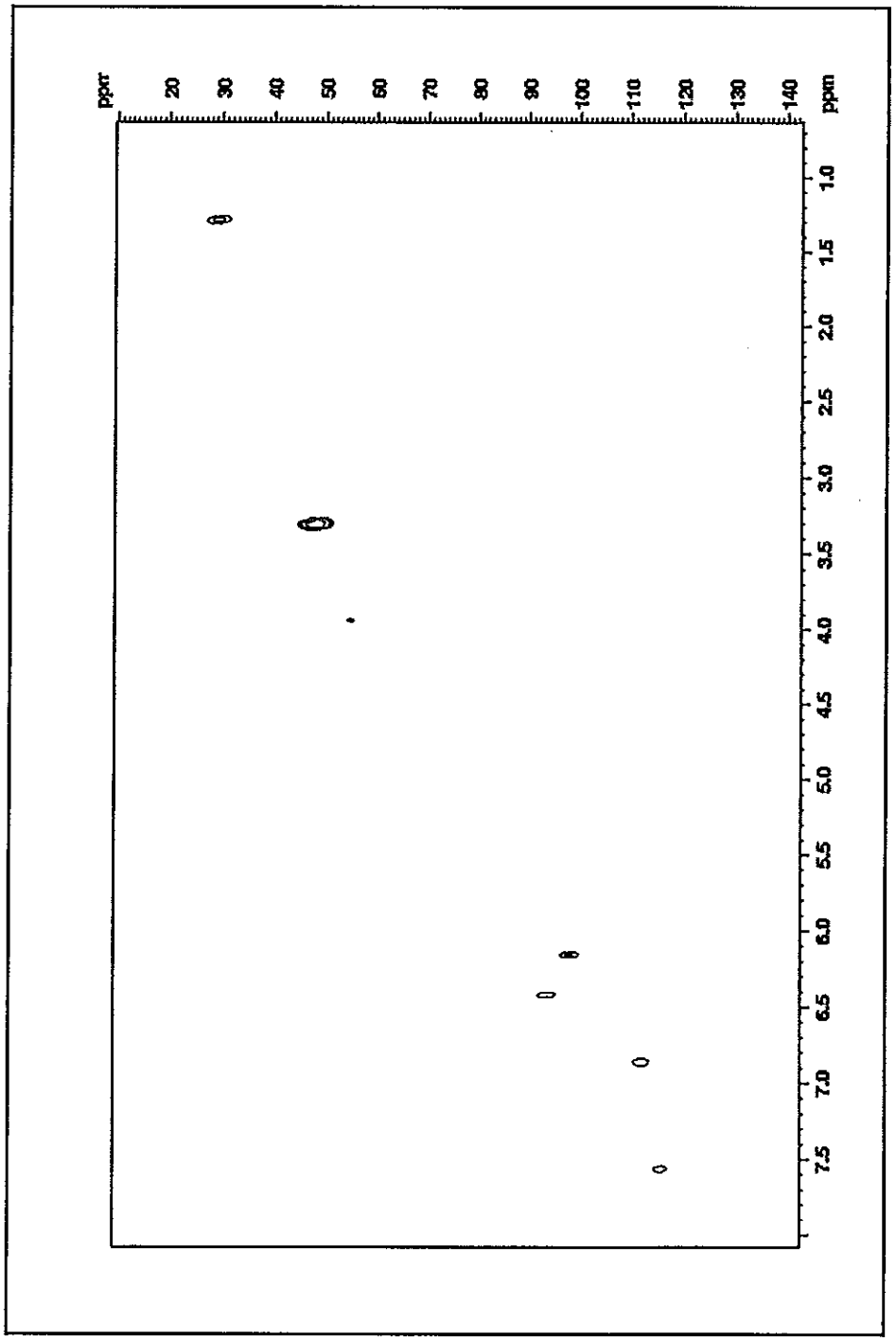

Figure 119 2D HMQC spectrum of compound GP19

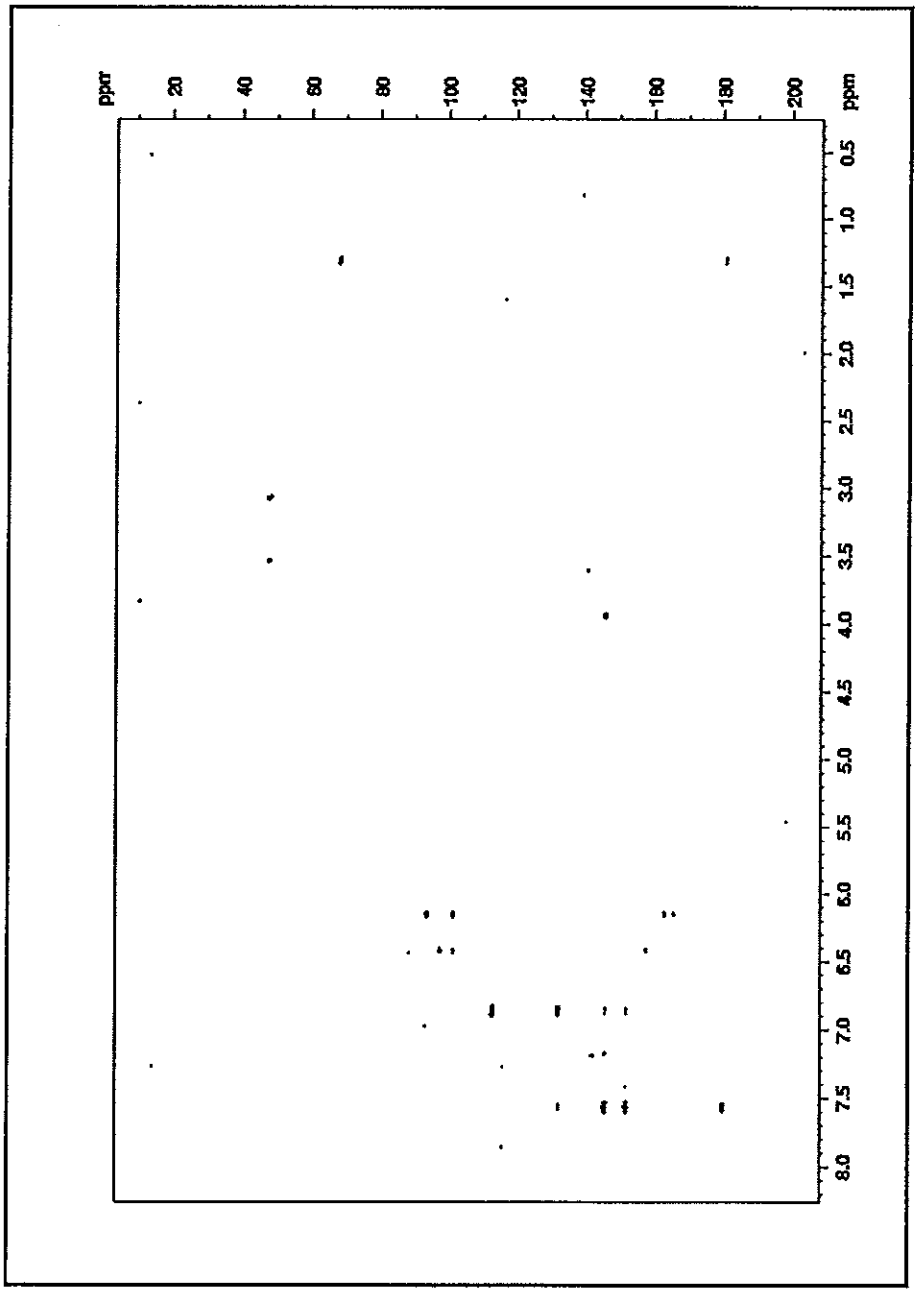

Figure 120 2D HMBC spectrum of compound GP19

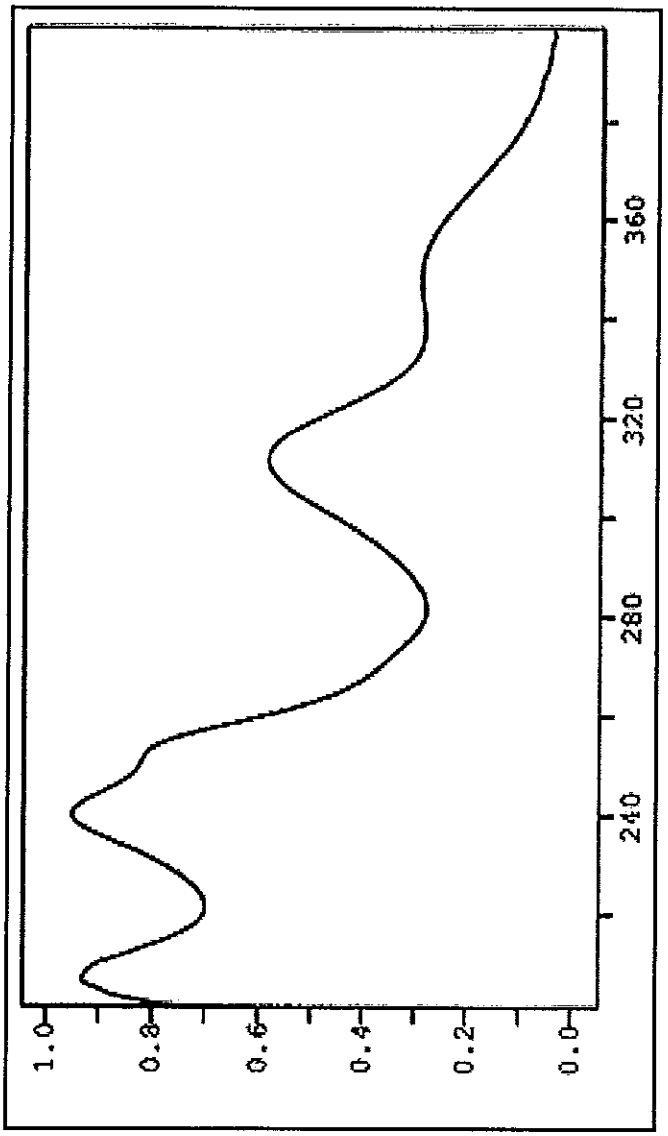

Figure 121 UV (MeOH) spectrum of compound GP17

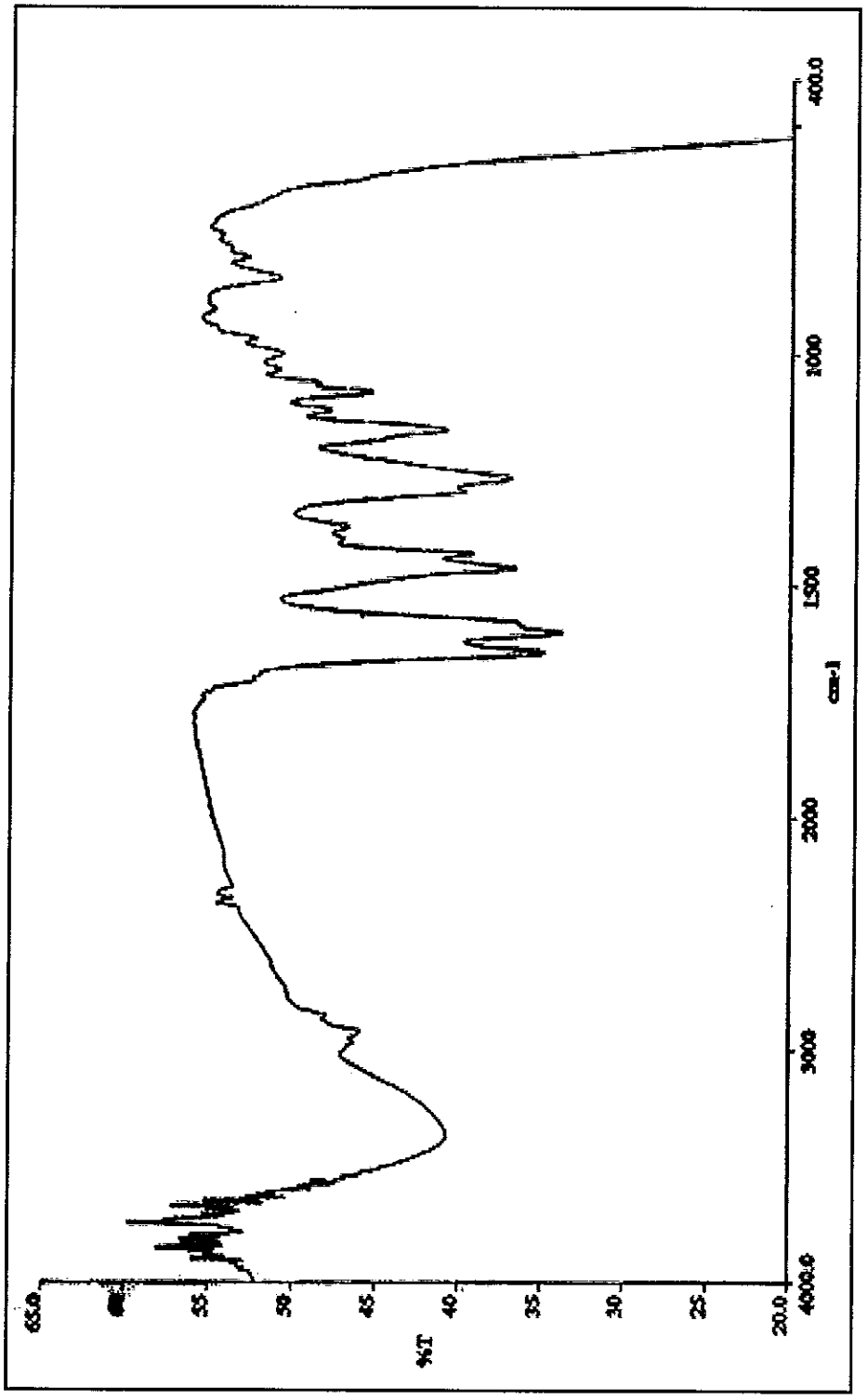

Figure 122 FT-IR (neat) spectrum of compound GP17

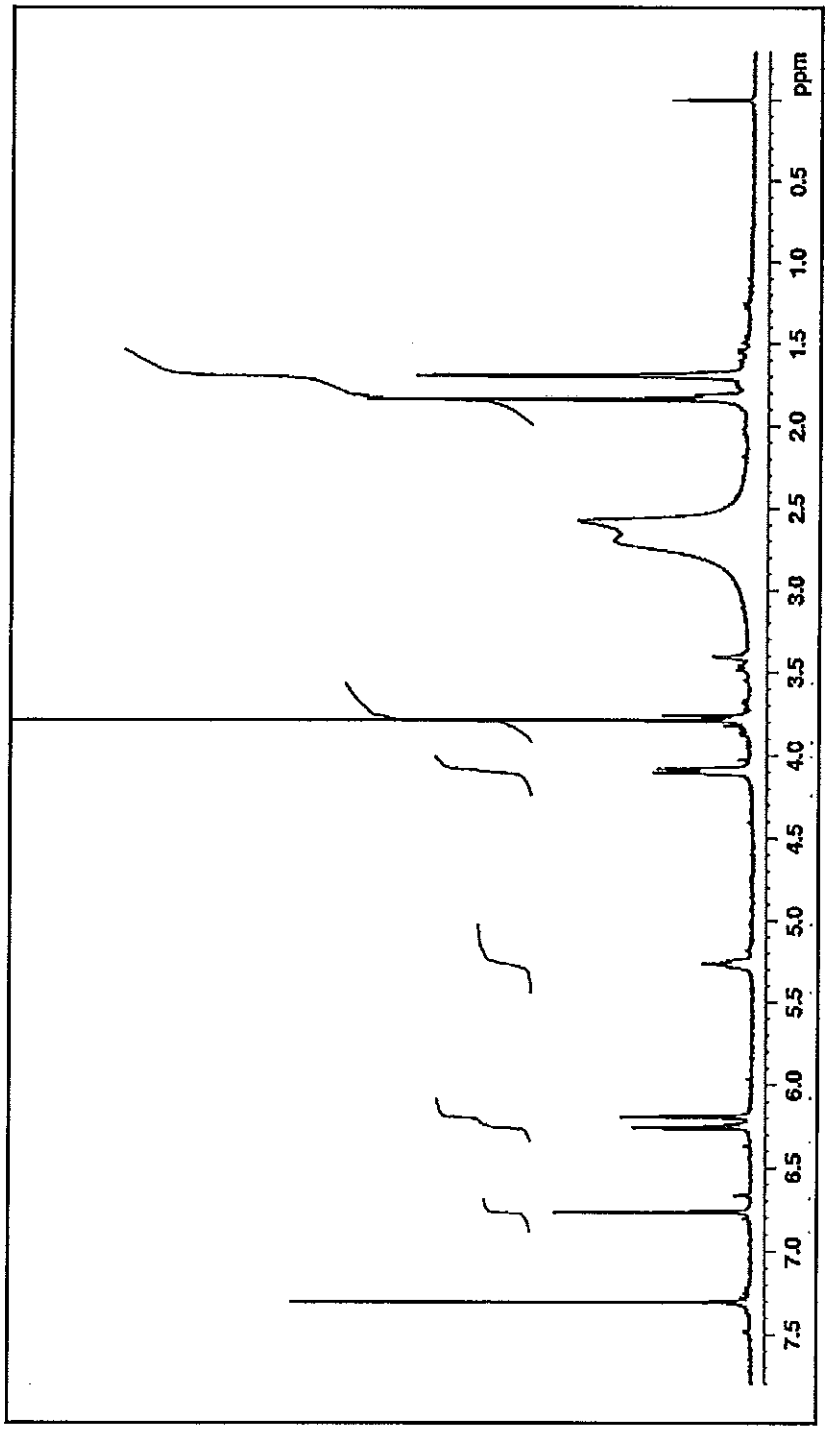

Figure 123 ^{1}H NMR (300 MHz) (CD_3Cl+CD_3OD) spectrum of compound GP17

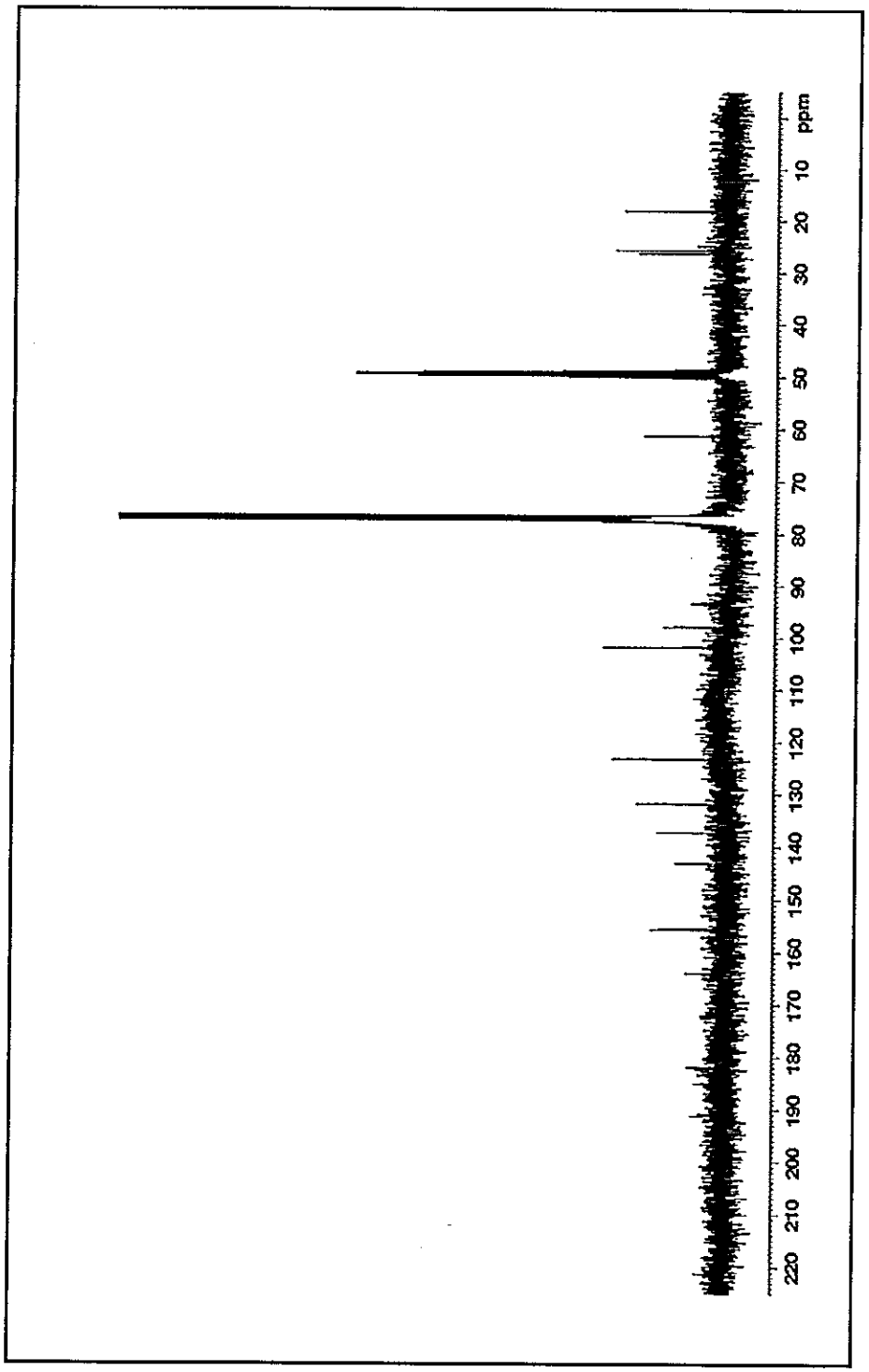

Figure 124 ^{13}C NMR (75 MHz) (CD_3Cl+CD_3OD) spectrum of compound GP17

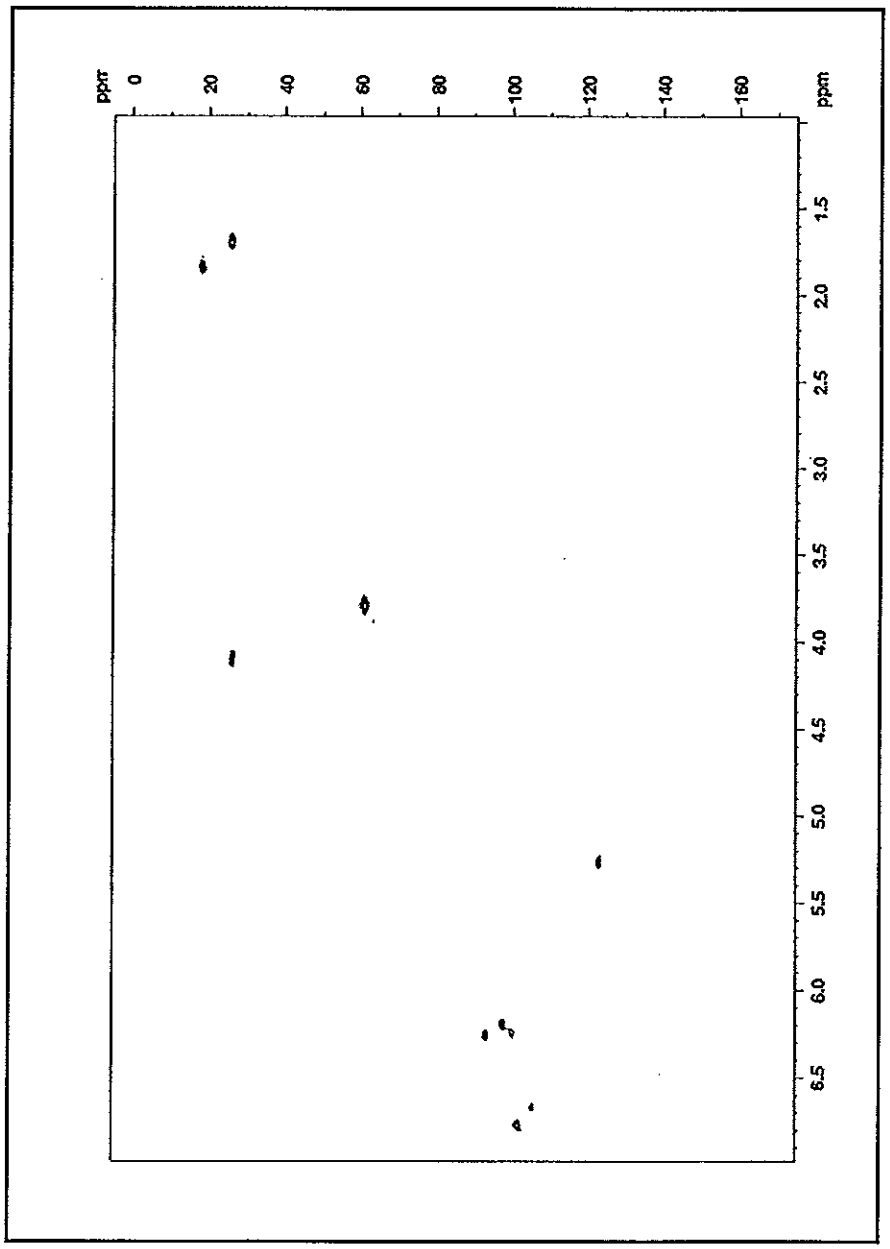

Figure 125 2D HMQC spectrum of compound GP17

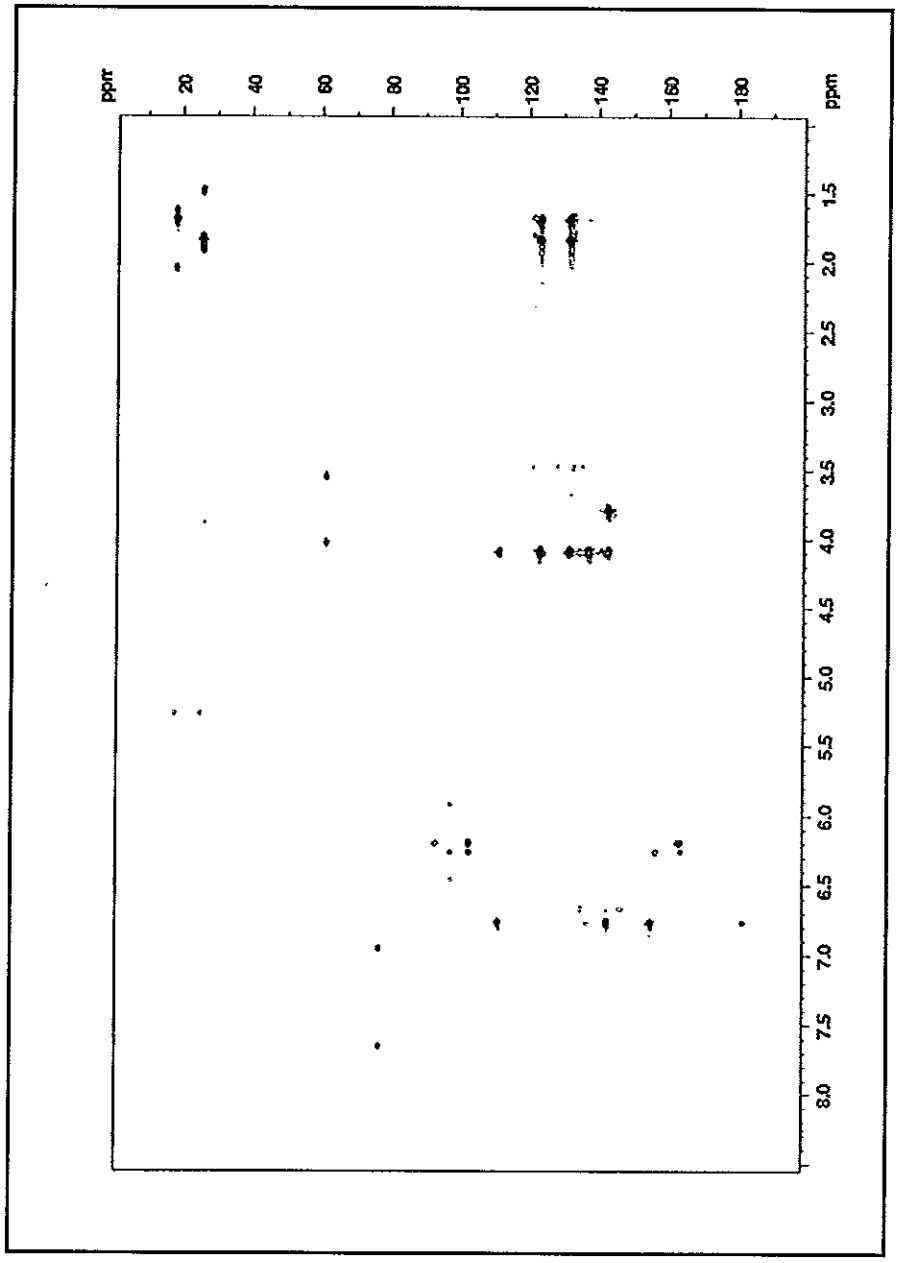

Figure 126 2D HMBC spectrum of compound GP17

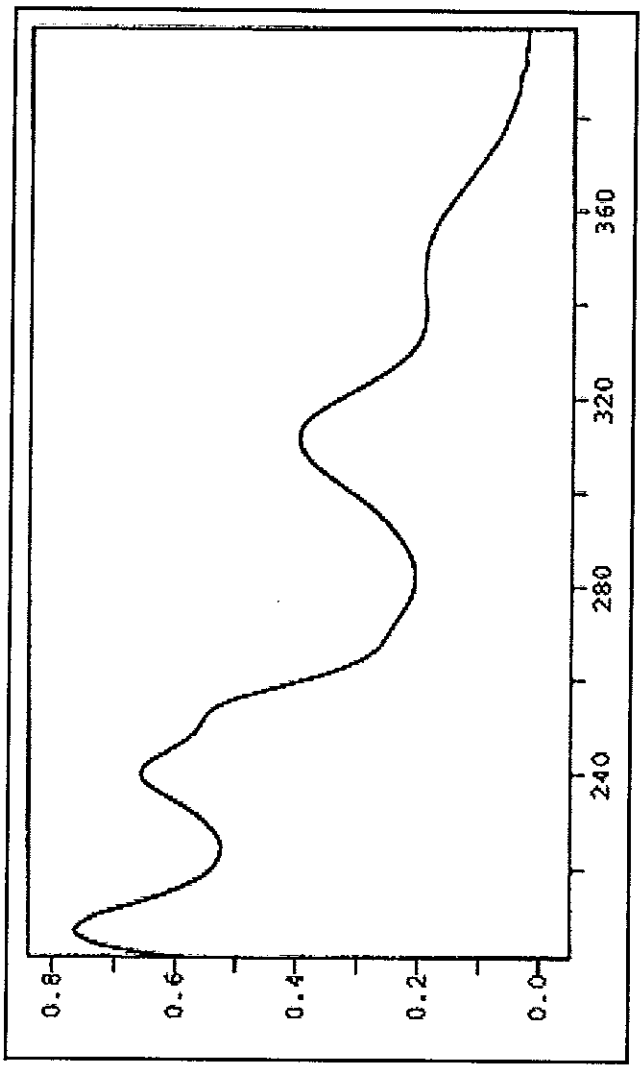

Figure 127 UV (MeOH) spectrum of compound GP16

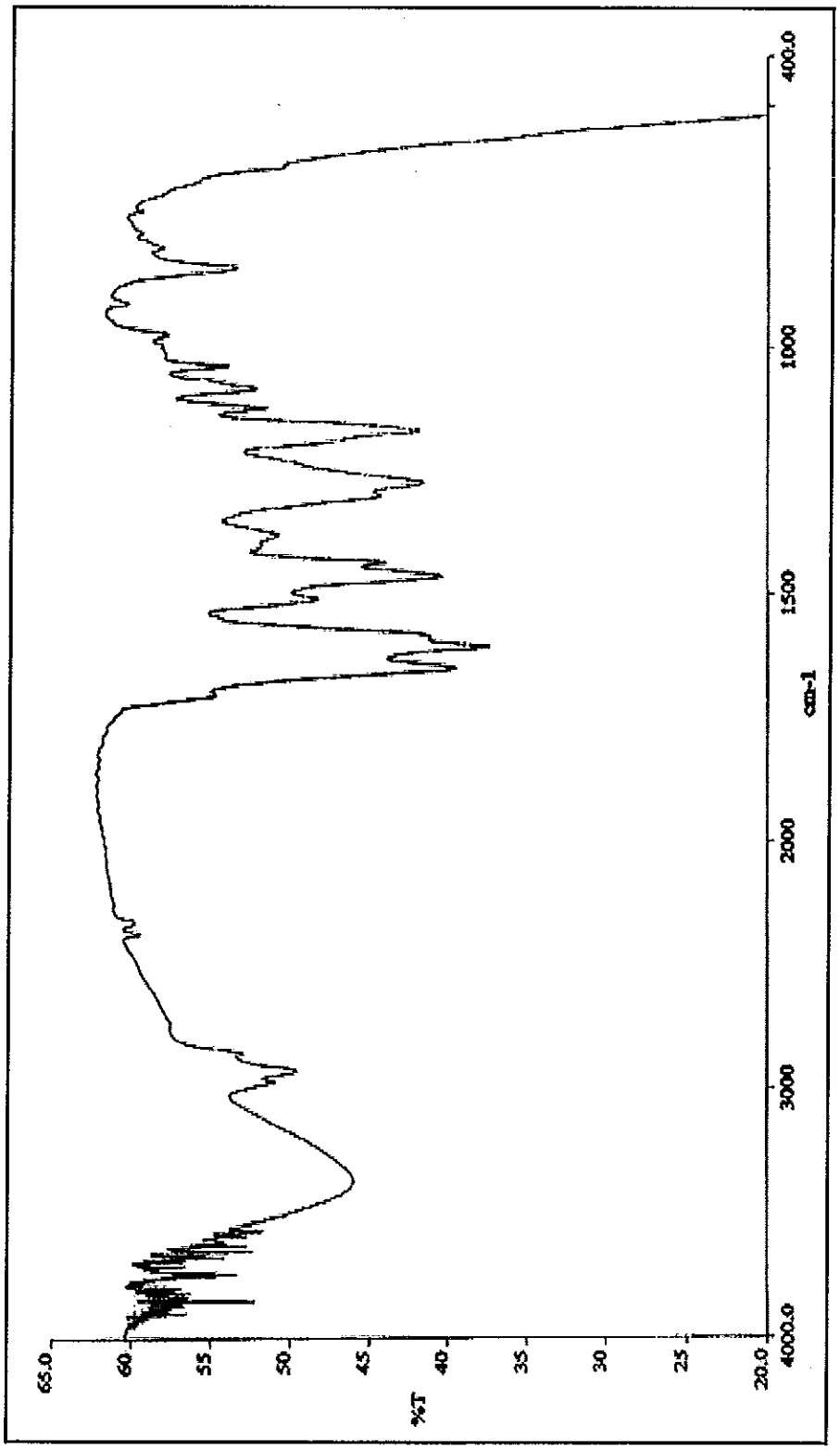

Figure 128 FT-IR (neat) spectrum of compound GP16

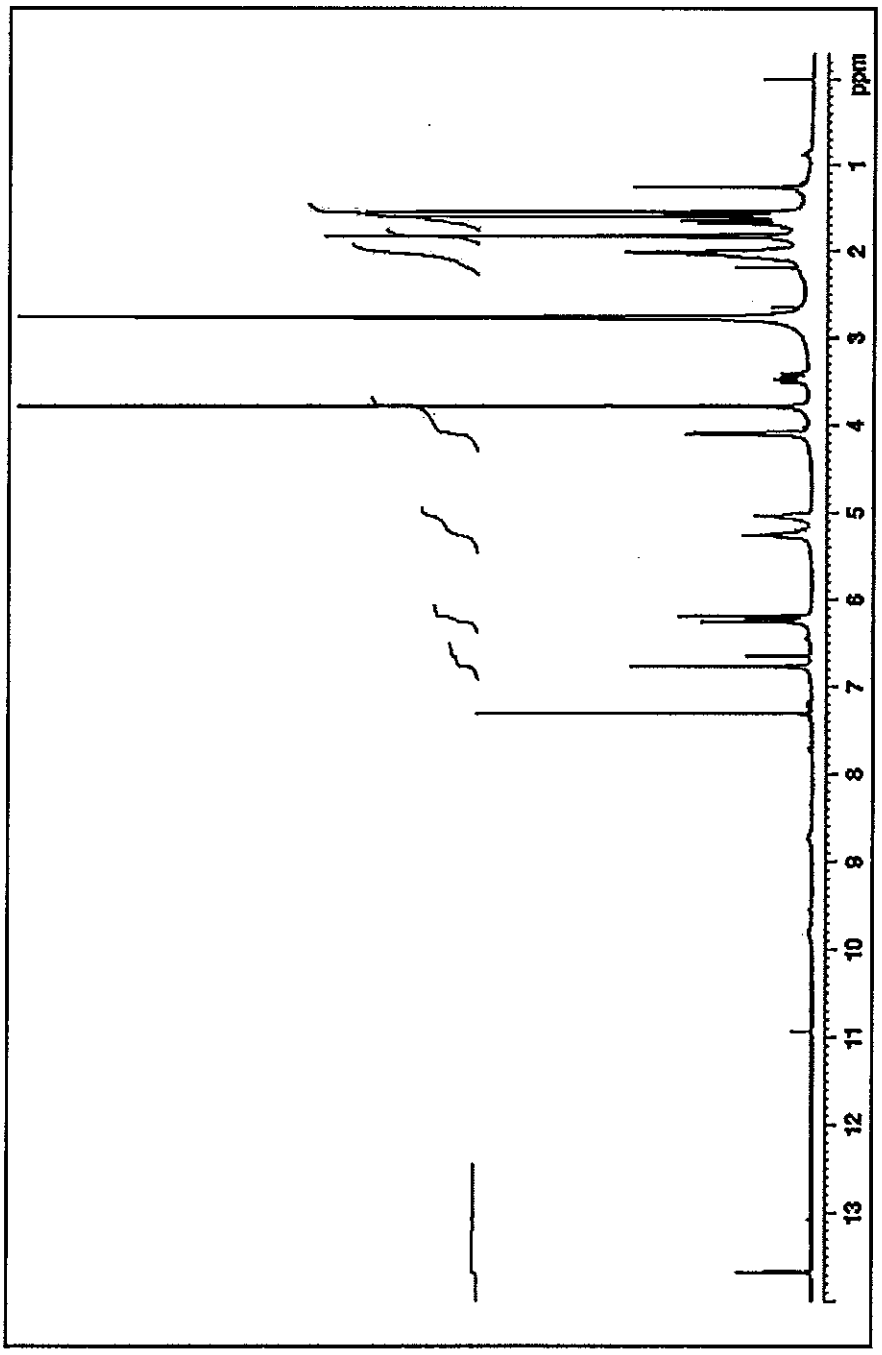

Figure 129 ^{1}H NMR (300 MHz) (CD_3Cl+CD_3OD) spectrum of compound GP16

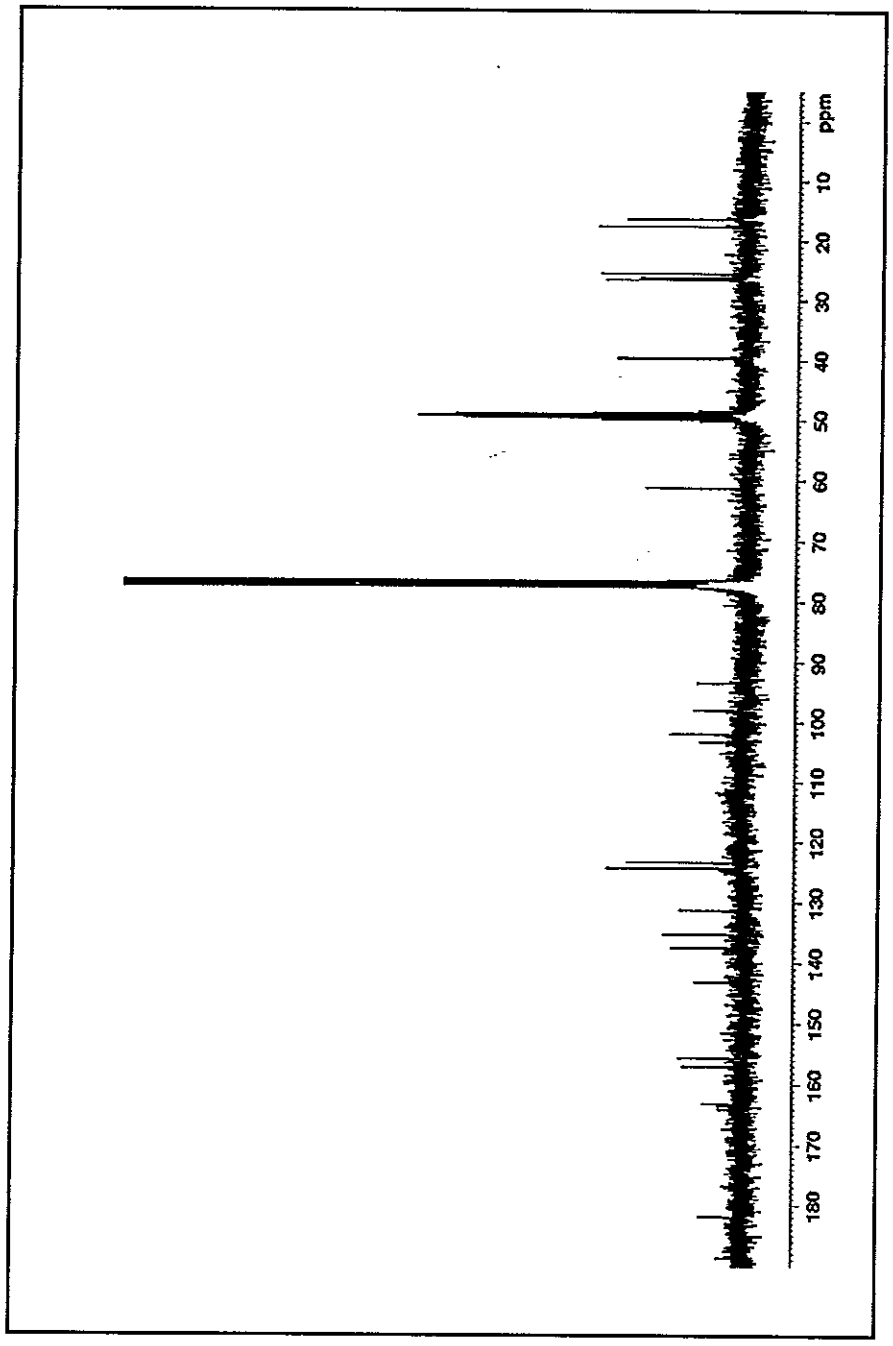

Figure 130 ^{13}C NMR (75 MHz) (CD_3Cl+CD_3OD) spectrum of compound GP16

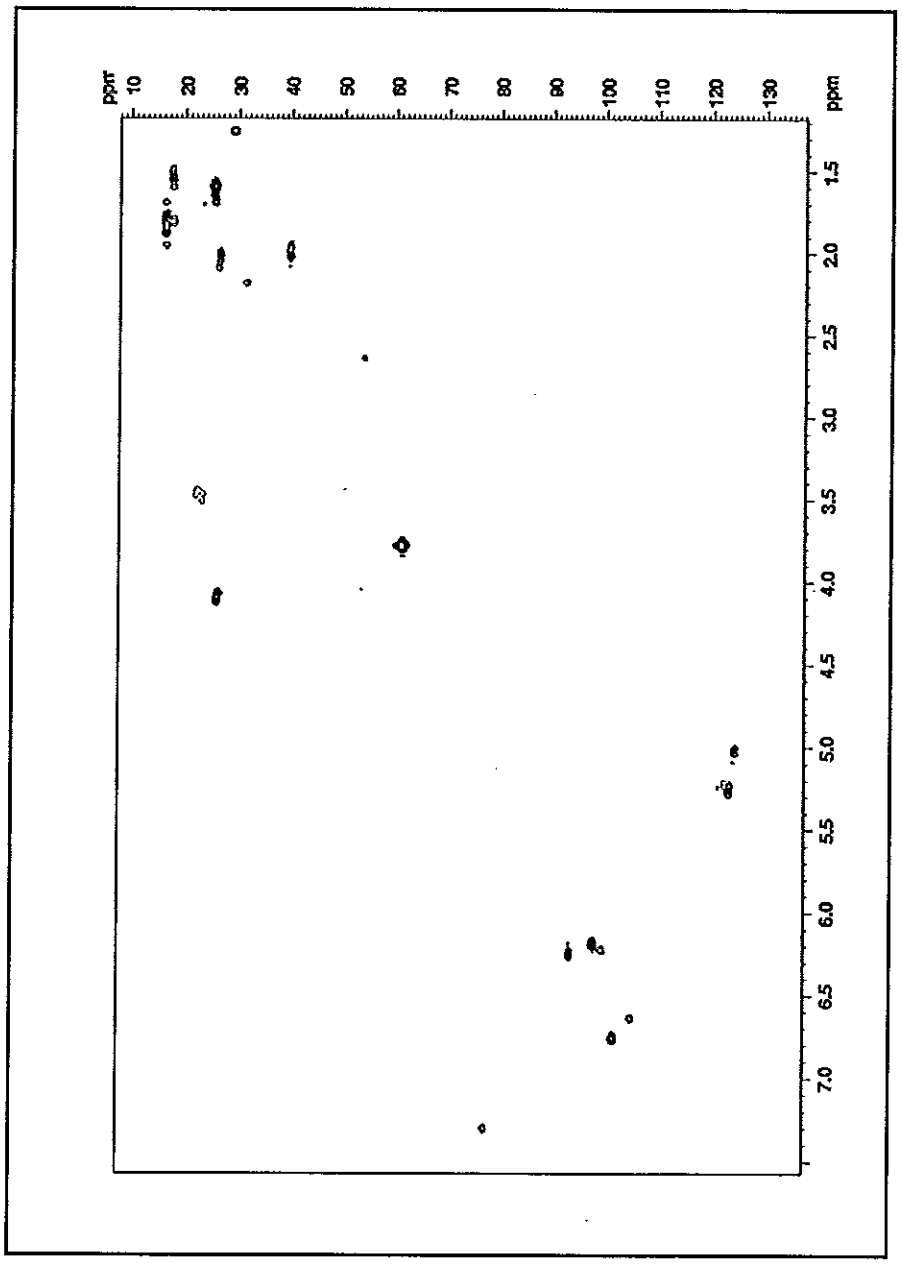

Figure 131 2D HMQC spectrum of compound GP16

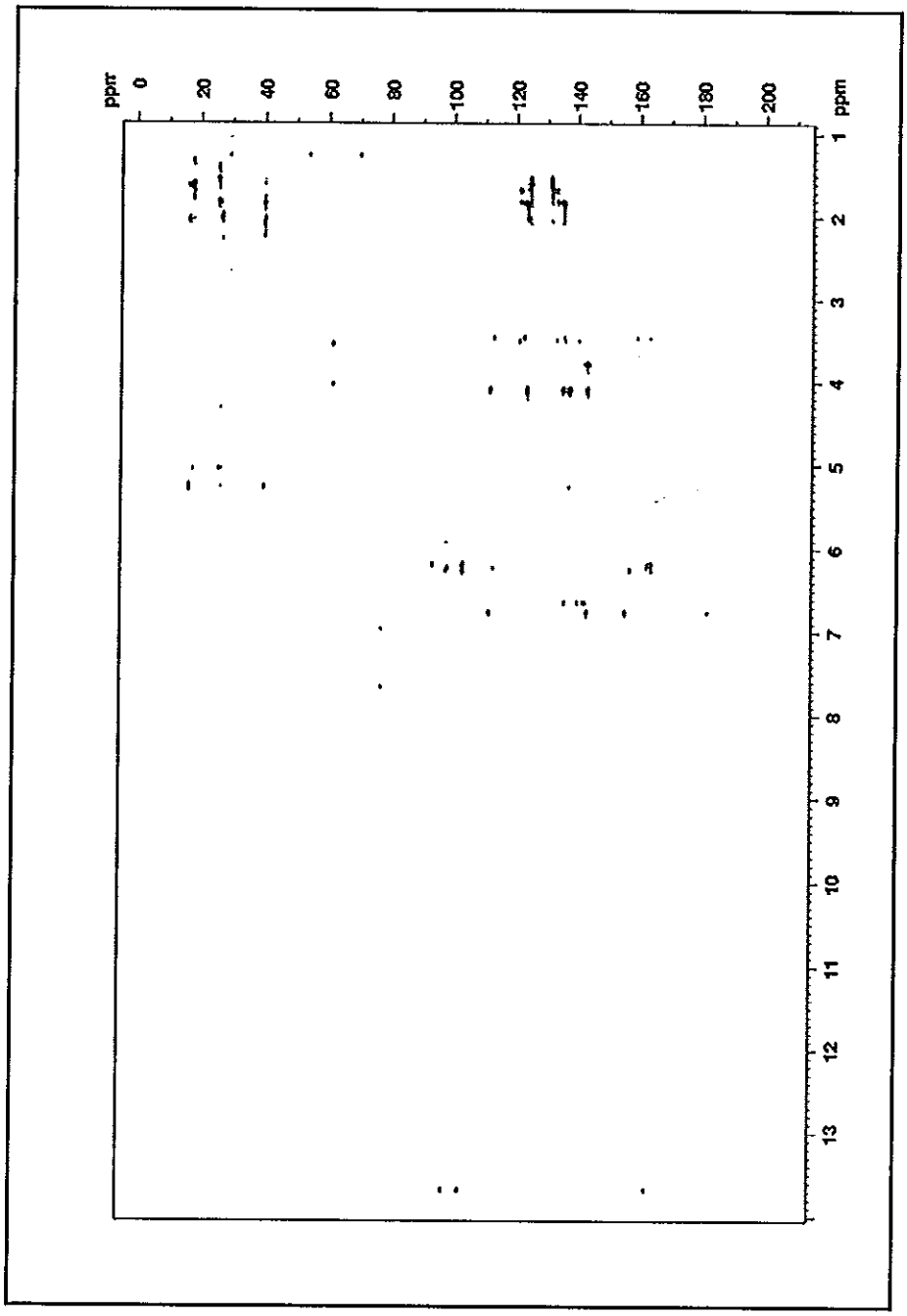

Figure 132 2D HMBC spectrum of compound GP16

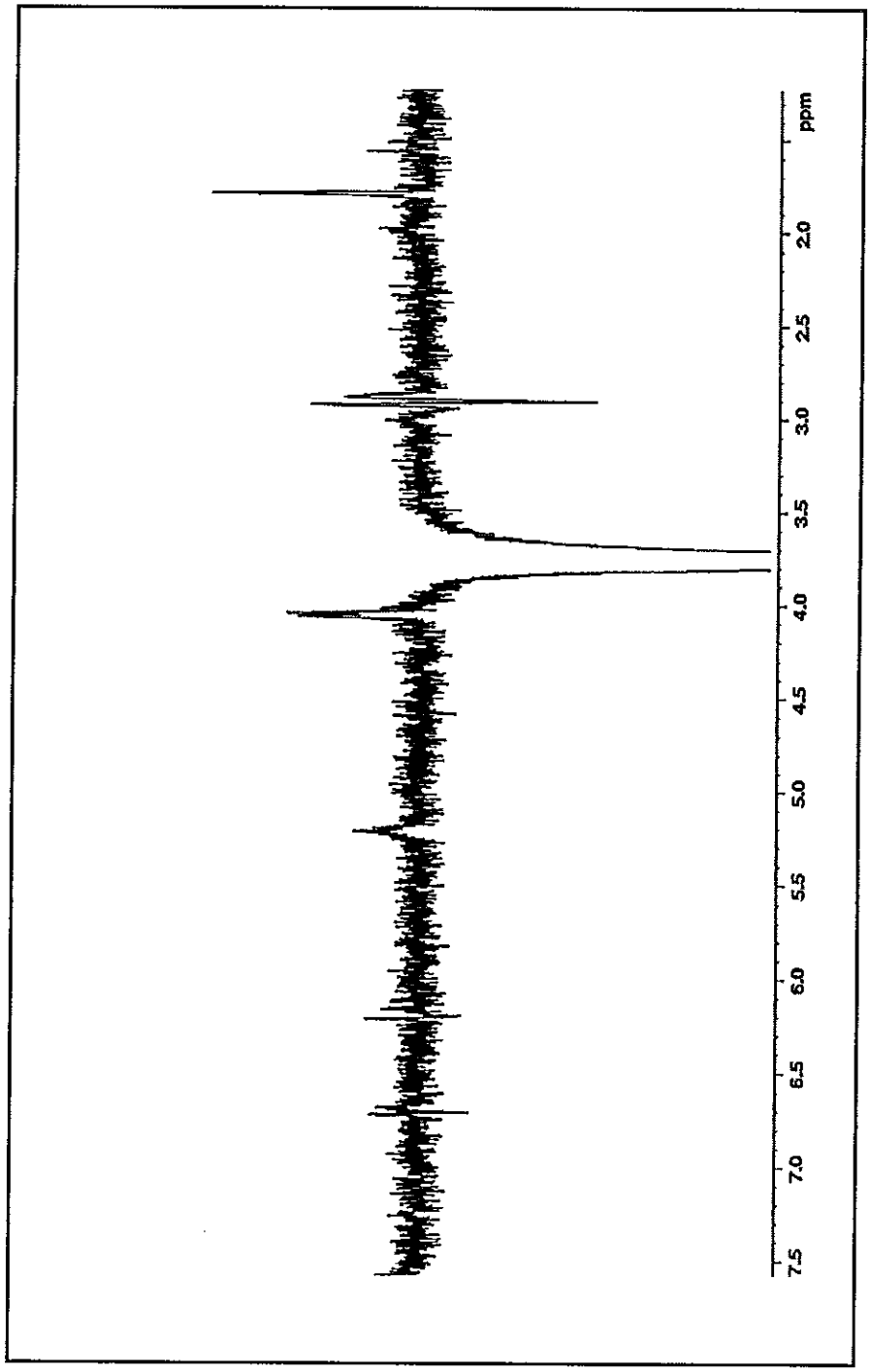

Figure 133 NOE difference spectrum of compound GP16 after irradiation at δ_H 3.78 (7-OCH_3)

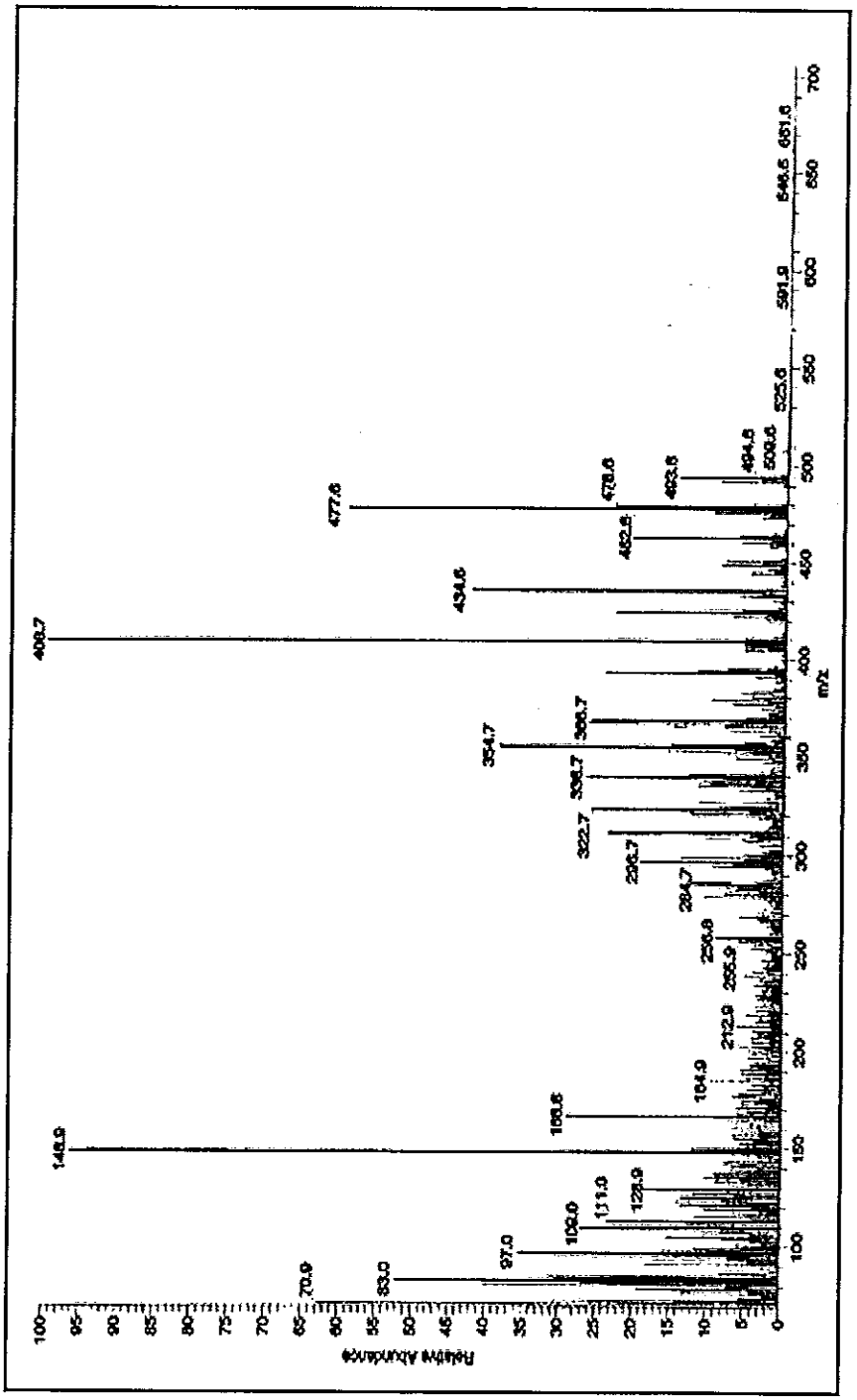

Figure 134 Mass spectrum of compound GP11

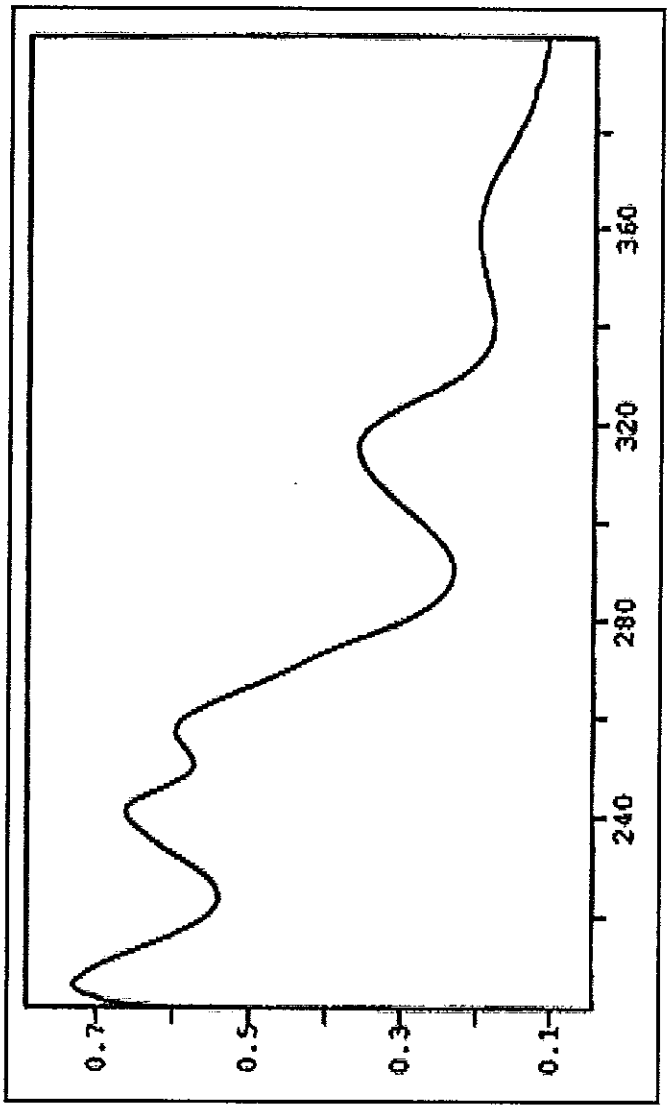

Figure 135 UV (MeOH) spectrum of compound GP11

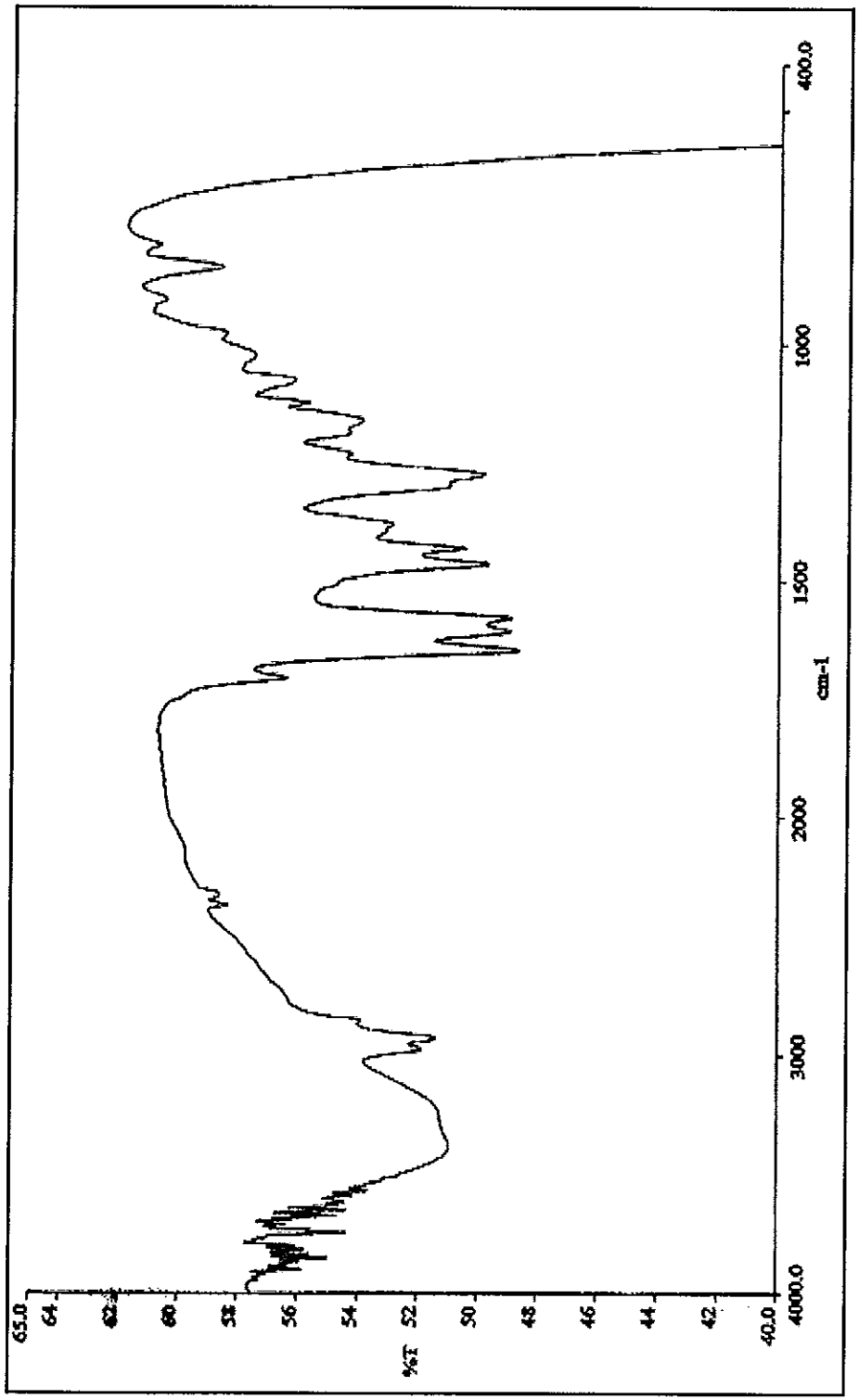

Figure 136 FT-IR (neat) spectrum of compound GP11

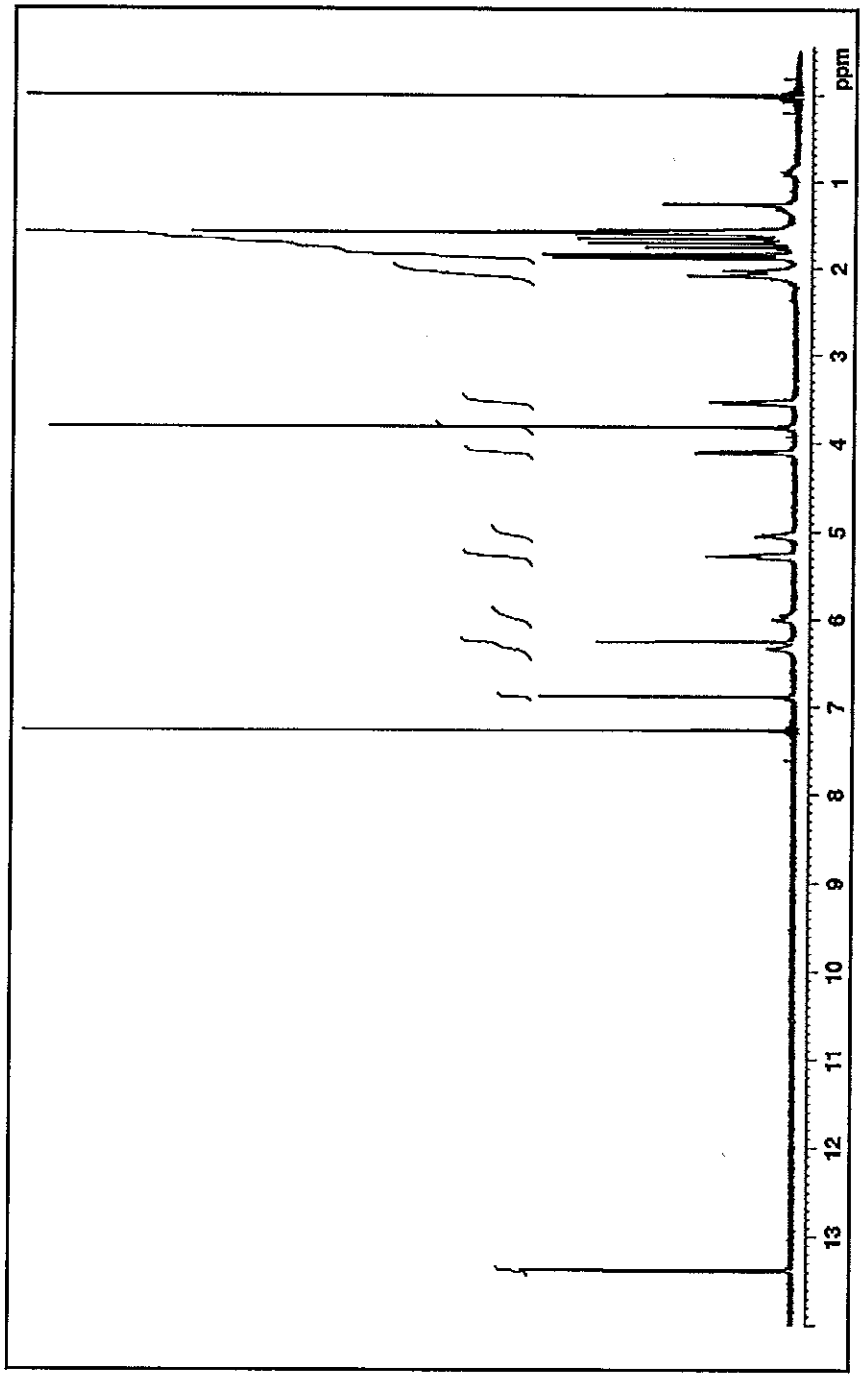

Figure 137 ^{1}H NMR (300 MHz) ($CDCl_3$) spectrum of compound GP11

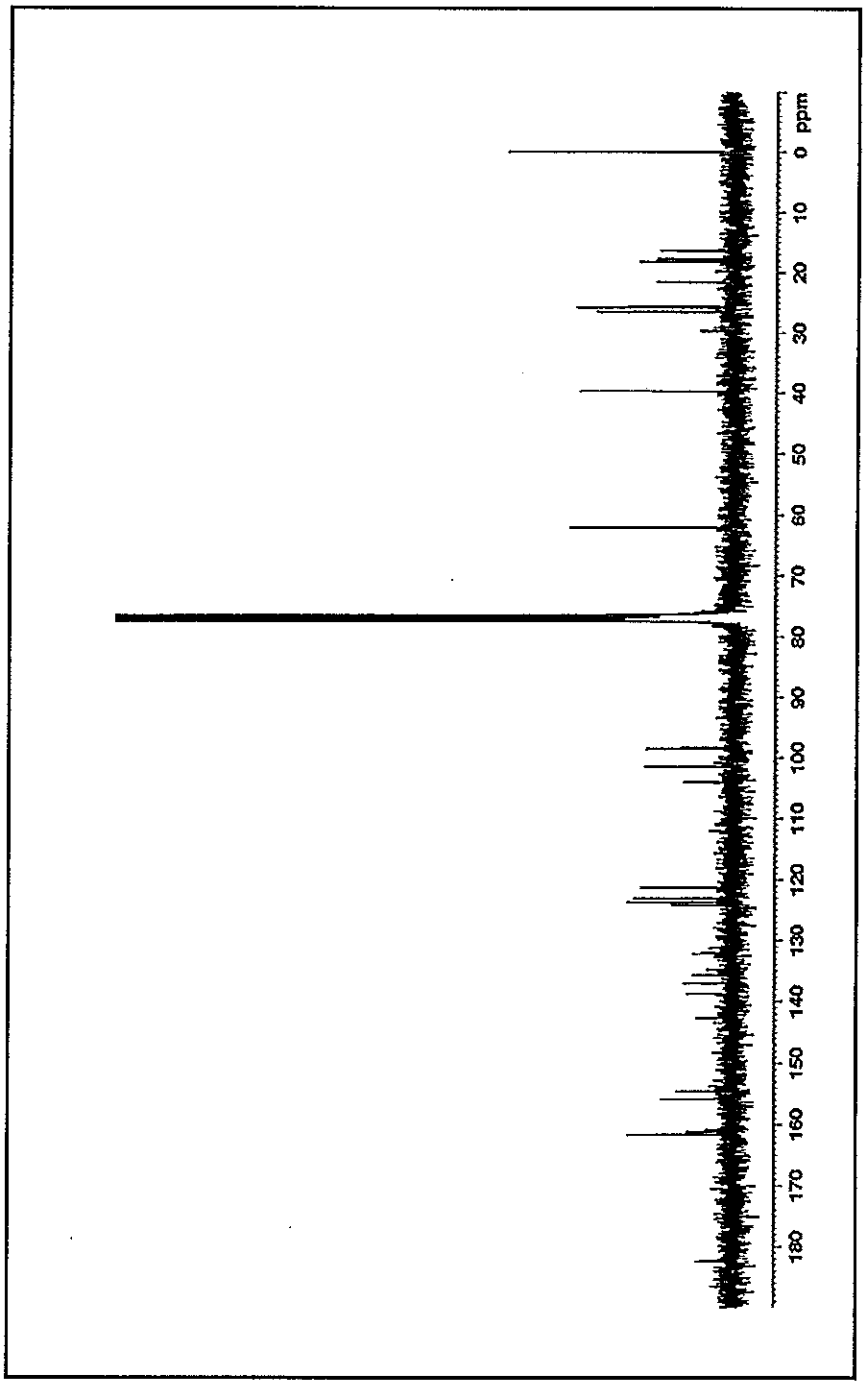

Figure 138 ^{13}C NMR (75 MHz) ($CDCl_3$) spectrum of compound GP11

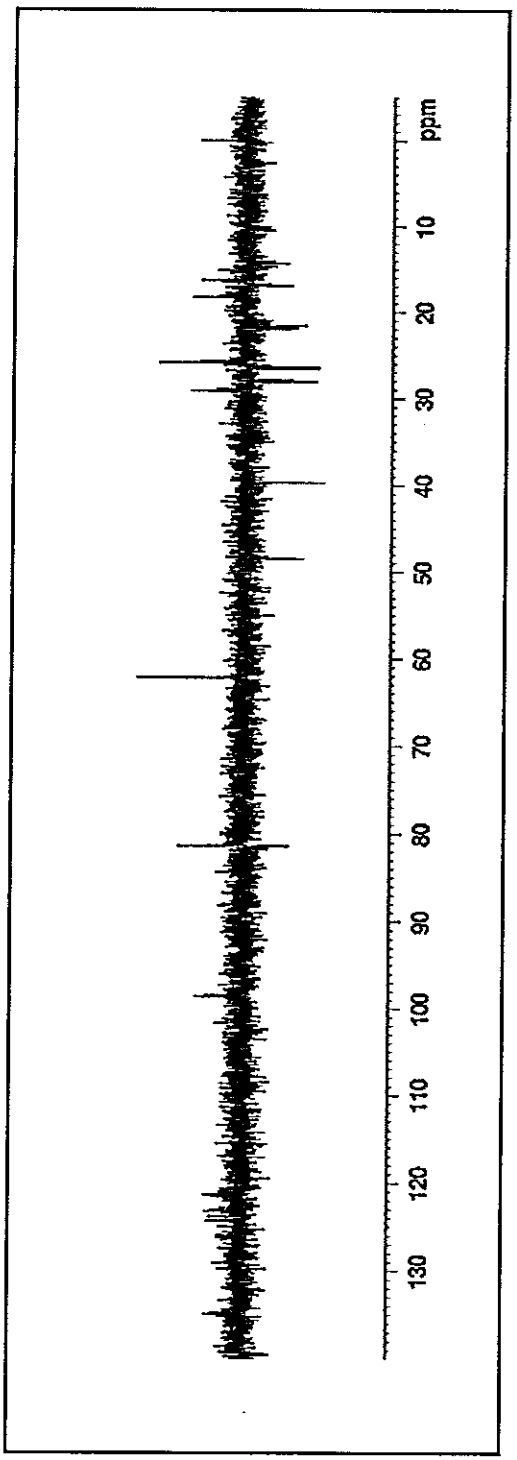

Figure 139 DEPT 135° spectra of compound GP11

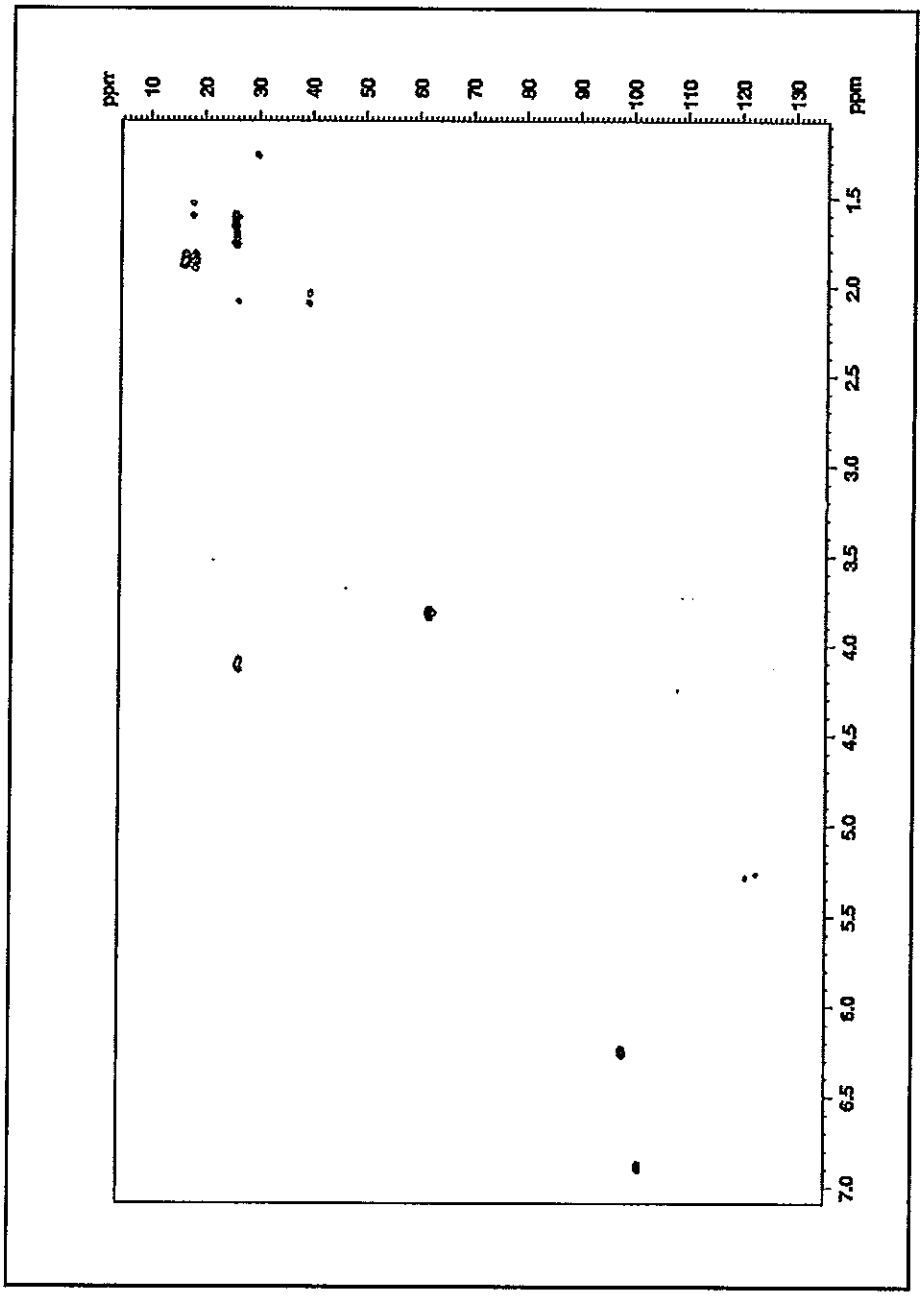

Figure 140 2D HMQC spectrum of compound GP11

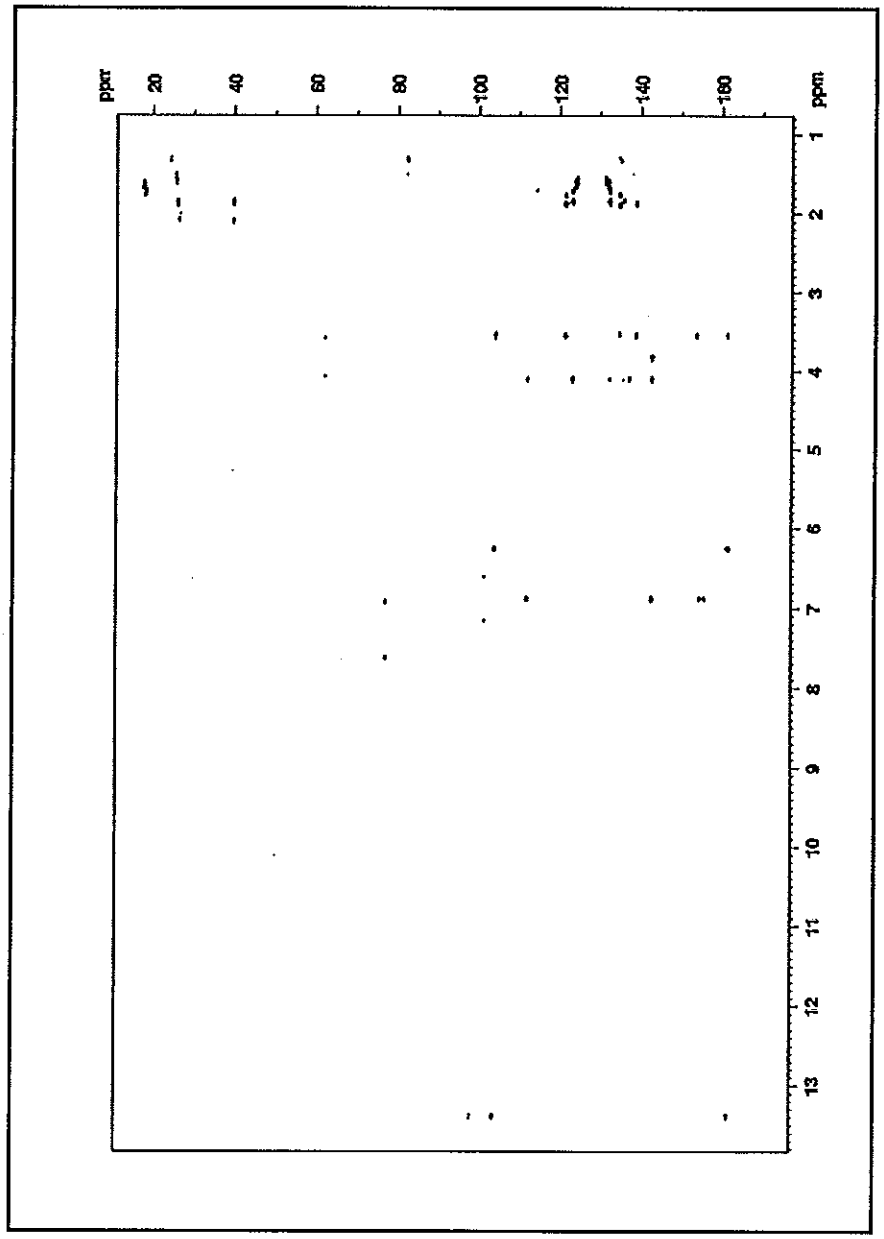

Figure 141 2D HMBC spectrum of compound GP11

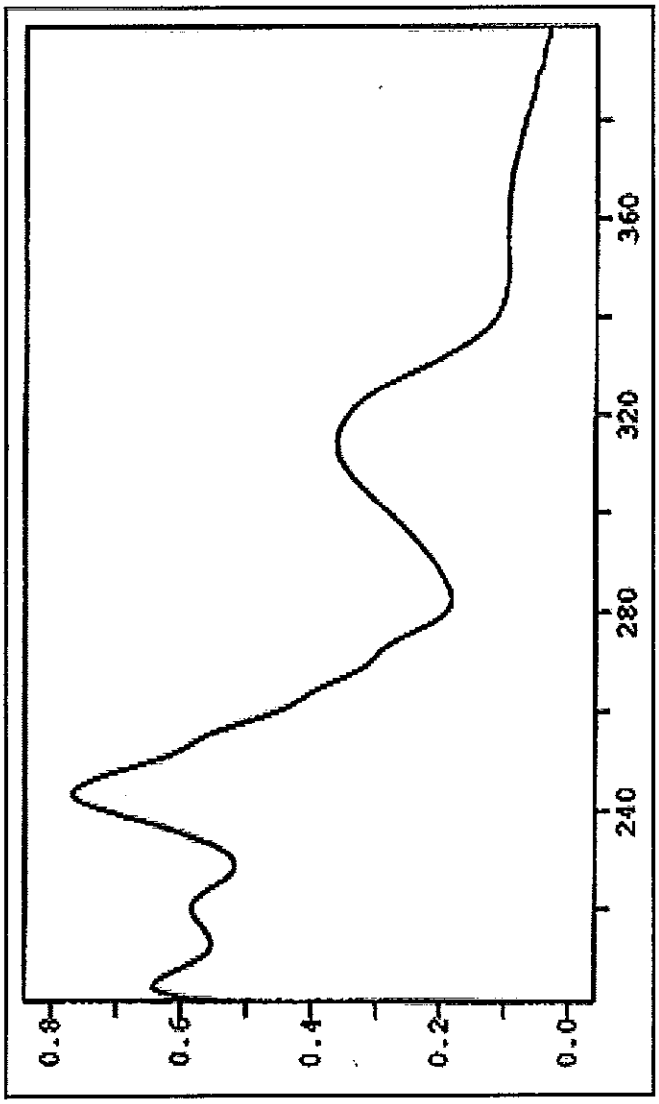

Figure 142 UV (MeOH) spectrum of compound GP15

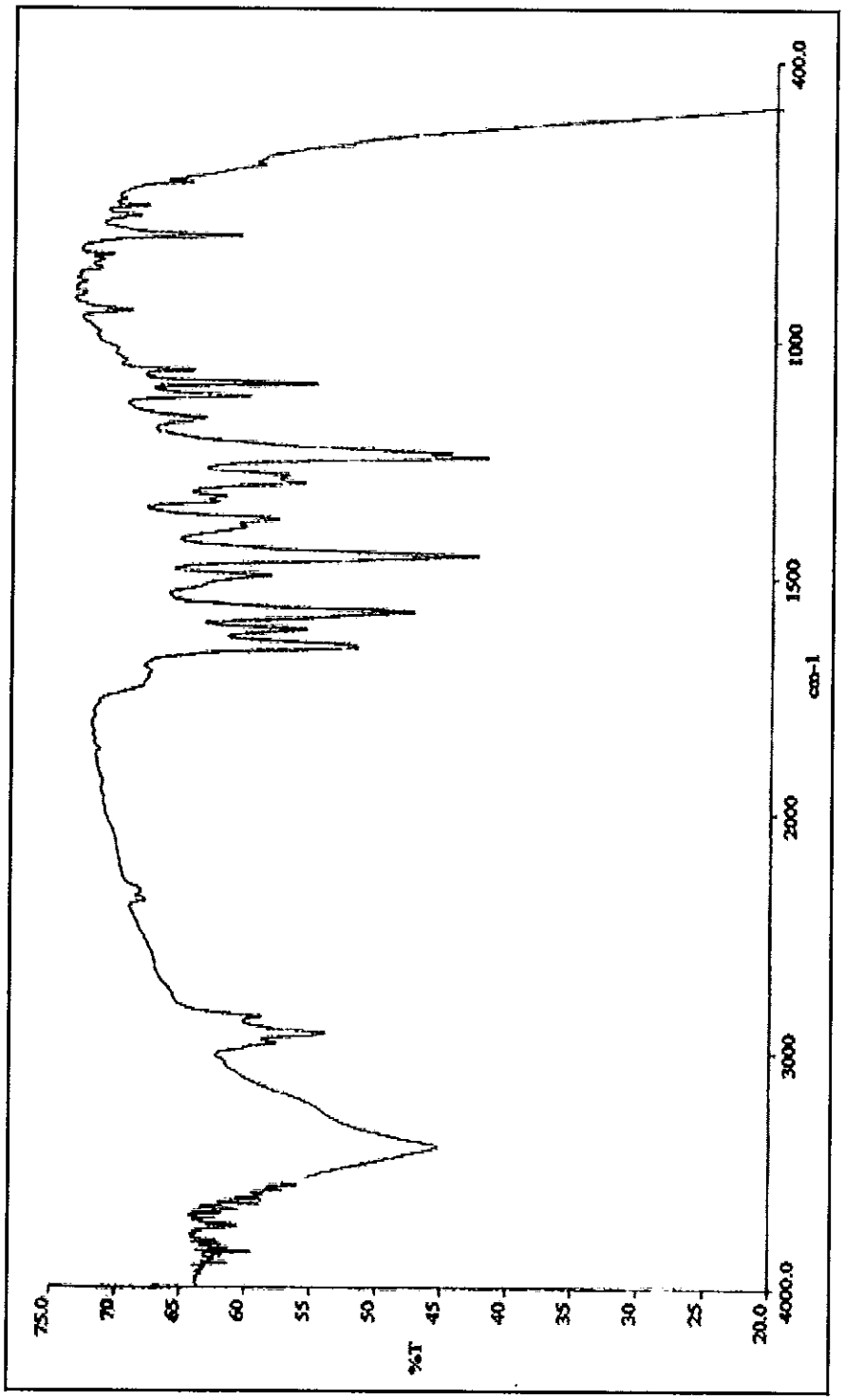

Figure 143 FT-IR (neat) spectrum of compound GP15

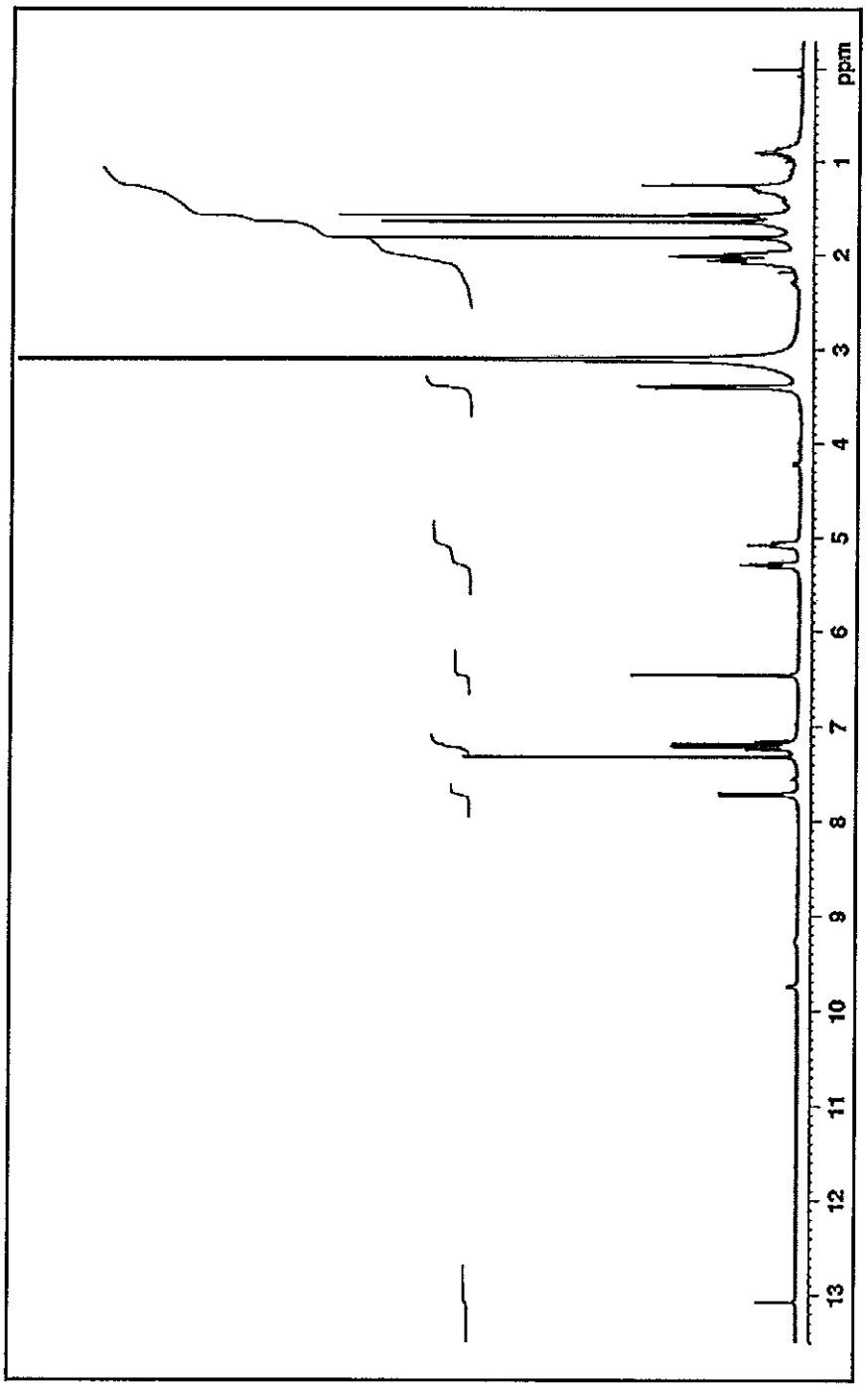

Figure 144 ^{1}H NMR (300 MHz) (CD_3Cl+CD_3OD) spectrum of compound GP15

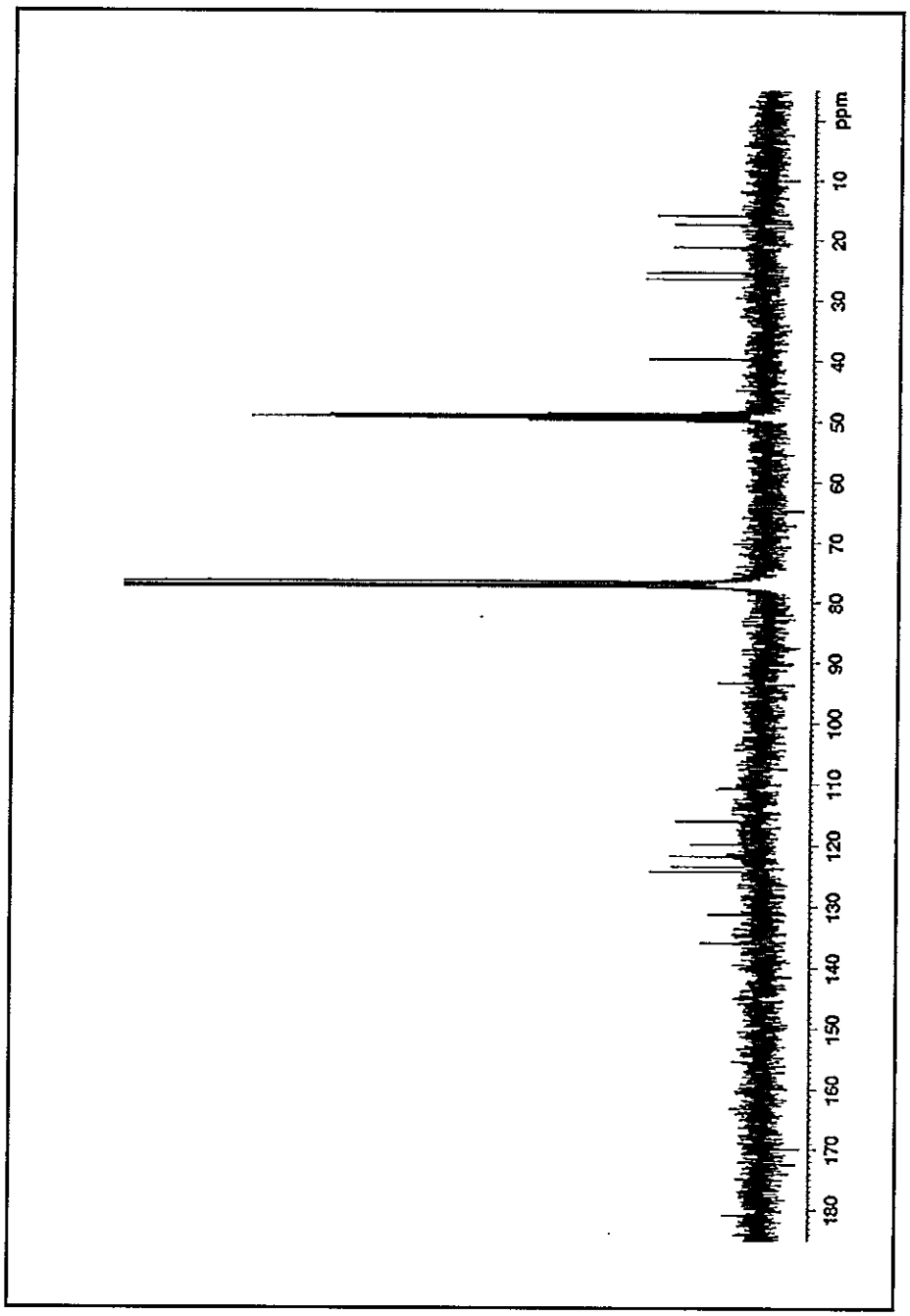

Figure 145 ^{13}C NMR (75 MHz) (CD_3Cl+CD_3OD) spectrum of compound GP15

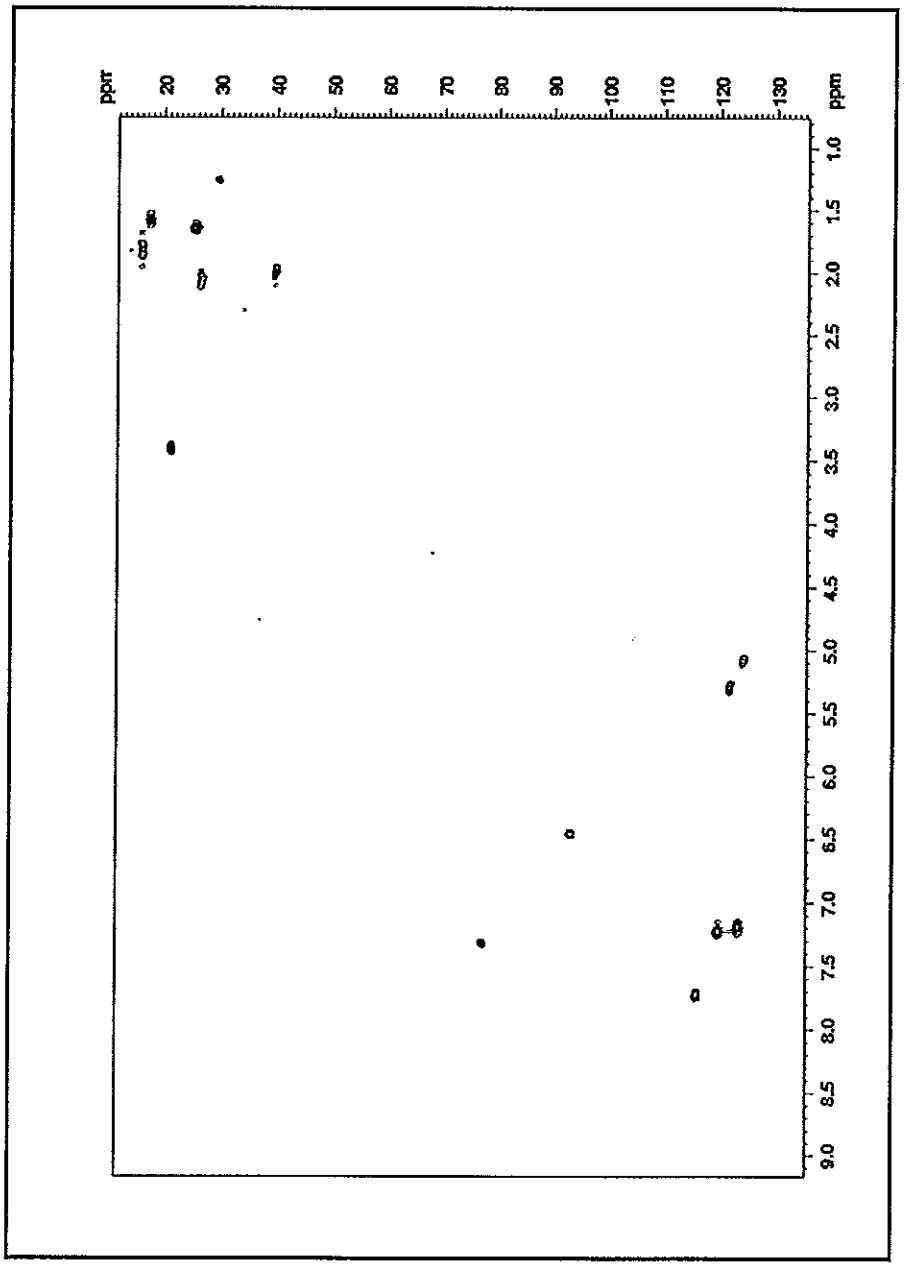

Figure 146 2D HMQC spectrum of compound GP15

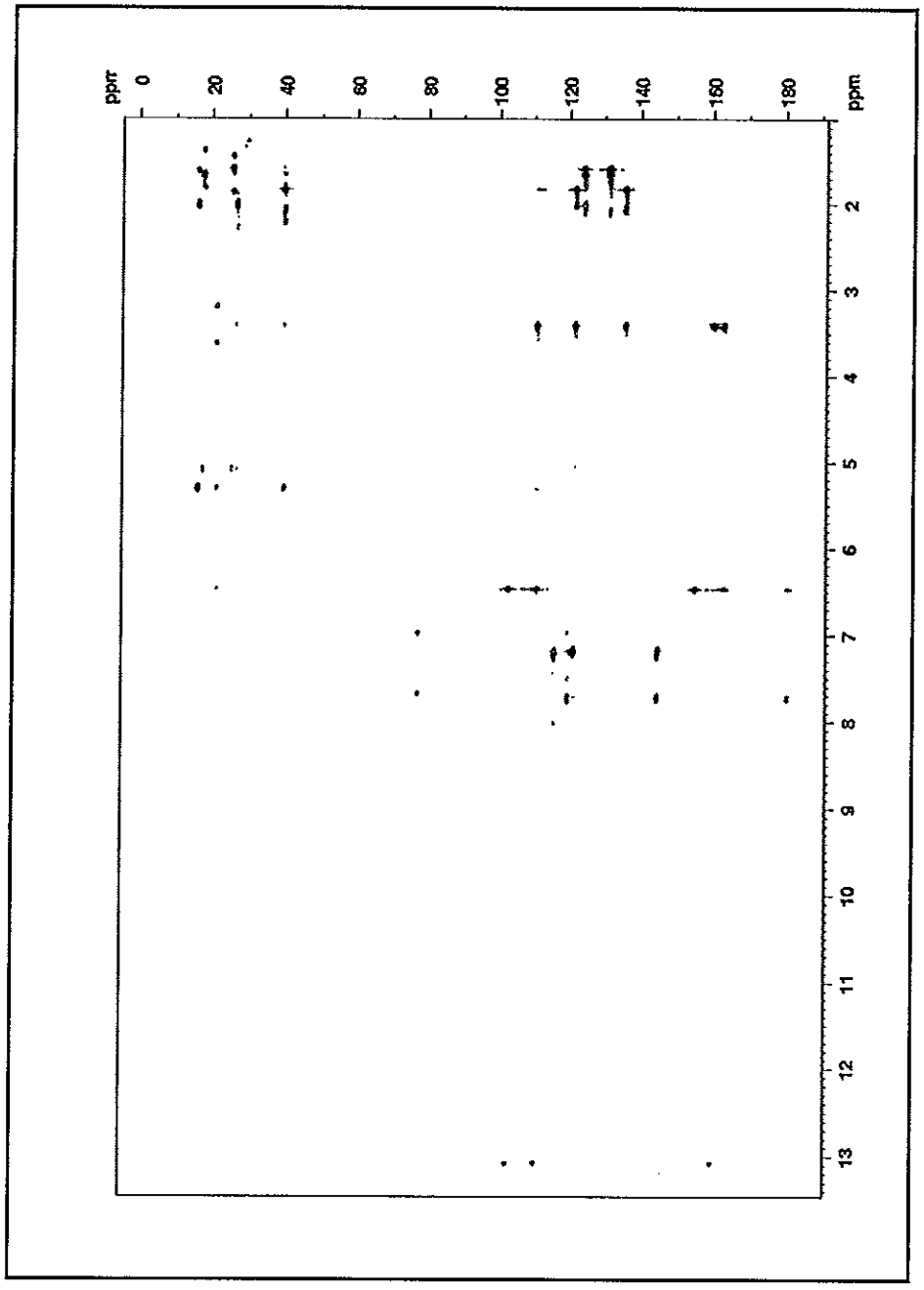

Figure 147 2D HMBC spectrum of compound GP15

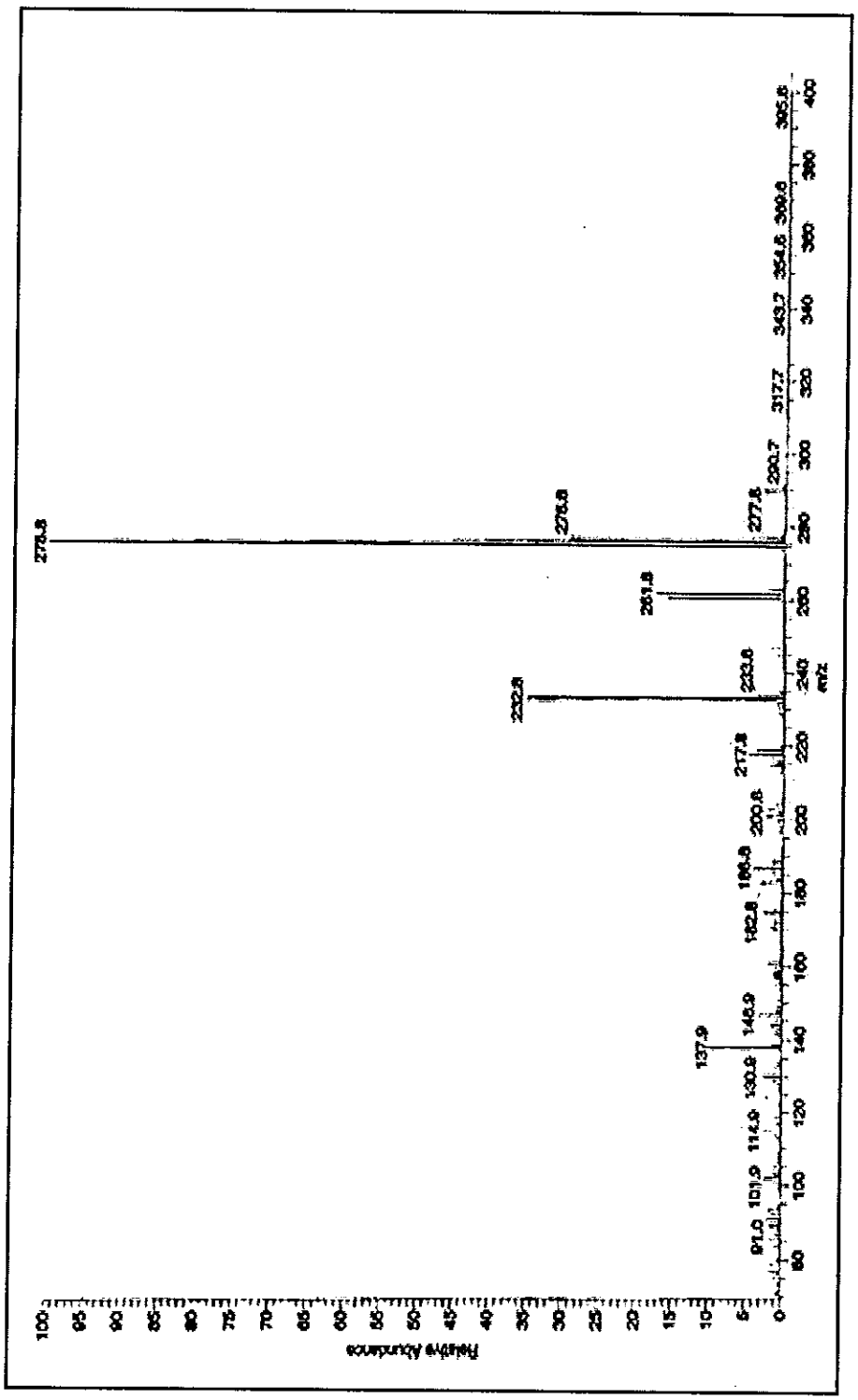

Figure 148 Mass spectrum of compound GP10

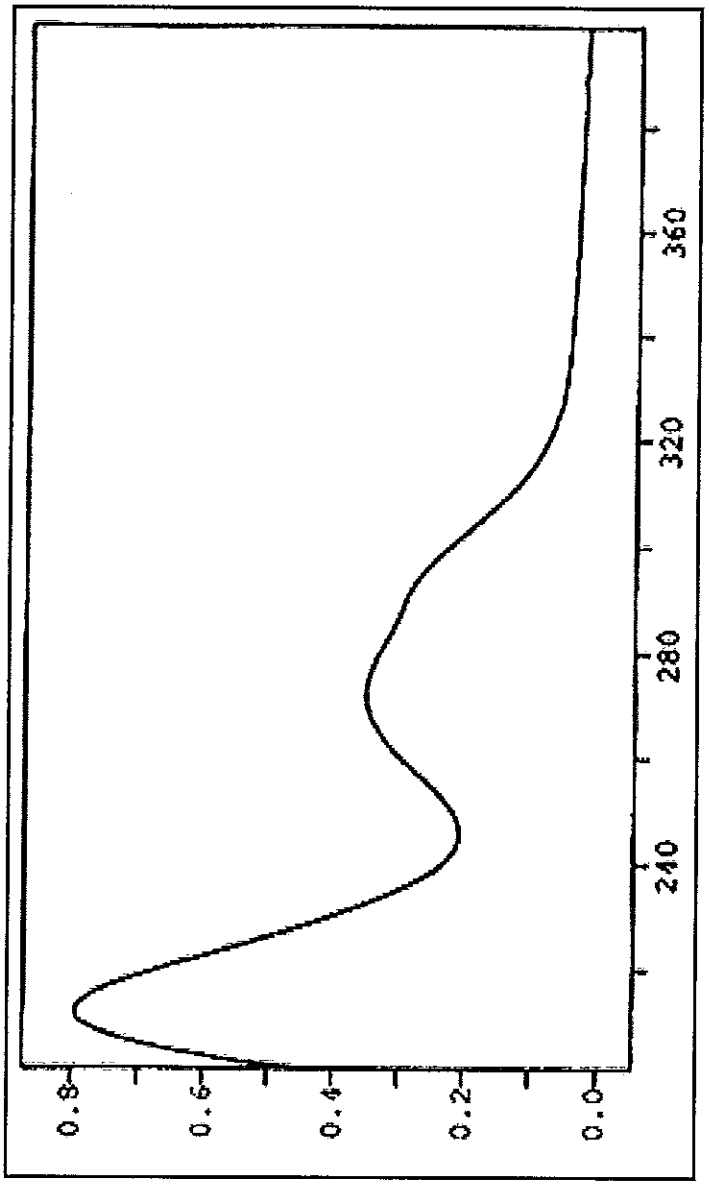

Figure 149 UV (MeOH) spectrum of compound GP10

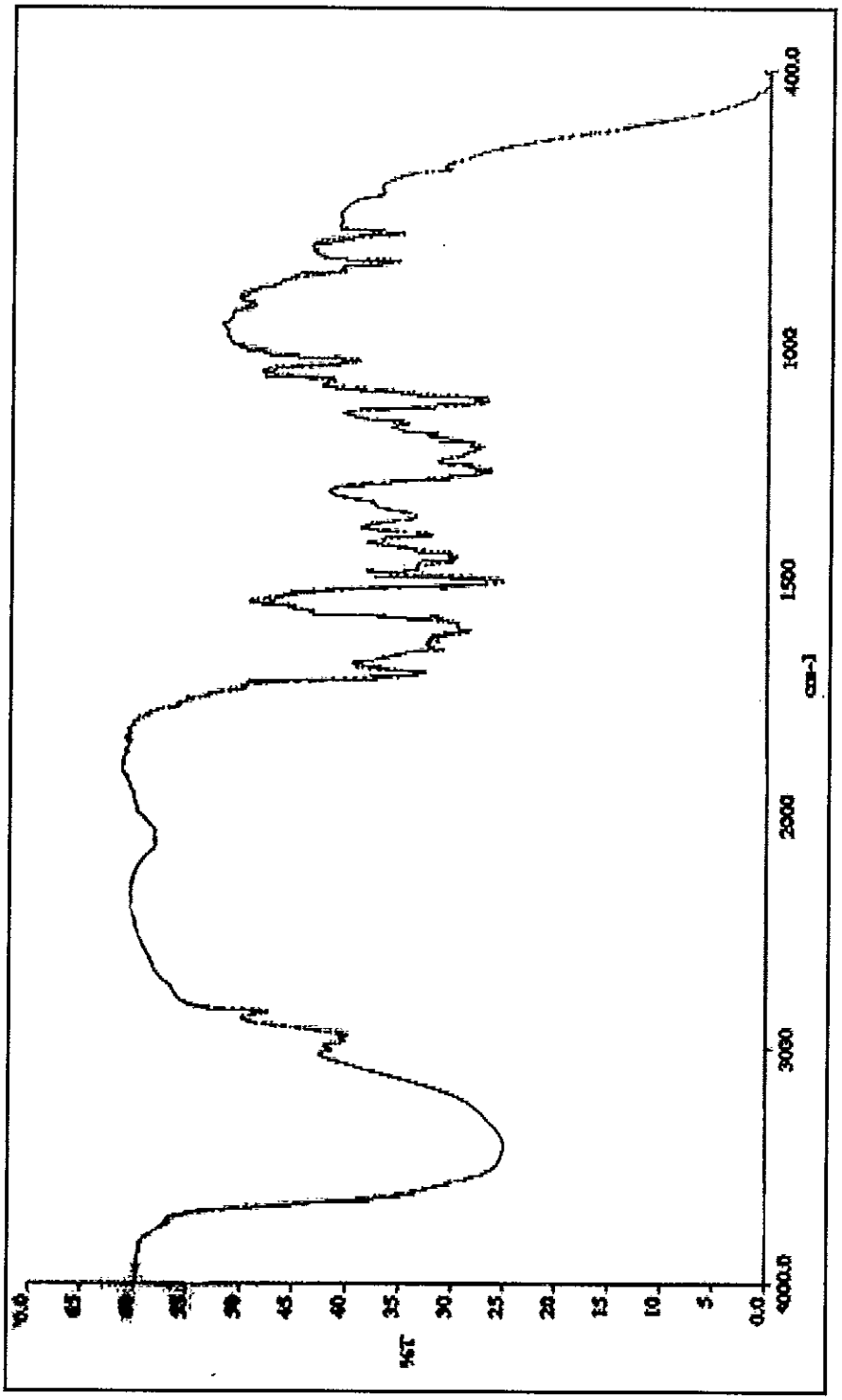

Figure 150 FT-IR (neat) spectrum of compound GP10

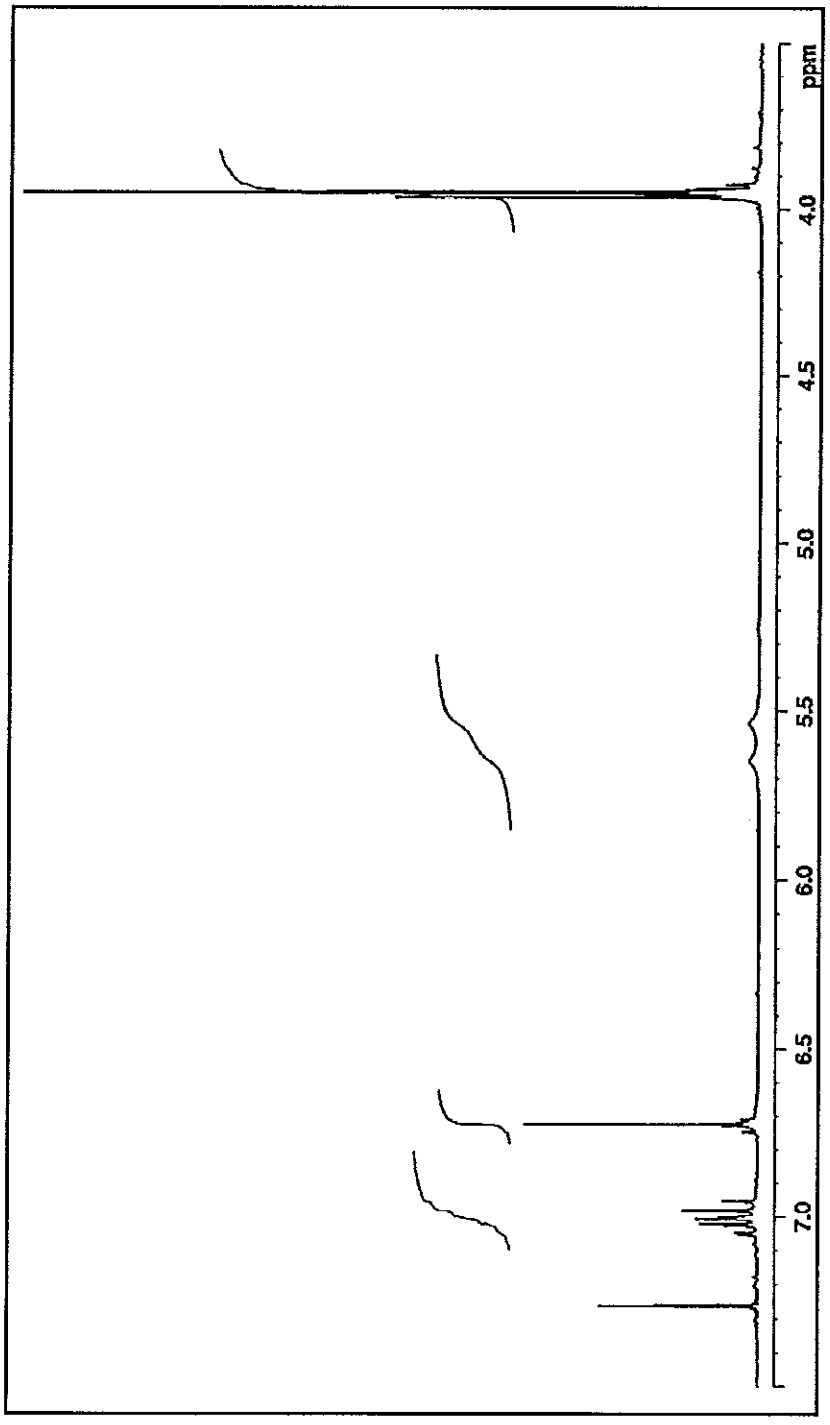

Figure 151 ^{1}H NMR (300 MHz) ($CDCl_3$) spectrum of compound GP10

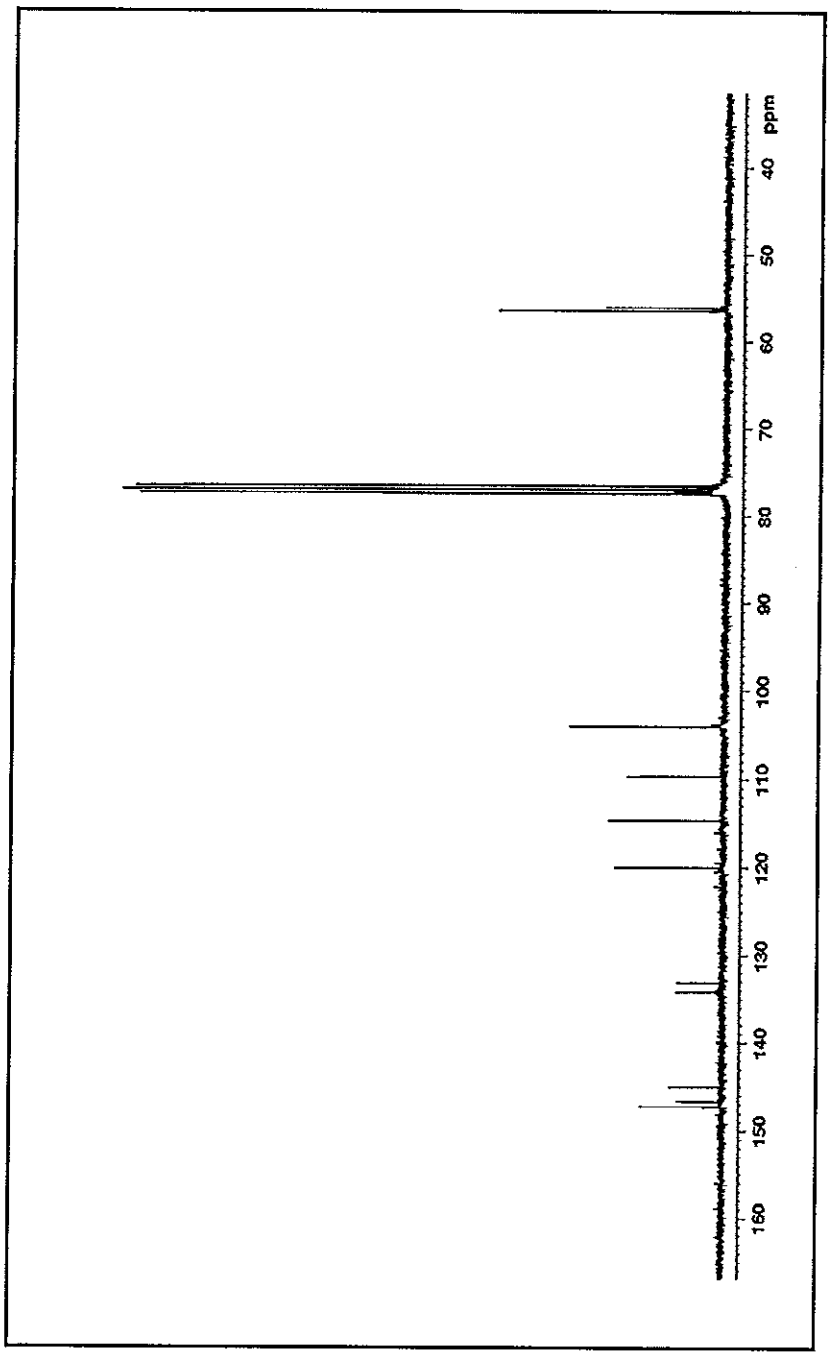

Figure 152 ^{13}C NMR (75 MHz) ($CDCl_3$) spectrum of compound GP10

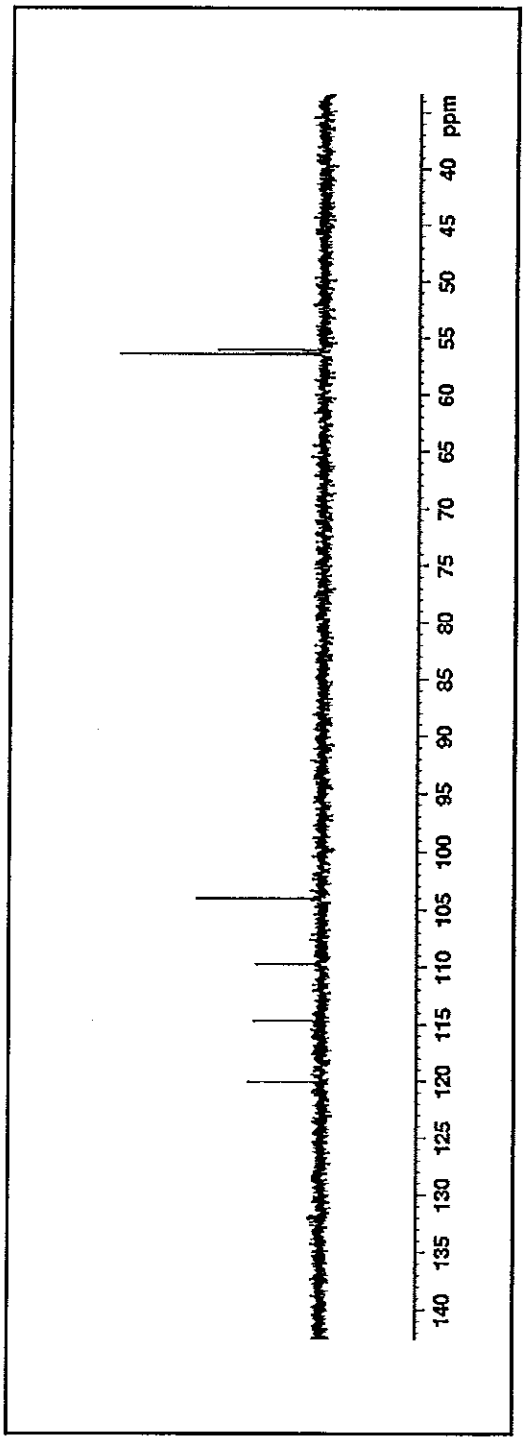

Figure 153 DEPT 90° spectra of compound GP10

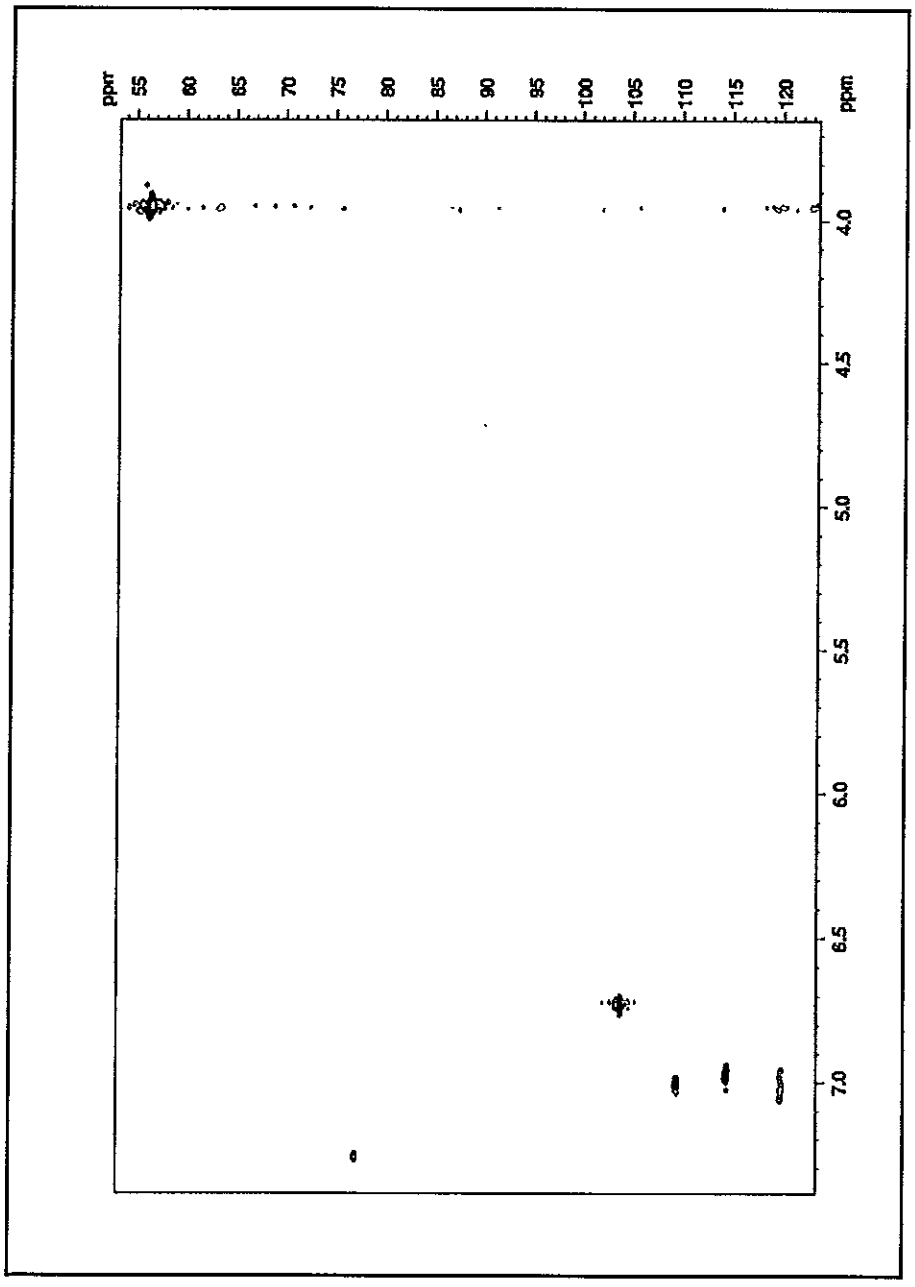

Figure 154 2D HMQC spectrum of compound GP10

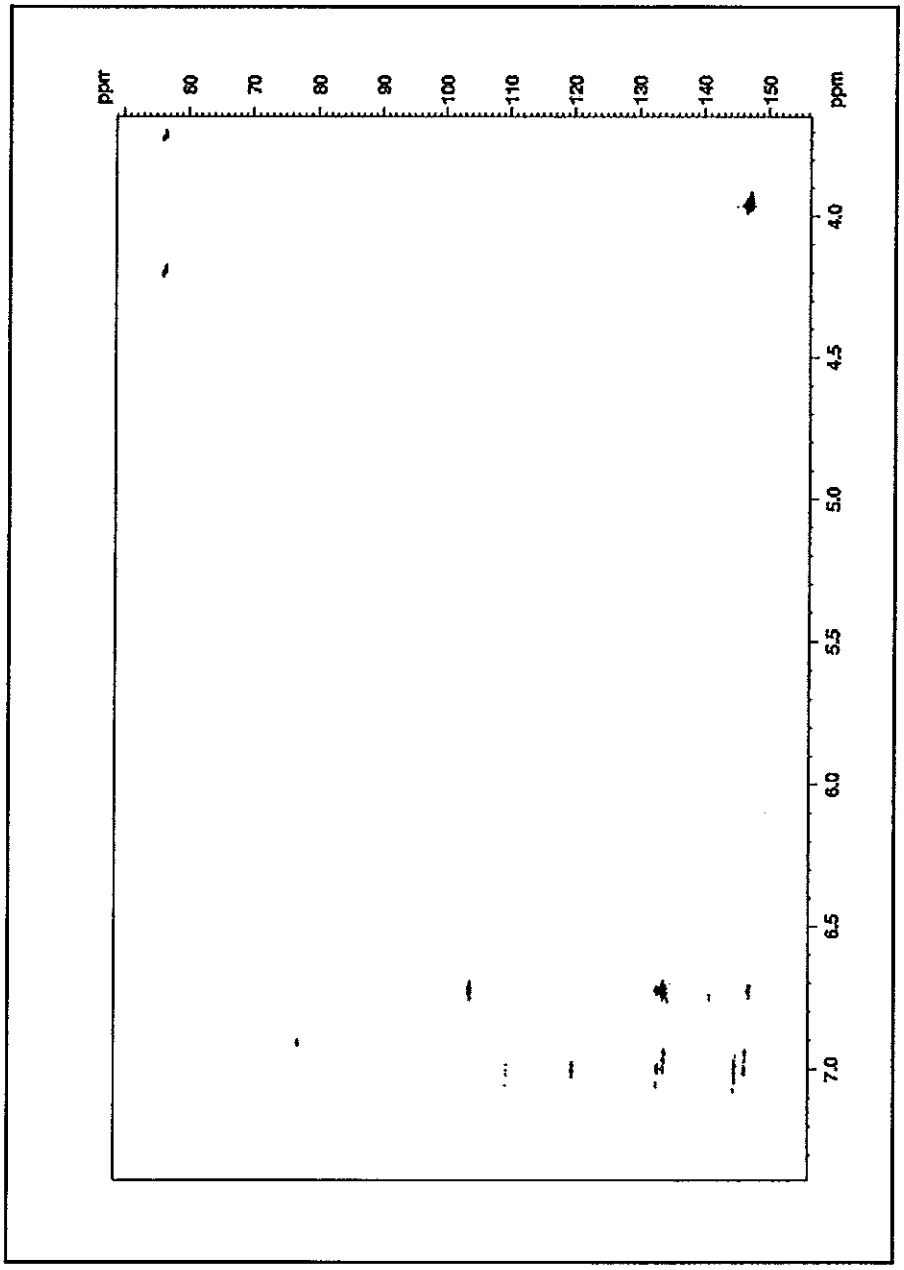

Figure 155 2D HMBC spectrum of compound GP10

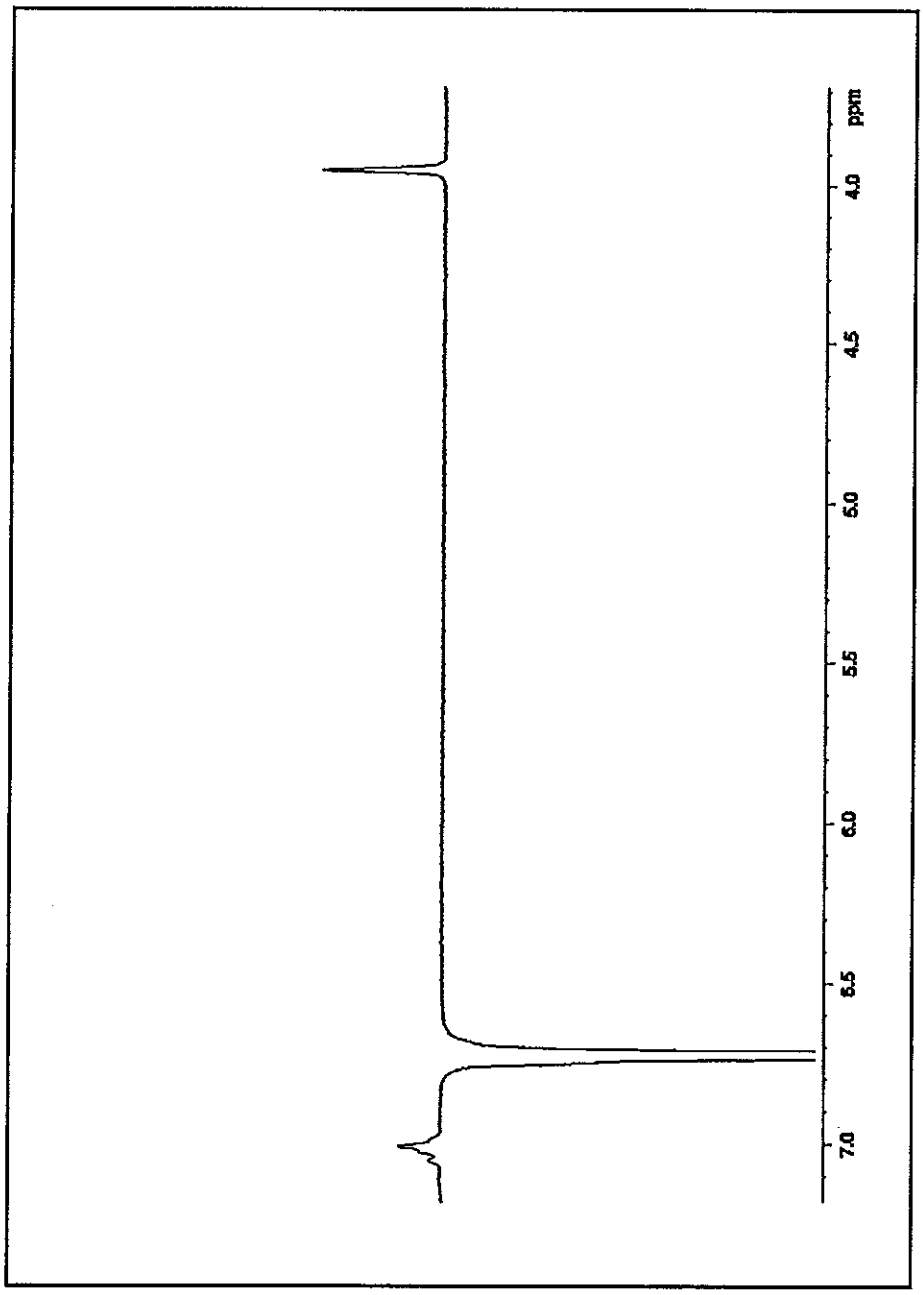

Figure 156 NOE difference spectrum of compound GP10 after irradiation at δ_H 6.72 (H-1 and H-6)

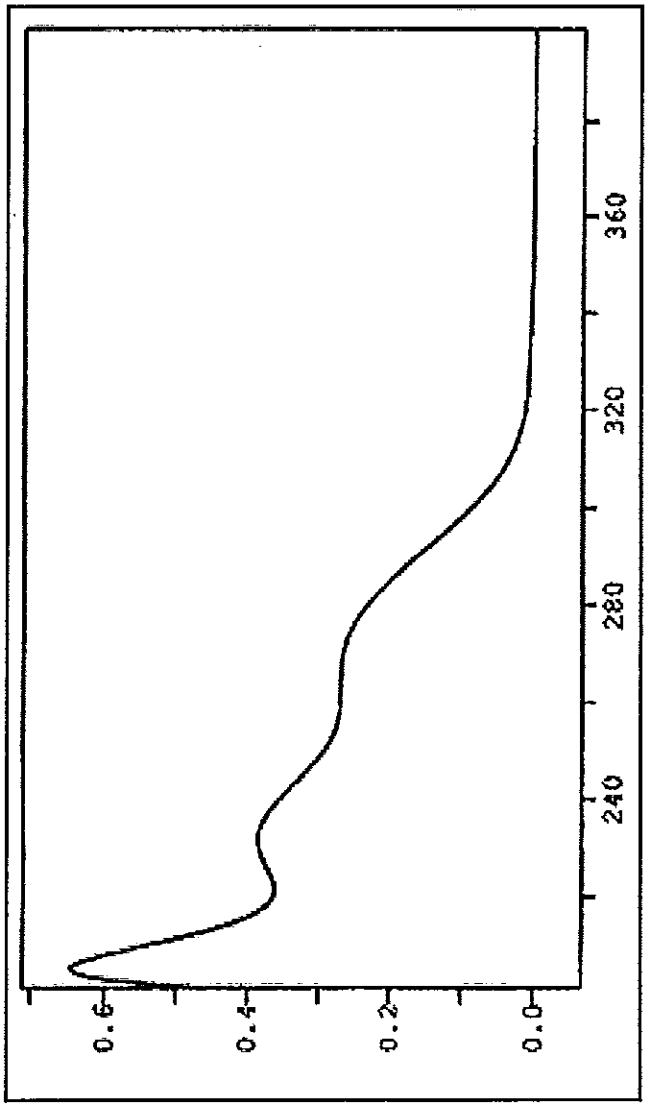

Figure 157 UV (MeOH) spectrum of compound GP13

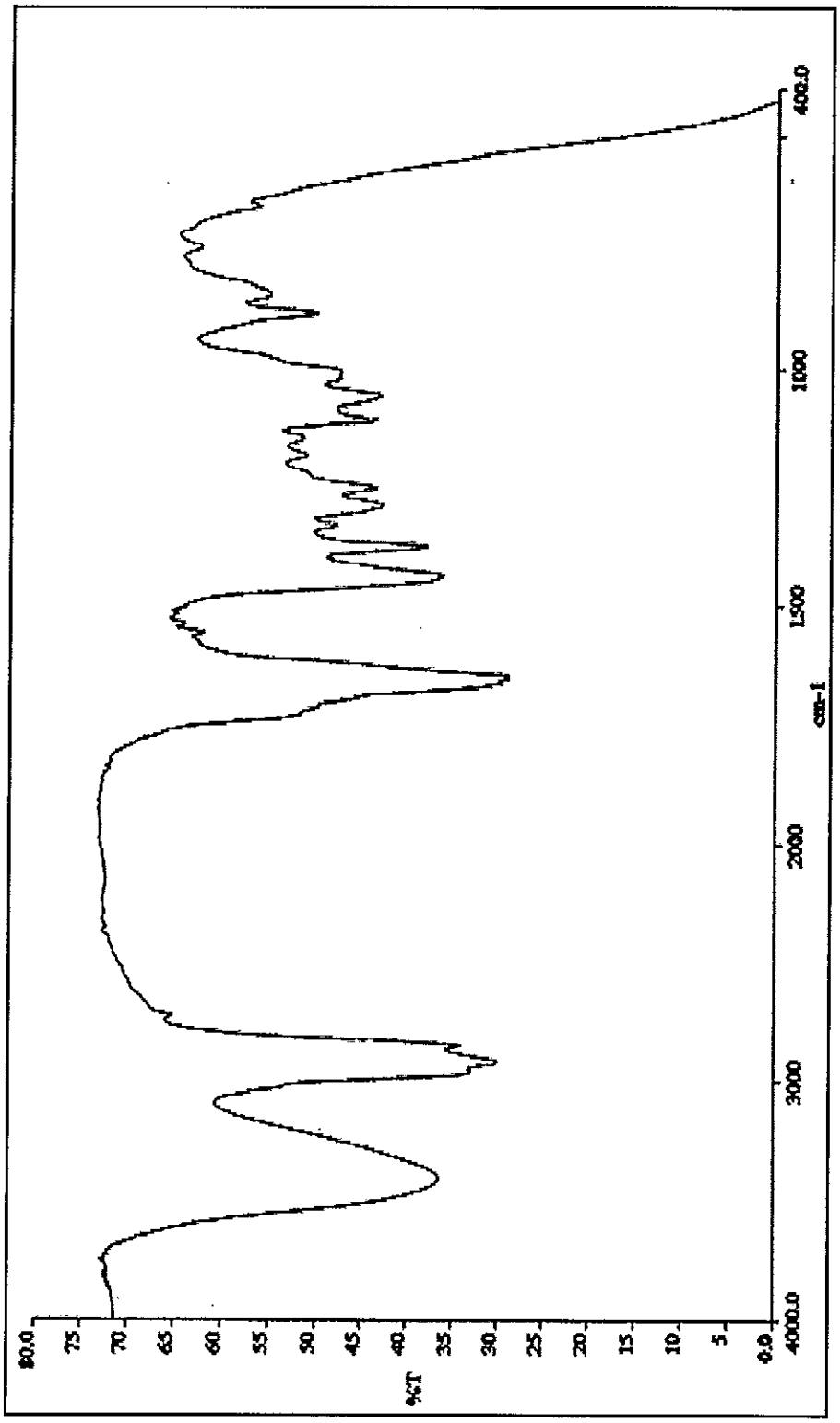

Figure 158 FT-IR (neat) spectrum of compound GP13

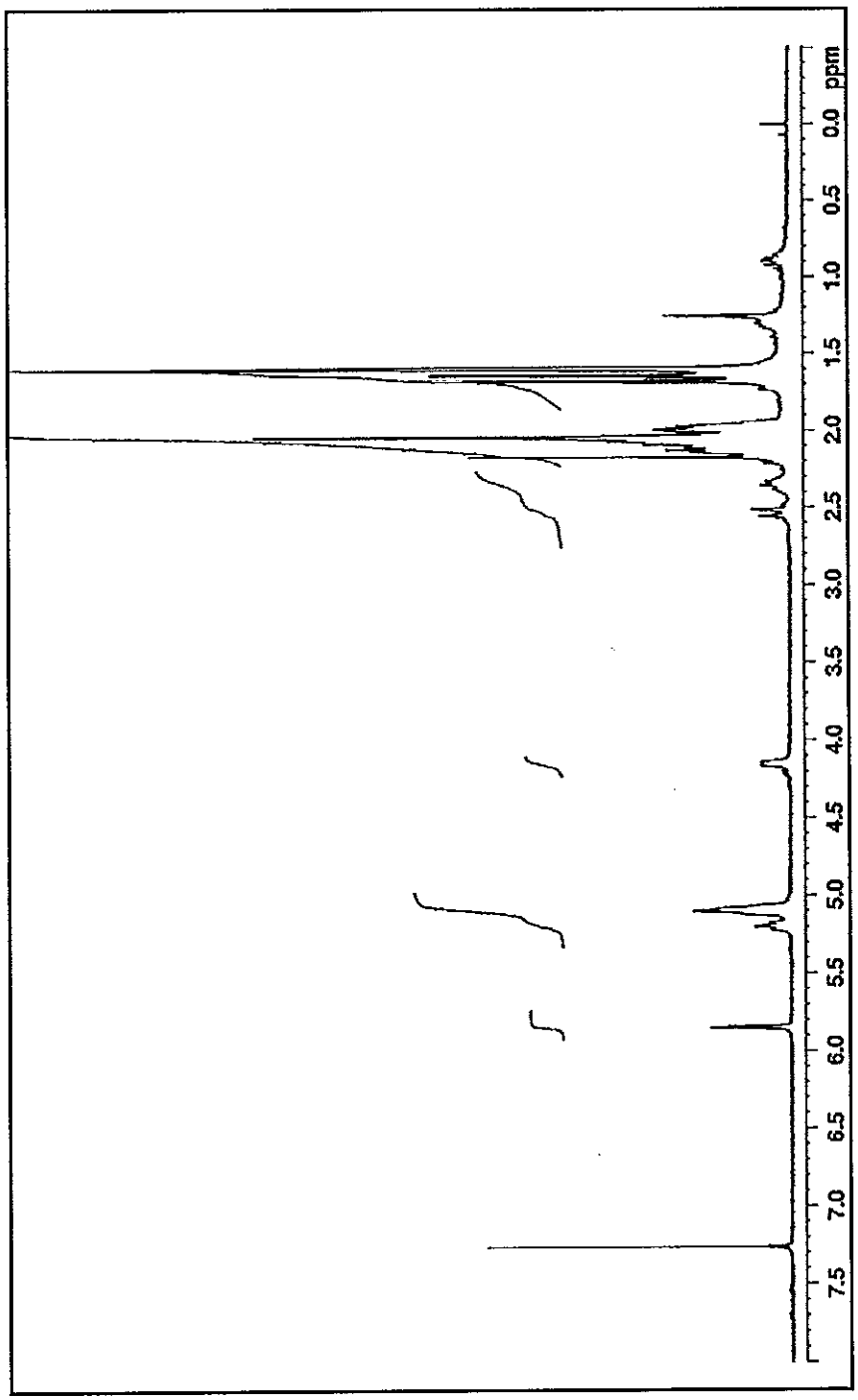

Figure 159 ^{1}H NMR (300 MHz) ($CDCl_3$) spectrum of compound GP13

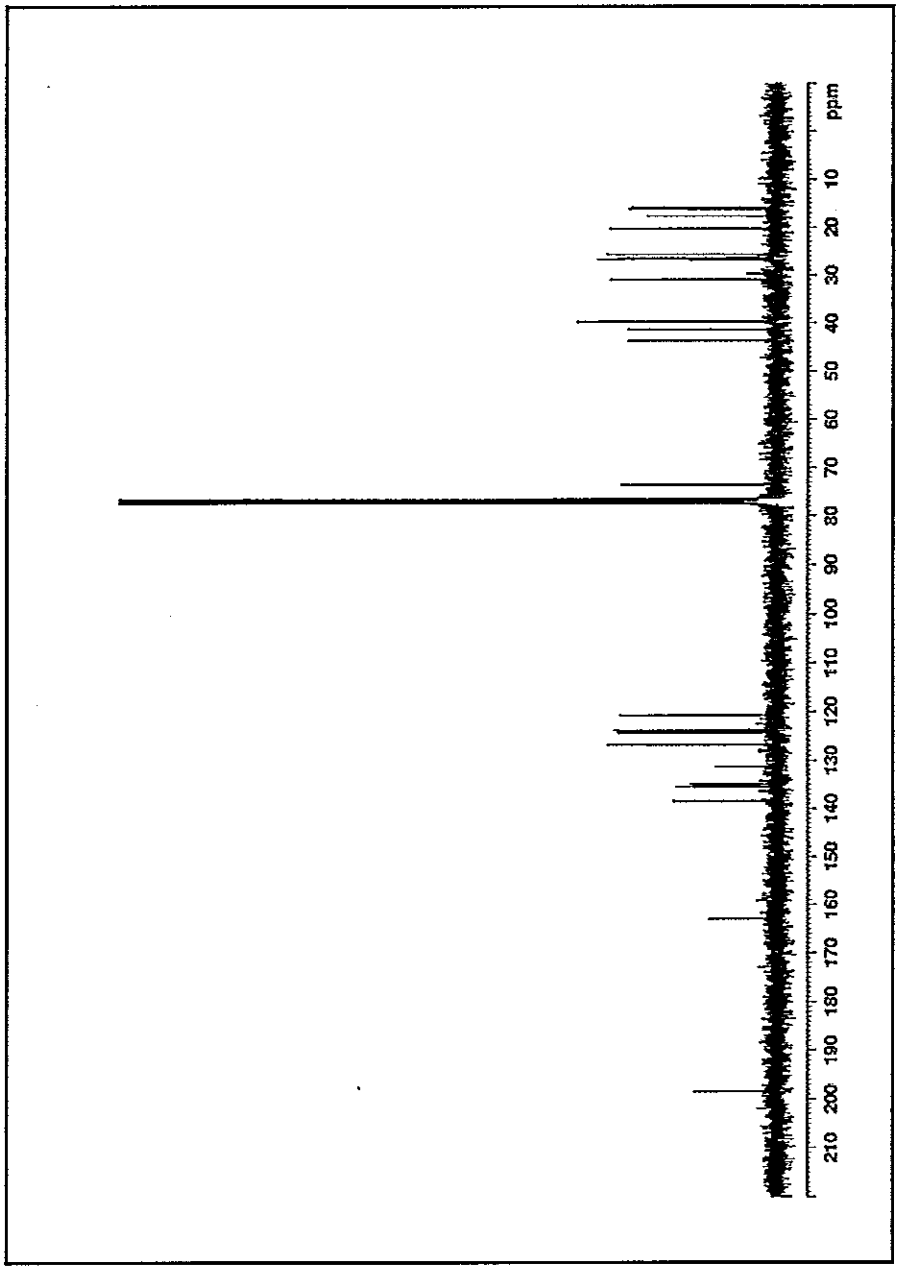

Figure 160 ^{13}C NMR (75 MHz) ($CDCl_3$) spectrum of compound GP13

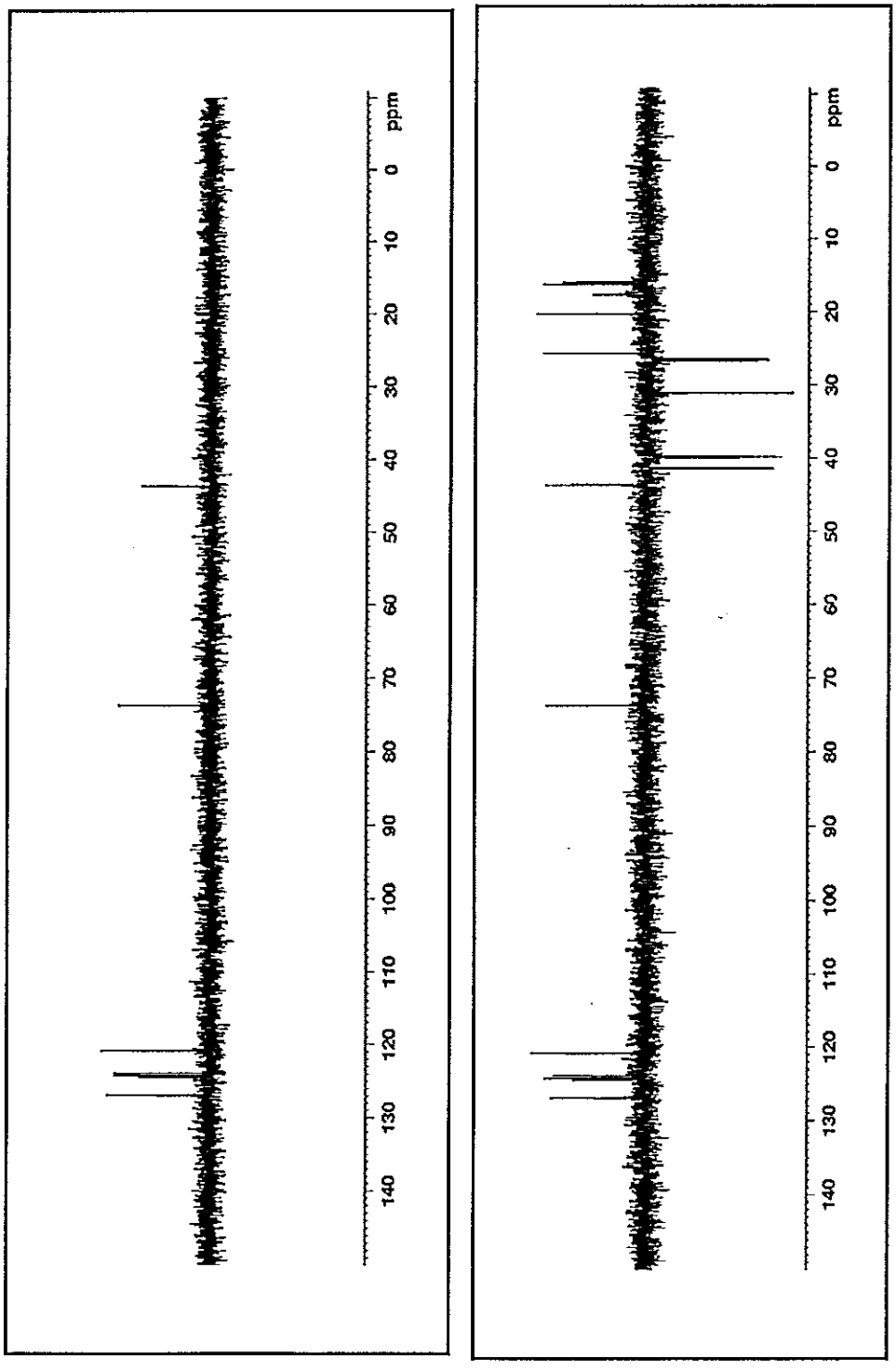

Figure 161 DEPT 90° and 135° spectra of compound GP13

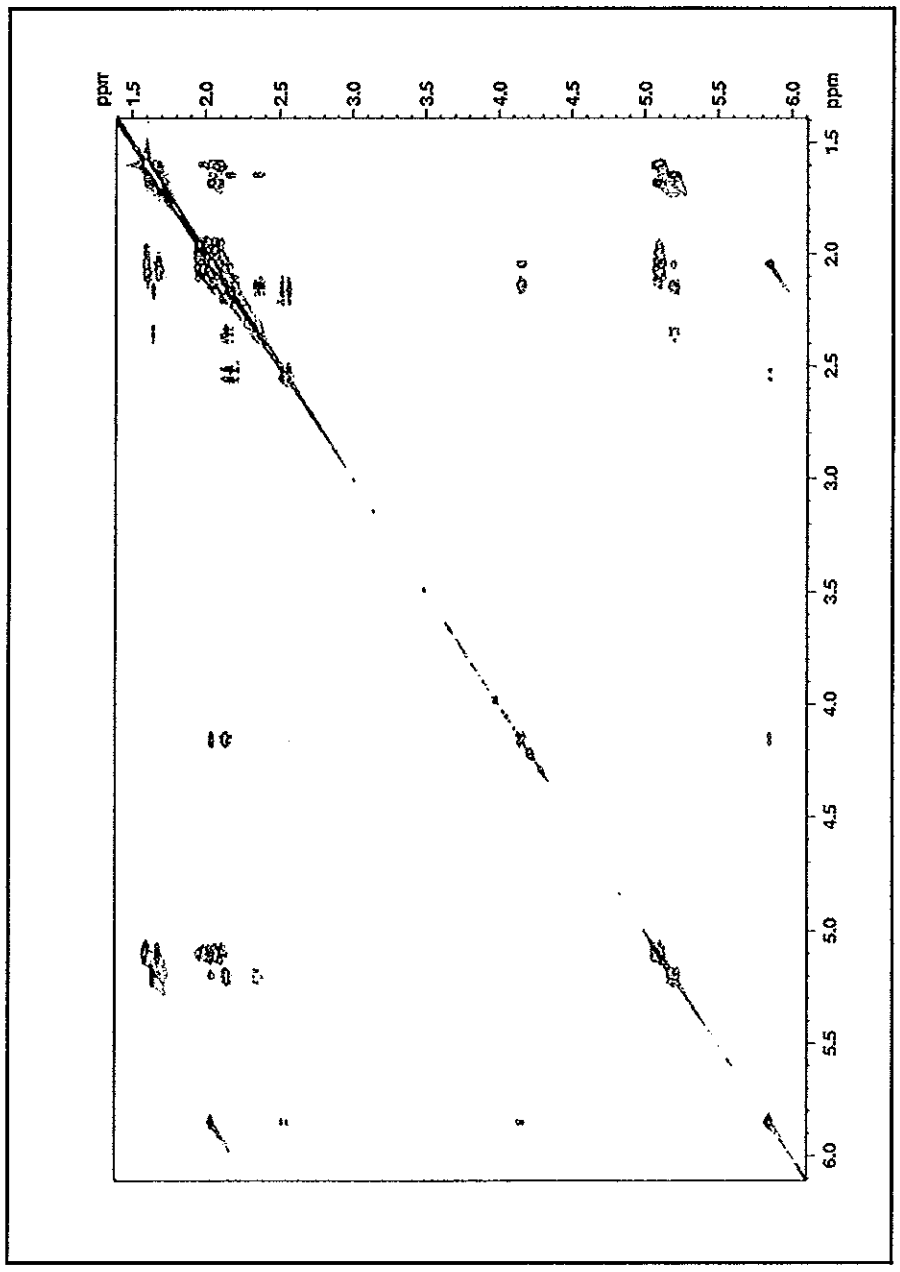

Figure 162 ^{1}H-^{1}H COSY spectrum of compound GP13

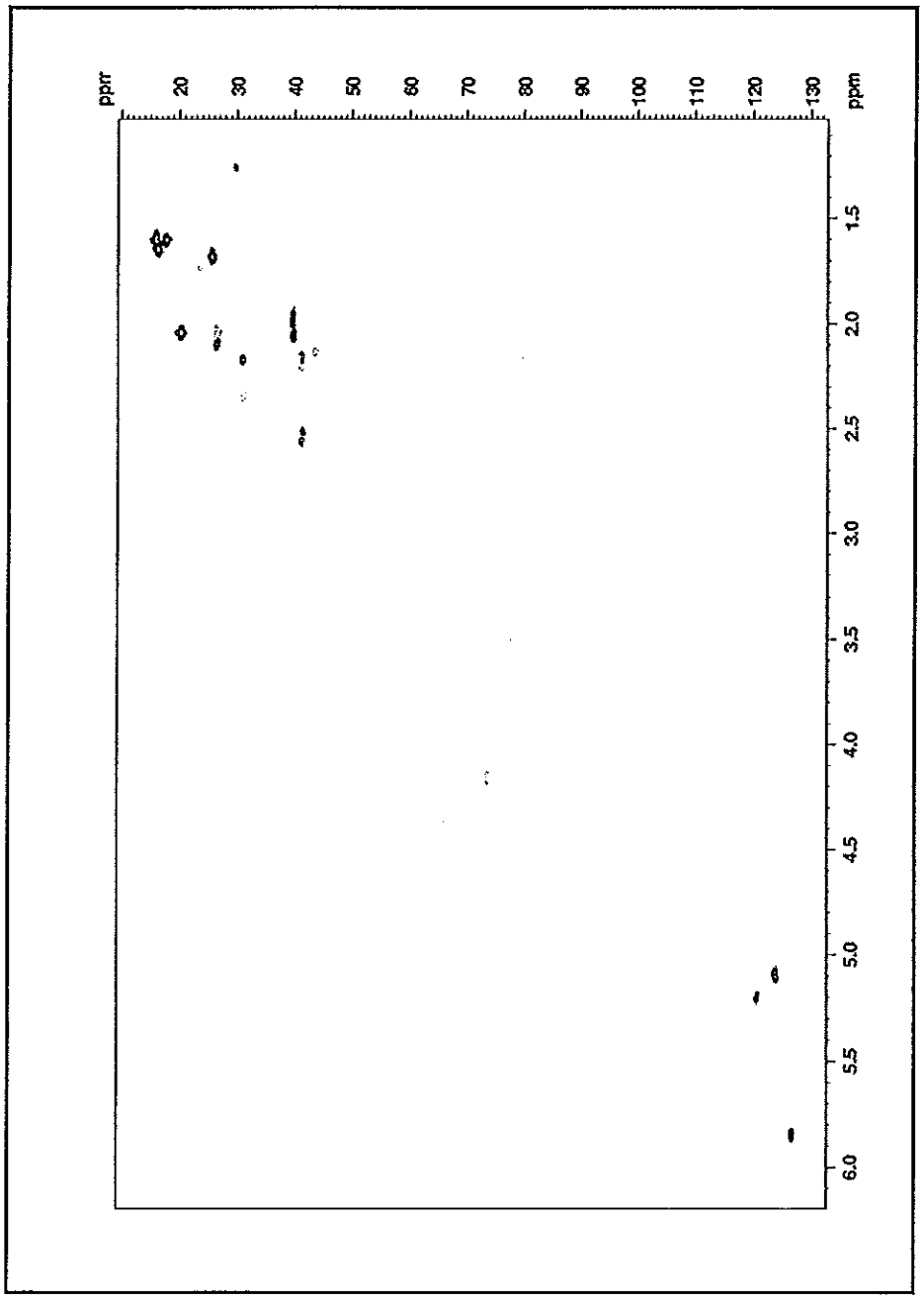

Figure 163 2D HMQC spectrum of compound GP13

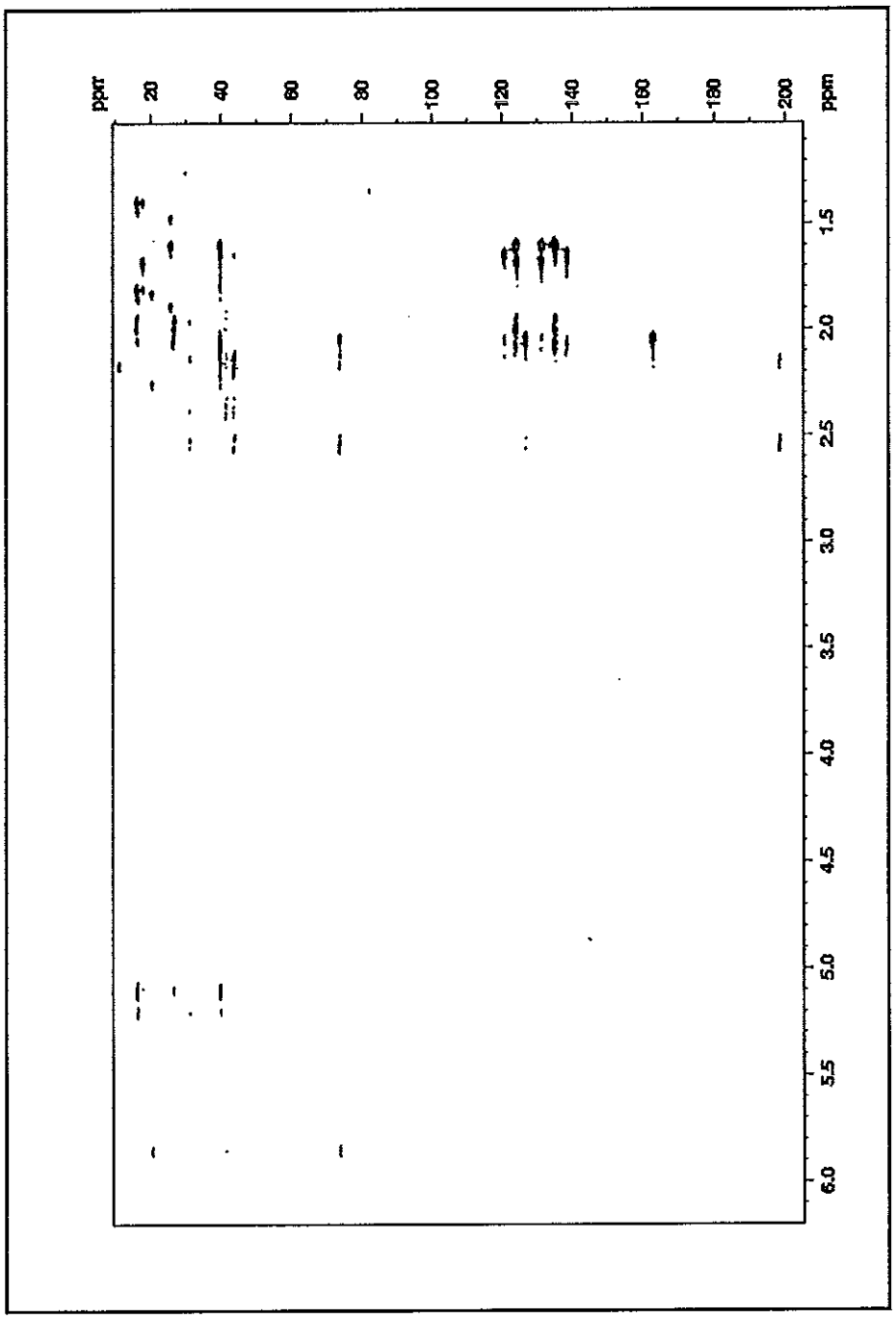

Figure 164 2D HMBC spectrum of compound GP13

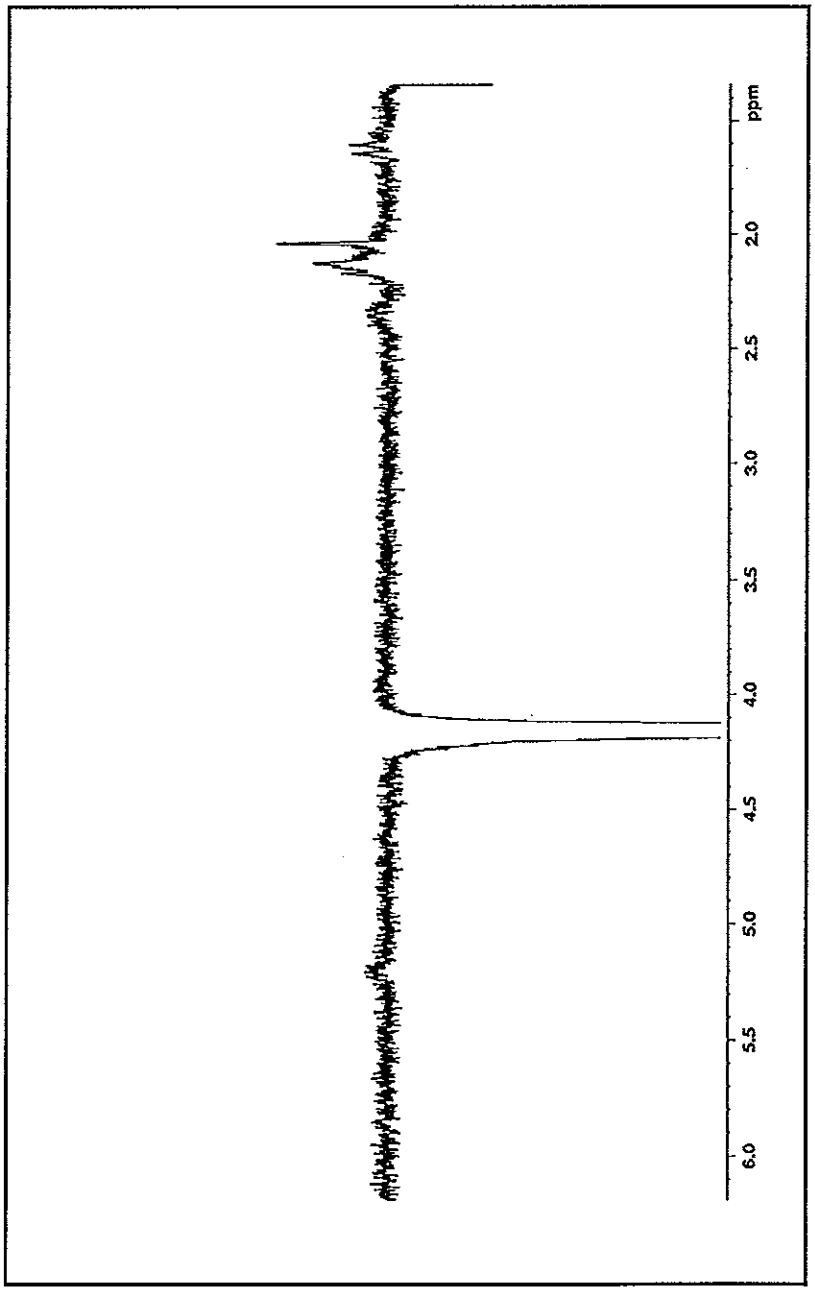

Figure 165 NOE difference spectrum of compound GP13 after irradiation at δ_H 4.15 (H-4)

REFERENCE

Abe, F., Nagafuji, S., Okabe, H., Higo, H. and Akahane, H. 2003. "Trypanocidal constituents in plants 2. Xanthones from the stem bark of *Garcinia subelliptica*", *Bio. Pharm. Bull.* 26(12), 1730-1733.

Abe, F., Nagafuji, S., Okabe, H., Akahane, H., Estrada-Muniz, E., Huerta-Reyes, M. and Reyes-Chilpa, R. 2004. "Trypanocidal constituents in plants 3. Leaves of *Garcinia intermedia* and heartwood of *Calophyllum brasiliense*", *Bio. Pharm. Bull.* 27(1), 141-143.

Ali, S., Goundar, R., Sotheeswaran, S., Beaulieu, C. and Spino, C. 2000. "Benzophenones of *Garcinia pseudoguttifera* (Clusiaceae)", *Phytochemistry.* 53, 281-284.

Baggett, S., Protiva, P., Mazzola, E.P., Yang, H., Ressler, E.T., Basile, M.J., Weinstein, I.B. and Kennelly, E.J. 2005. "Bioactive benzophenones from *Garcinia xanthochymus* fruits", *J. Nat. Prod.* 68(3), 354-360.

Chanmahasathien, W., Li, Y., Satake, M., Oshima, Y., Ishibashi, M., Ruangrungsi, N. and Ohizumi, Y. 2003a. "Prenylated xanthones from *Garcinia xanthochymus*", *Chem. Pharm. Bull.* 51(11), 1332-1334.

Chanmahasathien, W., Li, Y., Satake, M., Oshima, Y., Ruangrungsi, N. and Ohizumi, Y. 2003b. "Prenylated xanthones with NGF-potentiating activity from *Garcinia xanthochymus*", *Phytochemistry.* 64(5), 981-986.

Chen, J.J., Chen, I.S. and Duh, C.Y. 2005. "Cytotoxic xanthones and biphenyls from the root of *Garcinia linii*", *Planta Med.* 71(2), 196-201.

Chiang, Y.-M., Kuo, Y.-H., Oota, S. and Fukuyama, Y. 2003. "Xanthones and benzophenones from the stems of *Garcinia multiflora*", *J. Nat. Prod.* 66(8), 1070-1073.

Deachathai, S., Mahabusarakam, W., Phongpaichit, S. and Taylor, W.C. 2005. "Phenolic compounds from the fruit of *Garcinia dulcis*", *Phytochemistry.* 66(19), 2368-2375.

Don, M.-J., Huang, Y.-J., Huang, R.-L. and Lin, Y.-L. 2004. "New phenolic principles from *Hypericvm sampsonii*", *Chem. Pharm. Bull.* 52(7), 866-869.

Farombi, E.O., Akanni, O.O. and Emerole, G.O. 2002. "Antioxidant and scavenging activities of flavonoid extract (Kolaviron) of *Garcinia kola* seeds", *Pharm. Bio.* 40(2), 107-116.

Han, Q.-B., Lee, S.-F., Qiao, C.-F., He, Z.-D., Song, J.-Z., Sun, H.-D. and Xu, H.-X. 2005. "Complete NMR assignments of the antibacterial biflavonoid GB1 from *Garcinia kola*", *Chem. Pharm. Bull.* 53(8), 1034-1036.

Hay, A.-E., Helesbeux, J.-J., Duval, O., Labaied, M., Grellier, P. and Richomme, P. 2004a. "Antimalarial xanthones from *Calophyllum caledonicum* and *Garcinia vieillardii*", *Life Sciences.* 75(25), 3077-3085.

Hay, A.-E., Aumond, M.-C., Mallet, S., Dumontet, V., Litaudon, M., Rondeau, D. and Richomme, P. 2004b. "Antioxidant xanthones from *Garcinia vieillardii*", *J. Nat. Prod.* 67(4), 707-709.

Herath, K., Jayasuriya, H., Ondeyka, J.G., Guan, Z., Borris, R.P., Stijfhoorn, E., Stevenson, D., Wang, J., Sharma, N., MacNaul, K., Menke, J.G., Ali, A., Schulman, M.J. and Singh, S.B. 2005. "Guttiferone I, a new prenylated benzophenone from *Garcinia humilis* as a Liver X Receptor Ligand", *J. Nat. Prod.* 68(4), 617-619.

Huang, Y.-L., Chen, C.-C., Chen, Y.-J., Huang, R.-L. and Shieh, B.-J. 2001. "Three xanthones and a benzophenone from *Garcinia mangostana*", *J. Nat. Prod.* 64(7), 903-906.

Ilyas, M., Parveen, M., Shafiullah. and Ahmad, S.M. 2002. "A novel chalcone from *Garcinia nervosa*", *J. Chem. Res, Synop.* 5, 231-233.

Ito, C., Itoigawa, M., Miyamoto, Y., Onoda, S., Rao, K.S., Mukainaka, T., Tokuda, H., Nishino, H. and Furukawa, H. 2003a. "Polyprenylated benzophenones from *Garcinia assigu* and their potential cancer chemopreventive activities", *J. Nat. Prod.* 66(2), 206-209.

Ito, C., Itoigawa, M., Takakura, T., Ruangrungsi, N., Enjo, F., Tokuda, H., Nishino, H. and Furukawa, H. 2003b. "Chemical constituents of *Garcinia fusca* : Structure elucidation of eight new xanthones and their cancer chemopreventive activity", *J. Nat. Prod.* 66(2), 200-205.

Jantan, I., Pisar, M.M., Idris, M.S., Taher, M. and Ali, R.M. 2002. "In vitro inhibitory effect of rubraxanthone isolated from *Garcinia parvifolia* on platelet-activating factor receptor binding", *Planta Med.* 68(12), 1133-1134.

Komguem, J., Meli, A.L., Manfouo, R.N., Lontsi, D., Ngounou, F.N., Kuete, V., Kamdem, H.W., Tane, P., Ngadjui, B.T., Sondengam, B.L. and Connolly, J.D. 2005. "Xanthones from *Garcinia smeathmannii* (Oliver) and their antimicrobial activity", *Phytochemistry.* 66(14), 1713-1717.

Kosela, S., Hu, L.-H., Yip, S.-C., Rachmatia, T., Sukri, T., Daulay, T.S., Tan, G.-K., Vittal, J.J. and Sim, K.-Y. 1999. "Dulxanthone E : a pyranoxanthone from the leaves of *Garcinia dulcis*", *Phytochemistry.* 52, 1375-1377.

Kosela, S., Hu, L.-H., Rachmatia, T., Hanafi, M. and Sim, K.-Y. 2000. "Dulxanthones F-H, three new pyranoxanthones from *Garcinia dulcis*", *J. Nat. Prod.* 63, 406-407.

Lakshmi, C., Kumar, K.A. and Dennis, T.J. 2002. "Polyprenylated benzophenones from *Garcinia indica*", *J. Indian. Chem. Soc.* 79(12), 968-969.

Lannang, A.M., Komguem, J., Ngninzeko F.N., Tangmouo, J.G., Lontsi, D., Ajaz, A., Choudhary, M.I., Ranjit, R., Devkota, K.P. and Sondengam, B.L. 2005. "Bangangxanthone A and B, two xanthones from the stem bark of *Garcinia polyantha* Oliv", *Phytochemistry.* 66(19), 2351-2355.

Mahabusarakam, W., Chairerk, P. and Taylor, W.C. 2005. "Xanthones from *Garcinia cowa* Roxb. latex", *Phytochemistry.* 66(10), 1148-1153.

Merza, J., Aumond, M.-C., Rondeau, D., Dumontet, V., Le Ray, A.-M., Seraphin, D. and Richomme, P. 2004. "Prenylated xanthones and tocotrienols from *Garcinia virgata*", *Phytochemistry.* 65(21), 2915-2920.

Nguyen, L.H.D. and Harrison, L.J. 2000. "Xanthones and triterpenoids from the bark of *Garcinia vilersiana*", *Phytochemistry.* 53, 111-114.

Nilar and Harrison, L.J. 2002. "Xanthones from the hartwood of *Garcinia mangostana*", *Phytochemistry.* 60(5), 541-548.

Nilar., Nguyen, L.H.D., Venkatraman, G., Sim, K.Y. and Harrison, L.J. 2005. "Xanthones and benzophenones from *Garcinia griffithii* and *Garcinia mangostana*", *Phytochemistry.* 66(14), 1718-1723.

Parveen, M., Ilyas, M., Mushfiq, M., Busudan, O.A. and Muhaisen, H.M.H. 2004. "A new biflavonoid from leaves of *Garcinia nervosa*", *Nat. Prod. Res.* 18(3), 269-275.

Pattalung, P.N., Wiriyachitra, P., Ongsakul, M. 1988. "Antimicrobial activities of rubraxanthone isolated from *Garcinia parvifolia* (Miq.) Miq", *J. Sci. Soc. Thailand.* 14(1), 67-71.

Rukachaisirikul, V., Kaewnok, W., Koysomboon, S., Phongpaichit, S. and Taylor, W.C. 2000a. "Caged-Tetraprenylated xanthones from *Garcinia scortechinii*", *Tetrahedron.* 56(43), 8539-8543.

Rukachaisirikul, V., Adair, A., Dampawan, P., Taylor, W.C. and Turner, P.C. 2000b. "Lanostanes and friedolanostanes from the pericarp of *Garcinia hombroniana*", *Phytochemistry.* 55, 183-188.

Rukachaisirikul, V., Pailee, P., Hiranrat, A., Tuchinda, P., Yoosook, C., Kasisit, J., Taylor, W.C. and Reutrakul, V. 2003a. "Anti-HIV-1 protostane triterpenes and digeranylbenzophenone from trunk bark and stems of *Garcinia speciosa*", *Planta Med.* 69, 1141-1146.

Rukachaisirikul, V., Ritthiwigrom, T., Pinsa, A., Sawangchote, P. and Taylor, W.C. 2003b. "Xanthones from the stem bark of *Garcinia nigrolineata*", *Phytochemistry.* 64(6), 1149-1156.

Rukachaisirikul, V., Naklue, W., Sukpondma, Y. and Phongpaichit, S. 2005a. "An antibacterial biphenyl derivative from *Garcinia bancana* MIQ", *Chem. Pharm. Bull.* 53(3), 342-343.

Rukachaisirikul, V., Saelim, S., Karnsomchoke, P. and Phongpaichit, S. 2005b. "Friedolanostanes and lanostanes from the leaves of *Garcinia hombroniana*", *J. Nat. Prod.* 68(8), 1222-1225.

Rukachaisirikul, V., Phainuphong, P., Sukpondma, Y., Phongpaichit, S. and Taylor, W.C. 2005c. "Antibacterial caged-tetraprenylated xanthones from the stem bark of *Garcinia scortechinii*", *Planta Med.* 71, 165-170.

Rukachaisirikul, V., Tadpetch, K., Watthanaphanit, A., Saengsanae, N. and Phongpaichit, S. 2005d. "Benzopyran, biphenyl, and tetraoxygenated xanthone derivatives from the twigs of *Garcinia nigrolineata*", *J. Nat. Prod.* 68(8), 1218-1221.

Sherley, G., Kosela, S., Kardono, L.B.S., Hanafi, M. and Harrison, L.J. 2004. "Identification of cytotoxic and antibacterial pyranoxanthones from *Garcinia porrecta*", *New Technologies & Medicine*. 5(1), 39-43.

Smitinand, T. 2001. "Thai Plant Names", The Forest Herbarium, The Royal Forest Deparment.

Soemiati, A., Kosela, S., Hanafi, M. and Harrison, L.J. 2004. "Elucidation and cytotoxic L1210 evaluation of prenylated pyranoxanthonoids from the indonesian *Garcinia dulcis* fruit (Guttiferae) n-hexane extract", *New Technologies & Medicine*. 5(4), 389-393.

Sukpondma, Y., 2005. "Chemical constituents from the fruits of *Garcinia scortechinii* and *Garcinia hanburyi*", *Ph. D. Thesis*. Prince of Songkla University, Thailand.

Sukpondma, Y., Rukachaisirikul, V. and Phongpaichit, S. 2005a. "Antibacterial caged-tetraprenylated xanthones from the fruits of *Garcinia hanburyi*", *Chem. Pharm. Bull.* 53(7), 850-852.

Sukpondma, Y., Rukachaisirikul, V. and Phongpaichit, S. 2005b. "Xanthone and sesquiterpene derivatives from the fruits of *Garcinia scortechinii*", *J. Nat. Prod.* 68(7), 1010-1017.

Suksamrarn, S., Suwannapoch, N., Ratananukul, P., Aroonlerk, N. and Suksamrarn, A. 2002. "Xanthones from the green fruit hulls of *Garcinia mangostana*", *J. Nat. Prod.* 65(5), 761-763.

Suksamrarn, S., Suwannapoch, N., Phakhodee, W., Thanuhiranlert, J., Ratananukul, P., Chimnoi, N. and Suksamrarn, A. 2003. "Antimycobacterial activity of prenylated xanthones from the fruits of *Garcinia mangostana*", *Chem. Pharm. Bull.* 51(7), 857-859.

Tanaka, N., Takaishi, Y., Shikishima, Y., Nakanishi, Y., Bastow, K.,Lee, K.-H., Honda, G., Ito, M., Takeda, Y., Kodzhimatov, O.K. and Ashurmetov, O. 2004. "Prenylated benzophenones and xanthones from *Hypericum scabrum*", *J. Nat. Prod.* 67, 1870-1875.

Thoison, O., Fahy, J., Dumontet, V., Chiaroni, A., Riche, C., Tri, M.V. and Sevenet, T. 2000. "Cytotoxic prenylxanthones from *Garcinia bracteata*", *J. Nat. Prod.* 63, 441-446.

Thoison, O., Cuong, D.D., Gramain, A., Chiaroni, A., Hung, N.V. and Sevenet, T. 2005. "Further rearranged prenylxanthones and benzophenones from *Garcinia bracteata*", *Tetrahedron.* 61, 8529-8535.

Vieira, L.M.M., Kijjoa, A., Silva, A.M.S., Mondranondra, I.-O., Kengthong, S., Gales, L., Damas, A.M. and Herz, W. 2004a. "Lanostanes and friedolanostanes from the bark of *Garcinia speciosa*", *Phytochemistry.* 65, 393-398.

Vieira, L.M.M., Kijjoa, A., Wilairat, R., Nascimento, M.S.J., Gales, L., Damas, A.M., M.S.Silva, A., Mondranondra, I.-O. and Herz, W. 2004b. "Bioactive friedolanostanes and 11(10→8)-Abeolanostanes from the bark of *Garcinia speciosa*", *J. Nat. Prod.* 67, 2043-2047.

Wahyuni, F.S., Byrne, L.T., Dachriyanus, Dianita, R., Jubaha, J., Lajis, N.H. and Sargent, M.V. 2004. "A new ring-reduced tetraprenyltoluquinone and a prenylated xanthone from *Garcinia cowa*", *Aust. J. Chem.* 57(3), 223-226.

Weng, J.-R., Lin, C.-N., Tsao, L.-T. and Wang, J.-P. 2003a. "Novel and anti-inflammatory constituents of *Garcinia subelliptica*", *Chemistry—A European Journal.* 9(9), 1958-1963.

Weng, J.-R., Lin, C.-N., Tsao, L.-T. and Wang, J.-P. 2003b. "Terpenoids with a new skeleton and novel triterpenoids with anti-inflammatory effects from *Garcinia subelliptica*", *Chemistry—A European Journal.* 9(22), 5520-5527.

Whitmore, T.C. 1973. "Tree flora of Malaya", Vol. II, Hong Kong : Wing Tai Cheung Printing CO. Ltd.

Williams, R.B., Hoch, J., Glass, T.E., Evans, R., Miller, J.S., Wisse, J.H. and Kingston, D.G.I. 2003. "A novel cytotoxic guttiferone analogue from *Garcinia macrophylla* from the Surinam rainforest", *Planta Med.* 69(9), 864-866.

Williams, R.B., Hoch, J., Glass, T.E., Evans, R., Miller, J.S., Wisse, J.H. and Kingston, D.G.I. 2005. "A novel cytotoxic guttiferone analogue from *Garcinia macrophylla* from the Surinam rainforest", *Planta Med.* 71(4), 354-356.

Xu, Y.-J., Chiang, P.-H., Lai, Y.-H., Vittle, J.J., Wu, X.-H, Tan, B.K.H., Imiyabir, Z. and Goh, S.-H. 2000. "Cytotoxic prenylated depsidonees from *Garcinia parvifolia*", *J. Nat. Prod.* 63, 1361-1363.

Xu, Y.-J., Lai, Y.-H., Imiyabir, Z. and Goh, S.-H. 2001. "Xanthones from *Garcinia parvifolia*", *J. Nat. Prod.* 64(9), 1191-1195.

VITAE

Name Miss Wanpen Naklue

Student ID 4722071

Educational Attainment

Degree	Name of Institution	Year of graduation
Bachelor of Science (Chemistry)	Prince of Songkla University	2003

Scholarship Awards during Enrolment

1. The Development and Promotion of Science and Technology Talents Project
2. The Higher Education Development Project: Postgraduate Education and Research Program in Chemistry, funded by the Royal Thai Government.